UNIVERSITY OF Hull

Department of Biological and Marine Sciences

Thesis submitted for the Degree of Doctor of Philosophy

The molecular basis of circadian and seasonal rhythms in the blue mussel *Mytilus edulis*

Emma C. Chapman

BSc (Hons), MSc

Supervisors:

Professor Jeanette Rotchell

Professor Dan Parsons

October 2019

Abstract

Exposure to regular environmental oscillations such as day/night have allowed organisms to evolve biological mechanisms to adaptively anticipate and prepare for rhythmic environmental change. A network of gene-protein interactions between clock genes and their proteins comprise the molecular clock mechanism at the heart of regulating biological rhythms. Though this is an endogenous and self-regulating system, elements of this network can be entrained by exogenous biotic and abiotic factors. This synchronisation process between environmental cycles and endogenous rhythms is facilitated by cues like light and temperature, which influence clock gene expression patterns.

Marine bivalves often inhabit intertidal habitats under the influence of numerous oscillating environmental conditions, though little is known about how they regulate their biological timekeeping. In this thesis, we investigate the molecular regulation of biological rhythms in the ecologically and commercially important blue mussel, *M. edulis*, over different timeframes. For the first time in this species, we isolate and characterise a number of clock genes (*Clk*, *Cry1*, *ROR/HR3*, *Per* and *Rev-erb*) and clock-associated genes (*ARNT*, *Timeout*-like and *aaNAT*). Rhythmic clock gene expression is demonstrated in the absence of light cues, indicative of endogenous clock control. Differential expression of *Cry1* expression between males and females under the same conditions indicates sex-specific regulation and/or function. In addition, diurnal temperature cycles modulated the otherwise rhythmic expression of *Rev-erb* to constant levels demonstrating an interaction of temperature with clock function. Instances of seasonal clock mRNA expression differences were found, in addition to a number of other putative seasonal genes, indicating a possible mechanism

by which seasonal cues can inform rhythmic biological processes.

Understanding the influence of environmental cues on the molecular clock is essential in predicting the outcomes of future environmental change on fundamental rhythmic processes, in particular the impacts of decoupled environmental cues on the already highly dynamic and stressful intertidal zone.

Acknowledgements

I would especially like to thank my supervisors Prof Jeanette M. Rotchell and Prof Daniel R. Parsons for their help, support and guidance throughout this PhD. It wouldn't have been possible without you so thank you for everything.

I would also like to thank Jennie Brigham and the School of Biological, Biomedical and Environmental Sciences/ Department of Biological and Marine Sciences for supporting my part-time studies.

Many thanks also go to David O'Neill, Dr Rose Wilcox and Prof Jeanette M. Rotchell for helping with sample collection and mussel dissections at all sorts of hours of the day and night.

Finally, thank you to my family for their support and encouragement.

Publications

Some aspects of this work have been published. Research from Chapters 2 to 4 appears in:

Chapman, E.C., O'Dell, A.R., Meligi, N.M., Parsons, D.R. and Rotchell, J.M., 2017. Seasonal expression patterns of clock-associated genes in the blue mussel *Mytilus edulis*. *Chronobiology International*, *34*(9), 1300-1314.

Research from Chapters 5 and 6 appears in:

Chapman, E.C., Parsons, D.R. and Rotchell, J.M., 2020. Influence of light and temperature cycles on the expression of circadian clock genes in the mussel *Mytilus edulis*. *Marine Environmental Research, 159.* 104960

Author Statement

JR was responsible for conceptualization, funding and supervision in general for both papers. EC was also responsible for the conceptualization, and conducted sample investigation and formal analysis. AO, NM and BB conducted sample investigation. DP reviewed the work. EC and JR took the lead in preparing the manuscripts and the data visualization.

Contents

List of Figures

List of Tables

Abbreviations

18S/*18S*	18S ribosomal RNA
5-HT	5-hydroxytryptamine (serotonin)
5-HTP	5-Hydroxytryptophan
αTUB/*TUB*	Alpha tubulin
AADC	Aromatic-L-amino acid decarboxylase
aaNAT/*aaNAT*	Arylalkylamine N-acetyltransferase
AhR	Aryl hydrocarbon receptor (or dioxin receptor)
ARNT/*ARNT*	Aryl hydrocarbon Receptor Nuclear Translocator
ARNTL/*ARNTL*	Aryl Hydrocarbon receptor nuclear translocator-like (BMAL1)
ASO	Abdominal sense organ
ATP	Adenosine triphosphate
bHLH	Basic helix-loop-helix domain
BLAST	Basic local alignment search tool
BMAL1/*BMAL1*	Brain and Muscle ARNT-Like 1 (ARNTL)
bp	Base pairs
BSA	Bovine serum albumin
CaM	Calmodulin
CCA1/*CCA1*	Circadian and Clock Associated 1
cDNA	Complementary deoxyribonucleic acid
CDS	Coding deoxyribonucleic acid sequence
CCG	Clock-controlled genes
CKI	Casein kinase I
CK1δ/ *CK1δ*	Casein kinase I delta
CKIε/*CKIε*	Casein kinase I epsilon
CK2	Casein kinase 2
CLK/*Clk*	Clock
CoA	Co-enzyme A binding pocket
Cq	Threshold cycles
CRY/*Cry*	Cryptochrome
CV	Coefficient of variation
CWO/*Cwo*	Clockwork orange

CYC/*Cyc*	Cycle
DBT/*Dbt*	Doubletime
DD	Dark/dark exposure (constant darkness)
DMSO	Dimethyl sulfoxide $(CH_3)_2SO$
DNA	Deoxyribonucleic acid
dNTP	Deoxynucleotide
dsDNA	Double-stranded deoxyribonucleic acid
DTT	Dithiothreitol
EDTA	Ethylenediaminetetraacetic acid $C_{10}H_{16}N_2O_8$
EF1/*EF1*	Elongation factor 1
ELISA	Enzyme-linked immunosorbent assay
ER	Estrogen receptor
EST	Expressed sequence tag
EU	European Union
FA	Formaldehyde-agarose
FAD	Flavin adenine dinucleotide
FAO	Food and Agriculture Organization of the United Nations
FRQ/*FRQ*	Frequency
GAPDH	Glyceraldehyde-3-phosphate dehydrogenase
GMT	Greenwich Mean Time
GnRH	Gonadotropin-releasing hormone
H&E	Heamatoxylin and eosin
HIF-α/*HIF-α*	Hypoxia inducible factor alpha
HIOMT	Hydroxindole-*O*-methyltransferase
HPLC	High performance liquid chromatography
hr	Hour(s)
HR3/*HR3*	Hormone receptor 3
IgSF	Immunoglobulin superfamily
ISH	In situ hybridisation
JET	Jetlag
JTT	Jones-Taylor-Thornton
Kb	Kilo bases
LD	Light/dark cycles
LD PCR	Long distance polymerase chain reaction

LHY/*LHY*	Late Elongated Hypocotyl
LL	Light/light exposure (constant light)
MFP-1/*mfp-1*	*Mytilus* foot protein 1
MPP	Mitochondrial-processing peptidase
mRNA	Messenger ribonucleic acid
mt-rRNA	Mitochondrial ribosomal ribonucleic acid
NES	Nuclear export signal domain
NGS	Next-generation sequencing
NLS	Nuclear localisation signal domain
NNI	Nearest neighbor interchange
NOAA	National Oceanic and Atmospheric Administration
NR_DBD_ROR	Nuclear receptor DNA-binding domain of retinoid orphan receptors
NR_LBD_ROR-like	Nuclear receptor ligand-binding domain of retinoid orphan receptors
NV-aaNAT/*aaNAT*	Non-vertebrate type arylalkylamine N-acetyltransferase
PAS	Period-aryl hydrocarbon receptor nuclear translocator – single-minded domain
PAC	PAS-associated c-terminal motif
PDP/*Pdp1ε*	PAR-domain protein 1
PER/*Per*	Period
PCR	Polymerase chain reaction
PP1	Protein phosphatase 1
PP2A	Protein phosphatase 2A
PST	Paralytic shellfish poisoning
qPCR	Quantitative real time polymerase chain reaction
RACE	Rapid amplification of cDNA ends
REV-ERB/*Rev-erb*	Nuclear Receptor Subfamily 1 Group D Member 1
RFU	Relative Fluorescence Units
RHT	Retino-hypothalamic tract
RIA	Radioimmunoassay
RNA	Ribonucleic acid
RNAi	Ribonucleic acid interference
ROR/*ROR*	RAR-related orphan receptor

ROS	Reactive oxygen species
SCN	Suprachiasmatic nucleus
SD	Standard deviation
SDS	Sodium dodecyl sulphate
SDS-PAGE	Sodium dodecyl sulphate polyacrylamide gel electrophoresis
SEM	Standard error of the mean
SIM/*Sim*	Single-minded
SGG	Shaggy
SOL	Small optic lobes
ssDNA	Single-stranded deoxyribonucleic acid
SSH	Suppression Subtractive Hybridisation
SST	Sea surface temperature
TAE	Tris-base, acetic acid, ethylenediaminetetraacetic acid buffer
TBE	Tris-base borate ethylenediaminetetraacetic acid buffer
TEMED	Tetramethylethylenediamine
TIM/*Tim*	Timeless
Tm	Melting temperature
TPH	Tryptophan hydroxylase
UKBAP	United Kingdom Biodiversity Action Plan
VRI/*Vri*	Vrille
VT-aaNAT/*aaNAT*	Vertebrate-type arylalkylamine N-acetyltransferase
WC-1/*WC-1*	White Collar-1
WC-2/*WC-2*	White Collar-2
X-gal	5-bromo-4-chloro-3-indolyl-β-D-galactopyranoside

Standard protein and gene nomenclature conventions are followed throughout this thesis; protein names are fully capitalised and gene names are italicised.

Chapter 1

Introduction and literature review

1.1 BIOLOGICAL RHYTHMS

Biological rhythms are physiological or behavioural processes occurring within living organisms that cycle systematically over a regular time-period (Aschoff, 1981). This broad term encompasses a variety of types of rhythm which may be generally grouped according to frequency (i.e. timescale), biological system (i.e. spatial scale), underlying process (e.g. biochemical oscillations), or function (e.g. physiological, behavioural) (Aschoff, 1981). For example, biological rhythms are often broadly categorised according to the time-scale over which they operate and can be generally described as ultradian, circadian or infradian (Aschoff, 1981). Ultradian rhythms, such as such as 12.4 hr circatidal cycles, operate over a timeframe that is less than 24 hr (Tessmar-Raible et al., 2011), whereas circadian rhythms (term derived from Latin: *circa*, approximately; *diem*, day) endogenously cycle over a ~24 hr period (Figure 1.1) (Pittendrigh, 1960). Infradian rhythms are comparatively longer and include 29.5 day circalunar rhythms, and circannual cycles that oscillate on a yearly basis (Figure 1.1) (Tessmar-Raible et al., 2011). A number of common terms used to describe the temporal characteristics of a rhythm are described in Figure 1.2.

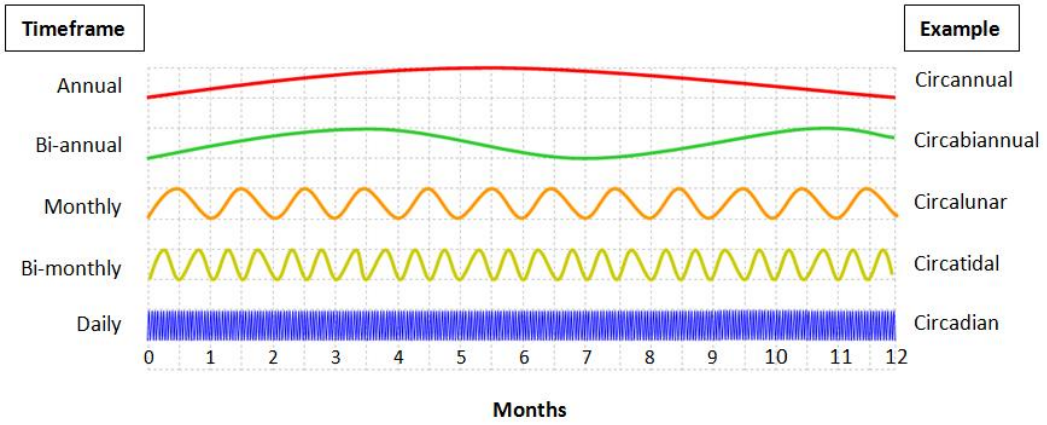

Figure 1.1 Simplified diagram illustrating examples of biological rhythm timescales (based on Aschoff, 1981).

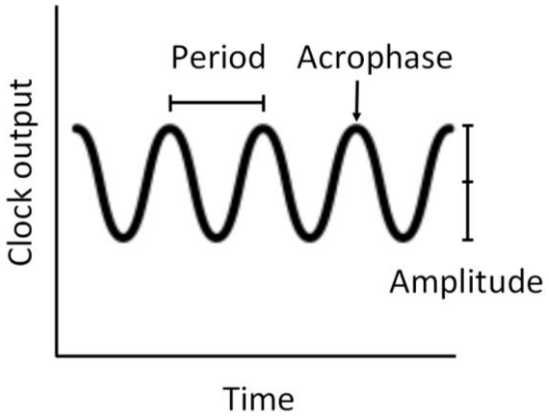

Figure 1.2 Diagram illustrating common terms used to describe characteristics of biological rhythms. Adapted from Vitaterna et al. (2001). Period refers to the time taken for a complete cycle, phase is the position of a distinct point in time in a cycle (i.e. activity onset), acrophase is the peak of the oscillation, and amplitude can refer to either the difference between maximum and minimum points of a biological oscillation or between the maximum and mean (Kreitzman and Foster, 2011).

The spatial scales over which biological rhythms operate range from molecular, cellular, whole-organism and population levels. These are exemplified by rhythmicity in gene expression patterns (Connor and Gracey, 2011), cycles of cell growth and division (Űnsal-Kaçmaz et al., 2005), and large-scale events like reproductive development/spawning (Norberg et al., 2004), migration (Gwinner,

1996) and diapause (Yamada and Yamamoyo, 2011). Chronobiology (derived from Greek: *chronos*, time; *bio*, life; *logos*, study/plan) is the term applied to the study of biological rhythms and their interactions with environmental cycles.

The majority of organisms are exposed to rhythmic environmental cycles, such as daytime/night-time due to the Earth's rotation on its axis, tidal and lunar cycles due to the rotation of the moon around the Earth (Naylor, 2010), and seasonal change as the planet rotates around the sun whilst tilting on its axis (Khavrus and Shelevytsky, 2010). Exogenous biological rhythms, described by Aschoff (1981) as "forced oscillations of passive systems", are simply direct responses to periodic external conditions such as photoreception in response to light or increased reaction rates in response to elevated temperature. However, regular environmental oscillations have allowed organisms to evolve biological mechanisms to adaptively anticipate and prepare for rhythmic environmental change (Vaze and Sharma, 2013; Yerushalmi and Green, 2009; McClung, 2006; Dodd et al., 2005). This has resulted in endogenous biological rhythms, the focus of this thesis, which are self-regulated internally on a molecular level (Dunlap, 1999; Reddy et al., 1984) and, though synchronised by external environmental cycles, can be sustained (free-running) in their absence (Pittendrigh, 1960). Notable examples of endogenous rhythms regulated by underlying endogenous molecular mechanisms, include circadian rhythms, such as sleep-wake cycles (Beersma and Gordijn, 2007) and core body temperature in humans (Kräuchi, 2002), and circannual rhythms including hibernation in golden-mantled ground squirrels (Hiebert et al., 2000) and seasonal migration in birds such as Sylvia warblers, *Sylvia borin* (Gwinner, 1996).

The remainder of this introduction chapter will discuss the key features of circadian rhythms and outline the molecular basis of circadian timing focusing on

vertebrate and invertebrate model species. Ultradian rhythms, in particular the influence of photoperiod on seasonal rhythms will be also be discussed as will the relationship between circadian and ultradian regulatory systems. Finally, after a brief overview of biological rhythms in aquatic molluscs, the relevance of blue mussel (*M. edulis*) chronobiology will be outlined and the aims of this thesis will be listed.

1.2 CIRCADIAN RHYTHMS

Given the daily shift in the environment between light and dark, circadian rhythms are particularly widespread and are considered ubiquitous as they have been documented in numerous bacteria (Sartor et al., 2019; Swan et al., 2018; Cohen and Golden, 2015), archaea (Maniscalco et al., 2014; Whitehead et al., 2009), plants (Linde et al., 2017; Dodd et al., 2013; Schulze et al., 2010; McClung, 2006), fungi (Larrondo and Canessa, 2019; Dunlap and Loros, 2006), invertebrates (Lam and Chiu, 2017; Tomioka and Matsumoto, 2015; Hardin, 2005) and vertebrates (Scheiermann et al, 2013; Wang et al., 2012; Oishi et al., 2010; Beersma and Gordijn, 2007; Zhdanova and Reebs, 2006). Specific examples of circadian rhythms in diverse organisms include photosynthesis in cyanobacteria (Golden et al., 1997), the release of floral scents in certain plants (Fenske and Imaizumi, 2016), metabolism in yeast (Eelderink-Chen et al., 2010), immunity in *Drosophila* (Stone et al., 2012), song communication in birds (Cassone, 2014), locomotion activity in rodents (DeCoursey et al., 2000) and hormone production in humans (Gnocchi and Bruscalupi, 2017). In addition to the endogenous approximate 24 hr cycling time necessary to classify a rhythm as circadian, further general characteristics have also been outlined (Roenneberg and Merrow, 2005; Pittendrigh, 1960). The most notable of which are that they are innate, self-sustaining, entrainable, and temperature compensated (Roenneberg and Merrow,

2005). This means that circadian rhythms are endogenously regulated (innate), can persist in the absence of external cues (self-sustaining) (Aschoff, 1960), are synchronised by environmental cycles (entrainment) (Golombek and Rosenstein, 2010), and have a period that can be maintained over a range of constant temperatures (temperature-compensation) (Ruoff, 2004; Rensing et al., 2001). As circadian rhythms are endogenous by their definition, the more general term of diurnal rhythm is often used when endogenous process has not been ascertained.

Entrainment of endogenous rhythms with external cycles can confer adaptive advantage as it allows organisms to gain benefits, or avoid costs associated with the timing of particular activities at a certain time of day (Vaze and Sharma, 2013; Dubruille and Emery, 2008; Dodd et al., 2005). For example, cyanobacterial strains with a functioning biological clock outcompete clock-disrupted strains when under rhythmic conditions (Woelfle et al., 2004). Among functional strains of cyanobacteria with different circadian periods, competitive advantage was shown when the endogenous and external cycles were similar (Woelfle et al., 2004). Competitive advantage, in terms of higher chlorophyll content, greater carbon fixation, faster growth, and survival, was apparent in the plant *Arabidopsis thaliana* when the period of their clock matched the environment (Dodd et al., 2005). Direct testing in the field has shown that mortality by predation was significantly greater in *Tamias striatus* chipmunks with impaired circadian function compared to controls, potentially as a result of increased nocturnal movement in the former (DeCoursey et al., 2000). Further supporting evidence includes the regression of circadian rhythms under constant conditions in nature (DeCoursey, 2004) and the occurrence of latitudinal gradients in circadian function (Costa et al., 1992).

Environmental cues used for entrainment, known as “zeitgebers” (derived

from German: *zeit*, time; *geber*, giver), most commonly include light and temperature (López-Olmeda et al., 2006; Sharma and Chandrashekaran, 2005; Glaser and Stanewsky, 2005; Millar, 2004) but can also include other stimuli like food availability (Williams and Pilditch, 1997), stress and exercise (Tahara et al., 2017), tidal and lunar cues (Tessmar-Raible et al., 2011) and moonlight (Payton and Tran, 2019; Bachleitner et al., 2007). Figure 1.3 is a linear diagram showing the key components of circadian entrainment; environmental cues act as zeitgebers to synchronise subcellular biochemical interactions, known as the molecular clock mechanism, which regulate rhythmic circadian processes.

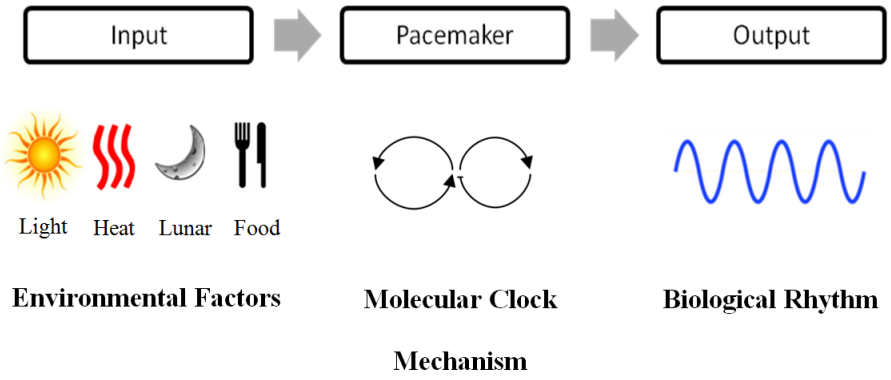

Figure 1.3 Concept diagram showing circadian rhythm entrainment by common zeitgebers (based on Golombek and Rosenstein, (2010)).

1.2.1 The molecular clock mechanism

The web of interactions at the heart of regulating circadian rhythms is referred to as the molecular clock mechanism. This subcellular timekeeping system comprises a variety of "clock genes" which autoregulate their expression patterns as their protein products interact with them via negative-feedback loops in a cycle that takes 24 hr to complete (Roenneberg and Merrow, 2005; Hardin et al., 1990). Evidence of these regulatory transcription-translation networks has been found in Bacteria (Sartor et al.,

2019; Swan et al., 2018), Archaea (Maniscalco et al., 2014), Plantae (McClung, 2019; Gardner et al., 2006), Fungi (Dunlap and Loros, 2006) and Animalia (Allada et al., 2001), with the latter including, though not limited to, the following major phyla: Mollusca (Connor and Gracey, 2011), Porifera (Jindrich et al., 2017), Cnidaria (Brady et al., 2011; Reitzel et al., 2010), Nematoda (Temmerman et al., 2011), Annelida (Tosches et al., 2014), Arthropoda (Häfker et al., 2017; Shirasu et al., 2003), Echinodermata (Petrone, 2016), and Chordata (Renthlei et al, 2019; Andreazzoli and Angeloni, 2017; Bertolucci et al., 2017; Mohawk et al., 2012; Zhdanova and Reebs., 2006).

There are both similarities and differences apparent between species in the specific clock genes/proteins involved in the molecular clock mechanism (Lam and Chiu, 2017; Hardin, 2005; Allada et al., 2001; Harmer et al., 2001; Young, 2000). Cyanobacterial circadian rhythms are post-translational oscillators involving the proteins KaiABC, SasA, CikA, and RpaA (Swan et al., 2018). Frequency (FRQ), White Collar-1 (WC-1) and White Collar-2 (WC-2) form an integral transcription–translation negative feedback loop in fungi (Dunlap and Loros, 2006) whereas Circadian and Clock Associated 1 (CCA1) and Late Elongated Hypocotyl (LHY) are involved in each of the three interlocked feedback loops in plants (McClung, 2006). Among animals, the majority of molecular chronobiology research has focused on mammals and arthropods, in particular insects. For example, central *Drosophila* clock genes include *Clock* (*Clk*), *Cycle* (*Cyc*), *Period* (*Per*), *Timeless* (*Tim*), *Doubletime (Dbt), Vrille* (*Vri), PAR-domain Protein 1* (*Pdp1ε*) and *clockwork orange* (*Cwo*) (Hardin, 2005). Key mammalian clock genes include *Clk*, *Bmal1*, *Period* genes (*Per1*, *Per2*, and *Per3*), *Cryptochrome* genes (*Cry1* and *Cry2*), *RAR-related orphan receptors* (*RORs*), *Rev-erb* and *Casein kinase I epsilon* (*CKIℰ*) (Shearman et al., 2000). The

molecular chronobiology of the core mammalian and *Drosophila* clocks are particularly well documented and are summarised below (Figure 1.4). In each case, the network of clock gene-protein interactions have evolved to cycle endogenously over a ~24 hr period.

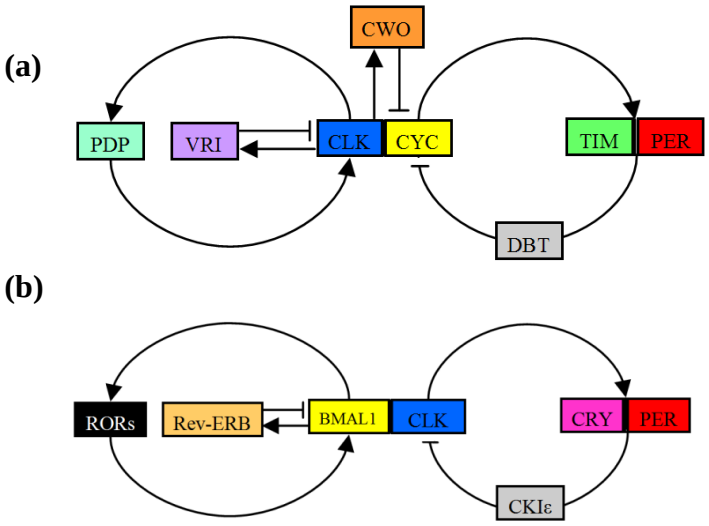

Figure 1.4 Generalised models of the negative-feedback loops at the heart of the regulatory core/central/master circadian molecular clock mechanism of (a) fruit fly (*Drosophila*) and (b) mammals. Arrows show a positive influence on gene expression and flat-ended lines denote inhibition. Adapted from Zhang and Kay (2010). Abbreviations: CLK, Clock; CYC, Cycle; PER, Period; TIM, Timeless; PDP, PAR-domain Protein 1; VRI, Vrille; CWO, Clockwork Orange; CRY, Cryptochrome; DBT, Double Time, BMAL1, Aryl hydrocarbon receptor nuclear translocator-like; CKIε, Casein kinase I epsilon; RORs, RAR-related orphan receptors; Rev-ERB, Rev-erbα protein.

Clk is a key clock gene involved in the primary negative feedback loops of the clock mechanism in both mammals and *Drosophila* (Steeves et al., 1999; Allada et al., 1998) (Figure 1.4). In *Drosophila*, the protein products of *Clk* and *Cyc* (CLK and CYC) heterodimerise with the assistance of an E-box (Enhancer Box) protein-binding site, and form a protein complex that triggers the expression of *Per* and *Tim* (Figure 1.4a) (Darlington et al., 1998). This results in a PER-TIM complex in the cytoplasm

which undergoes a series of phosphorylation reactions facilitated by kinases and phosphatases which add and remove phosphate groups respectively. For example, DBT and Casein Kinase II (CK2) phosphorylate PER, whereas Protein Phosphatase 2A (PP2A) removes these phosphate groups (Nawathean and Rosbash, 2004). Similarly, Shaggy (SGG) is the kinase acting upon TIM, and Protein Phosphatase 1 (PP1) is the antagonistic phosphatase (Dubruille and Emery, 2008). The resulting phosphorylated TIM-PER-DBT protein complex is translocated into the nucleus where it binds to the CLK-CYC heterodimers, thereby inhibiting transcription of *Per* and *Tim*. Upon degradation of the PER-TIM-DBT complex, the inhibitory effect is removed allowing CLK to accumulate once more and the process begins again (Hardin, 2005).

CLK is regulated by the second *Drosophila* feedback loop; the CLK-CYC heterodimer triggers the expression of *Vri* and *Pdp1ε* (Figure 1.4a) (Hardin, 2005), which lead to the repression and slightly delayed activation of *Clk* transcription respectively (Tomioka et al., 2012). A third, smaller feedback loop involves the CLK-CYC heterodimer triggering the expression of *Cwo*. Via competitive interactions with the E-Box sequence, CWO is able to inhibit CLK-CYC and therefore impact upon the expression of other clock genes, providing a mechanism by which the amplitude of clock activity can be controlled (Matsumoto et al., 2007). A more detailed graphical summary of the negative feedback interactions of the *Drosophila* molecular clock mechanism is shown in Figure 1.5.

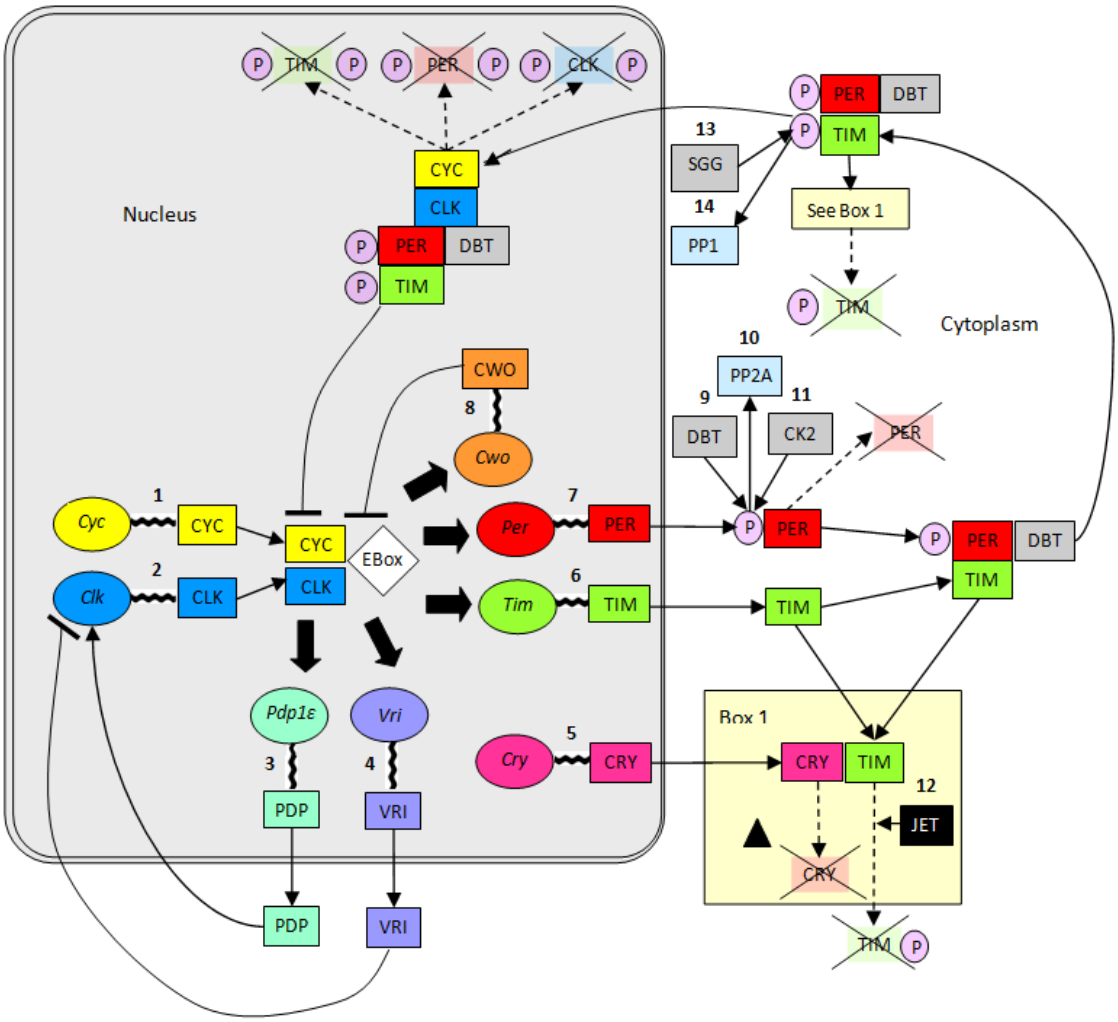

Figure 1.5 Model of the core feedback loops regulating circadian rhythm in *Drosophila.* Ovals represent genes, rectangular boxes represent proteins and circles show phosphorylation. Small arrows indicate process directionality and flat-ended lines denote inhibition. Large solid arrows show promotion of gene expression and dashed arrows denote degradation. The triangle symbol indicates the influence of light. Box 1 shows light-induced degradation of TIM. Adapted from Young, 2000; Hardin, 2005; Dubruille and Emery, 2008; Allada and Chung, 2010; Tomioka et al., 2012. Numbers 1 – 14 have been discovered in *Drosophila* and numbers 1, 2, 5-7, 9 and 13 have been found in molluscs (see Table 1.1). Abbreviations: *Clk*, *Clock*; *Cyc*, *Cycle*; *Per*, *Period*; *Tim*, *Timeless*; *Pdp1ε*, *PAR-domain Protein 1*; *Vri*, *Vrille*; *Cry*, *Cryptochrome*; *CWO*, *Clockwork Orange*; JET, Jetlag; DBT, Double Time; SGG, Shaggy; CK2, Casein kinase 2; PP1, Protein Phosphatase 1; PP2A, Protein phosphatase 2A.

In mammals, the process differs in that CLK heterodimerises with BMAL1 which triggers the expression of *Per* (*Per1-3*) and *Cry* genes (*Cry1* and *Cry2*), leading to the formation of a PER-CRY heterodimer (Figure 1.4b) (Shearman et al., 2000). The PER-CRY heterodimers are translocated to the nucleus where they repress their own transcription (Sato et al., 2006). As in the *Drosophila* system, the stability and nuclear translocation of clock proteins are regulated by post transcriptional modifications, such as the phosphorylation of PER proteins by casein kinase Iδ and Iε (CKIδ/ε) (Lee et al., 2009). The second mammalian regulatory feedback loop consists of RAR-related orphan receptors (ROR α, β and γ), which activate BMAL1 transcription, and REV-ERB (α and β) which repress its transcription (Figure 1.4b) (Guillaumond et al., 2005).

The cyanobacterial *kaiABC* genes are proposed to be the earliest genes to have evolved clock function (Tauber et al., 2004). Selection pressure to avoid harmful UV light irradiation during the pre-Cambrian period (4.5 billion to 542 million years ago) is thought to have led to the evolution of photoreceptive cryptochrome from DNA repairing photolyases, and resulted in rhythmic vertical migration in the oceans (Gehring and Rosbash, 2003). Multiple gene duplication events and functional divergence of clock gene paralogs have ultimately shaped the molecular clock components of extant species (Haug et al., 2015; Tauber et al., 2004). For example, the lack of *Period* genes outside of the Bilateria, suggesting they arose within these phyla, along with gene duplication of *Period* in mammals and gene loss of *Timeless* and some cryptochromes in certain insects, are thought to have resulted in the major differences in clock regulation in animals (Reitzel et al., 2010). For instance, mammalian *Per1*, *Per2* and *Per3* contrast with just *Per* in *Drosophila* (Young and Kay, 2001); *Per* is the most rapidly evolving family of clock genes (Tauber et al.,

2004). Furthermore, though *Cry1* is present in *Drosophila*, it is not directly involved in the core clock interactions like in mammals, but plays an important associated role as a blue light photoreceptor; CRY and the *Jetlag* protein JET co-facilitate the light-induced degradation of TIM providing the mechanism whereby light acts as a zeitgeber to entrain the clock with external day/night cycles (Peschel et al., 2009; Van Gelder, 2006). Mammalian photoentrainment involves retinal photoreception and melanopsin signalling (Liu and Panda, 2017).

The relative importance of particular clock genes to the rhythm-regulation function of the clock mechanism can vary, even among relatively closely related species (Young and Kay, 2001). For example, *Timeless* is not an essential clock gene in the cricket *Gryllus bimaculatus* or honeybee *Apis mellifera*, but it is in the firebrat *Thermobia domestica* (Tomioka et al., 2012) and flies of the Drosophilidae family (Pavelka et al., 2003). These differences between *Drosophila* and *A. mellifera* are thought to have arisen from divergence from an ancestral insect clock in the case of the former, and convergence with mammalian clocks specialising in mammalian-type CRY and TIM2 in the case of the latter (Rubin et al., 2006). However, in all cases, the molecular clock mechanism regulates the expression of multiple clock-controlled genes (CCGs) which impact upon the timing of a host of diverse physiological and behavioural processes giving rise to a variety of circadian rhythms (Bozek et al., 2009; Harmer et al., 2001; McDonald and Rosbash, 2001; Zhang et al., 2009). Furthermore, a number of clock genes also have pleiotropic functions and therefore influence other biological processes beyond their interactions in the molecular clock mechanism. For example, Figure 1.6 shows some examples of links between *Drosophila* clock genes and various other biological processes including the roles of *Tim* in the nocturnal upregulation of phagocytosis (Stone et al., 2012; Lee and Edery, 2008), replication

fork stabilisation (Errico and Costanzo, 2010) and its non-circadian role in oogenesis/reproductive output in *Drosophila* ovarian follicles (Rush et al., 2006; Beaver et al., 2003). Similarly, mammalian clock genes can also play non-circadian roles in peripheral tissues (Alvarez et al., 2003).

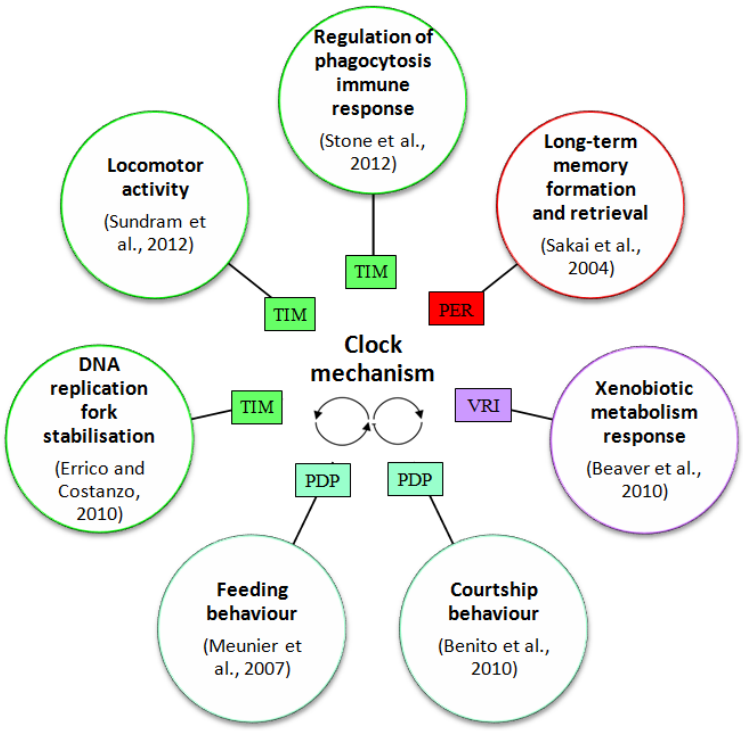

Figure 1.6 Diagram showing the influence of some *Drosophila* clock genes/proteins on biological processes. Abbreviations: PER, Period; TIM, Timeless; PDP, PAR-domain Protein 1; VRI, Vrille.

1.2.2 The central and peripheral clock mechanisms

The clock gene/protein interactions described in Section 1.2.1 summarise the typical interactions of the central, core or master clock mechanism often also referred to as the circadian pacemaker/oscillator. This central pacemaker is located in neuronal tissues, for example in the suprachiasmatic nucleus (SCN) of the hypothalamus in mammalian brains (Mohawk et al., 2012),in the pineal gland, hypothalamus and retina of birds (Gwinner and Brandstatter, 2001), in the ventro-lateral neurons in the brains

of *Drosophila* (Tomioka et al., 2012; Helfrich-Förster, 2006), the mid-brain of lepidopterans (Sauman et al., 2005), the optic lobes of crickets and cockroaches (Tomioka, 2014; Reischig and Stengl, 2003) and the eyestalks and/or brains of some decapod crustaceans (Grabek & Chabot, 2012; Escamilla-Chimal et al., 2010). The central clock mechanism is entrained by zeitgebers, in particular light/dark cycles (Liu and Panda, 2017; Golombek and Rosenstein, 2010; Tomioka and Matsumoto, 2010; Hiebert et al., 2000). This central pacemaker either directly influences rhythmic processes within an organism, or acts indirectly by influencing peripheral clocks located in non-neuronal tissues (Reppert and Weaver, 2002; Cermakian and Sassone-Corsi, 2000). However, it is now well known that different circadian clocks are present and active on a cellular level in numerous tissue types (Tomioka et al., 2012). For example, single rat fibroblast cells, which synthesise connective tissue, are able to support their own circadian rhythms *in vitro* lasting for a few days (Welsh et al., 2004) and the rhythmic expression of *Period* has been shown to occur in multiple *Drosophila* body parts which has been attributed to the presence of multiple circadian clocks operating on a cellular level (Plautz et al., 1997). The synchronisation of clocks in different cells and tissues is important for coordinating whole-organism level processes in many species (Welsh et al., 2004). The precise mechanisms and the extent to which the central pacemaker is involved with peripheral clocks not only vary on a species-level, but are also tissue-dependent (Tomioka et al., 2012).

Clocks in peripheral mammalian tissues are not responsive to light/dark (LD) cycles so the central circadian pacemaker exerts more influence over the clocks in peripheral tissues (Schibler, et al., 2003). Though insects such as *Drosophila* have a central pacemaker, they also possess self-sustained peripheral oscillators in other tissues outside of the brain (Dunlap et al., 2004). Examples include the circadian

pattern of sperm release in the cotton leafworm moth, *Spodoptera littoralis*, *in vitro* under LD and constant darkness (DD) (Bebas et al., 2001) and the circadian deposition of cuticle layers in the cockroach *Blaberus fuscus* with excised optic lobes demonstrating independence from the central clock tissues (Lukat, 1978). It is possible that these differences in circadian system organisation may be linked to the fact that in organisms with a small body size light perception is not necessarily limited to information received via photoreceptors (Tomioka et al., 2012). In insects, three potential mechanisms whereby light may entrain peripheral clocks have been suggested: (1) central and peripheral clocks directly (photoreceptors) or indirectly (CRY degradation) detect light leading to reciprocal synchronisation, (2) photoreceptors somehow transmit light information to peripheral clocks, and (3) via an unknown mechanism the central clock, once entrained by light, subsequently entrains peripheral clocks (Tomioka et al., 2012). It is possible that a number of these processes are applicable though further research is needed to investigate these mechanisms.

1.3 SEASONAL AND CIRCANNUAL RHYTHMS

Seasonal variations in environmental conditions influence the majority of plants and animals. As a result, biological rhythms with circannual periodicities are apparent in various aspects of physiology and behaviour including reproduction, moulting, growth, migration and hibernation, which are often favourable at particular times of the year (Kumar and Mishra, 2018; Gwinner, 2012). Type I seasonal rhythms require both endogenous and exogenous cues as they only persist for up to one cycle in constant conditions, whereas type II seasonal rhythms are true circannual rhythms that are endogenously sustained under constant conditions and only require exogenous

cues for entrainment (Dunlap et al., 2014). An example of the former is the reproductive cycles in the mouse *Peromyscus leucopus* (Johnston and Zucker, 1980) and examples of the latter include testicular and molt cycles in starlings (Gwinner, 2012), pupation and development of the beetle *Anthrenus verbasci* (Miyazaki et al., 2014), and endogenous seasonal rhythms of body mass and reproduction in ground squirrels (Hiebert et al., 2000). Photoperiod, the number of daylight hours per day, is a common seasonal influence on multiple ecological systems, influencing both types of circannual rhythm (Dunlap et al., 2004). Non-photoperiodic seasonal cues include water, food, ambient temperature and social cues but are generally thought to be as a result of "masking" in which the expression of a trait is influenced directly rather than affecting an endogenous mechanism (Paul et al., 2007).

1.3.1 Photoperiodism

Natural photoperiods are governed by day-length, which is linked to annually cycling seasonal variation. The tilt of the Earth on its axis as it orbits the sun means that photoperiod varies with predictable regularity over the year and that seasonal photoperiod difference is greater at higher latitudes (Forsythe et al., 1995). The physiological responses of organisms to circannual photoperiod cycles, known as photoperiodism, are often large-scale events benefiting from advanced preparation including seasonal reproduction, migration, diapause and hibernation (Denlinger, 2009). Instances have been documented in a wide range of taxa including annelids (Schierwater and Hauenschild, 1990), molluscs (Numata and Udaka, 2010; Bohlken and Joosse, 1981), arthropods (Toyota et al., 2017; Beck, 2012; Saunders, 2009), echinoderms (McClintock and Watts, 1990), fish (Borg, 2010; Davie et al., 2009), reptiles (Weil and Crews, 2010), birds (Bentley, 2010; Gwinner, 1996), mammals

(Bradshaw and Holzapfel, 2007; Tournier et al., 2003), amphibians (Weil and Crews, 2010), plants (Lumsden, 2002) and fungi (Tan et al., 2004). Advanced preparation is commonly required for organisms to favour from optimal conditions or to evade adverse conditions associated with particular points of the year, as the photoperiodic response is best exhibited in anticipation of the changing season to be advantageous (Denlinger, 2009). Photoperiodism can consequently be considered as a measure of fitness within a population as, in addition to the nature of the photoperiodic response, the advantages or disadvantages of the timing of the response can influence survival and/or reproductive success (Bradshaw and Holzapfel, 2007).

Photoperiodism comprises five key elements (Figure 1.7) (Denlinger, 2009; Dolezel, 2014). First, there must be a seasonal change in day to night ratio; the latitude of the habitat must be high enough that seasonal variation in daylight hours is evident. For example, photoperiod at latitudes above 30° (~4 hr annual photoperiod change) is considered a reliable cue of season over evolutionary time (Bradshaw and Holzapfel, 2007), though insect photoperiodic responses are exhibited at latitudes as low as 7° (Denlinger, 1986). Second, the organism requires the anatomical capability to be able to sense light via either ocular or extra-ocular receptors or a combination thereof (Dunlap et al., 2004). Third, some form of photoperiodic clock mechanism must exist, enabling the organism to detect daylight hours vs. hours of darkness. Fourth, a biological "counter" mechanism is required to keep track of consecutive days exhibiting the altered day to night ratio. The photoperiodic clock and counter mechanisms, which may or may not be linked to the circadian clock mechanism, are the least understood aspects, particularly for invertebrates (Nishiwaki-Ohkawa and Yoshimura, 2016; Koštál, 2011). Finally, the organism exhibits a photoperiodic response, as documented in many phyla (Nelson et al., 2009; Bradshaw and Holzapfel,

2007; Farner, 1961). Examples include the annual spawning of wild Atlantic cod *Gadus morhua* (Norberg et al., 2004), seasonal reproductive development in the polychaete *Nereis (Neanthes) limnicola* (Fong and Pearse, 1992), moulting, breeding and song in birds (Dawson, 2001), and immune function and reproductive development in deer mice *Peromyscus maniculatus* (Demas and Nelson, 1998). In insects the most common outcome of photoperiodism is the onset of diapause (Denlinger, 2009), a phase of suspended development. For example, the monarch butterfly *Danaus plexippus* enters reproductive diapause during shorter autumn photoperiods and migrates south to overwintering sites where diapause persists until photoperiod and temperature increase, whereupon they mate and return north (Saunders, 2009).

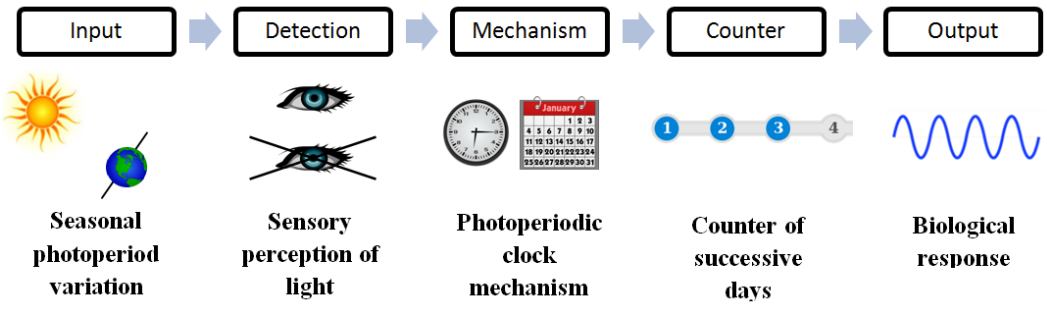

Figure 1.7 Concept diagram showing the photoperiodism process (Adapted from Dolezel, 2014).

In natural environments, photoperiod does not often act in isolation as it is one of many abiotic factors present that may affect an organism. Experimental photoperiod manipulations sometimes only show detectable results when other abiotic and biotic variables are present at relevant background levels, for example, a combination of both temperature and light (Wayne and Block, 1992) and food availability (Domínguez et al., 2010). These examples indicate that photoperiod can sometimes act as a secondary factor contributing to certain physiological or

behavioural processes and that it is particular combinations of environmental conditions that determine the overall effect on an organism. Furthermore, some organisms, including mammals (Lincoln et al., 2005) and birds (Dawson and Sharp, 2007; Nicholls et al., 1988) in particular, only show photoperiodic responses at particular times of year and are unresponsive to photoperiod during refractory periods. For example, photoperiodic testicular growth occurs during the spring in the Tree Sparrow *Passer montanus*, but testicular regression occurs after the breeding season and they experience a photorefractory period during which the reproductive system does not respond to changes in day length (Dixit and Singh, 2011). Therefore, photoperiodic responses may only be elicited during a period during which organisms are photoperiod-sensitive. In addition, non-photic cues such as temperature, social interactions and food availability can modify the timing of seasonal rhythms by interacting with photoperiod to modify the sensitive period or phase of the rhythm (Saunders, 2014; Helm et al., 2013; Dunlap et al., 2004). The molecular mechanisms of photoperiodism are less well understood than those of circadian rhythms.

1.3.2 Molecular regulation of photoperiodism

The circadian clock is involved in photoperiodic time measurement in mammals and is mediated by light-sensitive melatonin secretion, derived from serotonin, which responds to seasonal photoperiods (Nishiwaki-Ohkawa and Yoshimura, 2016; Dardente et al., 2010). The extent of the relationship between circadian timing and photoperiodism is less clear in invertebrates and has been debated among entomologists in particular (Goto, 2013; Saunders, 2005). Independence, co-operation and unity are different types of mechanism that have been proposed to describe the relationship between the circadian and photoperiodic systems (Dolezel,

2014; Koštál, 2011). A number of different models of insect photoperiodic clocks have been proposed which generally describe either independence from circadian influence or the involvement of one or more circadian oscillators (Danks, 2005; Nunes and Saunders, 1999). Three prominent models include the external coincidence model, in which a single oscillator (molecular clock mechanism) is both photo-induced and entrained by light (Saunders, 2005; Nunes and Saunders, 1999), the internal coincidence model, where light entrainment and the phase relationship between multiple different oscillators leads to photoperiodic induction (Nunes and Saunders, 1999) and a non-clock role for the circadian system in photoperiodism (Pittendrigh, 1972). No single model is all encompassing (Danks, 2005; Nunes and Saunders, 1999), likely due to difference between organisms in routes of photoreception; mammals rely on retinal photoreception (Golombek and Rosenstein, 2010) whereas extra-retinal photoreception is generally prevalent in other vertebrates, insects, crustaceans and molluscs (Kumar, 1997).

Similarly, relatively little is known about the degree of involvement between the regulation of photoperiodism and the clock genes of the circadian molecular clock system though links have been found in both mammals (Tournier et al., 2003) and invertebrates (Goto, 2013). For example, in the Syrian hamster, *Mesocricetus auratus*, the gene *casein kinase 1ε (tau)* affects both circadian and photoperiodic periods (Bradshaw and Holzapfel, 2007). *Timeless* has also been linked to both processes in flies (Pavelka et al., 2003). A number of clock genes (*Clk*, *Cyc*, *Per*, *Tim*, *Cry2*, and *vrille*) are differentially regulated in diapausing versus non-diapausing strains of the beetle *Colaphellus bowringi* (Zhu et al., 2017) and the rhythmicity and amplitude of *Per and Clk* expression varies between short day and long day conditions in the linden bug *Pyrrhocoris apterus* (Syrova et al., 2003). In addition, RNA interference (RNAi)

suppression of *Per*, *Cyc*, *Clk* and *Cry1* expression, has been shown to modulate photoperiodic responses in the bean bug *Riptortus pedestris* (Ikeno, et al., 2013; Ikeno et al., 2011b; Ikeno et al., 2010). Further differences and similarities between elements of the systems have been reviewed (Dolezel, 2014; Goto, 2013; Koštál, 2011; Bradshaw and Holzapfel, 2007a; Danks, 2005) however the full extent of any potential overlap remains unknown. Genetic approaches to ascertain the links between genes and phenotypes, examine photoperiodic traits in mutants and at different latitudes, and sequence transcriptomes of individuals under different lighting regimes will help to clarify photoperiodic mechanisms (Goto, 2013).

1.4 THE MELATONIN SYNTHESIS PATHWAY

Serotonin (5-hydroxytryptamine or 5-HT), which is ubiquitous among animals, is a neurotransmitter with broad physiological functions (Mohammad-Zadeh et al., 2008). It is involved in circadian function by modulating light input into the mammalian SCN, as well as influencing circadian rhythms via non-photic phase shifting (Morin, 1999). For example, wheel running in mice results in phase-dependent changes in serotonin levels in the SCN (Dudley et al., 1998) and disruption of the serotonin system results in altered circadian locomotor behaviour (Paulus and Mintz, 2012). In *Drosophila*, serotonin signalling also affects circadian photosensitivity, by impacting upon TIM stability (Yuan et al., 2005).

Melatonin (referred to chemically as *N*-acetyl-5-methoxytryptamine), an evolutionarily conserved hormone present in multiple taxa, is also linked to circadian function. Melatonin is derived from serotonin via the indoleamine pathway (Figure 1.8) which is sequentially facilitated by the enzymes arylalkylamine/serotonin N-acetyltransferase (aaNAT) and hydroxindole-*O*-methyltransferase (HIOMT), the

former of which is the rate-limiting factor and may be considered a proxy for the rate of melatonin synthesis (Foulkes et al., 1997).

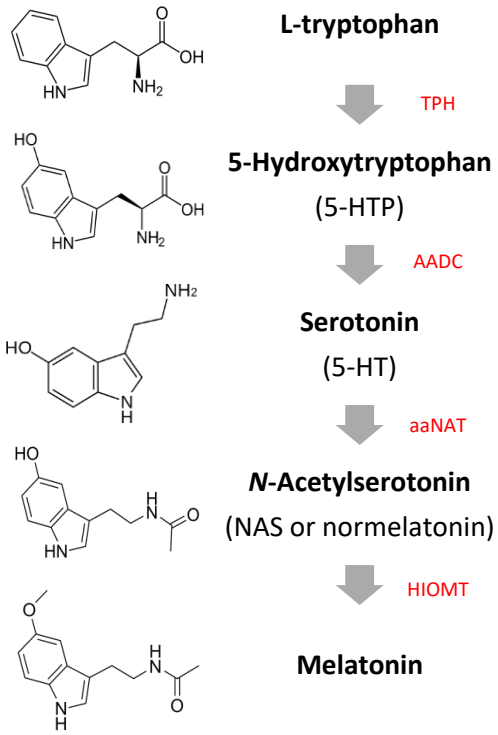

Figure 1.8 Schematic diagram showing a melatonin biosynthesis pathway with enzymes shown in red (adapted from Yanez and Meissl, 1996). Chemical structures obtained from www.chemicalbook.com. Abbreviations: TPH, tryptophan hydroxylase; AADC, aromatic-L-amino acid decarboxylase; aaNAT, arylalkylamineN-acetyltransferase; HIOMT, Hydroxyindole-O-methyltransferase.

Generally, aaNAT levels cycle in a circadian manner and peak during the night, a trend which is consequently reflected in melatonin levels (Foulkes et al., 1997; Mohamed et al., 2014). Both aaNAT and melatonin are light-sensitive, with particular sensitivity exhibited upon exposure to blue light (Izawa et al., 2009). As a result, melatonin is sometimes referred to as "the hormone of darkness" as it is a physiological signal for the length of night (Nelson et al., 2005). In diurnal mammals, light acting through the circadian system impacts upon melatonin production in the pineal gland and its nocturnal duration results in circadian sleep rhythms (Zisapel,

2018; Dunlap et al., 2014); photoreceptive retinal ganglion cells signal to the SCN by the retino-hypothalamic tract (RHT) via the neurotransmitter glutamate, and trigger a cascade resulting in transcriptional induction of clock genes and clock phase shift (Cermakian and Sassone-Corsi, 2000). As melatonin duration represents the day/night cycle, it is also a key endocrine messenger for photoperiod, linking the external light regime with the regulation of seasonal rhythms (Dunlap et al., 2014). As a result, melatonin can therefore influence reproductive development in mammals when administered at certain times of day (Vriend and Reiter, 2014). The relationship between melatonin signalling and circadian regulation is less well studied in invertebrates, though the two have been linked (Tosches et al., 2014; Yuan et al., 2005).

1.5 RHYTHMS AND CLOCK GENES IN AQUATIC MOLLUSCS

As previously discussed, the molecular basis of animal circadian timing is particularly well documented in mammals and insects (Hardin, 2005; Harmer et al., 2001; Shearman et al., 2000). Though molluscs are a large, diverse phylum, little is known about the molecular clock mechanism governing their biological rhythms – an important but understudied aspect of their ecology with relevance to commercial applications in the case of edible aquatic species such as bivalves (Gosling, 2015). This section outlines a number of examples of rhythmic biological processes exhibited by aquatic molluscs and considers the suspected underlying genetic mechanisms as well as the relevant environmental cues.

1.5.1 Biological rhythms in aquatic molluscs

Intertidal organisms are exposed to both terrestrial and aquatic environments

and are therefore under the influence of multiple fluctuating conditions, many of which occur with predictable rhythmicity. For example, cycles of diurnal light/dark, tidal immersion/exposure and annual seasonal change provide environmental cues, which can reliably inform biological timekeeping. A number of different environmental factors, both biotic and abiotic, can influence biological rhythms in aquatic molluscs (Figure 1.9).

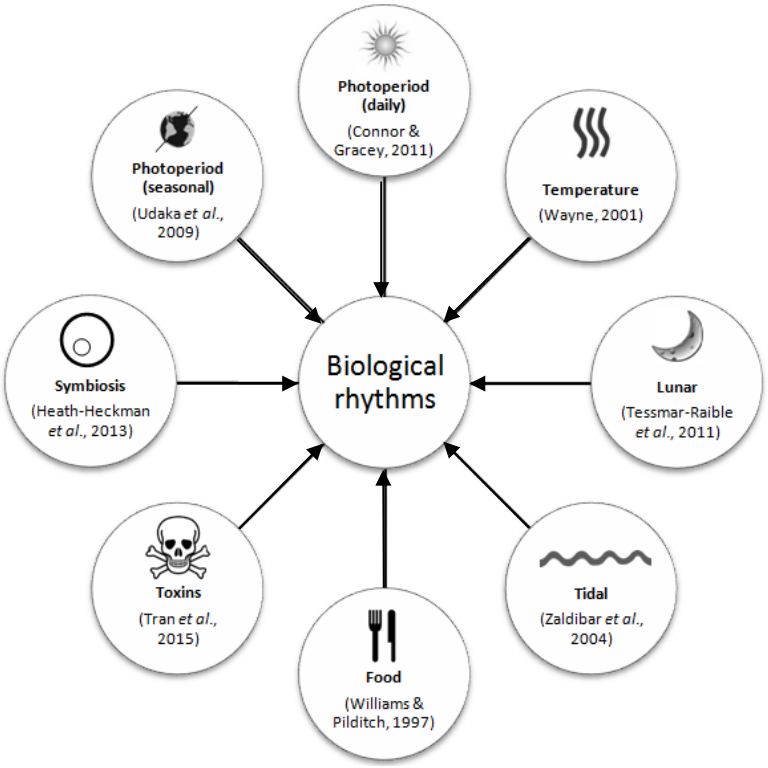

Figure 1.9 Diagram showing biotic and abiotic factors influencing biological rhythms in molluscs.

Marine biological rhythms, encompassing a variety of essential physiological and behavioural processes, have generally evolved to operate over timescales that are daily (circadian), tidal, lunar and seasonal in nature (Tessmar-Raible et al., 2011). Typical examples from marine molluscs that manifest over a wide range of spatial and temporal scales, include rhythmic gene expression (Payton et al., 2017b; Connor and Gracey, 2011; Constance et al., 2002), optic nerve impulses (Jacklet, 1969), cell

renewal (Zaldibar et al., 2004), locomotion (Schnytzer et al., 2018; Newcomb et al., 2014; Gray and Hodgson, 1999), respiration (Kim et al., 1999; Rao, 1980), feeding (Houki et al., 2015) and reproduction (Maneiro et al., 2017; Tessmar-Raible et al., 2011; Wayne, 2001; Seed, 1969).

The eyes of the gastropod sea snail *Bulla sp.* and the sea slug *Aplysia sp.*, have been used as invertebrate models of circadian pacemakers on a cellular level (Block et al., 1993) as optic nerve impulses show a circadian pattern persisting in constant darkness (McMahon et al., 1984; Jacklet, 1969). Other examples of circadian rhythms in molluscs include circadian valve activity in various species of mussel (Garcia-March et al., 2016; Gnyubkin, 2010; Wilson et al., 2005; Ameyaw-Akumfi and Naylor, 1987) and in the oyster *Crassostrea gigas* (Mat et al., 2012). In addition, circadian locomotor activity has been observed in the sea slug *Melibe leonine* (Newcomb et al., 2014), circadian siphon extension/feeding occurs in the clam *Ruditapes philippinarum* (Houki et al., 2015) and a circadian pattern of bioluminescence is evident in the squid *Euprymna scolopes* (Heath-Heckman et al., 2013). Furthermore, gene expression rhythms with circadian and ultradian periodicities are apparent in the gills of *M. californianus*; 40% of the transcriptome showed rhythmic gene expression, of which at least 80% was attributed to circadian cycling (Connor and Gracey, 2011). This illustrates that even when limited rhythmic behavioural or physiological processes are observable, rhythmic subcellular processes are in operation. Some further examples of ultradian (<24 hr) and circadian (~24 hr) rhythms in bivalves, gastropods and cephalopods are listed in Table 1.1, focusing on examples in which rhythms have been investigated for their endogenous nature, and including studies published after experiments in this thesis were conducted.

Table 1.1 Examples of biological rhythms with circadian (~24 hr) and ultradian (<24 hr) periods in marine molluscs

Species name	Common name	Rhythm	Location	Rhythm periodicity	Evidence for endogenous regulation	Description	Reference
Bivalves							
Austrovenus stutchburyi	New Zealand cockle	Shell gape	Valves	Circatidal	Yes	- Gaping response to pulsed food treatment with tidal periodicity continues for two cycles in absence of food	Williams and Pilditch (1997)
C. gigas	Pacific oyster	Shell gape	Valves	Circatidal and diurnal	Yes (tidal)	- Dominant tidal rhythm under constant immersion *in situ* - Weak circadian contribution *in situ*	Tran et al. (2011)
				Circadian and ultradian	Yes	- Circadian and ultradian activity persisting in DD	Mat et al. (2016)
				Circadian	Yes	- Daily pattern under LD subtidal conditions in the lab - Circadian rhythm was entrainable - No evidence for endogenous circatidal rhythm in the lab - Nocturnal in autumn/winter and diurnal in spring/summer *in situ* and in the lab	Mat et al. (2012)
		Clock gene expression	Adductor muscle	Diurnal and circatidal	No	- Diurnal *Cry1* expression in LD lost in DD - Circatidal pattern with tidal current in DD	Mat et al. (2016)
		Clock gene expression	Gills	Diurnal and ultradian	Some	- Differences multiple clock gene expression patterns in LD compared to DD: *Clk, Bmal1, Cry, Cry1, Cry2, Per, Tim* and *Rev-erb*	Perrigault and Tran (2017)

Donax variabilis	Coquina clam	Locomotion	Whole organism	Circatidal	Yes	- Circatidal pattern in responsiveness to tidal cues in the laboratory, independent of light regime	Ellers (1995)
Mya arenaria	Soft-shell clam	Siphon opening and closing (filtration)	Siphons	Circatidal	Some	- Rhythm with 12.4 hr period phase shifted in response to single or periodic draining stimulus. - No phase shift under different LD conditions, under different temperatures or in response to water turbulence	Gusev and Golubev (2001)
M. californianus	California mussel	Gene expression	Gills	Diurnal and circatidal	Not tested	- Circadian pattern for majority of rhythmically expressed genes - Some tidal transcripts	Connor and Gracey (2011)
		Clock gene expression		Diurnal	Not tested	- Rhythmic expression of *Cry1* and *ROR* but not *Tim* or *Bmal1*	
M. edulis	Blue mussel	Byssus thread production	Foot	Diurnal	Not tested	- More show higher activity at night than in the day	Martella (1974)
		Shell gape	Valves	Circadian under some conditions	Yes	- Weak circadian activity under LL and constant immersion, in unfed but not fed mussels - No evidence of circatidal rhythmicity	Ameyaw-Akumfi and Naylor (1987)
				Ultradian	Yes	- Ultradian (~90 min) shell closures under constant conditions with LL	Rodland et al. (2006)
		Gape angle, exhalent pumping and valve adduction rate	Valves and siphons	Diurnal	Not tested	- Greater activity at night under natural LD (including moonlight), constant temperature and constant immersion (experiment conducted in July)	Robson et al. (2010)
		Maximum gape angle and gaping frequency	Valves	Diurnal under some conditions	Not tested	- Diurnal rhythm with activity higher at night in the wild but not apparent under laboratory conditions	Wilson et al. (2005)

						(experiment conducted in March/April)	
M. galloprovincialis	Mediterranean mussel	Renewal of epithelial cells	Stomach; digestive gland	Circatidal	Yes	- Circatidal rhythm found in subtidal organisms	Zaldibar et al. (2004)
		Valve activity	Valves	Diurnal	Not tested	- Circadian pattern - Phase shift triggered by light	Gnyubkin (2010)
		Water propulsion rate	Whole organism	Circatidal	Yes	- Circatidal rhythm persists in lab under LD, LL and DD - Failed to be replicated by others (See references in Kim et al., 1999 and Robson et al. 2010)	Rao (1954)
Pinna nobilis	Fan mussel	Shall gaping	Valves	Circadian	Not tested	- Circadian periodicity in subtidal environment measured *in situ* - Seasonal patterns in gaping activity	Garcia-March et al. (2016)
R. philippinarum	Manila clam	Siphon extension (feeding)	Siphon	Circadian	Yes	- Circadian activity that persists under LL and DD	Houki et al. (2015)
		Oxygen consumption rate	Whole organism	Circadian and circatidal	Yes	- Initial circadian pattern gives way to more persistent circatidal periodicity under non-tidal conditions	Kim et al. (1999)
		Shell micro-growth increments	Shell	Circatidal	Yes	- Circatidal periodicity in subtidal environment	Poulain et al. (2011)
Saxidomus purpuratus	Washington clam	Oxygen consumption rate	Whole organism	Circatidal	Yes (tidal)	- Circadtidal periodicity for 7-9 days under constant immersion followed by a unimodal diurnal pattern	Kim et al. (2003)
Gastropods							
Aplysia californica	California sea slug	Optic nerve impulses	Optic nerve	Circadian	Yes	- Circadian rhythm persists in DD - Free-running rhythm in DD of LL treated samples	Jacklet (1969)

Bulla gouldiana	California bubble (sea snail)	Optic nerve impulses	Basal retinal neurons of the eye	Circadian	Yes	- Circadian rhythm that persists in DD	McMahon et al., 1984
		Gene expression		Diurnal	No	- Rhythmic *Per* expression under LD but not DD - Constitutive expression of *Per* in other tissue types	Constance et al. (2002)
Cellana radiata	Rayed wheel limpet	Oxygen consumption	Whole organism	Diurnal and circatidal	Not tested	- Diurnal and tidal rhythms with activity higher during high tide especially at night	Rao (1980)
Cellana rota	Limpet	Locomotion	Whole organism	Circadial and mixed circatidal/ circadian	Yes	- Circatidal or mixed circatidal/circadian rhythm *in situ* - Seasonal affects activity which is higher during the winter - Moon phase affects activity which is highest during the first quarter - Circatidal (~12.4h) rhythm in the lab under constant water spray and constant and varying light regimes	Schnytzer et al. (2018)
		Gene expression	Head	Circatidal	Not tested	- Tidally expressed transcripts - Clock genes were either non-rhythmic or weakly circadian but not significant	
Helcion pectunculus	Prickly limpet	Locomotor activity	Whole organism	Circadian and circatidal	Yes	- Both circadian and circatidal components under free-running conditions	Gray and Hodgson (1999)
Melibe leonina	Lion's mane sea slug	Locomotor activity	Whole organism	Circadian	Yes	- Circadian pattern persists in DD	Newcomb et al. (2014)
Nerita (Melanerita) atramentosa	Black nerite sea snail	Activity/ position representing feeding and respiration	Whole organism	Circadian and circatidal	Yes	- Circatidal rhythm persists for ~5 days in LL under constant submergence - Circadian activity persist up to 10 days in LL under constant submergence	Zann (1973)

Olivella semistriata	Sea snail	Locomotion	Whole organism	Circatidal	Yes	- Endogenous circatidal behaviour discriminating between incoming and outgoing tides	Vanagt et al. (2008)
Patella vulgata	Common limpet	Locomotion	Whole organism	Circatidal	Not tested	- Circatidal rhythm synchronised by time of emersion	Santina and Naylor (1994)
Cephalopods							
Eledone cirrhosa	Lesser/curled octopus	Locomotion	Whole organism	Diurnal	No	- Nocturnal activity under LD which did not persist under DD	Cobb et al. (1995)
E. scolopes	Hawaiian bobtail squid	Bioluminescence	Light organ	Diurnal	Not tested	- Daily cycles of luminescence levels produced by bacterial symbionts	Boettcher et al. (1996)
		Cryptochrome gene expression	Head, Light organ	Diurnal	Not tested	- Circadian *Cry1* and *Cry2* expression in head - Circadian *Cry1* expression in the light organ influenced by symbiont luminescence	Heath-Heckman et al. (2013)

*Abbreviations: LD, light/dark cycles; LL, light/light (constant light); DD, dark/dark (constant dark).

Along with a variety of other invertebrates, marine molluscs have also been observed to show biological rhythms under aspects of lunar influence, including circatidal rhythms (12.4 hr period) (Table 1.1) (Tessmar-Raible et al., 2011; Naylor, 2005). For example, circatidal rhythms of shell micro-growth increments are exhibited under non-tidal conditions by the Manila clam, *Ruditapes philippinarum*, (Poulain et al., 2011) and circatidal rhythms of locomotion are apparent in some intertidal marine gastropods (Vanagt et al., 2008; Santina and Naylor, 1994). The molecular mechanisms governing endogenous circatidal rhythms in marine organisms remain to be established.

In practice, multiple types of rhythm can occur in an organism, either influencing a single process where one rhythm may be considered a dominant contributory factory over the other, or simultaneously impacting different processes. In the case of the former, rhythmic oxygen consumption in the clam *R. philippinarum* is initially circadian but gives way to an endogenous circatidal pattern persisting for a number of weeks under subtidal conditions (Kim et al., 1999). In another example, peaks of locomotor activity in the limpet *Helcion pectunculus*, one corresponding to a circadian period and a second to a circatidal period, were evident under constant darkness and constant aerial exposure indicating the possible presence of two endogenous clock mechanisms (Gray and Hodgson, 1999). Finally, valve behaviour in the oyster *C. gigas* is influenced by a number of rhythmic environmental processes, resulting in circadian (Mat et al., 2012), circatidal (Tran et al., 2011) and circannual periodicities (Payton et al., 2017c). It has been proposed that, as different marine bivalves inhabit different geographical locations globally, tidal and solar intensities may vary over a species range to the extent that a background rhythm in one location could potentially be exhibited as dominant rhythm elsewhere (Tran et al., 2011; Place

et al., 2008).

Different rhythms operating in the same mollusc over different timescales include the tidally-synchronised renewal of epithelial cells in the stomach and digestive gland of the mussel *M. galloprovincialis* (Zaldibar et al., 2004), in addition to circadian valve activity that is phase shifted by light (Gnyubkin, 2010). As previously mentioned, the rhythmic transcriptome *M. californianus* gills comprises genes that are expressed in circadian and circatidal patterns respectively (Connor and Gracey, 2011). It is therefore apparent that different biological rhythms operating over different temporal scales may coexist within individuals but have varying relevance to specific tissues or processes. The regulation of daily and tidal rhythms have been hypothesised to be interconnected to varying degrees, though the extent to which they are linked remains to be established in order to gain a deeper understanding of the chronobiology of marine organisms (Tessmar-Raible et al., 2011; Naylor, 2010).

1.5.2 Seasonal rhythms and photoperiodism in molluscs

Evidence of photoperiodism in molluscs is less well known than in arthropods (Nelson et al., 2009) and mainly documents reproductive activities such as oviposition and growth in terrestrial gastropods (Numata and Udaka, 2010). For example, photoperiod influences seasonal variation in super-cooling ability in the terrestrial snail *Helix aspersa* in which shorter photoperiods induce lower temperatures of crystallisation (Ansart et al., 2001), and longer photoperiods resulted in higher rates of reproduction in the slug *Limax valentianus* (Hommay et al., 2001). Among aquatic molluscs, many of which are seasonal spawners (Maneiro et al., 2017; Osada et al., 2007; Rodríguez-Rúa et al., 2003; Duinker et al., 2000; Li et al., 2000; Seed, 1969),

photoperiod affects the rate of egg laying in the freshwater snail, *Lymnaea stagnalis* (Joosse, 1984) and short days, in conjunction with warmer temperatures, are correlated with an increase in egg-laying behaviour in the sea slug *Aplysia californi*a, which breeds in late summer/autumn (Wayne and Block, 1992).

Although photoperiod is the most reliable environmental indicator of season, in aquatic habitats temperature is a comparatively more reliable seasonal cue than in terrestrial habitats (as water temperature is less variable than air temperature) and therefore seems to be used more in conjunction with photoperiod as a cue by aquatic molluscs than by their terrestrial counterparts (Numata and Udaka, 2010). The duration the mussel *M. galloprovincialis* was under favourable conditions of food supply and temperature was a greater contributory factor to number of spawns than photoperiod, however the authors suggest that the mussels may not have had enough time to reach the stage of gonad maturity where a response is perhaps more likely to occur and suggest further study to clarify the effects of photoperiod (Domínguez et al., 2010). Work on great scallops (*Pecten maximus*) has shown that the rebuilding of the gonads after spawning occurred to a greater extent (larger gonad growth) in scallops kept at constant or increasing photoperiod conditions than in those exposed to a natural/decreasing photoperiod regime, which showed no significant changes (Duinker et al., 1999). The same significant effect was also seen in scallop gonad growth when increasing photoperiod and temperature were combined under conditions of excess food availability (Saout et al., 1999). Finally, the oyster *C. gigas* has been found to progressively change from being nocturnal during the autumn/winter to being diurnal in the spring/summer in both environmental and laboratory conditions, suggesting the presence of an endogenous circannual clock, although the mechanisms for this are currently unknown (Mat, et al., 2012). At present

there is not yet an encompassing explanation of the mechanism(s) by which reproductive development in aquatic molluscs is influenced by photoperiod (Domínguez et al., 2010; Numata and Udaka, 2010), and the relationship between regulation of their short-term biological rhythms and photoperiodic trends are also yet to be fully understood.

1.5.3 Clock genes in aquatic molluscs

To date, there has been little investigation into the molecular mechanisms underlying biological rhythm regulation of molluscs. As a result, there are relatively few instances where molluscan clock genes have been identified. However, homologs of the core clock genes including *Clk*, *Cry1/2*, *Cyc*, *Tim*, *Per*, *Dbt*, *ROR* and *Rev-erb* have been isolated from molluscs (Table 1.2) as have some clock-associated genes (Table 1.2 and phototransduction genes (Sun et al., 2016). Table 1.2 contains examples of the few sequenced molluscan clock genes, a number of which were isolated since research in this thesis was completed (Cook et al., 2018; Duback et al., 2018; Schnytzer et al., 2018; Bao et al., 2017; Perrigault and Tran, 2017).

These findings point to the existence of a regulatory molecular clock mechanism in the phylum, as is to be expected given the ubiquitous presence of this mechanism in all phyla investigated. These few sequences have provided the initial insights into how the molluscan molecular clock mechanism is hypothesised to be arranged. For example, PER from the sea snail *Bulla gouldiana* (GenBank accession number AF353619) has sequence similarities to *Drosophila* PER (AF033029.1) in the region attributed to TIM binding, and has more sequence homology with *Drosophila* PER than mouse PER, leading to the hypothesis that molluscs may exhibit *Drosophila*–type PER-TIM binding rather than mammalian-type PER-CRY binding

(Constance et al., 2002) (Figure 1.4). In terms of rhythmic clock gene expression in molluscs, *Per* expression is rhythmic but not endogenously so in *B. gouldiana* eyes (Constance et al., 2002) and *Cry1* and *ROR* are rhythmic in the gills of the California mussel, *M. californianus*, though it is yet to be investigated whether the rhythm persists under constant conditions (Connor and Gracey, 2011). More research is required to identify further putative clock genes from molluscs and to establish their interactions, rhythmic properties and functional importance. The molecular basis of non-circadian rhythms, such as tidal and seasonal rhythms, are also yet to be established.

Table 1.2 Nucleotide/amino acid sequences of mollusc clock and clock-associated genes

	Clock genes										**Clock-associated genes**				
	Clock	*Cry1*	*Cry2*	*Cyc/ARNTL/ Bmal1*	*Timeless*	*Period*	*ROR/HR3*	*Rev-erb (nr1d1)/E75*	*Dbt/ CK1ε*	*Shaggy/GSK3*	*Timeout*	*6-4 photolyase*	*ARNT*	*aaNAT*	**Reference/ GenBank Accession #**
Bivalves															
M. californianus	✓	✓		✓	✓		✓								Connor and Gracey (2011); Gracey et al. (2008)
M. galloprovincialis						*		✓						✓	EF644354.2 FL488956.1
Palcopecten magellanicus	✓	✓		✓	✓	✓			✓						Pairett and Serb (2013)
Patinopectan yessoensis	✓	✓		✓	✓	✓			✓					✓	Sun et al. (2016) XM_021523366
C. gigas	✓	✓	✓	✓	✓	✓	✓	✓	✓		✓	✓	✓		Perrigault and Tran (2017) Bao et al. (2017) EKC31717.1 KU127505.1 XP_011441580.1
Crassostrea angulata										✓					Zeng et al. (2013)
Pinctada fucata	✓			✓									✓		Bao et al. (2017)

Mizuhopecten yessoensis						✓								XM_021519834.1
Gastropods														
B. gouldiana						✓								Constance et al. (2002)
Lottia gigantea	✓	✓		✓			✓		✓		✓		✓	Bao et al. (2017) XP_009051269.1 ESO86573.1 XP_009046363.1 XP_009060168.1 XM_009063510
Haliotis discus hannai		✓												HM107828
Haliotis diversicolor													✓	KC256820.1
A. californica	✓	✓				✓			✓		✓			XP_005112430.1 XP_005089742.1 XP_005099695.1 XP_005111020 XP_005098675.1
Hermissenda crassicornis	✓	✓	✓		✓	✓					✓	✓		Cook et al. (2018)
Melibe leonina	✓	✓	✓	✓	✓	✓					✓	✓		Cook et al. (2018); Duback et al. (2018)
Tritonia diomedea	✓	✓	✓	✓	✓	✓					✓	✓		Cook et al. (2018)
Cellana rota		✓		✓	✓	✓								Schnytzer et al. (2018)
Patella vulgata	✓			✓									✓	Bao et al. (2017)
Biomphalaria glabrata	✓			✓									✓	Bao et al. (2017)
Cephalopods														
E. scolopes		✓	✓											Heath-Heckman et al. (2013)

*The putative *M. galloprovincialis* period sequence with accession number **BM66066**, is omitted due to low sequence homology lending support to this identification.

1.5.4 The melatonin synthesis pathway and molluscs

Though components of the melatonin synthesis pathway (Figure 1.8) are involved in circadian and photoperiodic timing in mammals (Zisapel, 2018; Dunlap et al., 2014; Morin, 1999) comparatively little is known about invertebrates. Circadian

photosensitivity is influenced by serotonin signalling in *Drosophila* (Yuan et al., 2005) and melatonin signalling is involved in circadian control of swimming behaviour in the marine annelid *Platynereis dumerilii* (Tosches et al., 2014). Aspects of the melatonin synthesis pathway have been linked to reproductive development in aquatic invertebrates. For example, melatonin has been detected in the gonads of cnidarians including a sea star *Echinaster brasiliensis* and a sea pansy *Renilla köllikeri*; in the former, melatonin in gonad tissues is produced rhythmically with a night time peak and thought to be regulated by aaNAT (Peres et al., 2014). In the latter, no daily pattern in melatonin level was detected which was in keeping with the absence of detected circadian rhythms in the species, however a seasonal pattern was discovered where the timing of melatonin level increase and gonad maturation were correlated suggesting a potential for the provision of seasonal information (Mechawar and Anctil, 1997).

In molluscs serotonin, melatonin, and HIOMT have been detected using radioimmunoassay (RIA) and high-performance liquid chromatography (HPLC) techniques; serotonin acts as both a neurohormone and neurotransmitter in molluscs and has a large variety of different functions including involvement of developmental events such as the induction of larval metamorphosis (Couper and Leise, 1996), induction of oocyte maturation (Tanabe et al., 2006), triggering of spawning (Ram et al., 1993) and regulation of aspects of male copulatory behaviour (De Lange et al., 1998). Both melatonin and HIOMT have been found in neural and ocular tissues of the gastropod *Helix aspersa maxima,* although reasonably little variation was able to be detected, just a small peak at the end of the dark period in the cerebroid ganglions (Blanc et al., 2003). The same study failed to detect aaNAT although the authors attribute this to the likely presence of low levels beyond the detection limits of the

assay used (Blanc et al., 2003). Melatonin levels in the cephalopod mollusc *Octopus vulgaris* showed rhythmic fluctuations in the optic lobe, retina and hemolymph, which peaked during darkness with retinal serotonin levels showing the opposite pattern (Muñoz et al., 2011). Diurnal oscillation in melatonin content in the cerebral ganglia of the sea slug *A. californica* similarly peaked at night although, conversely, in the eyes peak levels were actually detected in the daytime, opposite to the pattern in most vertebrates (Abran et al., 1994).

As these existing molluscan studies focus on the detection of chemicals in tissues, there is a lack of work investigating variation in the expression of the genes encoding the enzymes that catalyse the process. Based on sequence similarities to other species, the gene *aaNAT* appears to have been sequenced from the bivalve *M. galloprovincialis* (GenBank accession FL488956.1), however any daily and seasonal variations in the expression of this gene, and their significance to physiological processes, are yet to be investigated in molluscs.

1.6 THE BLUE MUSSEL *M. EDULIS*

1.6.1 Description, habitat and distribution

The blue mussel *M. edulis*, also sometimes known as the common mussel, is a filter-feeding marine bivalve belonging to the family Mytilidae. With two equally-sized asymmetric valves, blue mussels are roughly triangular in shape and are sessile as adults, anchoring themselves to the substrate by depositing proteinaceous byssus threads from glands in their muscular foot (Gosling, 2015). They predominantly inhabit the intertidal zone, but also occur at subtidal level, and are a gregarious species forming patches which can progress into dense mussel beds (Suchanek, 1978; Bayne, 1976). As a biogenic reef-building organism, *M. edulis* plays a crucial role in

transforming habitats dominated by sediment into reefs with a higher level of biodiversity, to the extent that loss or removal of mussels from reefs can detrimentally impact upon the biota of such habitats (Gutiérrez et al., 2003). Reefs, biogenic and geogenic (non-biogenic substrata) in origin, are listed under Annex I of the EU Habitat Directive (Joint Nature Conservation Committee (JNCC), 2016a) and blue mussel beds on sediment are also currently a UK Biodiversity Action Plan (UKBAP) priority habitat, identified as requiring conservation action (JNCC, 2016b). Relatively tolerant to a wide range of temperatures and salinities (Bayne, 1976), the species has a widespread global distribution and is found along the coastlines of North America, Asia, North Africa and Europe, including being common along UK shores (Seed, 1976).

1.6.2 Life cycle and gametogenesis

Blue mussels are considered gonochoristic (distinct sexes), despite the occasional occurrence of hermaphrodites and recently discovered sex inversion in environmentally stressed post-spawned females (Chelyadina et al., 2018). There are no external morphological characteristics to distinguish the sexes (Seed, 1976). Reproductive maturity occurs at 1 to 2 years old; adults experience seasonal reproductive development where resting/spent mussels lacking sexual structures undergo gametogenesis. Gametes develop in follicles in the mantle tissue, increasing in quantity, size and maturity (Seed, 1969). The reproductive status of an individual may be broadly classified as developing, mature, spawning or resting/spent, although more detailed arbitrary schemes of classification have been described (Seed, 1969). The timing of gametogenesis and spawning varies with location and is influenced by microhabitat (summarised by Seed, 1976), but in the UK gametogenesis commences

in the winter, generally progressing until early spring when maturity/ripeness is attained which is followed by spawning (Seed, 1969). A brief redevelopment period followed by a second spawning event can occur if local conditions are favourable, and the resting phase generally coincides with the end of the summer (Seed, 1969). Spawning occurs directly into the water column, with seawater inducing spermatozoa motility as well as the maturation of oocytes (Chipperfield, 1953). External fertilisation results in embryos which develop into larvae and then progress through the following stages of development: trochophore (ciliated embryo), young veliger (functional gut and begins to secrete prodissoconch shell I), straight-hinge veliger (fully formed prodissoconch shell I), veliconcha (secretes prodissoconch II shell), eyed-veliger (develops a pair of eyespots), and pediveliger (develops a foot), which is followed by metamorphosis (including organ reorganisation, dissoconch shell development and secretion of byssus threads) resulting in the post-larval plantigrade stage (Bayne, 1976; Bayne, 1964b). Proposed to be an adaptive strategy to avoid competition and inhalation by adults, juveniles (plantigrades) then generally undergo two settlement stages, initially on filamentous algae and subsequently, following further development, on a solid substrate such as a mussel bed (Bayne, 1964a). The major stages in the life cycle of a blue mussel are summarised in Figure 1.10.

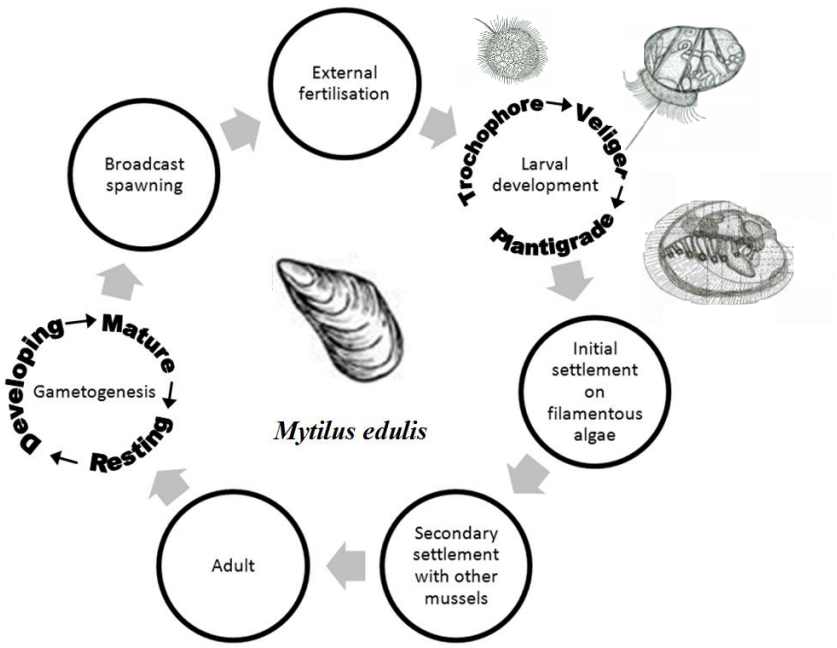

Figure 1.10 Summary of the major stages in the life cycle of the blue mussel *M. edulis*. Diagrams of larval stages are from Field (1922).

1.6.3 Light perception

The larvae of *M. edulis* develop a pair of photosensitive eyespots that are retained as cephalic eyes into adulthood (Morton, 2001). Located on the gill filaments between the outer and inner gills (Northrop, 2000) these simple cup-shaped structures are open to seawater and lack a lens, cornea and pinhole aperture making them incapable of forming images (Rosen, 1977). However, in the valve adjacent to each eye is a small translucent area of shell referred to as a "Shell window" through which light may penetrate (Rosen, 1977). The eye has been described as an "off" visual system as optic nerve activity spikes occur only in response to darkness, their activity pattern dependent on the characteristics of the preceding light period (Northrop, 2000). Valve closure observed in response to dimmed light in both individuals with functioning and non-functioning eyes indicates the presence of other photoreceptor cells (Northrop, 2000). Indeed, *M. edulis* larvae show positive or negative phototaxis at different developmental stages, including prior to eyespot development (Bayne,

1964b). Conflicting findings, where blind and sighted mussels respond to changes in light (Northrop, 2000) and sighted mussels show no light sensitivity (Rosen, 1977), have both led to authors hypothesising that the adult eyes may be used to sense photoperiod. Though circadian pacemakers have been revealed in the more complex eyes of gastropods (Block et al., 1993; Jacklet, 1969), the function of the simpler cephalic eyes such as those found in *Mytilus* are unclear.

1.6.4 Temperature perception

In the oyster *C. gigas* and the soft-shell clam *Mya arenaria*, the relationship between heart rate and the temperature in both the mantle and pericardial cavities, led to the proposal that these bivalves may possess thermoreceptors in the mantle tissue to detect temperature change, in addition to experiencing the effects directly (Lowe, 1974). It is unclear whether this is the case for *Mytilus*, however specialised thermosensors are not essential for temperature entrainment, as exemplified by *Drosophila* in which the process is tissue-autonomous; temperature synchronisation of *Per* expression can occur in a variety of isolated tissues and in individuals lacking functional antennae (Glaser and Stanewsky, 2005).

1.6.5 Mechanoreception

Mechanoreception involves sensing and responding to touch, sound or vibration. Many bivalves have statocycts which are fluid-filled sacs, surrounded by ciliated sensory cells, which contain single (statolith) or multiple (statoconia) denser granules allowing the structure to act as a gravity receptor and assist with orientation (Cragg and Nott, 1977). Mussels of the genus *Mytilus* develop a pair of statocycts as pediveliger larvae that are attached to the pedal ganglia (Bayne, 1971) and contain a

single statolith (Cragg and Nott, 1977). In addition to this internal sensory system, *Mytilus* spp. also possess superficial mechanoreceptors such as those located in the anterior byssus retractor muscle (LaCourse and Northrop, 1978) and the gill cilia (Murakami and Machemer, 1982). They also have a pair of well-developed abdominal sense organs (ASO) located outside the gill axes on the posterior adductor muscle that detect water current (Haszprunar, 1985; Haszprunar, 1983) and potentially water-borne vibrations (Zhadan, 2005). Indeed, *M. edulis* are known exhibit behavioural changes in valve movements in response to vibration stimulus (Roberts et al., 2015). Finally, *M. edulis* also have osphradia, sensory receptors located near the visceral ganglion (Haszprunar, 1987). Historically thought to be mechanoreceptors, bivalve osphradia are now generally considered to be chemoreceptors involved in detecting chemical spawning cues and synchronisation of gamete release by the secretion of the spawning stimulant serotonin (Beninger et al., 1995; Haszprunar, 1987).

1.6.6 Relevance of *M. edulis* chronobiology

As a species that inhabits the intertidal zone, *M. edulis* is under the influence of multiple environmental factors, such as alternating periods of tidal immersion and emersion, daily light/dark cycles, as well as bi-monthly/monthly lunar cycles (Figure 1.9). At higher latitudes, seasonal long day/short day (photoperiod) variations are also relevant. Though biological rhythms are present in bivalves (Table 1.1) and examples of clock genes isolated from the class are emerging (Table 1.2), there is still little known about how mussels, and indeed all bivalves, synchronise their biological rhythms with environmental cycles via molecular clockwork mechanisms.

The chronobiology of *M. edulis* is a poorly understood aspect of the ecology of this species which also has commercial relevance as a harvested edible species

(Smaal, 2002); approximately 182,000 tonnes of blue mussels were harvested worldwide in 2016 worth an estimated US $280 million (FAO, 2016). The two major challenges faced by mussel aquaculturists are a reliance on the supply of wild mussel spat, which is seasonal and linked to environmental conditions, and the reduced economic value of spawning and post-spawned mussels due to their lower meat content (Domínguez et al., 2010). Blue mussels are also frequently-used bioindicators of water quality; their sensitivity to absorption of various anthropogenically-derived organic and inorganic pollutants, combined with a constrained metabolising ability and hardiness to different chemically detrimental conditions, results in concentrated contaminants in their tissues (Rittschof and McClellan-Green, 2005; O'Connor, 2002). For instance, the ongoing NOAA National Status and Trends 'Mussel Watch' program has monitored trace chemical contaminant levels in mussels since 1986 to gain insights into spatial and temporal contamination trends (Farrington et al., 2016; O'Connor, 2002). Recent research also highlights the requirement for studies examining the natural seasonal changes undergone by bio-monitoring species in order to avoid falsely attributing results to pollutants; a number of genes commonly used as biomarkers of pollution-stress in *M. galloprovincialis* have now been shown to exhibit seasonal variation in expression levels in unpolluted waters (Jarque et al., 2014). Similarly, temporal expression patterns of other genes have also been recorded in *Mytilus* (Banni et al., 2011; Connor and Gracey, 2011). Insights into the chronobiology of *M. edulis* are therefore highly relevant to multiple applications.

In addition to being an ecologically, toxicologically and economically relevant species with seasonal gametogenesis cycles, the sedentary lifestyle, widespread distribution, abundance, and ease of sampling of *M. edulis* makes it an ideal study organism for investigating bivalve biological rhythm regulation on a molecular level

and the influence of biotic and abiotic factors on this process. A wider understanding of the chronobiology of this species is relevant to researchers investigating the effects of both natural and anthropogenic environmental change on keystone marine species and intertidal zone inhabitants.

1.7 THESIS AIMS AND OBJECTIVES

This research investigates the little-known molecular mechanisms involved in regulating marine bivalve biological rhythms. The aim of this thesis was to identify components of the molecular clock mechanism in the blue mussel *M. edulis* and to investigate whether clock genes were expressed in rhythmic patterns over different timescales (24 hr and seasonal). The responses of clock mRNA expression patterns to environmental cues including light and temperature were investigated as entrainment of clocks by zeitgebers is essential in maintaining synchrony between endogenous and external cycles (Mohawk et al., 2012; Dubruille and Emery, 2008; Rensing and Ruoff, 2002). Of particular interest herein is the potential involvement of clock genes in provisioning environmental information used to time the seasonal reproductive development of *M. edulis* (Figure 1.11). It was hypothesised that a molecular clock mechanism exists in *M. edulis* and that the expression patterns of the genes involved would be influenced by changes in environmental light and temperature regimes.

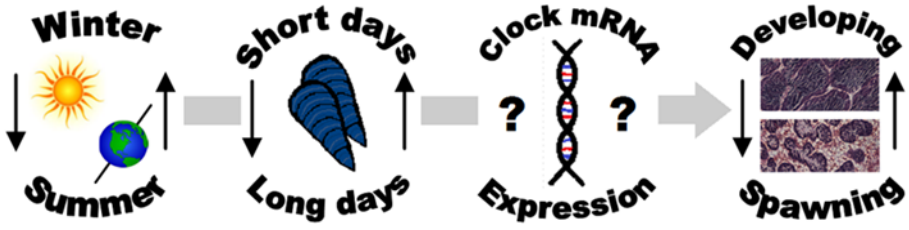

Figure 1.11 Summary of the hypothesised link between environmental cues e.g. photoperiod, the molecular clock mechanism, and rhythmic outputs e.g. seasonal gametogenesis.

Using a targeted approach, the genes *Clk*, *Cry1*, *ROR/HR3*, *Per*, *Rev-erb*, *Timeout*-like, *ARNT* and *aaNAT* were selected for isolation and were quantified in *M. edulis* based on their key functions in the molecular clock of other species (Tomioka et al., 2012; Jetten, 2009; Kewley et al., 2004; Allada et al., 2001; Foulkes et al., 1997). The effect of season on the mRNA expression of these clock-associated genes was investigated during an experiment in which differences between winter and summer were examined in both sexes. To complement this work, a laboratory-based exposure experiment was conducted to investigate the response of diurnal expression patterns to modulated light and temperature regimes to ascertain endogenous circadian expression and to identify potential zeitgebers. In addition, a non-targeted global approach was also applied to identify the molecular-level responses of wild *M. edulis* to natural seasonal differences to reveal other candidate genes with a potential role in the provisioning of environmental information. All field and laboratory experiments were conducted on wild-caught adult *M. edulis* from the UK and gonadal tissue sections were prepared to identify the sex and gametogenesis stage of all individuals.

To achieve the proposed aims, the following hypotheses and research objectives were identified:

1. Isolate and characterise key clock genes in *M. edulis* using molecular biology techniques including RNA extraction, cDNA synthesis, PCR, agarose gel electrophoresis and sequencing (Chapters 2 and 4). It was hypothesised that *M. edulis* contain homologs of clock genes known to be involved in the molecular-level regulation of timekeeping in other organisms.
2. Quantify mRNA expression levels of the identified clock genes and assess how they vary between seasons (winter and summer) in a wild population using optimised qPCR assays to quantify relative expression differences (Chapters 3

and 4). Differences in photoperiod can be used as an environmental cue of season by influencing the light-entrainable molecular clock mechanism. It was hypothesised that *M. edulis* clock gene expression will vary between seasons at equivalent time-points during the day.

3. Isolate *M. edulis* clock proteins using Western blotting, which allows the identification of specific clock proteins based on antibody binding (Chapter 4). It was hypothesised that *M. edulis* possess clock proteins.
4. Investigate the rhythmic and endogenous nature of *M. edulis* clock gene activity by examining mRNA expression responses to modulated light cycles (light/dark, LD; and constant darkness, DD) and temperature cycles (warm/cold under constant darkness, TCDD) in a laboratory-based exposure experiment (Chapter 5). It was hypothesised that diurnal clock gene expression occurs in *M. edulis* under LD conditions and persists under DD, indicative of endogenous regulation. It was also hypothesised that temperature cycles can modulate clock gene expression patterns.
5. Identify further genes potentially involved in seasonal response using a global molecular-level approach (Suppression Subtractive Hybridisation) to detect mRNA transcripts that show seasonal differences in expression levels (Chapter 6). It was hypothesised that seasonally-expressed transcripts can provide molecular-level information on environmental cycles.

Chapter 2

Isolation and characterisation of circadian rhythm-related genes from the blue mussel *M. edulis*

2.1 INTRODUCTION

Circadian rhythms are cyclical biological processes operating over a ~24 hr period. Though they are synchronised by external environmental cycles, they are regulated endogenously on a molecular-level by clock genes that form negative feedback interactions with the proteins they encode (Young, 2000; Hardin, 2005). These gene-protein interactions oscillate in a regular manner forming a network referred to as the molecular clock mechanism that is considered ubiquitous across virtually all phyla, though the constituent clock genes vary between organisms (Allada et al, 2001).

Transcription factors, which activate or repress transcription of other genes, are integral to both vertebrate and invertebrate molecular clock interactions, and include the basic helix-loop-helix PAS (bHLH-PAS) transcription factors CLK, BMAL1 and PER (Tomioka and Matsumoto, 2015; Kewley et al., 2004; Shirasu et al., 2003). The core interactions of the clock mechanism are formed by CLOCK, which heterodimerises with the protein encoded by *Cyc* in *Drosophila* (Darlington et al., 1998) and *Bmal1/ARNTL* in mammals (Gekakis et al., 1998). PER subsequently forms a protein complex with TIM in *Drosophila* and with CRY1 in mammals to form the first negative feedback loop (Figure 1.4). Though *Cry1* exists in *Drosophila*, it

encodes a blue light-sensitive flavoprotein that facilitates the light-induced degradation of TIM (Peschel et al., 2009). The second loop generally comprises RAR-related orphan receptors (*ROR*) and *RevErb* in mammals (Jetten, 2009). Vertebrate ROR, of which there are three forms (α, β and γ), are nuclear hormone receptors which influence *Bmal1* transcription along with members of the REV-ERB family which act antagonistically as transcriptional repressors (Guillaumond et al., 2005). Similar negative feedback loop functions are performed by *Pdp1ε* and *Vri* in *Drosophila* which repress and activate *Clk* transcription respectively. (Tomioka et al., 2012) (Figure 1.4).

The majority of invertebrate chronobiology to date focuses on terrestrial arthropods. Although molluscs are a large phylum, containing a number of commercially important bivalve species such as scallops, oysters, mussels and clams (Gosling, 2015), the molecular regulatory mechanisms comprising the molluscan circadian pacemaker remain largely undiscovered. There are few cases of clock genes having been isolated or characterised from molluscs including bivalves (Table 1.2). When the current chapter was compiled, the few known examples of bivalve clock genes included homologs of the six *Drosophila* core clock genes *clock (Clk), cryptochrome (Cry1), cycle (Cyc/Bmal1/ARNTL), timeless (Tim), period (Per) and doubletime (Dbt)*, which were isolated from the eye of the Atlantic sea scallop *Placopecten magellanicus* (Pairett and Serb, 2013) and were discovered in the sequenced genome of the Pacific oyster *C. gigas* (Zhang et al., 2012). *Clk*, *Cry1*, *Bmal1* and a *RAR-related orphan receptor beta* (*RORβ)* homolog were also isolated from the gill tissue of the California mussel *M. californianus* (Connor and Gracey, 2011). The clock-associated gene *arylalkylamine N-acetyltransferase* (*aaNAT*), had been isolated from the mussel *M. galloprovincialis* (GenBank accession FL488956.1).

Vertebrate-type *aaNAT* (*VT-aaNAT*) encodes a light-sensitive enzyme which catalyses a stage of the vertebrate melatonin synthesis pathway (Foulkes et al., 1997) and non-vertebrate type *aaNAT* (*NV-aaNAT*) is a CCG in insects, linking photoperiod to endocrine response via the clock mechanism (Mohamed et al., 2014). The few cases where clock proteins have been isolated from molluscs include PER from *B. gouldiana* (Constance et al., 2002) and CRY1 from *E. scolopes* (Heath-Heckman et al., 2013). However, mollusc antibodies are not commercially available for this purpose, so testing antibodies from model species for cross-species reactivity can be a cost-effective alternative to developing specific antibodies, which has been previously been applied to mollusc clock protein detection (Constance et al., 2002).

The blue mussel *M. edulis*, a commercially and ecologically important species of bivalve (FAO, 2018; Gutiérrez et al., 2003) under the influence of multiple environmental cycles (Tessmar-Raible et al., 2011), is an ideal candidate organism for the investigation of circadian rhythm-related genes in an intertidal bivalve. Mussels undergo seasonal reproductive cycles so their aquaculture is challenged by seasonal variations in mussel value and spat supply (Domínguez et al., 2010). However, the mechanism(s) regulating *M. edulis* biological timekeeping, including links to their seasonal cycles of sexual development, are presently unknown. The aims of this chapter are to establish whether clock genes exist in *M. edulis* by isolating putative clock gene sequences from the species. Candidate genes selected for isolation were chosen based on their relevance to circadian function in other species and were as follows: *Clk*, *Cry1*, Aryl Hydrocarbon Receptor Nuclear Translocator (*ARNT*), the *Tim* homolog *Timeout*-like, *ROR/HR3*, and *aaNAT*. The secondary aim is to investigate cross-species reactivity of commercially available mammalian antibodies as a means of identifying *M. edulis* clock proteins.

2.2 MATERIALS AND METHODS

2.2.1 Sampling

Adult blue mussels were collected from a single wild population at low tide from Brighton Beach, East Sussex, UK (50°49′ longitude and 0°8′ latitude) between March and September 2005 (*n*=50). Approximately 1.0 cm^2 of mantle tissue was dissected from each individual and immersed in 0.5 mL RNA*later* solution (Qiagen Ltd., Manchester, UK) to preserve the sample integrity for RNA extraction. Samples were stored at -20 ˚C.

2.2.2 Total RNA isolation

Prior to commencing, work surfaces and equipment were treated with RNase Away (Molecular Bioproducts, UK) to protect the samples from DNA and Ribonuclease (RNase) contamination. The reagents and protocol from the High Pure RNA Tissue Kit (Roche, Burgess Hill, UK) were used; RNA, liberated via sample homogenisation, was bound to glass fibres in a column, treated for residual genomic DNA, and washed to remove impurities before elution.

Intact total RNA was isolated from *M. edulis* mantle samples by homogenising ~20 mg of tissue in 400 µL Lysis/Binding Buffer (4.5 M guanidine-HCl, 100 mM sodium phosphate pH 6.6) using a rotor stator homogeniser (IKA, Staufen, Germany). Centrifugation for 2 min at 13,000 x *g* formed a pellet of insoluble cell debris. The supernatant was mixed with 200 µL absolute ethanol in a sterile tube (Fisher Scientific, UK) then transferred into a High Pure Filter Tube. Samples were centrifuged at 13,000 x *g* for 30 sec and the flow-through was discarded. 10 µL DNase I Working Solution (0.18 kU) combined with 90 µL DNase Incubation Buffer (1 M NaCl, 20 mM Tris-HCl, 10 mM $MnCl_2$, pH 7.0) was added to the glass fleece of each Filter Tube and

incubated for 15 min at room temperature to digest residual genomic DNA. To remove cellular impurities, 500 µL Wash Buffer I (5 M guanidine-HCl, 20 mM Tris-HCl, pH 6.6) was added followed by 15 sec centrifugation at 8,000 x *g*. This step was repeated with Wash Buffer II (20 mM NaCl, 2 mM Tris-HCl, pH 7.5). Finally 300 µL Wash Buffer II was added followed by centrifugation at 13,000 x *g* for 2 min. 100 µL of Elution Buffer (sterile nuclease-free double distilled water) was incubated with the sample for 1 min at room temperature before the RNA was eluted for 1 min at 8,000 x *g*. RNA was subsequently stored at -20 ˚C or -80 ˚C.

2.2.3 RNA quantification

RNA was quantified using a Qubit 1.0 Fluorometer (Life Technologies, Paisley, UK) which measures relative fluorescence of sample assays using a curve-fitting algorithm calibrated by standard assays to calculate sample RNA concentration. The Qubit RNA BR Assay Kit, with an assay range of 20 ng/mL to 1000 ng/mL, was used with thin-walled polypropylene Qubit Assay Tubes (Life Technologies, UK). A working solution was created containing 200 µL Qubit RNA Buffer and 1 µL Qubit RNA Reagent (200X concentrate in DMSO) per assay. Two standard solutions were prepared to calibrate the instrument by combining 190 µL of the working solution with 10 µL of either Qubit RNA Standard #1 (0 ng/µL in TE buffer) or #2 (10 ng/µL in TE Buffer) respectively. For sample assays, 199 µL of working solution was mixed with 1 µL RNA. Assays were incubated at room temperature for 2 min and the instrument was calibrated with the two standard assays before sample readings were taken.

2.2.4 Denaturing formaldehyde-agarose (FA) RNA gel

RNA samples were run on a formaldehyde-agarose gel to confirm RNA

integrity. The denaturing conditions of the gel prevent secondary and tertiary RNA structures forming which can inhibit separation during electrophoresis. The gel was prepared as follows: 10 mL of 10X concentrated FA gel buffer (containing 200 mM MOPS, 50 mM sodium acetate anhydrous and 10 mM EDTA in RNase-free water, adjusted to pH 7 using NaOH) (all reagents supplied by Fisher Scientific, UK), 1.2 g agarose (Fisher Scientific, UK) and RNase-free water (Fisher Scientific, UK) to a total volume of 100 mL. After heating in the microwave to dissolve the agarose, the gel was cooled to approximately 65 ˚C before the addition of 1.8 mL 37% (12.3 M) formaldehyde (Fisher Scientific, UK) and ethidium bromide (Invitrogen, UK) was added to a final concentration of 0.15 ug/mL. The gel was poured into a gel tray and left to set at room temperature. A 1X concentration FA gel running buffer was made by mixing 100 mL 10X FA gel buffer, 20 mL 37% (12.3 M) formaldehyde (Fisher Scientific, UK), and 880 mL RNase-free water (Fisher Scientific, UK). Once set, the gel was left to equilibrate in the 1X FA gel running buffer for a minimum of 30 min. A 5X RNA loading buffer was made by combining 16 µL of saturated bromophenol blue solution (Fisher Scientific, UK) with 80 µL EDTA (Fisher Scientific, UK), 720 µL 37 % (12.3 M) formaldehyde (Fisher Scientific, UK), 2 mL glycerol (Fisher Scientific, UK), 3.084 mL formamide (Fisher Scientific, UK), 4 mL 10X RNA FA gel buffer and RNase-free water (Fisher Scientific, UK) to complete the volume to 10 mL. Before loading samples on the gel, 3 µL of 5X RNA loading buffer was mixed with 5 µL RNA sample and heated for 3 min at 65 ˚C, and then chilled on ice. 6.5 µL of 1 Kb Full Scale DNA ladder (Fisher Scientific, UK) was loaded alongside the samples. Samples were then separated by electrophoresis for at least 40 min at 90 v and viewed using a UV transilluminator (Gel Doc™ EZ System, BioRad, UK).

2.2.5 cDNA synthesis and Ribonuclease H Treatment

Complementary DNA (cDNA) was synthesised from RNA using the SuperScript® VILO™ cDNA Synthesis Kit (Life Technologies, UK), as cDNA is comparatively less susceptible to degradation. The following reagents were used: 14 µL RNA (~150 ng minimum), 2 µL 10X SuperScript® Enzyme Mix (SuperScript® III Reverse Transcriptase, RNaseOUT™ Recombinant Ribonuclease Inhibitor, and a proprietary helper protein) and 4 µL 5X VILO™ Reaction Mix (buffer containing random primers, $MgCl_2$ and dNTPs; exact concentrations not provided by manufacturer). Samples were gently mixed and heated in a thermal cycler as follows: 25 ˚C for 10 min, 42 ˚C for 60 min and 85 ˚C for 5 min before cooling to 4 ˚C. To digest any remaining RNA in RNA-DNA hybrid structures, 1 µL Ribonuclease H (RNase H) (5 U/µL in 25 mM HEPES-KOH pH 8.0, 50 mM KCl, 1 mM EDTA, 0.1 mg/mL BSA and 50% v/v glycerol) (Thermo Fisher Scientific, Loughborough, UK) and 2 µL of accompanying 10X Reaction Buffer (200 mM Tris-HCl pH 7.8, 400mM KCl, 80 mM $MgCl_2$, 10 mM DTT) were added followed by incubation at 37 ˚C for 45 min. cDNA was stored at -20 ˚C.

2.2.6 Species Identification

The *M. edulis* complex consists of three mussel taxa (*M. edulis*, *M. galloprovincialis* and *M. trossulus*) which are difficult to distinguish based on morphology and can form hybrids. PCR was therefore used to amplify the non-repetitive region of *Mytilus foot protein-1* (*mfp-1*) to confirm species identity as *M. edulis* (Inoue et al., 1995). The “Me15” and “Me16” primers used were designed by Inoue et al. (1995) and the thermal cycling conditions were optimised by Bignell et al. (2008). PCR products were separated by electrophoresis on a 4% TBE agarose gel

stained with GelRed™ Nucleic Acid Gel Stain (10,000X in water) (Biotium, Cambridge Bioscience, UK) and band sizes were assessed by comparison with O'RangeRuler 20 bp DNA Ladder (0.1 µg/µL) (Thermo Fisher Scientific, UK).

2.2.7 PCR Primer design and selection

Specific primer sequences designed for the amplification of *Clk* from *M. californianus* were kindly provided by Dr Andrew Gracey, University of Southern California, as were nucleotide sequences for *M. californianus Clk*, *Cry1*, *Bmal1* and *RORβ* (Personal communication, 2013) from which new primers were designed for testing and optimisation on *M. edulis* (Table 2.1.). Primers for *aaNAT* were designed based on a sequence from the Mediterranean mussel *M. galloprovincialis* (GenBank accession FL488956.1). Primers were designed using the Primer-BLAST tool (http://www.ncbi.nlm.nih.gov/tools/primer-blast/) and self-complementarity was checked using Oligo Calc (www.basic.northwestern.edu/biotools/OligoCalc.html) to ensure low likelihood of primer self-annealing and secondary structure formation. Where *Mytilus* sequence data was unavailable, other sequences of the desired gene were located on the GenBank database on the National Center for Biotechnology Information (NCBI) website (http://www.ncbi.nlm.nih.gov/). Sequence alignments were created using the NCBI Basic Local Alignment Search Tool (BLAST) or the ClustalW2 sequence alignment tool (http://www.ebi.ac.uk/Tools/msa/clustalw2/). The following *M. edulis* 18S rRNA positive control primers were used: forward 5'-GTGCTCTTGACTGAGTGTCTCG-3' and reverse 5'-CGAGGTCCTATTCCATTATTCC-3' (Ciocan et al., 2011). Primers were from Eurofins Genomics (Ebersberg, Germany) or Integrated DNA Technologies (IDT) (Leuven, Belgium) and were diluted to 200 pmol/µL or 100 pmol/µL in molecular-

grade water (Fisher Scientific, UK).

Table 2.1 PCR primers used for the amplification and sequencing of *M. edulis* genes.

Target Gene	Primer	Sequence 5'-3'	Tm (˚C)	% GC	Amplicon Size (bp)
Clk	*Clock*_3F	TATGCATCAGAAAGTATTAC	49.1	30.0	452
	*Clock*_ Right	GGTGATGCCCTATGGTCAAG*	59.4	55.0	
	*Clock*_New_6R	TCGGGTTTAGAGTTCCACTG	54.1	50.0	666
Cry1	*Cry1*_3F	GGTTGTCTGTCTGTCAGGAGG	61.8	57.1	443
	*Cry1*_5R	AATGCTGAACTGGACACCCA	57.3	50.0	
	*Cry1*_8F	TGGACCCTGTAGCAGTATGGAAA	57.7	47.8	801
	*Cry1*_8R	AGCAGGCTACAGCATGTCTAC	56.8	52.4	
	*Cry1*_14F	GATGGCRAAGTWGCMGGAAC	56.6	55.0	1684
	*Cry1*_12R	GAGATTTTCTATTCCAGGACAGAG	52.7	41.7	
ARNT	*Bmal1*_1F	CGACCAGAGGGTAACAGCTT	59.4	55.0	578
	*Bmal1*_3R	CCGAAGCAGATTGTGGCATT	57.3	50.0	
Tim	*Tim*_New_1F	TTCCGAGAACAGARCCCWGA	56.8	52.5	475
	*Tim*_New_1R	CTCATKGCCCACAGGTAGT	55.6	55.3	
	*Tim*_New_F2	CAAAGAACCAGACTGCTTGGA	55.2	47.6	898
	*Tim*_RACE_R1	CCTCCTGTCCTTTAATTGGTTGTGC	58.2	48.0	
ROR/ HR3	*ROR*_3F	GCTGCATCACAGATCTCCCC	61.4	60.0	569
	*ROR*_5R	GGTGATACCATGCCTGTCGG	61.4	60.0	
	*ROR*_8F	GCTTGATTATTTAGGTCGATCTGG	53.5	41.7	513
	*ROR*_8R	CCCTGACTGCTGATGGGATA	56.2	55.0	
	*ROR*_9F	GATCTTGGAGAAGTAAACTGAC	50.7	40.9	1053
	*ROR*_12R	AGTTCTTTCTGWARKGCAGGG	54.8	47.6	
aaNAT	*aaNAT*_F3	CGTTTGAAGCTGACAGCACAC	57.0	52.0	624
	*aaNAT*_R4	CAATGCATGCAAGTATGGGCA	56.5	47.6	

*sequence provided by Dr Andrew Gracey, University of Southern California (Personal communication, 2012). Amplicon sizes predicted from sequence lengths in other species. Underlined degenerate nucleotides as follows: R, G or A; W, A or T; K, G or T.

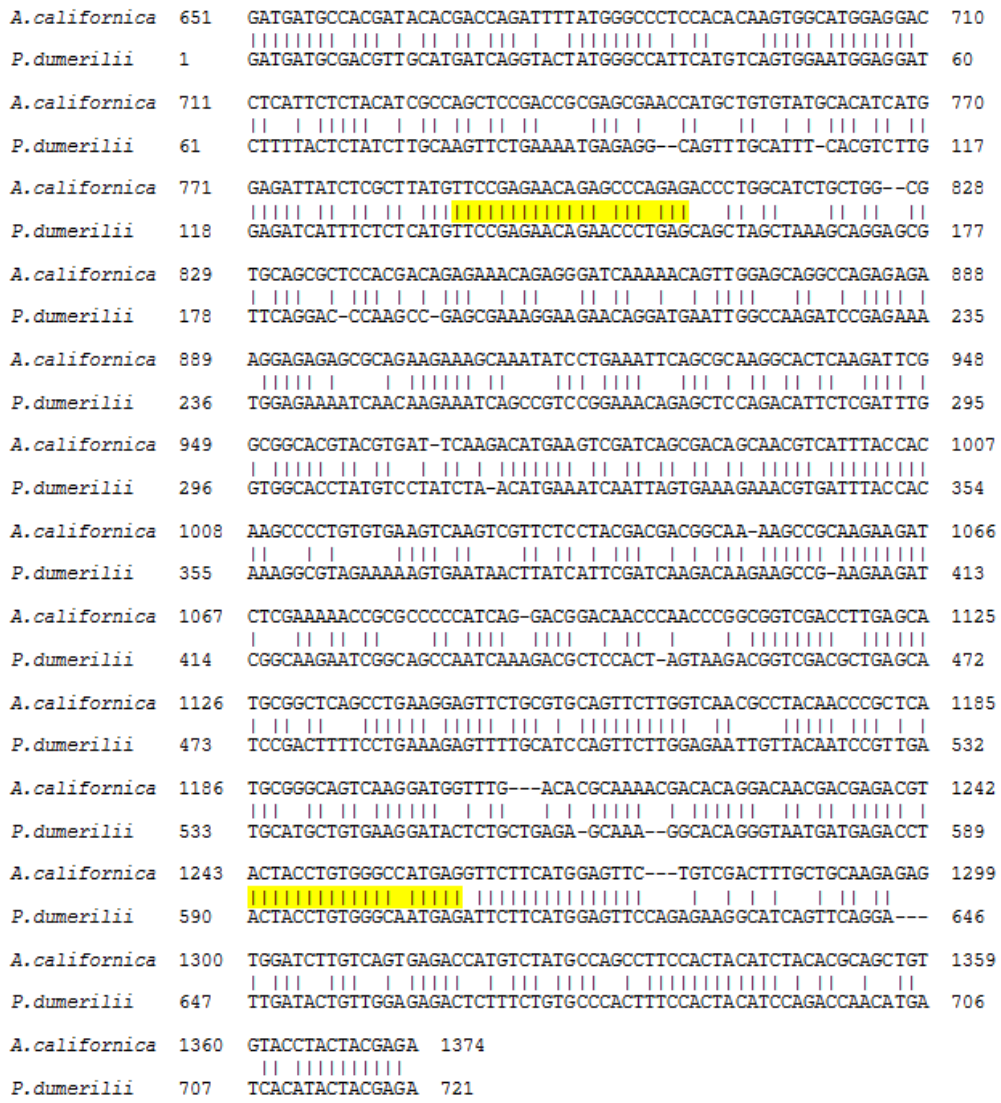

Figure 2.1 Partial alignment of the sea slug *A. californica Timeless* homolog (GenBank accession XM_005099638.1) with polychaete *P. dumerilii Timeout* (KF316923.1). Vertical lines show identical nucleotides and highlighted areas show the locations of the degenerate primer pair, *Tim*_New_1F and *Tim*_New_1R (Table 2.1), designed for testing on *M. edulis*. Numbers show the nucleotide positions in each sequence.

2.2.8 Polymerase Chain Reaction (PCR) amplification

All PCR reactions were performed on either a Techne TC-4000 Thermal Cycler (Bibby Scientific, Stone, UK) or a Veriti 96 Well Thermal Cycler (Applied Biosystems, Loughborough, UK). Thermal cycling programs used are shown in Table 2.2.

Table 2.2 Thermal cycling programs used for PCR reactions.

Program A

Stage	N° of Cycles
94 °C for 30 sec	x 1
94 °C for 30 sec 55 °C for 30 sec 72 °C for 30 sec	x 35
72 °C for 2 min	x 1

Program B

Stage	N° of Cycles
94 °C for 30 sec	x 1
94 °C for 30 sec 55 °C for 30 sec 72 °C for 1 min	x 35
72 °C for 7 min	x 1

Program C

Stage	N° of Cycles
94 °C for 30 sec	x 1
94 °C for 30 sec 60 °C for 30 sec 72 °C for 30 sec	x 35
72 °C for 2 min	x 1

Program D

Stage	N° of Cycles
94 °C for 30 sec	x 1
94 °C for 30 sec 65 °C for 30 sec 72 °C for 30 sec	x 35
72 °C for 2 min	x 1

Program E

Stage	N° of Cycles
94 °C for 30 sec	x 1
94 °C for 30 sec 50 °C for 30 sec 72 °C for 1 min	x 35
72 °C for 2 min	x 1

2.2.8.1 Isolation of *Clk*

The first *Clk* PCR product was generated by mixing 1 µL cDNA with 0.5 µL of 200 pmol/µL *Clock*_3F and *Clock*_Right respectively (Table 2.1), 0.5 µL 40 mM dNTP mix (Thermo Fisher Scientific, Loughborough, UK), 0.5 µL of 50X Advantage cDNA polymerase mix (including KlenTaq-1 DNA polymerase, minor amounts of a proofreading polymerase, and 1.1 µg/µL TaqStart Antibody for hot start reactions) (Clontech, TaKaRa BioEurope SAS, Saint Germain-en-Laye, France), 2.5 µL of the

associated 10X PCR Buffer (400mM tricine-KOH pH 9.2, 150 mM KOAc, 35 mM Mg(OAC)2, 37.5 µg/mL Bovine serum albumin (BSA) (Clontech, France), 0.5 µL 100% dimethyl sulfoxide (DMSO) (Agilent Technologies, Wokingham, UK), 0.5 µL 25 mM $MgCl_2$ (Thermo Fisher Scientific, UK) and 18.5 µL molecular biology-grade water (Fisher Scientific, UK). Thermal cycling program A was used (Table 2.2).

The second *Clock* PCR product was obtained by mixing 1 µL of cDNA with 0.5 µL of 200 pmol/µL *Clock*_3F, 0.5 µL 100 pmol/µL *Clock*_New_6R (Table 2.1), with the following reagents from the Expand High FidelityPLUS PCR System (Roche, UK): 0.5 µL PCR Nucleotide Mix (40 mM), 0.375 µL Expand High FidelityPLUS Enzyme Blend (5 U/µL, containing a mixture of Taq polymerase and a proofreading polymerase), 5.0 µL Expand High FidelityPLUS Reaction Buffer 5X (containing 7.5 mM $MgCl_2$), and molecular-grade water (Fisher Scientific, UK) to a total reaction volume of 25 µL. Thermal cycling program E was used (Table 2.2).

After subsequent agarose gel electrophoresis (Section 2.2.9), the first product was cloned (Section 2.2.12) and sequenced (Section 2.2.15). The second product was purified from the gel (Section 2.2.10) and 5 µL of the resulting DNA was substituted for cDNA as the template in a further PCR reaction under the same conditions outlined above. This sample was also sequenced following gel purification.

2.2.8.2 Isolation of *Cry1*

The first *Cry1* PCR product was generated by combining 1 µL cDNA, 0.5 µL *Cry1*_3F and *Cry1*_5R (both 100 pmol/µL) (Table 2.1), 0.5 µL 40 mM dNTP mix (Agilent Technologies, UK), 0.25 µL Herculase II Fusion DNA Polymerase (containing a Pfu-based DNA polymerase and ArchaeMaxx PCR enhancing factor) (Agilent Technologies, UK), 5 µL of 5X PCR buffer (providing a final Mg_2+

concentration of 2 mM) (Agilent Technologies), 0.5 µL 100% DMSO (Agilent Technologies, UK), 0.5 µL 25 mM $MgCl^2$ (Fisher Scientific, UK) and 16.25 µL sterile nuclease-free water (Fisher Scientific, UK). Thermal cycling program B was used (Table 2.2). A re-PCR was later performed by substituting cDNA with 1 µL of correctly sized purified band DNA cut from an agarose gel (see Sections 2.2.9 and 2.2.10), in order to obtain the final PCR product lacking non-specific multiple bands.

The second *Cry1* PCR product, designed to overlap the first, was obtained by mixing 0.5 µL 100 pmol/µL *Cry1*_8F and *Cry1*_8R (Table 2.1) with 1 µL cDNA, 0.5 µL 40 mM dNTP mix (Agilent Technologies, UK), 0.5 µL 50X Advantage cDNA polymerase mix (Clontech, France), 2.5 µL 10X PCR Buffer (Clontech, France) and 19.5 µL sterile nuclease-free water (Fisher Scientific, UK). The thermal cycling conditions were as described above. The PCR product was visualised (Section 2.2.9), quantified (Section 2.2.11) and sent directly for sequencing (Section 2.2.15).

The third *Cry1* PCR product was generated, purified, subjected to Re-PCR and sequenced by performing the same protocol described for second *Clk* PCR product (Section 2.2.8.1) except that the following primers were used: 100 pmol/µL of both *Cry1*_14F and *Cry1*_12R (Table 2.1).

2.2.8.3 Isolation of *ARNT*

The *ARNT* PCR product was obtained by combining 1 µL template cDNA with 0.5 µL of 100 pmol/µL *Bmal1*_1F and *Bmal1*_3R (Table 2.1), 0.5 µL 40 mM dNTP mix (Agilent Technologies, UK), 0.5 µL 50X Advantage cDNA polymerase mix (Clontech, France), 2.5 µL 10x PCR Buffer (Clontech, France), 0.5 µL 100% DMSO (Agilent Technologies, UK), 0.5 µL 25mM $MgCl_2$ (Fisher Scientific, UK) and 18.5 µL sterile nuclease-free water (Fisher Scientific, UK). Thermal cycling program C

was used (Table 2.2). A single PCR product was obtained which was sequenced directly (Section 2.2.15). The remainder of the gene's coding DNA sequence (CDS) was obtained using RACE PCR (see Section 2.2.16).

2.2.8.4 Isolation of *Tim*

The *Tim* PCR product was obtained by mixing 1 µL cDNA with 0.5 µL 100 pmol/µL *Tim*_New_F1 and *Tim*_New_R1 primers (Table 2.1), 0.5 µL 40 mM dNTP mix (Agilent Technologies, UK), 0.25 µL of Herculase II Fusion DNA Polymerase (Agilent Technologies, UK) and 17.25 µL sterile nuclease-free water (Fisher Scientific, UK). Thermal cycling program D was used (Table 2.2). The PCR product displayed multiple bands during electrophoresis so the correctly sized band was purified from the gel (Section 2.2.10) and 5 µL purified DNA was used as a template in a subsequent PCR. This resulting single-PCR product was purified from the gel prior to sequencing (Section 2.2.15).

A second *Tim* PCR product was obtained by pairing the 100 pmol/µL primer *Tim*_New_F2, which was designed from *A. californica Timeless* homolog (GenBank accession XM_005099638.1), with the *M. edulis Tim*-specific primer *Tim*_RACE_1R designed from the first *Tim* PCR product sequence described above (Table 2.1). The same reagents and concentrations used previously were combined with PCR program B (Table 2.2). After agarose gel electrophoresis (Section 2.2.9), the band was cut from the gel and purified (Section 2.2.10) before sequencing (Section 2.2.15).

2.2.8.5 Isolation of *ROR/HR3*

The first *ROR/HR3* PCR product was generated using the same reagents, quantities and thermal cycling conditions used to generate the first *Cry1* PCR product

(Section 2.2.8.2) except the primers were 0.5 µL of 100 pmol/µL *ROR*_3F and *ROR*_5R respectively (Table 2.1). The second PCR product, designed to overlap the first, was obtained using 0.5 µL 10 pmol/µL *ROR*_8F and *ROR*_8R with the same reagents and thermal cycling conditions previously described for the second *Cry1* PCR product (Section 2.2.8.2). Both *ROR/HR3* PCR products were visualised (Section 2.2.9) quantified (Section 2.2.11) and sequenced (Section 2.2.15). The third PCR product was generated, purified, subjected to Re-PCR and sequenced by performing the same protocol that was used to isolate the second *Clk* PCR product (Section 2.2.8.1) except that the following primers were used: 100 pmol/µL *ROR*_9F and *ROR*_12R (Table 2.1).

2.2.8.6 Isolation of *aaNAT*

An *aaNAT* PCR product was generated using 1 µL of cDNA, 0.5 µL of 100 pmol/µL primers *aaNAT*_F3 and *aaNAT*_R4 (Table 2.1), 0.5 µL 40 mM dNTP mix (Agilent Technologies, UK), 0.25 µL of Herculase II Fusion DNA Polymerase (Agilent Technologies, UK), 5 µL of 5X PCR buffer (Agilent Technologies), and 17.25 µL molecular-grade water (Fisher Scientific, UK). Thermal cycling Program D was used (Table 2.2). Agarose gel electrophoresis (Section 2.2.9) revealed a correctly sized band which was cut and purified (Section 2.2.10) and 5 µL of the resulting DNA was used as a template in a second PCR in a total reaction volume of 25 µL under the same conditions reaction conditions. Gel electrophoresis resulted in the reappearance of the same-sized band, which was purified from the gel and sequenced (Section 2.2.15).

2.2.9 Agarose gel electrophoresis

All PCR products were separated and visualised by agarose-gel electrophoresis on 1% Tris/Borate/EDTA (TBE) agarose gels. For each 100 mL of gel required, 1 g of agarose (Fisher Scientific, UK) was combined with 100 mL 1X TBE buffer (89 mM Tris Base, 89 mM boric acid and 2 mM ethylenediamine tetraacetic acid, EDTA) (Fisher Scientific, UK) and heated in the microwave for 30 sec increments at 450 watts until fully dissolved. Molten gels were cooled at room temperature until ~ 50 ˚C and were stained with either SYBR® Safe DNA gel stain (10,000X concentrate in DMSO) (Life Technologies, UK), as was the case for *Clk* PCR products, or with GelRed™ Nucleic Acid Gel Stain (10,000X in water) (Biotium, Cambridge Bioscience, Cambridge, UK) for all other PCR products. Samples were prepared by mixing 10 µL of PCR product with 2 µL 6X DNA Loading Dye (10 mM Tris-HCl pH 7.6, 0.03% bromophenol blue, 0.03% xylene cyanol FF, 60% glycerol, 60 mM EDTA) (Thermo Scientific, UK) to facilitate gel loading and visualisation of electrophoresis progress. 10 µL of 50 µg/mL Quick-Load® 100 bp DNA Ladder (supplied in 2.5% Ficoll-400, 11 mM EDTA, 3.3 mM Tris-HCl pH 8.0, 0.017% SDS and 0.015% bromophenol blue) (New England BioLabs, Hitchin, UK) was loaded onto each gel to provide a comparable size reference for PCR products. Where larger PCR products were anticipated, an alternate molecular weight marker was used: 1 kb DNA Ladder (supplied in 3.3 mM Tris-HCl, 11 mM EDTA, 0.015% bromophenol blue, 0.017% SDS, 2.5% Ficoll®-400; pH 8.0 at 25 °C) (New England Biolabs, UK). Gels were run at 70 volts for 45 to 60 min and photographed with a UV transilluminator (Gel Doc™ EZ System, BioRad, UK) using Image Lab™ Software (BioRad, UK).

2.2.10 Purification of DNA from agarose gels

When multiple bands were obtained per lane from agarose gel electrophoresis, indicating the presence of a mixed PCR product, the desired band was cut from the gel under UV light using a scalpel and was purified using the NucleoSpin® Gel and PCR Clean-up Kit (Macherey Nagel, UK). This technique uses a chaotropic salt solution that disturbs the hydrogen bonding of nucleic acids and facilitates their binding to a silica membrane. Subsequent washing steps remove contaminants including primers, nucleotides, salts and dyes allowing pure DNA to be eluted.

For each 100 mg of excised agarose gel, 200 µL Binding Buffer NTI (containing guanidinium thiocyanate, chaotropic salt and a pH indicator) was added. Samples were incubated on a heat block at 50 °C for up to 10 min with intermittent vortexing to dissolve the gel slice. The sample was loaded into a NucleoSpin® Gel and PCR Clean-up Column and centrifuged for 30 sec at 11,000 x *g*. Flow-through was discarded and 700 µL of Buffer NT3 (6 mL concentrate diluted with 24 mL absolute ethanol) was added. After centrifugation for 30 sec at 11,000 x *g*, flow-through was again discarded. This NT3 washing step was then repeated to minimise chaotropic salt carry-over. An additional centrifugation for 1 min at the same speed ensured removal of residual buffer from the column. For sample elution, 15 µL to 30 µL Buffer NE (5 mM Tris/HCl, pH 8.5) was added, incubated for 1 min at room temperature, and centrifuged for 1 min at 11,000 x *g*. The sample was then re-applied to the column and the final centrifugation step was repeated in order to maximise DNA yield obtained. Samples were stored at -20 °C.

2.2.11 DNA quantification

To ascertain DNA concentration prior to sequencing, DNA quantification was

performed using a Qubit 1.0 Fluorometer (Life Technologies, UK). The method was the same as was previously described for RNA quantification (Section 2.2.3) except that the dsDNA BR Assay Kit (Life Technologies, UK), with a range of 0.01 µg/mL to 10 µg/mL, was used. This kit consisted of Qubit dsDNA BR Reagent (200X concentrate in DMSO), Qubit dsDNA BR Buffer, Qubit dsDNA BR Standard #1 (0 ng/µL in TE buffer) and Qubit dsDNA BR Standard #2 (100 ng/µL in TE buffer).

2.2.12 Cloning of PCR products

The first *Clk* PCR product (Section 2.2.8.1) was cloned using the Original TOPO TA Cloning Kit for Sequencing with One Shot TOP10 Chemically Competent *Escherichia coli* (Life Technologies, UK) to obtain a single product for sequencing. The ligation reaction, in which a plasmid takes up the PCR insert, was prepared by combining 6 µL PCR product with 1 µL T4 DNA ligase (4.0 Weiss units/µL), 2 µL of 1/10 diluted pCR®2.1 vector (25 ng/µL in 10 mM Tris-HCl, 1 mM EDTA pH 8.0) and 1 µL 10X Ligation Buffer (60 mM Tris-HCl pH 7.5, 60 mM MgCl2, 50 mM NaCl, 1 mg/mL BSA, 70 mM, β-mercaptoethanol, 1 mM ATP, 20 mM dithiothreitol, 10 mM spermidine) and incubated overnight at 14 °C in a Techne TC-4000 Thermal Cycler (Bibby Scientific, UK). The following day, 2 µL of the reaction mix was added to the chemically competent TOP10 *E. coli* and incubated on ice for 30 min. Heat shock at 42 °C was performed in a water bath for 30 sec to transform the *E. coli* with the plasmid. Samples were then immediately placed on ice. 250 µL of room temperature SOC medium (2% tryptone, 0.5% yeast extract, 10 mM NaCl, 2.5 mM KCl, 10 mM $MgCl_2$, 10 mM $MgSO_4$, 20 mM glucose) was added and samples were incubated at 37 °C at 200 rpm for 1 hr to encourage cell growth.

Blue/white screening was performed to enable identification of successfully

transformed colonies. Selective media was made by combining 37 g LB Agar Miller granules (consisting of 10 g tryptone, 5 g yeast extract, 10 g sodium chloride, 12 g agar) (Fisher Scientific, UK) per 1 L of purified water. Once autoclaved and cooled to ~50 °C, kanamycin sulphate (Fisher Scientific, UK) was added to a final concentration of 50 µg/mL. Only cells successfully transformed with the plasmid, which contains a kanamycin-resistance gene, are able to grow on the selective media. Plates were poured and set under aseptic conditions then spread with 40 µL of 20 mg/mL X-gal (5-bromo-4-chloro-3-indolyl-β-D-galactopyranoside) in DMSO (Fisher Scientific, UK). Plates were pre-warmed to 37 °C prior to the addition of 50 µL transformed *E. coli* and each sample was plated in duplicate. When dry, plates were inverted and incubated at 37 °C overnight to allow colony growth.

Growth of white colonies indicates successful ligation and transformation as disruption of the plasmid's *lacZ* gene during the ligation prevents X-gal digestion which would otherwise result in blue colonies. Individual white colonies were used to inoculate 10 mL sterile LB Miller Broth (containing 10 g tryptone, 5 g yeast extract and 10 g sodium chloride per litre of distilled water) (Fisher Scientific, USA) containing 50 mg/mL kanamycin (Fisher Scientific, UK). These liquid cultures were incubated overnight at 37 °C at 200 rpm. Cloudiness of the broth the following day indicated successful cell growth.

2.2.13 Purification of plasmid DNA from *E. coli* liquid cultures

6 mL of overnight bacterial culture was centrifuged at 20,000 x *g* for 5 min. The supernatant was discarded and the plasmid DNA was isolated from the *E. coli* cell pellet using the Wizard® *Plus* SV Minipreps DNA Purification System (Promega, Southampton, UK). Cell pellets were thoroughly resuspended in 250 µL Cell

Resuspension Solution (50mM Tris-HCl pH 7.5, 10mM EDTA, 100 µg/mL RNase A) by vortexing. 250 µL of Cell Lysis Solution (2 M NaOH, 1% SDS) was added to degrade cell membranes, and samples were inverted 4 times to gently mix. 10 µL of Alkaline Protease Solution was added to inactivate released proteins such as endonucleases which could negatively affect DNA quality, and samples were again inverted 4 times to mix. Samples were incubated for 5 min at room temperature before 350 µL of Neutralisation Solution (4.09 M guanidine hydrochloride, 0.759 M potassium acetate, and 2.12 M glacial acetic acid at a final approx. pH of 4.2) was added to reduce sample alkalinity. Samples were inverted 4 times to mix before being centrifuged at 20,000 x *g* for 10 min. Without disturbing the precipitate, the cleared lysate was transferred into a Wizard® SV Minicolumn and centrifuged at 20,000 x *g* for 1 min to bind the plasmid DNA to the column. The flow-through was discarded. 750 µL of Column Wash Solution (60% ethanol, 60 mM potassium acetate, 8.3 mM Tris-HCl, 0.04 mM EDTA) was added to purify the DNA from remaining cellular impurities. The samples were centrifuged for 1 min at 20,000 x *g* and the flow-through was discarded. This wash step was repeated using 250 µL of the same solution followed by 2 min centrifugation at the same speed. The column was placed in a sterile tube and 100 µL Nuclease-Free Water was added. A final centrifugation of 1 min at 20,000 x *g* was used to elute the DNA which was then stored at -20 °C.

2.2.14 PCR on purified plasmid DNA

PCR was performed on purified plasmid DNA from the *Clk*-transformed *E. coli* (Sections 2.2.12 and 2.2.13) to confirm the inclusion of the correct insert. The gene-specific primer *Clock*_ 3F was paired with the M13R primer 5'-CAGGAAACAGCTATGAC-3' (Invitrogen, UK) and 0.5 µL of each at 100 pmol/µL

were mixed with 1 µL purified plasmid DNA, 2.5 µL 10X PCR Buffer (Clonetch, France), 0.5 µL 50X Advantage cDNA polymerase mix (Clontech, France), 0.5 µL 40 mM dNTP mix (Thermo Fisher Scientific, UK), 0.5 µL 25 mM $MgCl_2$ (Thermo Fisher Scientific, UK), 0.5 µL 100% DMSO (Agilent Technologies, UK) and 18.5 µL sterile nuclease-free water (Fisher Scientific, UK). Thermal cycling conditions were: 94 °C for 30 sec, followed by 35 cycles of 94 °C for 30 sec, 55 °C for 30 sec and 72 °C for 60 sec, followed by a final extension of 72 °C for 7 min. PCR products were analysed by agarose gel electrophoresis (Section 2.2.9).

2.2.15 Sequencing

PCR products or purified band DNA were sent for sequencing using EZ-seq DNA sequencing service (Sanger sequencing) provided by Macrogen Europe (Amsterdam, The Netherlands), using the PCR primers as sequencing primers (Table 2.1). A minimum of 6 ng/µL DNA was combined with 0.25 µL 100 pmol/µL primer and molecular-grade water (Fisher Scientific. UK) to a total volume of 10 µL. A minimum of 50 ng/µL plasmid DNA containing the *Clk* sequence insert was sequenced using primers M13R 5'-CAGGAAACAGCTATGAC-3' and M13F 5'-GTAAAACGACGGCCAGT-3' (Invitrogen, UK). Obtained sequences were manually edited and assembled with the software Bioedit version 7.2.5.

2.2.16 Rapid Amplification of cDNA Ends (RACE)

Rapid Amplification of cDNA Ends (RACE) PCR reactions were performed using the SMARTer RACE cDNA Amplification Kit (Clontech, France) to isolate the full 5' and 3' ends of the genes of interest to obtain the full CDS. This technique involves generating complete cDNA copies of the mRNA in reverse transcription

reactions using modified primers, followed by RACE PCR pairing a gene-specific primer with universal primers.

2.2.16.1 Preparation of RACE-ready cDNA

RACE-ready *M. edulis* cDNAs were generated according to the manufacturer's protocol (Clontech, France). For the 5' RACE-ready cDNA, 2.75 µL *M. edulis* RNA (184 ng/µL) was combined with 1 µL 5'-RACE CDS primer A (12 µM), whereas for the 3' RACE-ready cDNA, 2.75 µL of RNA (184 ng/µL) was combined with 1 µL 3'-RACE CDS primer A (12 µM) and 1 µL deionised water. After briefly mixing and centrifuging, samples were heated at 72 °C for 3 min followed by 42 °C for 2 min in a thermal cycler. After brief centrifugation, 1 µL SMARTer IIA Oligonucleotide (12 µM) was added to the 5' reactions only and the following was added to all samples: 2 µL 5X First-Strand Buffer (250 mM Tris-HCl at pH 8.3, 375 mM KCl, 30 mM $MgCl_2$), 1 µL dithiothreitol (20 µM), 1 µL dNTP mix (10 mM), 0.25 µL RNase Inhibitor (40 U/µL) and 1 µL SMARTScribe Reverse Transcriptase (100 U/µL). Samples were mixed by pipetting, centrifuged briefly and heated in a thermal cycler at 42 °C for 90 min followed by 70 °C for 10 min. Samples were then diluted using either 20 µL or 100 µL of Tricine-EDTA buffer (10 mM Tricine-KOH at pH 8.5, 1 mM EDTA) depending on whether the initial RNA concentration used was less than or greater than 200 ng respectively. RACE-ready cDNAs were stored at -20 °C.

2.2.16.2 RACE PCR Reactions

ARNT RACE PCR products were obtained by combining: 2.5 µL of either 3' or 5' RACE-ready cDNA, 5 µL 10X Universal Primer A Mix (containing 0.4 µM 5'-CTAATACGACTCACTATAGGGCAAGCAGTGGTATCAACGCAGAGT-3' and 2 µM 5'-CTAATACGACTCACTATAGGGC-3'), 1 µL of 100 pmol/µL gene-specific primer (Table 2.3), 1 µL 40 mM dNTP mix (Clontech, France), 1 µL 50X Advantage cDNA polymerase mix (Clontech, France), 5 µL 10X PCR Buffer (Clontech, France) and 34.5 µL of PCR-grade water (Clontech, France). Thermal cycling programs were: Touchdown A for the 3' product and Touchdown B for the 5' product (Table 2.4).

Table 2.3 Primers used for RACE PCR and for sequencing of RACE PCR products.

Target Gene	Application	Primer	Sequence 5'-3'	Tm (˚C)	% GC
Bmal1/ ARNT	3' RACE, Sequencing	*Bmal1*_1F	CGACCAGAGGGTAACAGCTT	59.4	55.0
	Sequencing	*Bmal1*_ 7F	GGTGCCCCTACTTATACACAGC	57.3	54.5
	5' RACE, Sequencing	*Bmal1*_ 6R	GCTACTGGTCCTTAGCCATACCC	58.9	56.5
	Sequencing	*Bmal1*_8R	ATCGACTGATGAAGAACTGGTGT	56.0	43.4

After agarose gel electrophoresis (Section 2.2.8), both the 3' and 5' RACE products showed faint bands of the anticipated sizes (~1167 bp and 1306 bp respectively), which were cut from the gel and purified (Section 2.2.9). 5 µL of the each purified DNA was then substituted for cDNA as a template in a further PCR reaction of 25 µL total volume, using the same amplification conditions as before. The brighter bands obtained were cut from the gel, purified and sequenced (Section 2.2.14) with the appropriate primers (Table 2.3).

Table 2.4 Thermal cycling conditions for RACE PCR of ARNT 5' and 3' cDNA ends.

Program Name	**Touchdown A**			**Touchdown B**		
Stage	**Temperature (°C)**	**Time**	**No. of cycles**	**Temperature (°C)**	**Time**	**No. of cycles**
Initial denaturation	94	30 sec	1	94	30 sec	1
Annealing/Extension	68	3 min		68	3 min	
Denaturation	94	30 sec		94	30 sec	
Annealing	60	30 sec	20	65	30 sec	5
Extension	72	3 min		72	3 min	
Denaturation	94	30 sec		94	30 sec	
Annealing	55	30 sec	10	60	30 sec	5
Extension	72	3 min		72	3 min	
Denaturation	94	30 sec		94	30 sec	
Annealing	50	30 sec	10	55	30 sec	5
Extension	72	3 min		72	3 min	
Denaturation	-	-	-	94	30 sec	
Annealing	-	-	-	50	30 sec	20
Extension	-	-	-	72	3 min	
Final Extension	72	5 min	1	72	5 min	1

2.2.17 Gene characterisation and analysis of sequence data

2.2.17.1 BLAST comparison searches

The BLAST search tool was used to compare *M. edulis* sequences with those on the Genbank database (http://blast.ncbi.nlm.nih.gov/Blast.cgi) to confirm sequence identity. Nucleotide blast searches (megablast and blastn) were used to compare nucleotide sequences with the nucleotide database and protein blast (blastp) was used to compare amino acid sequences to other amino acids sequences. Blastx was used to compare translated nucleotide sequences with the protein database, allowing the identification of functional protein domain coverage. Two-way blastn searches allowed pairwise comparison between two nucleotide sequences.

2.2.17.2 Multiple sequence amino acid alignments

M. edulis nucleotide sequences were conceptually translated into amino acid sequences (http://in-silico.net/tools/biology/sequence_conversion) and aligned with sequences of the same gene from other species, downloaded from the GenBank database (https://www.ncbi.nlm.nih.gov/) using the ClustalW2 sequence alignment tool (http://www.ebi.ac.uk/Tools/msa/clustalw2/). This allowed sequence similarities and differences between different species to be visualised for each gene. Sequences chosen included those from model species of vertebrates and insects as well as available marine invertebrate sequences from molluscs and crustaceans.

2.2.17.3 Generation of phylogenetic trees

Phylogenetic analysis was performed for each gene using Mega5.2 software. The outgroups selected were sequences from closely related genes from model organisms. Sequences were aligned using the inbuilt ClustalW feature and alignments were edited manually with the ends cropped based on the shortest sequence. Maximum likelihood analysis was performed. The Jones-Taylor-Thornton (JTT) model was used and for heuristic searches the Nearest Neighbor Interchange (NNI) method was used. The bootstrap method with 1000 replicates was used to ascertain support for the tree and bootstrap values were shown on the nodes. Species names and Genbank accession numbers for the sequences used were displayed on the trees.

2.2.18 Identification of clock proteins

2.2.18.1 Protein extraction

A pilot study was performed to extract total proteins from portions of *M. edulis* mantle tissue from the same individual that had been stored under the following three

conditions: TRI Reagent® (Sigma Aldrich, UK) at -80 °C, RNA*later* solution (Ambion, Life Technologies, USA) at -80 °C and no buffer at -20 °C. All samples were from the same sexually developing male at gametogenesis stage βIII (Seed, 1969), sampled from the late-morning time-point in winter 2014. Extractions from rat liver tissue (*Rattus norvegicus*) and whole fruit flies (*D. melanogaster*) (Animal Husbandry, Southampton, UK) stored in RNA*Later* at -20 °C were also prepared to serve as controls in subsequent Western blotting procedures.

Total protein was extracted by placing weighed tissue samples in 9X volume per weight filter-sterilised ice-cold PBS solution (0.01M, pH 7.4) and homogenising with a rotor-stator homogeniser (IKA, Staufen, Germany) before centrifugation at 20,000 x *g* for 5 min. The supernatant containing soluble material was retained and the insoluble pellet was extracted by incubating with 1% sodium dodecyl sulphate (SDS) for 10 min on ice. The centrifugation step was repeated and both the soluble and insoluble extractions were stored at -20 °C.

2.2.18.2 Protein quantification

Protein concentrations were quantified using the Qubit 1.0 Fluorometer (Life Technologies). Assays were performed in the same way as described previously for RNA quantification (section 2.2.3) but with the Qubit™ Protein Assay Kit (Life Technologies, Paisley, UK) with a detection range of 12.5 µg⁄mL to 5 mg⁄mL, being used in this case. The kit consists of Qubit Protein Reagent (200X concentrate in 1,2-propanediol), Qubit Protein Buffer, Qubit Protein Standard #1 (0 ng/µL in TE buffer with 2 mM sodium azide) and Qubit Protein Standard #2 (200 ng/µL in the same buffer) and Qubit Protein Standard #3 (400 ng/µL in the same buffer).

2.2.18.3 SDS-PAGE

Sodium dodecyl sulphate polyacrylamide gel electrophoresis (SDS-PAGE) was performed to separate proteins based on their molecular weights. First a 12% separating gel (1 mm thickness) was made by combining 1.3 mL 4X separating gel buffer (1.5M Tris, pH 8, 0.4% SDS) with 2 mL acrylamide solution (30% w/w acrylamide/bis-acrylamide 37.5:1) (Sigma Aldrich, UK) and 1.65 mL of purified water. 100 µL of 10% ammonium persulphate solution (Fisher Scientific, UK) and 4 µL of Tetramethylethylenediamine (TEMED) (Fisher Scientific, UK) were then added to catalyse the polymerisation of the gel which was then poured and left to set with an overlay of butanol (Fisher Scientific, UK) to straighten the level the gel and remove bubbles. After approx. 1 hr, the gel was set and the butanol was removed. A 4% stacking gel was prepared by mixing 1.3 mL of 4X stacking buffer (0.5M Tris, pH 6.8, 0.4% SDS) with 0.65 mL acrylamide solution (30% w/w acrylamide/bis-acrylamide 37.5:1) and 3.3 mL purified water. As before, gel polymerisation was induced by the addition of 100 µL of 10% ammonium persulphate solution and 4 µL of TEMED. The stacking gel was poured on top of the separating gel and left to set with a comb in for 30 min. Gels were kept moist at 4 °C for a maximum of 3 days with the comb intact before use.

Prior to gel loading, protein samples were combined with 2X Laemmli sample buffer (4% SDS, 20% glycerol, 10% 2-mercaptoethanol, 0.004% bromophenol blue and 0.125 M Tris HCl, pH ~6.8) and heated to 100 °C for 4 min to denature the proteins. 20 µg total proteins were loaded per well and 5 µL (~11 ug) of broad-range pre-stained protein marker (7-175 kDa) (New England Biolabs, UK) was run alongside the samples. Electrophoresis was performed in 1X gel running buffer (25 mM Tris, 192 mM glycine, 0.1% SDS) at 100 v for 30 min followed by 150 v for 1 hr

45 min in a cold room at 4 °C.

2.2.18.4 Coomassie blue staining

In order to visualise proteins separated by SDS-PAGE, Coomassie blue staining was performed. Gels were placed in prefixing solution (50% methanol, 10% acetic acid, 40% distilled water) for at least 1 hr before being stained in the same solution containing 0.25% Coomassie blue R-250 (Fisher Scientific, UK) for 30 min. Gels were then transferred to destain solution (20% methanol and 10% acetic acid in distilled water) and heated in a microwave at 900 w for 40 sec. After 30 min this step was repeated with fresh destain solution. The gel was de-stained at room temperature overnight with fresh buffer to obtain a clear background. The gel was then transferred to distilled water and photographed.

2.2.18.5 Western blotting

As antibodies are not commercially available for blue mussel clock proteins, species cross-reactivity was tested using the following rabbit polyclonal antibodies with reactivity in humans to the following proteins: CLOCK, CRY1, BMAL1, TIM and ROR2 (Bethyl Laboratories, Texas, USA). SDS-PAGE was performed as described in section 2.2.18.3. Rat and fruit fly protein extractions were used as mammalian and invertebrate controls respectively.

Electroblotting was performed at 4 °C to transfer the proteins from the gel onto a nitrocellulose membrane (GE Heathcare Life Sciences, UK) by submersion in transfer buffer (20 mM Tris, 150 mM glycine, 20% methanol, pH8) and applying 100 v for 1 hr 15 min. The membrane was washed with Tris Buffered Saline with Tween® 20 (TBST) buffer (0.5 M Tris, 0.138M NaCl, and 0.0027M KCl at pH8, with 0.05%

Tween® 20) for 5 min. Blocking was performed in TBST buffer containing 5% w/v skimmed dry milk powder (blocking buffer) for 3 hr with constant gentle agitation at room temperature. The primary antibodies were diluted 1:1000 in blocking buffer as per manufacturer's instructions. Membranes were incubated with 10 ml of the antibody dilutions at 4 °C overnight with gentle spinning.

The following day, membranes were washed 3 times with TBST buffer for 10 min each time. The secondary antibody, Goat anti-Rabbit IgG-heavy and light chain Alkaline Phosphatase Conjugated Antibody (Bethyl Laboratories, Texas, USA) was diluted 1:5000 and incubated with the membrane for 1 hr at room temperature. As before, 3 TBST wash steps were performed followed by a rinse with distilled water. Finally, 2 mL Western Blue® Stabilized Substrate for Alkaline Phosphatase (Promega, Southampton, UK) was added to the membrane which was developed at room temperature and washed with distilled water when clear bands appeared.

Protein molecular weights were predicted by inputting full amino acid sequences into the online Protein Molecular Weight calculator http://www.bioinformatics.org/sms/prot_mw.html. In cases where the full amino acid sequence was unavailable for a species, such as was the case for *M. edulis* clock genes, a sequence from a closely related species available was used as an alternative.

2.3 RESULTS

2.3.1 Isolation of *M. edulis* target genes

Sequencing of the *mfp-1* gene confirmed species identity as *M. edulis*. Nucleotide sequences were obtained via PCR and RACE PCR for the six *M. edulis* circadian rhythm-related genes: *Clk*, *Cry1*, *ARNT*, *Tim*, *ROR/HR3* and *aaNAT*.

Sequence length, coverage and Genbank accession numbers are given in Table 2.5. The top three blastn (nucleotide vs nucleotide database comparison) and blastx (translated nucleotide vs protein database comparison) matches for each of the sequences are summarised in Table 2.6.

Table 2.5 Sizes of the isolated gene sequences (cDNA) from *M. edulis* along with their corresponding GenBank accession numbers.

Gene	Sequence length (bp)	GenBank Accession Number	Conceptual translation (amino acids)	CDS coverage
Clk	626	KJ671527	208	Partial
Cry1	1087	KJ671528	362	Partial
ARNT	2037	KJ671529	679	Complete
Tim	851	KX576716	283	Partial
ROR/HR3	1825	KJ671530	608	Complete
aaNAT	540	KX576715	179	Complete

Table 2.6 Summary of blastn and blastx GenBank database search results. Query cover is the percentage coverage of the *M. edulis* query sequence which overlaps the database hit sequence, and ident is the percentage of matches within the coverage area. *molluscs

***M. edulis* sequence (bp)**	**Blastn search results**					**Blastx search results**				
	Species	**Gene**	**GenBank Accession Number**	**Query Cover (%)**	**Ident (%)**	**Species**	**Gene**	**GenBank Accession Number**	**Query Cover (%)**	**Ident (%)**
Clk (626 bp)	*C. gigas**	*Clock*-like	XM_01131329.1	29	78	*C. gigas**	CLOCK	ECK28478.1	99	48
	Gavia stellata	*Clock* variant X1	XM_009819246.1	20	81	*C. gigas**	CLOCK-like	XP_011429631.1	99	48
	G. stellata	*Clock* variant X2	XM_009819245.1	20	81	*Sus scrofa*	CLOCK	XP_003356992.1	99	48
Cry1 (1087 bp)	*C. gigas**	*Cry1*-like variant X2	XM_011424995.1	92	67	*C. gigas**	CRY1-like isoform X2	XP_011423247.1	99	67
	*C. gigas**	*Cry1*-like variant X1	XM_011424944.1	88	75	*C. gigas**	CRY1-like isoform X1	XP_011423246.1	99	65
	*C. gigas**	*Cry1*-like protein	GQ415324.1	56	69	*C. gigas**	CRY-like protein	ACU53158.1	94	65
ARNT (2037 bp)	*Lottia gigantea**	bHLH & PAS family	XM_009063510	38	79	*C. gigas**	ARNT-like	EKC32806	95	70
	*Chlamys farreri**	*ARNT*	JN166934	19	81	*H. diversicolor**	ARNT	AGG55386	76	74
	*Haliotis diversicolor**	*ARNT*	KC256820	29	84	*A. californica**	ARNT homolog	XP_005096897	95	61
Tim (851 bp)	*C. gigas**	*Timeless* homolog	XM_011443276.1	99	71	*C. gigas**	TIMELESS homolog	XP_011441580.1	99	77
	*L. gigantea**	Hypothetical protein (*Timeless*)	XM_0090481151	90	69	*L. gigantea**	Hypothetical protein (TIMELESS)	XP_009046363.1	99	65
	*A. californica**	*Timeless* homolog	XM_005099638.1	69	67	*A. californica**	TIMELESS homolog	XP_005099695.1	99	62
ROR/HR3 (1825 bp)	*L. gigantea**	Unnamed	XM_009064558.1	39	82	*C. gigas**	Probable HR3 isoform X1	XP_011437283.1	70	66
	*C. gigas**	Probable *HR3*, transcript variant X1	XM_011438981.1	47	67	*C. gigas**	Putative HR3	EKC18621.1	69	66
	*C. gigas**	Probable *HR3*, transcript variant X5	XM_011438980.1	17	77	*C. gigas**	Probable HR3 isoform X2	XP_011437284.1	70	64
aaNAT (540 bp)	*Danio rerio*	Unnamed clone	BX927368.13	8	83	*P. dumerilii*	aaNAT	AIT11917.1	86	49
	Anisakis simplex	Genome assembly	LL319197.1	7	88	*Branchiostoma floridae*	N-Acyltransferase superfamily protein	XP_002608038.1	88	50
	Clostridium saccharobutylicum	Complete genome	CP006721.1	6	91	*Capitella teleta*	N-Acyltransferase superfamily protein	ELU18274.1	88	47

2.3.1.1 Characterisation of *Clk*

The 626 bp *M. edulis* partial *Clk* sequence (Table 2.5) matched other *Clk* sequences, with the best overall match (78%) being to *Clock*-like from *C. gigas* (Table 2.6). In addition, a two-way blastn comparison showed that there was a 93% identity similarity between this *M. edulis* sequence and *Clk* from *M. californianus*. A multiple-species amino acid alignment of CLK revealed partial coverage of two PAS functional protein domains by the translated *M. edulis Clk* sequence (Figure 2.2), providing further supporting evidence that it belongs to the bHLH-PAS family. The phylogenetic tree showed that *M. edulis* CLK clustered most closely with CLK from the other molluscs *C. gigas* and *A. californica*, which formed a clade distinct from arthropods and comparatively more similar to vertebrate CLK (Figure 2.3).

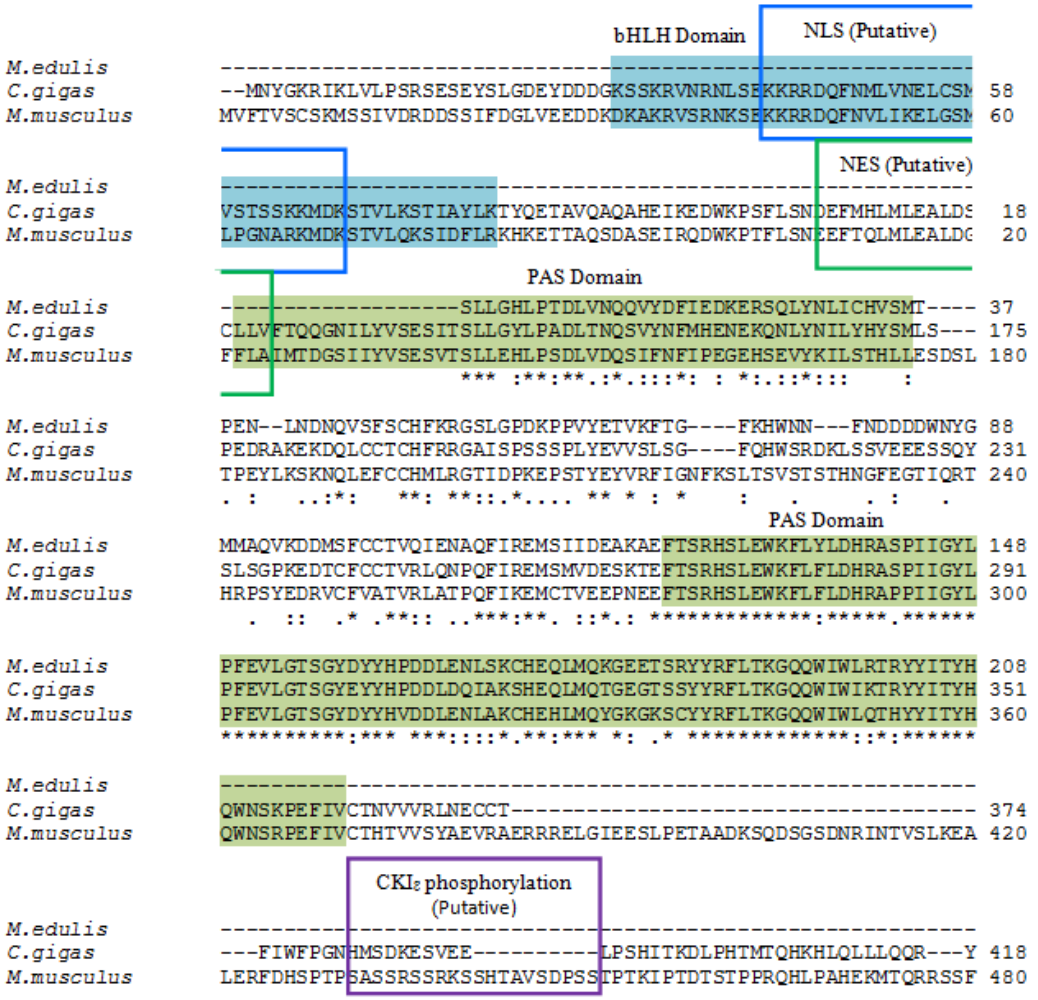

```
M.edulis        ------------------------------------------------------------
C.gigas         LNQATNSEPKAHRYTEPTANSNN-----------------LLQAGPDRMET-----TCL 455
M.musculus      SSQSINSQSVGPSLTQPAMSQAANLPIPQGMSQFQFSAQLGAMQHLKDQLEQRTRMIEAN 540

M.edulis        ------------------------------------------------------------
C.gigas         IKRVWRNFRRI---------------------------------------------- 466
M.musculus      IHRQQEELRKIQEQLQMVHGQGLQMFLQQSNPGLNFGSVQLSSGNSNIQQLTPVNMQGQV 600
```

Figure 2.2 Partial multiple species amino acid alignment of partial blue mussel *M. edulis* CLK (GenBank accession KJ671527) with CLK from the Pacific oyster *C. gigas* (EKC28478) and the mouse *M. musculus* (AAD30565). The 3' end of the alignment has been cropped. Dashes represent gaps in the alignment, asterisks represent homology, colons represent conserved amino acid substitutions (similar chemical properties) and dots represent semi-conserved amino acid substitutions (similar conformation). Functional protein domains are denoted by both the shaded (Marchler-Bauer *et* al., 2011) and boxed (Hirayama and Sassone-Corsi, 2005) regions. Abbreviations: bHLH, basic helix-loop-helix; NLS, nuclear localisation signal; NES, nuclear export signal; PAS, PER-ARNT-SIM; CKI, casein kinase I.

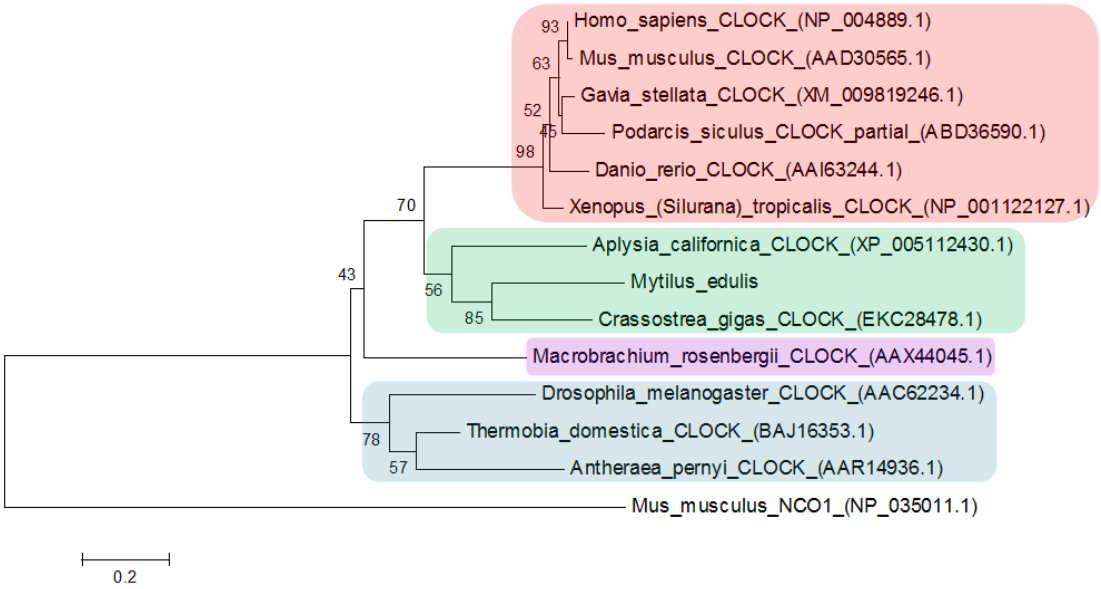

Figure 2.3 Phylogenetic tree of partial CLK amino acid sequences manually edited to a length of 230 amino acids with gaps with 1000 bootstrap replicates. Sequence GenBank accession numbers shown in brackets. Shading represents: vertebrates, red; molluscs, green; crustaceans, purple; insects, blue. A Nuclear Receptor Coactivator 1 (NCOA1) sequence, another member of the bHLH transcription factor family, was used as the outgroup.

2.3.1.2 Characterisation of *Cry1*

Blast searches using the 1087 bp partial *Cry1* nucleotide sequence obtained from *M. edulis* (Table 2.5) showed that the top three matches were all to *Cry1*-like sequences from the oyster *C. gigas* (Table 2.6). Furthermore, there was a 92% identity similarity between the *M. edulis* and *M. californianus Cry1* nucleotide sequences when compared directly with pairwise blastn. A multiple-species amino acid alignment of molluscan CRY sequences revealed partial coverage of a flavin adenine dinucleotide-binding domain 7 (FAD-binding 7) by the translated *M. edulis* sequence (Figure 2.4). The phylogenetic tree for cryptochrome sequences demonstrated clustering of the *M. edulis* sequence with that of CRY1 from the squid *E. scolopes*, whereas squid CRY2, which was more closely related to insect-type CRY2 and vertebrate-type CRY sequences, grouped separately. This indicates that the *M. edulis* sequence is most similar to insect-type CRY1 sequences (Figure 2.5).

```
M.edulis        ------------------------------------------------------------
C.gigas         -MNTNREEVVVHWFRHGLRFHDNPSLIDGLSECDRFYPVFIFDGEVAGTKTAGYNRFRFL 59
E.scolopes      MDVKMKKKIAVHWFRRGQRIHDNPALIDALKDCDEFYPIFIFDGKVAGTEICGYNRWRFL 60

M.edulis        -----DLDRNLRKFGGRLYVFHGQPVDILTNLFKEWGVTKLTFEQDPEAVWKQRDDAVKE 55
C.gigas         LECLQDLDKNLKAAGTRLYCFQGQPTDILERLIEEWGVTKVTFEADPEPIWQERDRLVRE 119
E.scolopes      LENLKDLDDTFSQFGGRLYCFHGQPVDIFKNMFEEWGVNYITAEEDPEPIWKERDDSARE 120
                     *** .:   * *** *:***.**: .:::****. :* * ***.:*::**  .:*

M.edulis        LCERKEIECVERVSHTLYEPMKIIEKNDGQPPLTYSLFNLVASALGDPPRPVSYPVFHNI 115
C.gigas         LLDKKNVQCVEKVSHTLWDPYEIIENNGGSPPLTFSLFNLVTSTIGPPPRPVEDPDFTDI 179
E.scolopes      LCEESGITCKFFTSHTLYSPQDIISKNGGTPPLTLELFQLVISSLGDPMRPIPEPNLEGV 180
                * :.. : *   .****:.* .**.:*.* **** .**:** *::* * **:  * : .:

M.edulis        DLPVYPDHEKKFGIPKPQTVGVFPDCKEQNNRINEWKGGESKALDLLEKRLAIEKKAYED 175
C.gigas         SLPVSQNHDKQFGIPTLEDLNVRPECEEQNKRLVEWLGGESKALELLAIRMKHEETAYEN 239
E.scolopes      NMPVPENFEK-FALPNLSYFGIEPECEEQKKPINVFVGGEKRALALLKARLEKEKLFFEQ 239
                .:**  :.:* *.:*. . ..: *:*:**:: :  : ***.:** **  *:  *:  :*:
                                                    FAD-Binding 7
M.edulis        GYVLPN-QYIPDLLGEPMSMSAHLRFGCLSVRRFHWTIHDLFE-----------KVKPKE 223
C.gigas         GYVMPN-QYHPDLLSPPLSLSAHLRFGCLSVRKFYWSIHDKFEEQNTRSTALHFKVKPSI 298
E.scolopes      GSCLPNHQENPELLAKAISLSPYLRFGCVSIRKTYWGICDTYK-----------QVCHKE 288
                *  :** *  *:**. .:*:*.:*****:*:*: :* * * ::          :*  .

M.edulis        SKPDALTCQLIWREYFYVMSANNINYDKMEGNPICLNIPWYRNDEVLKKWEMGQTGYPWI 283
C.gigas         GAPVSLSAQLMWREYFYTMAINNININYDKMETNPICLNIPWYDNPEHEEKWTKGETGYPWI 358
E.scolopes      T-PSEVICQLHWREYFYVMCVGNINFDRIEGNPICLKINWAKNDELLKKWEFGQTGYPWI 347
                  *  : .** ******.*. .***:*::* *****:* *  * *  :**  *:******

M.edulis        DAIMNQLRHEGWIHHVGRHAVACFLTRGDLWISWVDGLKIFLKYLIDADWSVSSGNWMWV 343
C.gigas         DAIMKQLRYEGWVHHVARHAVSCFLTRGDLWLNWEVGLKVFYKYLLDADWSVCAGNWMWV 418
E.scolopes      DAIMNQLRFEGWNHHVGRHAVSCFLTRGDLWISWEEGLKVFLKYQLDADWSVCAGNWMWV 407
                ****:***.*** ***.****:*********:.*  ***:* ** :******.:******
```

```
M.edulis        SSSAFEKVLQCPKCFCPVG---------------------------------------- 362
C.gigas         SSSAFEKVLQCPNCFCPVRYGKRMDPSGEYVRRYLPVLKDMPLRYLFEPWKAPLPVQQKA 478
E.scolopes      SSSAFEKALQCPTCYSPIMYGMRMDRNGEFVRTYLPVLKDMPLKYLFCPWKAPLGVQEKA 467
                *******.****.*:.*:

M.edulis        ----------------------------------------------------------
C.gigas         KCIVGVDYPKPMVDHQKASKECIQNMKAVKDALMGKEIPHCAPSEEIEARRFSWLPDHTP 538
E.scolopes      NCIIGKDYPEPICSHRDMSRENMAKMYKIKEELLKGHIPHCAPTCEMEVWKFVWLP---P 524

M.edulis        ------------------
C.gigas         SGGHCTANFLCDGLKDMN 556
E.scolopes      IEHHEFAHNL-------- 534
```

Fig ık

accession KJ671528) with CRY1 from the Hawaiian bobtail squid *E. scolopes* (AGJ94014) and CRY-like protein from the Pacific oyster *C. gigas* (ACV53158). Symbols are as described for Figure 2.2. Shading denotes a functional protein domain identified based on the *M. edulis* sequence. Abbreviation: FAD, flavin adenine dinucleotide.

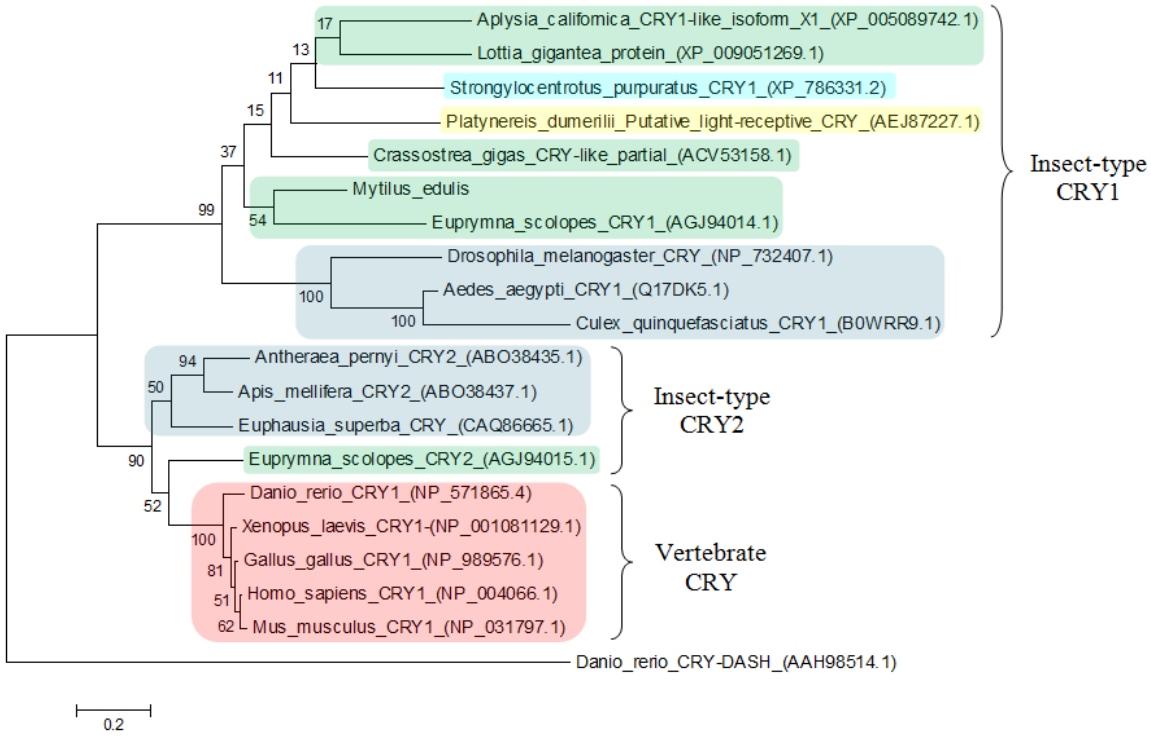

Figure 2.5 Phylogenetic tree of partial CRY amino acid sequences manually edited to a length of 359 amino acids with gaps with 1000 bootstrap replicates. GenBank accession numbers are shown in brackets. Shading represents: molluscs, green; echinoderms, aqua; annelids, yellow; insects, blue; vertebrates, red. A CRY-DASH sequence, another member of the photolyase/cryptochrome protein family, was used as the outgroup.

2.3.1.3 Characterisation of *ARNT*

BLAST search results using the full 2037 bp CDS of *M. edulis ARNT* (Table 2.5) showed matches to *Aryl Hydrocarbon Receptor Nuclear Translocator* (*ARNT*) and *ARNT-like* (*ARNTL*, alternatively known as *Bmal1*) sequences (Table 2.6), two different but closely related genes belonging to the same group of bHLH-PAS transcription factors. A multiple-species amino acid alignment using the translated *M. edulis* sequence revealed coverage of a basic helix-loop-helix (bHLH) domain, two PER-ARNT-SIM (PAS) protein domains and a PAS-associated c-terminal motif (PAC) (Figure 2.6), all characteristic of bHLH-PAS transcription factors.

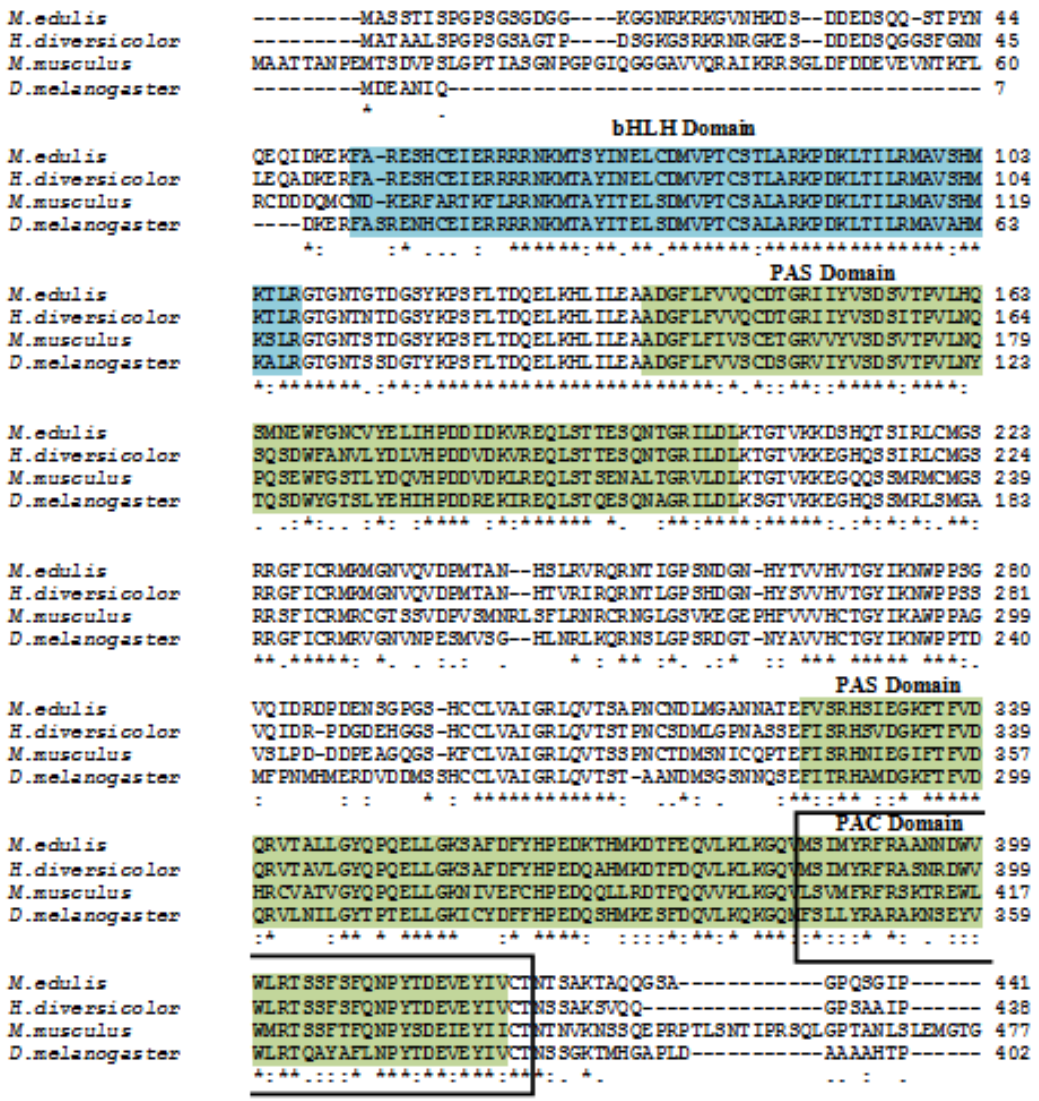

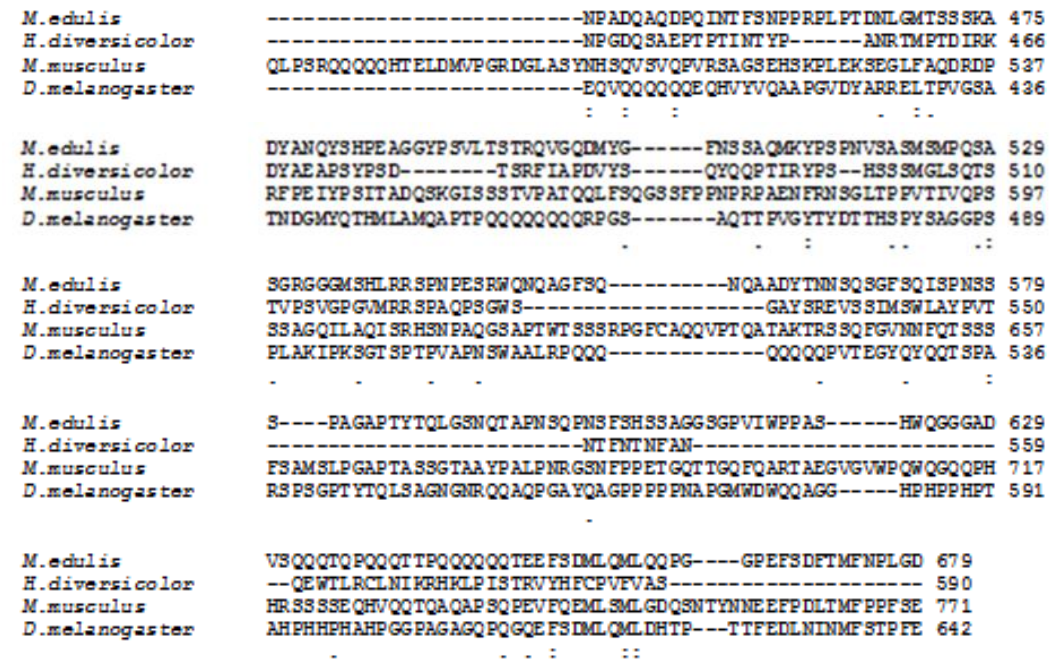

Figure 2.6 Multiple species amino acid alignment of blue mussel *M. edulis* ARNT (GenBank accession KJ671529) with abalone *H. diversicolor* ARNT (AGG55386.1), mouse *M. musculus* ARNT (U14333.1) and fruit fly *D. melanogaster* TANGO (NM_169254.2). Symbols are as described for Figure 2.2. Shaded and boxed areas represent functional protein domains identified in the *M. edulis* sequence. Abbreviations: bHLH, basic helix-loop-helix; PAS, PER-ARNT-SIM; PAC, PAS-associated C-terminal motif.

A phylogenetic tree containing sequences from two closely related bHLH-PAS transcription factor proteins, ARNT/TANGO (TANGO being the insect homolog of ARNT) and ARNTL/BMAL1/CYCLE showed that the *M. edulis* sequence clustered within a group of molluscan ARNT-homologs and was more closely related to other ARNT/TANGO sequences than to the ARNTL/BMAL1/CYCLE sequences, which clearly formed a separate clade (Figure 2.7). This suggests that the *M. edulis* sequence is ARNT; the 70% blastx identity match to *C. gigas* ARNT-like (EKC32806) (Table 2.6) may be the result of confusing gene nomenclature where the suffix "-like" may mean "similar to" rather than in reference to the gene named ARNT-like (*ARNTL*) in its own right, as this sequence is 100% identical to the *C. gigas* ARNT-homolog

sequence (XP_011419459.1) which clustered with the *M. edulis* sequence on the phylogenetic tree (Figure 2.7).

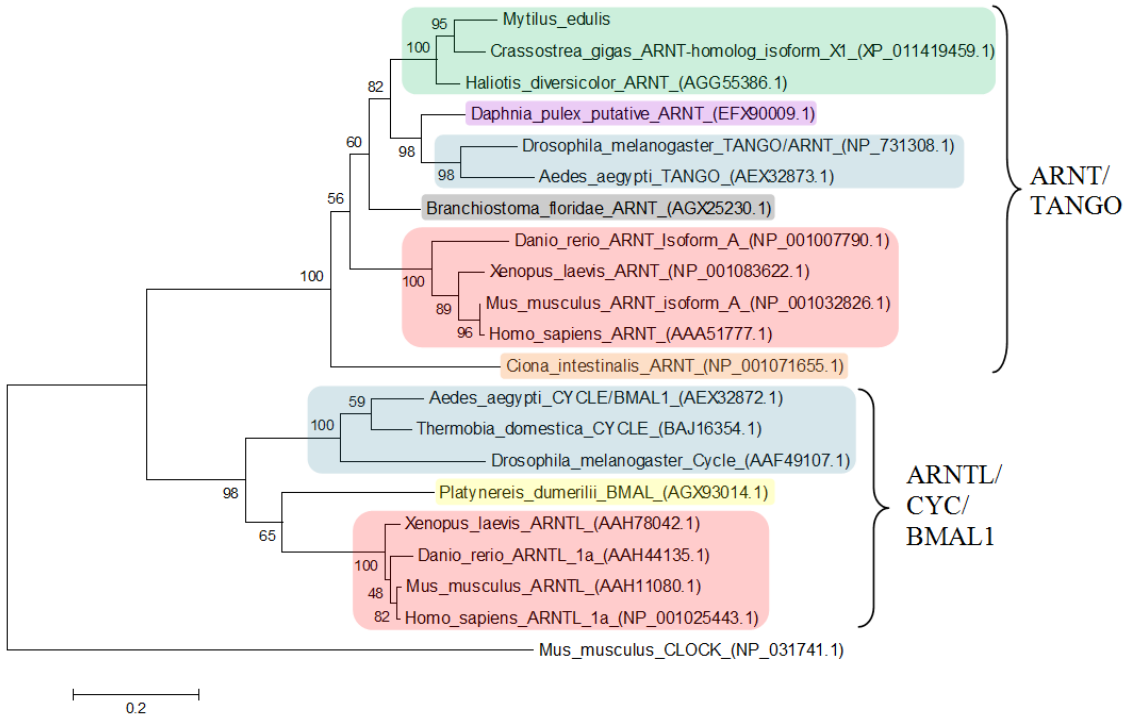

Figure 2.7 Phylogenetic tree of ARNT/TANGO and ARNTL/CYC/BMAL1 amino acid sequences manually edited to a length of 395 amino acids with gaps using 1000 bootstrap replicates with values displayed on the nodes. GenBank accession numbers shown in brackets. Shading represents: molluscs, green; crustacean, purple; insects, blue; grey, lancelet; red, vertebrates; orange, tunicate; yellow, annelid. A CLOCK sequence, another member of the bHLH transcription factor family, was used as the outgroup (unshaded).

2.3.1.4 Characterisation of *M. edulis Tim*-like

BLAST searches using the 851 bp *Timeless-Timeout* family nucleotide sequence (Table 2.5) showed high percentage matches to *Tim* homologs from different mollusc species (Table 2.6). TIM proteins lack conspicuous functional domains however a partial-gene multiple species alignment of molluscan TIM amino acid sequences showed sequence similarities (Figure 2.8).

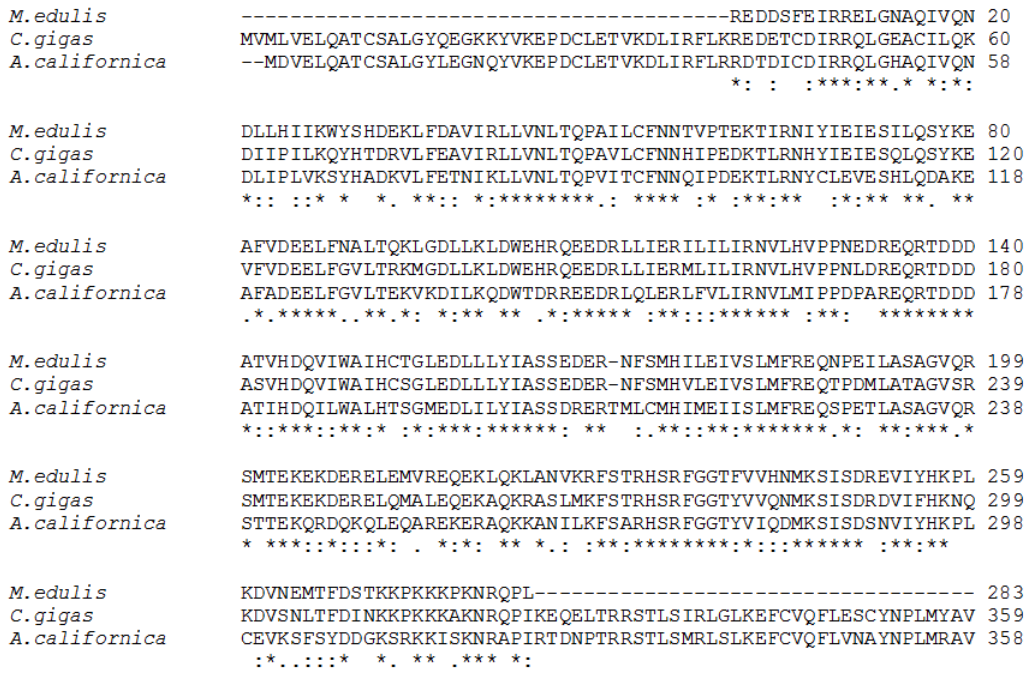

Figure 2.8 Multiple species amino acid alignment of partial *M. edulis* TIM (GenBank accession KX576716) with Pacific oyster *C. gigas* predicted *Timeless* homolog (XP_011441580.1) which has a full length of 1416 amino acids (not shown here in full) and sea slug (*A. californica*) predicted *Timeless* homolog (XM_005099638.1) which has a full length of 685 amino acids (also not shown in full). Symbols as described for Figure 2.2.

A phylogenetic tree of *Tim-Timeout* family protein sequences (TIM and TIMEOUT) shows that the partial *M. edulis* sequence clusters most closely with molluscan TIM homolog sequences, particularly *C. gigas* TIM homolog (XP_011441580.1), and is more closely related to TIMEOUT sequences than to TIM sequences, which form a distinct group which includes *C. gigas* TIM (EKC41755.1) (Figure 2.9). This suggests that the *M. edulis* sequence is TIMEOUT rather than the more ancestral homolog TIM, although the full gene protein sequence would be required in order to more conclusively determine which of the two homologs it bears most similarity to overall.

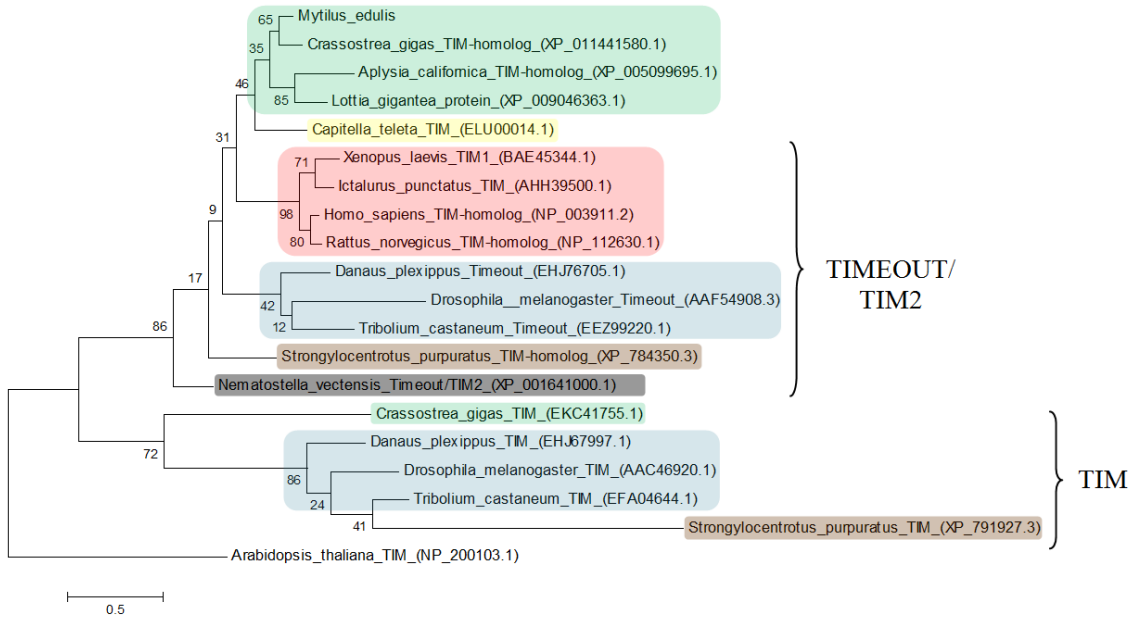

Figure 2.9 Phylogenetic tree of amino acid sequences of the homologs TIM and TIMEOUT manually edited to a length of 293 amino acids with gaps (based on the length of the partial *M. edulis* sequence), using 1000 bootstrap replicates with values displayed on the nodes. Sequence GenBank accession numbers shown in brackets. Shading represents: molluscs, green; annelid, yellow; vertebrates, red; insects, blue; echinoderm, brown; cnidarians, black. A plant TIM sequence was used as the outgroup (unshaded).

2.3.1.5 Characterisation of *ROR/HR3*

The isolated 1825 bp *M. edulis ROR/HR3* sequence, covering the complete CDS (Table 2.5), matched *HR3* sequences from the oyster *C. gigas* evidenced by BLAST searches (Table 2.6). Furthermore, blastn results showed that there was a 92% similarity between the *M. edulis* sequence and *M. californianus RORβ.* A multiple-species amino acid alignment of the conceptually translated *M. edulis* sequence with other invertebrate HR3 amino acid sequences shows coverage of two functional protein domains (a nuclear receptor DNA binding ROR domain and nuclear receptor ligand ROR binding domain-like), placing the sequence within the ROR/HR3 subfamily of nuclear receptors (Figure 2.10).

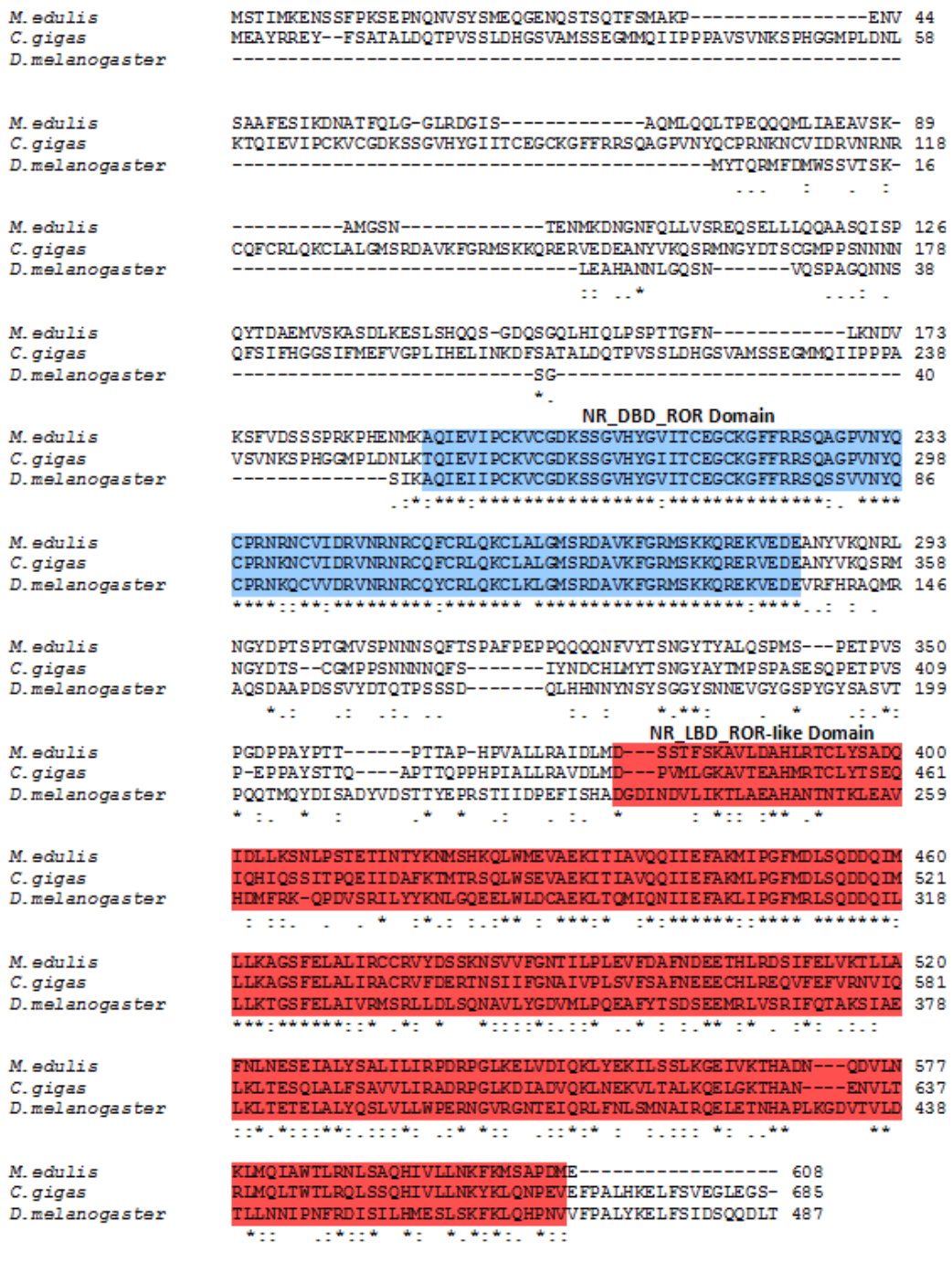

Figure 2.10 Multiple species amino acid alignment of partial *M. edulis* ROR/HR3 (GenBank accession KJ671530) with putative HR3 from the oyster *C. gigas* (EKC18621.1) and *Drosophila* HR3 (DHR3) from the fruit fly *D. melanogaster* (AAA28461). Symbols as described for Figure 2.2. Shading represents functional protein domains. Abbreviations: NR_DBD_ROR, Nuclear Receptor DNA-Binding Domain of Retinoid Orphan Receptors; NR_LBD_ROR-like, Nuclear Receptor Ligand-Binding Domain of Retinoid Orphan Receptors.

A phylogeny including invertebrate HR3 amino acid sequences and vertebrate RORα, RORβ and RORγ sequences, showed that *M. edulis* ROR/HR3 clustered with other mollusc sequences. Vertebrate RORs and insect HR3 grouped separately (Figure 2.11).

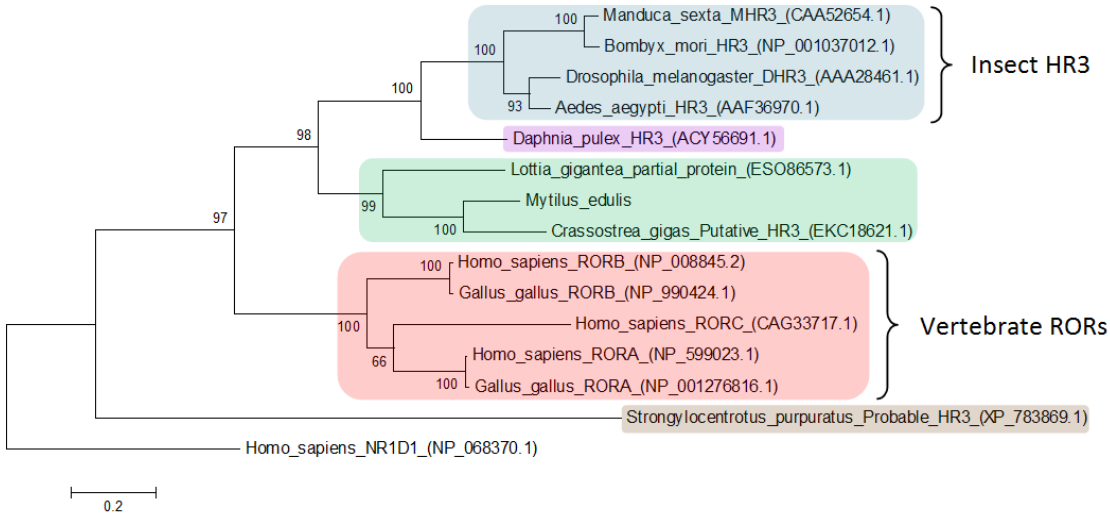

Figure 2.11 Phylogenetic tree of partial ROR/HR3amino acid sequences manually edited to a length of 450 amino acids with gaps with 1000 bootstrap replicates (See Section 2.2.17.3). Sequence GenBank accession numbers shown in brackets. Shaded boxes represent: insects, blue; crustacean, purple; molluscs, green; vertebrates, red; echinoderm, brown. The nuclear receptor gene *NR1D1* which encodes the protein Rev-ErbA alpha was used as the outgroup.

2.3.1.6 Characterisation of *M. edulis aaNAT*

A 540 bp nucleotide sequence covering the full CDS was obtained for *M. edulis aaNAT* (Table 2.5), which conceptually translates to a 179 amino acid sequence. Blastx searches revealed the amino acid sequence shared 49% similarity with the marine ragworm *P. dumerilii* Arylalkylamine N-acetyltransferase, 50% with a marine lancelet (amphioxus) *B. floridae* N-Acyltransferase superfamily protein, and 47% with a *C. teleta* N-Acyltransferase superfamily protein (Table 2.6). Furthermore, there was found to be a 98.9% amino acid sequence similarity between the *M. edulis* sequence and the *M. galloprovincialis* sequence from which the PCR primers were originally

designed (GenBank accession FL488956.1). Coverage of an Acetyltransferase/GNAT domain was detected in the *M. edulis* sequence and the multiple-species amino acid alignment shows that, even among only invertebrates, there are low levels of homology overall between protein sequences (Figure 2.12).

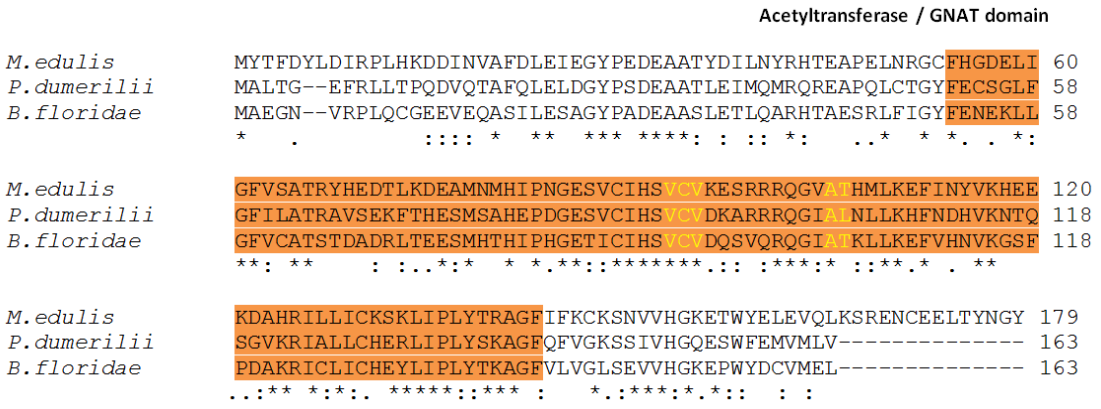

Figure 2.12 Multiple species alignment of the full CDS of *M. edulis* aaNAT amino acid sequence (GenBank accession KX576715) with lancelet *B. floridae* protein (XP_002608038.1) and marine ragworm *P. dumerilii* arylalkylamine N-acetyltransferase (AIT11917.1). Symbols as described for Figure 2.2. The shaded area shows coverage of the Acetyltransferase/GNAT domain in the *M. edulis* sequence and the coloured text shows a Coenzyme A (CoA) binding pocket.

A phylogenetic tree of aaNAT protein sequences shows that, as expected, the *M. edulis* sequence groups with that of *M. galloprovincialis* (Figure 2.13). Insects are clearly shown to form their own clade, which does not contain sequences from other invertebrates. Vertebrate aaNAT sequences also form their own clade, with the exception of cartilaginous fish that are distinct and are shown to group separately.

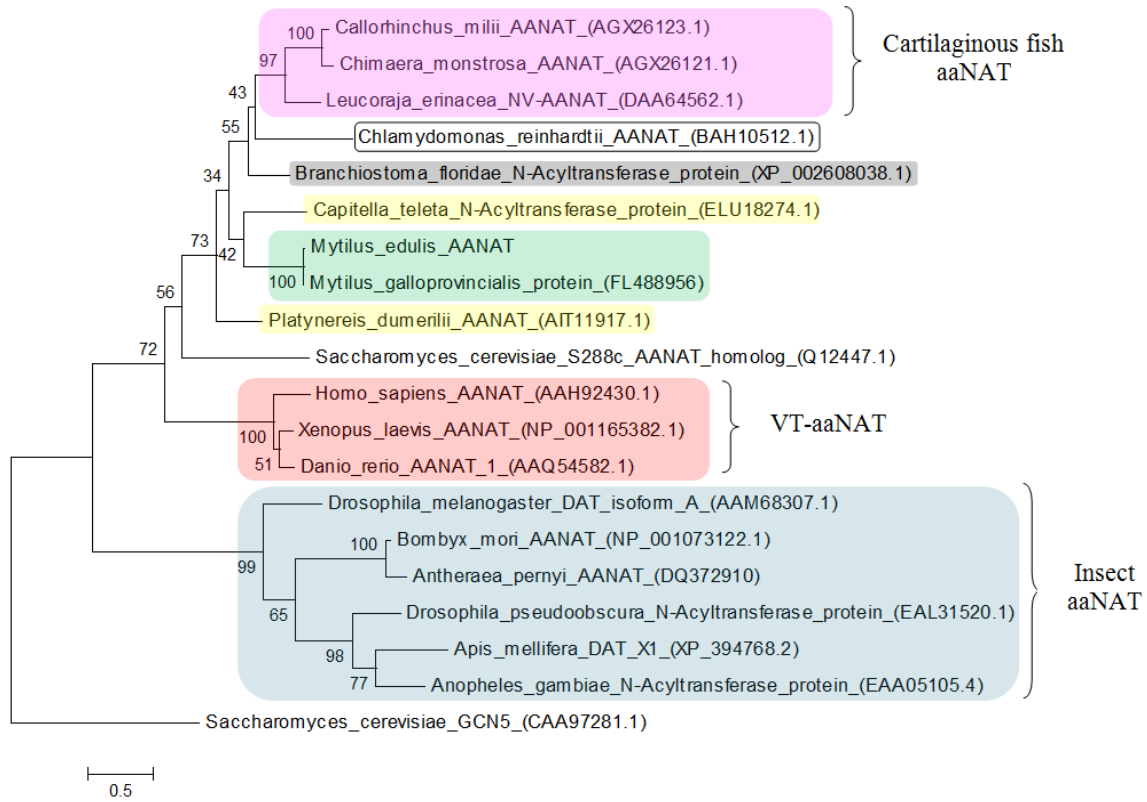

Figure 2.13 Phylogenetic tree generated using the full amino acid sequences of aaNAT homologs from different species manually edited to a length of 231 amino acids with gaps with 1000 bootstrap replicates. GenBank accession numbers shown in brackets. Shaded boxes represent cartilaginous fish, pink; plants, white; lancelets, grey; annelids, yellow; unshaded, yeast; molluscs, green; vertebrates excluding cartilaginous fish, red; insects, blue.

2.3.2 Protein extraction comparison

A comparison made between total protein extractions from *M. edulis* gonad tissue dissected from a single individual but stored under different conditions, indicated the suitability of tissue stored in RNAlater solution at -80 °C in particular for protein extraction, as demonstrated by the strong staining on a Coomassie blue stained SDS PAGE gel (Figure 2.14).

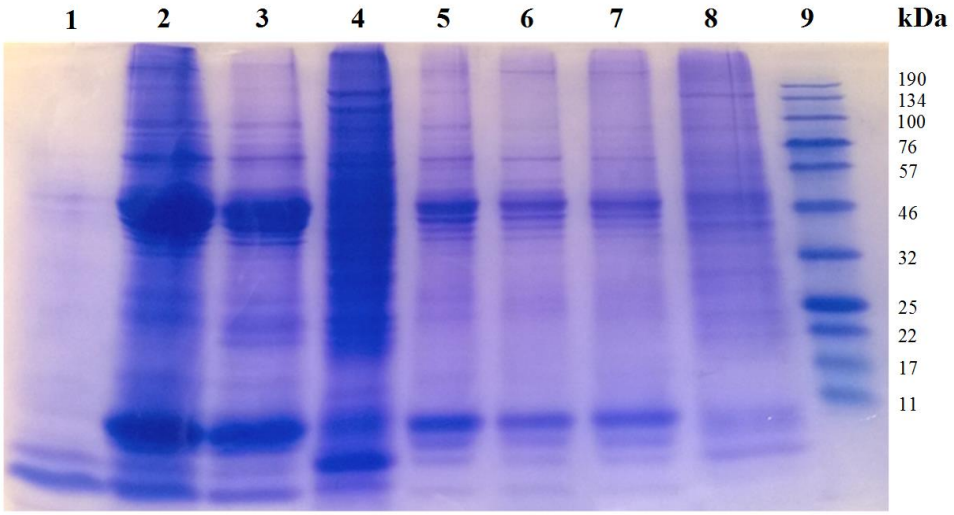

Figure 2.14 SDS-PAGE gel (12%) loaded with 5 µg protein per well and stained with Coomassie blue R-250. Lanes 1-3 show PBS extractions from mussel tissue stored in TRI reagent (-80 °C), RNALater (-80 °C) and no buffer (-20 °C) and lanes 5-7 show the corresponding insoluble cell-pellet extractions using 1% SDS. Lane 4 is a positive control PBS extraction from rat liver and lane 8 is the corresponding cell-pellet extraction. Lane 9 shows the broad-range pre-stained protein marker (7-175 kDa) (New England Biolabs, UK).

2.3.3 Western blotting to detect clock proteins

As antibodies for mollusc clock genes are not commercially available to be tested, antibodies designed to detect human clock genes were tested against protein extractions from mussel (*M. edulis*), as well as rat (*R. norvegicus*) and fruit fly (*D. melanogaster*), to test cross-species reactivity using Western blotting. Cross-species reactivity with at least one species was detected by CLOCK, CRY1, BMAL1 and TIMELESS, but not ROR2 (Figure 2.15; Table 2.7). In particular, a mussel protein of ~76 kDa was detected by the CLOCK antibodies (Figure 2.15b) and a protein of ~108 kDa was detected by the TIMELESS antibodies (Figure 2.15e), both of which are consistent with the molecular weights predicted for Pacific oyster *C. gigas* (Table 2.7); the full *M. edulis* amino acids sequences are unavailable. Both of these proteins were only detected in the soluble protein extract and not the insoluble faction (Figure 2.15b,

e). This was also the case for a ~47 kDa protein detected in *D. melanogaster* by BMAL1 antibodies (Figure 2.15d). Proteins consistent with the predicated molecular weight of CLOCK, CRY1 and BMAL1 from *R. norvegicus* were detected in both protein extraction factions (Figure 2.15b-d).

Table 2.7 Predicted molecular weights of clock gene proteins (kDa) in mussel, rat and fruit fly based on amino acid sequence composition with GenBank accession numbers given. Where full protein sequences were unavailable, predictions were based on *C. gigas** and *Drosophila serrata*†. Proteins consistent with these sizes identified by Western blotting are highlighted in grey.

	Predicted size (kDa)		
Protein	Mussel	Rat	Fruit fly
CLOCK	**~76.69*** KX371073.1	**97.04** AB019258.1	**116.19** AF069997.1
CRY1	**~63.24*** KT991835.1	**66.24** NM_198750.2	**62.52** AF099734.1
BMAL1	**~73.29*** KX371075.1	**68.68** NM_024362.2	**47.56** AF067206.1
TIMELESS	**~108.37*** KX371077.1	**138.59** NM_031340.1	**155.69** U37018.1
ROR2	**~97.18*** XP_011441184.1	**105.04** NM_001107339.1	**~82.07†** XM_020959253.1

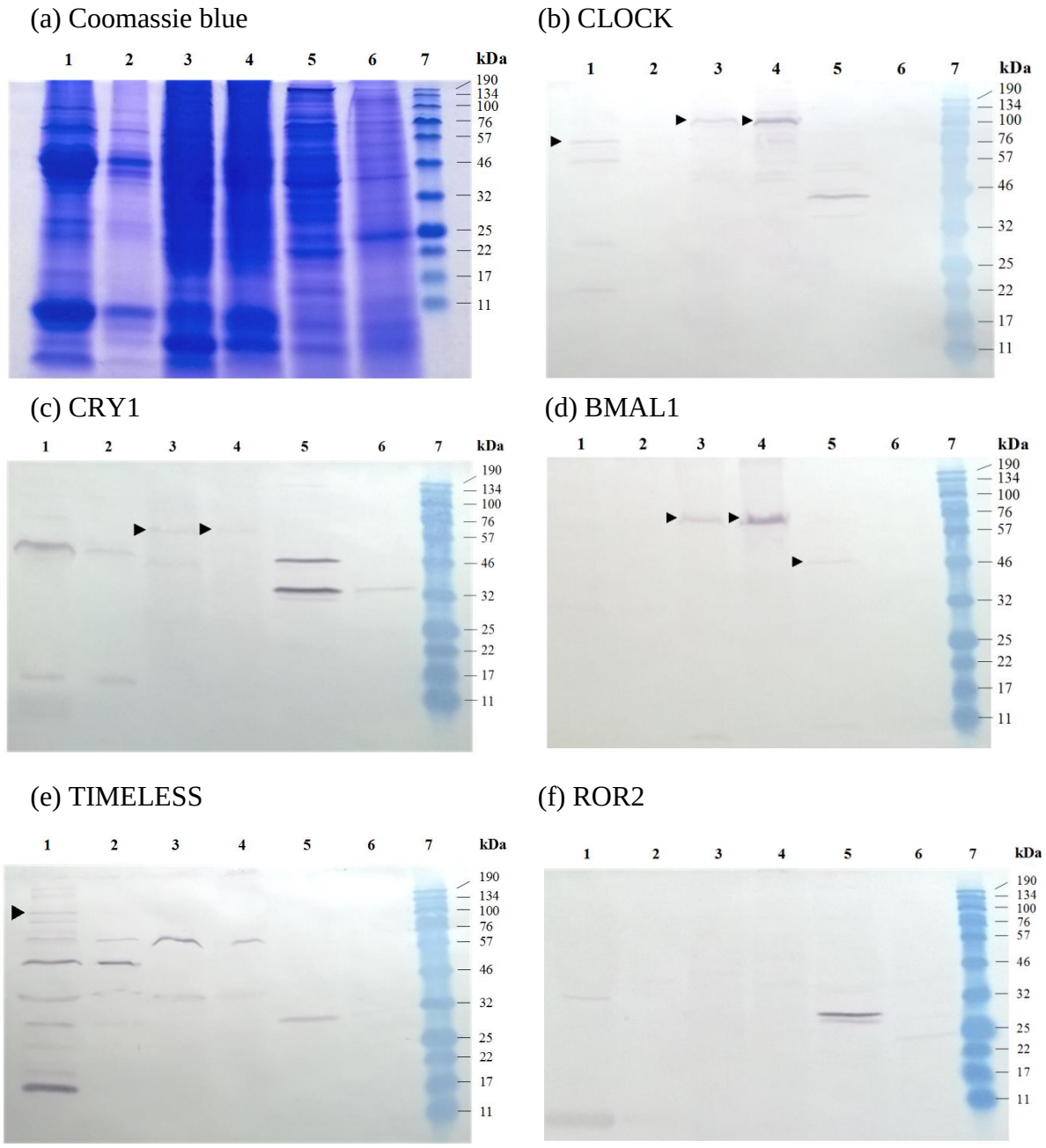

Figure 2.15 SDS PAGE gel showing total proteins stained with (a) Coomassie blue and Western blots showing reactivity of antibodies for human (b) CLOCK, (c) CRY1, (d) BMAL1, (e) TIMELESS and (e) ROR2 with aqueous and non-aqueous protein extraction fractions from *M. edulis* (lanes 1-2 respectively), rat liver (lanes 3-4) and whole *D. melanogaster* (lanes 5-6) alongside broad-range pre-stained protein marker (7-175 kDa) (New England Biolabs, UK). Arrowheads indicate bands consistent with the predicted molecular weights.

2.4 DISCUSSION

In this chapter, genes with putative molecular clock function were isolated from the blue mussel *M. edulis* for the first time as follows: *Clk, Cry1, ARNT, Timeout*-like, *ROR/HR3* and *aaNAT* (Table 2.5). Gene identities were confirmed by BLAST sequence comparison searches, multiple species amino acid alignments and construction of phylogenetic trees (Section 2.3). Furthermore, Western blotting detected *M. edulis* proteins consistent with the predicted molecular weights of CLOCK and TIMELESS (Figure 2.15; Table 2.7). Each gene will be discussed briefly in turn.

The *Clk* sequence isolated from *M. edulis* in this chapter (Table 2.5) shared a high degree of similarity with *Clk* from *M. californianus* (93%) and other bivalves (Table 2.6). The sequence encoded PAS domains characteristic of the bHLH-PAS family (Figure 2.2) and, like other mollusc CLK sequences, grouped closer phylogenetically to vertebrate sequences than insects (Figure 2.3). *Clk* is crucial to circadian function in diverse phyla as it is a key component of the transcription-translation interactions at the heart of the molecular clock mechanism (Allada et al, 2001).

The partial *M. edulis* cryptochrome sequence isolated here, encoded part of a FAD-Binding 7 protein domain (Figure 2.4) characteristic of flavoproteins, of which cryptochromes are a class (Cashmore et al., 1999). The conceptually translated sequence was most similar to *C. gigas* CRY1 (Table 2.6) and clustered with invertebrate CRY1 homologs on the phylogenetic tree rather than with insect-type CRY2 or vertebrate-type CRY sequences (Figure 2.5). This indicates a greater degree of shared sequence similarity between *M. edulis* CRY1 and insect CRY1 (Type I cryptochrome), encoding a photosensitive signal molecule that relays environmental light information to the clock mechanism (Peschel et al., 2009), than to vertebrate

CRY (Type II cryptochrome) which acts as a light-independent core clock component (Griffin et al., 1999). Other types of cryptochromes that have been identified in molluscs based on sequence similarities include *Cry2* (Heath-Heckman et al., 2013), *Cry5* believed to encode a 6–4 photolyase enzyme (Haug et al., 2015), and *Cry6* which is specific to invertebrates (Haug et al., 2015).

The full CDS of a second gene encoding a bHLH protein was isolated from *M. edulis* (Figure 2.6), which showed a high degree of similarity to mollusc *ARNT* homologs (Table 2.6). Phylogenetic analysis of the *M. edulis* sequence revealed grouping among ARNT and its *Drosophila* homolog TANGO, whereas sequences for BMAL1/ARNT-LIKE and its insect homolog CYC grouped separately (Figure 2.7). This evidence supports the identification of the *M. edulis* gene as *ARNT*. Of the three mammalian *ARNT* isoforms, *ARNT1* and *ARNT2* encode homologous proteins with the same functions, whereas *Bmal1/ARNT-like* (*ARNTL*) shares less sequence homology and its protein dimerises with fewer partners, CLK being one such example (Brunnberg et al., 2003). The multiple bHLH-PAS partners of mammalian ARNT1 and 2 include the ligand-activated AhR, involved in xenobiotic response, the hypoxia inducible factor alpha (HIF-α) involved hypoxia response, and the single-minded (SIM) protein linked to neural development (Kewley et al., 2004). Gene sequences of these ARNT partner-proteins have also previously been isolated from bivalves as follows: *AhR* (Butler et al., 2004; Liu et al., 2010; Zhou et al., 2010), *HIF-α* (Piontkivska et al., 2011) and SIM (XM_011422636.1).

The partial Timeless-Timeout family sequence isolated from *M. edulis* herein (Table 2.5) grouped among TIMEOUT/TIM2 sequences when translated, rather than with the distinct TIM group (Figure 2.9), supporting the identification of the gene as *Timeout*-like. Both *Timeless* and *Timeout*/*Tim2* paralogs occur in molluscs including

L. gigantea and *C. gigas* as a result of gene-duplication before the protostome-deuterostome divergence, with subsequent gene loss of one or more paralog evident in more recently evolved phyla such as chordates (Reitzel et al., 2010). Mammalian *Tim* (*mTim)* is actually thought to be a homolog of *Drosophila Timeout* (Reitzel et al., 2010) explaining the non-circadian vs. circadian roles respectively. Both genes are of developmental importance with experimental disruption resulting in embryonic lethality in mice (Gotter et al., 2000), worms (Chan et al., 2003) and *Drosophila* (Benna et al., 2010). Whereas *Tim* is involved in the core-clock interactions of many insects (Pavelka et al., 2003; Tomioka et al., 2012) *mTim* is not expressed rhythmically and is involved in responding to replication fork damage during DNA synthesis (Gotter et al, 2007), assisting chromosome cohesion (Benna et al., 2010; Errico and Costanzo, 2010) and embryonic cell death (O'Reilly et al., 2011). However, additional evidence points towards *Timeout* involvement in the circadian clock too. In mammals, the longer of the two *mTim* isoforms can bind with both PER (Barnes et al., 2003) and CRY1 (Engelen et al., 2013), and downregulation of mTIM results in an altered period for the cells (Engelen et al., 2013). Furthermore, *Drosophila Timeout* is thought to play a role in light entrainment of the circadian clock (Benna et al., 2010).

HR3, encoding an invertebrate orphan nuclear receptor, is the ortholog of the *ROR*s found in vertebrates (Giguère et al., 1994). The *ROR/HR3* sequence isolated from *M. edulis* (Table 2.6) matched other bivalve *HR3* sequences (Figure 2.11) and contained the characteristic DNA and ligand binding domains (Figure 2.10). *HR3* is mainly involved in regulating moulting-hormone pathways in insects (Carney et al., 1997), nematodes (Kostrouchova et al., 2001) and crustaceans (Hannas and LeBlanc, 2010) as its expression is induced by the molting/sex hormone ecdysteroid. It is also essential for insect embryogenesis (Carney et al., 1997). ROR is required for normal

circadian function in vertebrates as its interaction with *Bmal1* forms a transcription-translation feedback loop of the core clock mechanism (Jetten, 2009; Guillaumond et al., 2005). This function is not exclusive to vertebrates as, *HR3* and *E75* rhythmicity are required for locomotor rhythms in the insect *T. domestica*, with *HR3* disruption altering the expression patterns of *Cyc*, *Tim*, and *Clk* (Kamae et al., 2014). This is consistent with the roles of the vertebrate orthologs of *HR3* (*ROR*) and *E75* (*Rev-Erb*) (Jetten, 2009).

Finally, the full CDS of *M. edulis aaNAT* was isolated (Table 2.5; Table 2.6), covering an Acetyltransferase/GNAT domain characteristic of the gene family (Figure 2.12). The conceptually translated sequence grouped closest to non-insect invertebrate sequences, with insects, cartilaginous fish, and other vertebrates forming distinct clades (Figure 2.13). This is consistent with previous findings that the vertebrate version of the gene, *VT-aaNAT*, arose from a duplication event, and evolved separately from the more ancestral *NV-aaNAT* (Falcón et al., 2014), with a distinct isoform forming a separate clade in cartilaginous fish (Cazaméa-Catalan et al., 2014). *aaNAT* is involved in circadian melatonin synthesis in vertebrates (Foulkes et al., 1997) and is also a CCG linking photoperiodism with the endocrine system in some insects (Mohamed et al., 2014), however the *M. edulis* aaNAT sequence does not cluster with these groups (Figure 2.13). Circadian function has been dismissed for *aaNAT* from the lancelet *B. floridae* in favour of detoxification and neurotransmitter functions, as its expression does not cycle rhythmically and there is no evidence of melatonin or melatonin receptors in the species (Pavlicek et al., 2010). This, however, contrasts with molluscs as melatonin, including rhythmically fluctuating content, has been documented, as have melatonin receptor sequences (Abran et al., 1994; Blanc et al., 2003; Muñoz et al., 2011).

Western blotting using human antibodies revealed cross-species reactivity with *M. edulis* in the case of CLOCK and TIMELESS antibodies where ~76 kDa and ~108 kDa proteins were detected respectively (Figure 2.15). These proteins were consistent with the predicted molecular weights (Table 2.7), though other sized bands were also obtained (Figure 2.15). No consistent proteins were detected in *M. edulis* for CRY1, BMAL1 or ROR2 using this non-species specific antibody approach (Figure 2.15; Table 2.7). The development of species-specific antibodies would therefore be a valuable tool to isolate and quantify mussel clock proteins in the future.

2.5 CONCLUSIONS

The relationship between rhythmic biological processes and external environmental cycles is a little studied aspect of bivalve ecology despite the ecological and commercial importance of many bivalve species. In this chapter, *Clk*, *Cry1*, *ARNT*, *Timeout*-like, *ROR/HR3* and *aaNAT* sequences were isolated from the blue mussel, *M. edulis*, for the first time. The isolation of these circadian rhythm-related genes is the first step in identifying the putative components of the mussel circadian pacemaker. *M. edulis* proteins consistent with the anticipated molecular weights of CLOCK and TIMELESS were also detected. As such, this work provides a foundation for the further characterization of the blue mussel clock mechanism, which is expanded upon by investigating quantitative gene expression patterns in subsequent chapters.

Chapter 3

Development of quantitative real-time qPCR assays for circadian rhythm-related genes and reference genes from seasonally sampled *M. edulis*

3.1 INTRODUCTION

The mechanisms regulating circadian timekeeping operate on a molecular level, with rhythmic clock gene mRNA expression being an essential component. Quantification of clock mRNAs has revealed temporal and spatial expression patterns and has helped characterise the molecular clock mechanisms of diverse organisms (Allada et al., 2001). Quantitative Real-Time PCR (qPCR) is a powerful molecular technique allowing the detection and quantification of nucleic acids including mRNA. The benefits of this widely-used approach include a high degree of specificity and sensitivity over a wide dynamic range, producing reproducible results (Wong and Medrano, 2005). The approach is preferable to other techniques such as RNase protection assays and Northern blotting analysis as more detailed real-time data is generated, rather than end-point data, and even low abundance RNAs can be quantified in a time-efficient manner (Wang and Brown, 1999).

A number of different detection chemistries have been developed for qPCR including non-sequence-specific DNA binding dyes and different types of fluorescently labelled sequence-specific probes or primers (VanGuilder et al., 2008;

Wong and Medrano, 2005). SYBR Green I detection, one of the most commonly used approaches, utilises a dye molecule which fluoresces when intercalated with dsDNA, allowing fluorescence data to be used as a proxy for target DNA content. This technique has the advantage of being cost-effective to set up and run, as expensive sequence-specific fluorescent probes are not required, and it is flexible as the same dye reagent can be used to measure the expression of different target genes (VanGuilder et al., 2008). Furthermore, qPCR may be performed as either a one-step or a two-step reaction; cDNA synthesis and PCR may occur in a single protocol or be carried out separately. The two-step method, though more time consuming, minimises the handling of temperature-sensitive RNA and provides greater flexibility in terms of assay optimisation (Wong and Medrano, 2005). In all cases, the quantitative data are generated during the exponential phase of qPCR where an optimised reaction will experience a doubling of target DNA with each thermal cycle; Ct values (also known as Cq values) are the cycle at which a sample's exponential amplification crosses a threshold set above background fluorescence levels (Bustin et al., 2009).

An important consideration of qPCR assay optimisation is that the quality and integrity of the RNA must be as high as possible to ensure a high degree of accuracy (Bustin et al., 2009). RNA concentrations should be quantified and standardised for all samples (Bustin et al., 2009). Additionally, due to the non-specific nature of SYBR Green I-dsDNA intercalation, any dsDNA present will indiscriminately contribute to detectable fluorescence in SYBR reactions. It is therefore essential to the validity of the technique that SYBR Green I qPCR reactions are highly optimised to eliminate the presence of non-target DNA (Bustin et al., 2009). It is for this reason that the sample preparation method used prior qPCR must include a step to digest genomic

DNA and qPCR reactions must include sequence-specific primers with no propensity to self-anneal or to form hairpin structures (Taylor et al., 2010). Furthermore, primer and cDNA concentrations must be carefully selected to avoid creating reaction conditions where non-specific primer-binding, such as that which results in primer dimers, is likely to occur. Non-template negative controls must therefore be included alongside the samples of each run to confirm the absence of amplification including a lack of dimer formation and a lack of contamination. Melt curves must also be generated for all samples at reaction completion to confirm the successful amplification of the single desired qPCR product and the absence of non-specific primer binding. This is achieved by heating the DNA over a range of temperature increments and measuring the temperature at which fluorescence decreases, indicative of the dye dissociating from the denatured dsDNA (BioRad Laboratories, 2006). Also, to reduce any potential variation in the fluorescence that is detected, the qPCR machine, plates and plate-seals used should also be standardised for all samples (Bustin et al., 2009).

The relative quantification approach to qPCR is a widely-used method whereby expression levels for each gene of interest are normalised with stably-expressed reference genes. This counteracts the contribution of any variation in reverse-transcription efficiency between samples and allows comparisons of total relative gene expression levels between different treatments to be investigated (Hruz et al., 2011). This approach provides biologically relevant data without the need to quantify absolute values, however selection of reliable reference genes is integrally important to the method and their suitability in the relevant tissues from organisms exposed to each of the experimental treatment conditions must be verified (Bustin et al., 2009). The use of combined data from multiple reference genes is recommended

to improve accuracy (Vandesompele et al, 2002). Relative quantification is commonly performed by using the comparative Ct method, also known as the $2^{-\Delta\Delta Ct}$ method (Livak and Schmittgen, 2001), or one of its variations such as the $2^{-\Delta Ct}$ method (Schmittgen and Livak, 2008). An assumption of these approaches, which must be satisfied, is that the efficiency of the primer pairs used to detect both the genes of interest and the reference genes are the same; efficiencies are ideally as close to 100% as possible, indicating an exponential increase in template with each PCR cycle. This can be demonstrated by creating standard curves based on fluorescence values generated over a template cDNA dilution series, ideally spanning at least three orders of magnitude (Bustin et al., 2009; Taylor et al., 2010). Differences in PCR efficiency would mean that the ratio of expression of the gene of interest and the reference gene would not be the same at different template concentrations, leading to inaccuracies (Bustin et al., 2009) and must therefore be avoided.

The aim of this chapter is to develop and optimise qPCR assays for seasonally-collected wild *M. edulis* circadian rhythm-related genes: *Clock, Cry1, ARNT, Timeout*-like, *ROR*/*HR3* and *aaNAT*. Stable reference genes will also be selected and optimised. The rationale and application of these optimised qPCRs as a tool to investigate seasonal variation in *M. edulis* clock gene expression is discussed at length in Chapter 4. In brief, natural photoperiod progression can confer seasonal information by influencing clock gene expression patterns (Herrero and Lepesant 2014; Ikeno et al., 2010; Tournier et al., 2003). For example, seasonal photoperiod differences modulate the expression of *Clk*, *Bmal1*, *Per2*, and *Cry2* in Atlantic salmon, *Salmo salar*, (Davie et al., 2009) and the same genes in addition to *Per1*, *Per3* and *Cry1* are also modulated by photoperiod in the core clock of the hamster (Tournier et al., 2003). Photoperiod and latitude also affect the circadian oscillation patterns of

Clk, *Cyc*, *Per* and *Cry2* in the wasp *Nasonia vitripennis* (Benetta et al., 2019). Sampling wild mussels exposed to short and long photoperiods (winter and summer solstices) will allow the seasonal expression patterns of *M. edulis* clock genes to be investigated for the first time, as presented in Chapter 4.

3.2 MATERIALS AND METHODS

3.2.1 Sample collection

Wild adult blue mussels, *M. edulis* were collected from the intertidal zone at low tide from Filey Bay, North Yorkshire, UK (54° 13' longitude and 0° 16' latitude) in winter (20/22.12.14), spring (18/20.03.15), summer (14/16.06.15) and autumn (11/13.09.15) (Figure 3.1). Full details of the sampling regime and rationale are given in Chapter 4, Section 4.2.1.

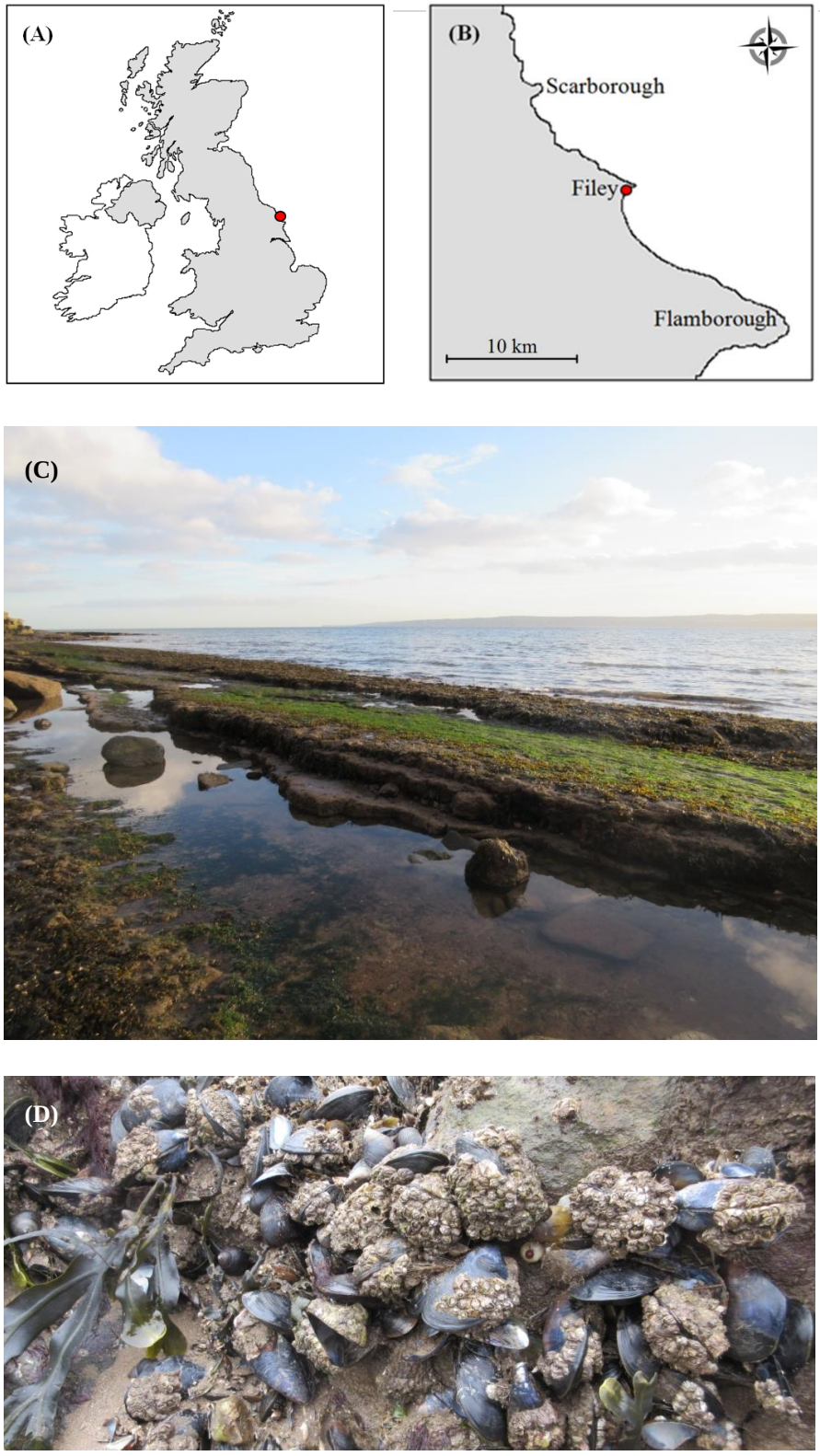

Figure 3.1 The sampling site at Filey Beach Brigg, North Yorkshire, UK (54° 13' longitude and 0° 16' latitude) on a map of (A) the UK and (B) the North Yorkshire coast. Photographs of (C) the intertidal zone sampling site and (D) blue mussels, *M. edulis*, attached to a rocky substrate.

3.2.2 Mussel dissection, tissue storage and species identification

The length of each mussel was measured before ~1 cm^3 portions of mantle tissue were dissected and stored for subsequent analyses as follows: in 1 mL of neutral buffered 10% formalin solution (Sigma Aldrich, Gillingham, UK) at room temperature to preserve tissue for histological determination of sex and gametogenesis stage for samples from all seasons (see Chapter 4, Section 4.2.2), in 1 mL RNA*later* solution (Ambion, Life Technologies, USA) at -20 °C to preserve RNA for molecular analyses for winter and summer samples, and in 1 mL TRI Reagent® (Sigma Aldrich, UK) at -20 °C to preserve proteins in winter and summer samples. In each case, the same portion of gonad tissue was removed from each mussel for each type of analysis to minimise variation resulting from potential tissue heterogeneity. Mussel mantle tissue was selected for analysis in order to examine seasonal clock gene expression patterns in the tissue which houses the seasonally developing gonads – a biological rhythm operating on an infradian (greater than 24 hr) timescale (Seed, 1969). Species identification was determined by performing PCR on *mfp-1* for a random 5% of the sample set as previously described (Section 2.2.6). Samples were confirmed as being *M. edulis*.

3.2.3 Total RNA extraction and concentration

Samples from winter and summer were used for molecular work and were randomly numbered for blind analysis. Tissue samples were not thawed until immediately prior to the RNA extraction procedure to avoid freeze-thaw RNA degradation, and the maximum number of extractions performed in one batch was 16 which is within the range of 10-20 recommended by Taylor et al. (2010), to reduce the time spent working with these sensitive samples. Total RNA isolation was performed

on *M. edulis* mantle tissue that had been preserved in RNA*later* solution (Qiagen Ltd., UK), using the High Pure RNA Tissue Kit (Roche, UK) as previously described (Section 2.2.2.) The protocol included a DNase I digestion step to digest genomic DNA. RNA integrity was checked for a random 5% subset of samples using a denaturing FA gel (Section 2.2.4). RNA concentrations were measured using the Qubit 1.0 Fluorometer (Life Technologies, UK) as previously described (Section 2.2.3.). RNA was successfully extracted from all samples with concentrations ranging from 20 ng/µL to 1020 ng/µL.

3.2.4 cDNA Synthesis for gene expression analysis

A two-step qPCR procedure was used where cDNA was synthesised prior to performing the qPCR reactions. cDNA was synthesised using the Transcriptor High Fidelity cDNA Synthesis Kit (Roche, UK) according to the manufacturer's instructions. To standardise the samples as recommended (Bustin et al., 2009), the same concentration of RNA (190 ng) was used for all cDNA reactions. RNA was combined with 2 µL 600 pmol/µL random hexamer primers and PCR-grade water to a total volume to 11.4 µL. This template-primer mix was then denatured by heating at 65 ^{o}C for 10 min in a thermal cycler and then immediately chilled on ice. The following reagents were then added: 4 µL 5X concentrated Transcriptor High Fidelity Reverse Transcriptase Reaction Buffer (250 mM Tris/HCl, 150 mM KCl, 40 mM $MgCl_2$, pH approx. 8.5 at 25 ^{o}C), 0.5 µL Protector RNase Inhibitor (40 U/µL) (in a storage buffer containing 20 mM HEPES-KOH, 50 mMKCl, 8 mM dithiothreitol (DTT), 50% glycerol (v/v), pH approx. 7.6 at 4 ^{o}C), 2 µL dNTP mix (10 mM each), 1 µL 0.1 M DTT, and 1.1 µL Transcriptor High Fidelity Reverse Transcriptase (9.09 U/µL) (in a storage buffer containing 200 mM potassium phosphate, 2 mM DTT, 0.2%

Triton X-100 (v/v), 50% glycerol (v/v), pH approx. 7.2). After brief mixing, samples were incubated as follows: 29 ºC for 10 min, 48 ºC for 60 min and 85 ºC for 5 min before chilling at 4 ºC. Samples were then stored at -20 ºC.

3.2.5 qPCR primer design and selection

As qPCR works well with small amplicon sizes (Bustin et al., 2009), new primers were designed from the sequences obtained from the six genes of interest (*Clk*, *Cry1*, *ARNT*, *Timeout*-like, *ROR/HR3* and *aaNAT*) in the previous chapter. The online tool Primer-BLAST (http://www.ncbi.nlm.nih.gov/tools/primer-blast/) was used to generate gene- and species-specific primers with an optimum annealing temperature in close to 60 ºC. The reference genes selected for validation were e*longation factor 1-alpha* (*EF1α*), *alpha tubulin* (*TUB)*, and *18S* which have previously been validated in wild-caught UK *M. edulis* at different stages of gametogenesis, based on their stable gene expression in the gonads (Cubero-Leon et al., 2012). Primer sequences for *EF1α* and *TUB* were designed by Cubero-Leon et al. (2012) and for *18S* by Ciocan et al. (2011). Although *β-actin* is commonly used as a reference gene, its variable expression levels detected in the gonads of seasonally collected *Mytilus* mussels in previous studies makes it an unreliable choice (Jarque et al., 2014; Cubero-Leon et al., 2012) and it is therefore not considered here. Lyophilised primers (IDT, Belgium) were resuspended in molecular grade water (Fisher Scientific, UK) to a concentration of 100 µM prior to being aliquoted and stored at -20 ºC.

Table 3.1 qPCR primers for *M. edulis* genes of interest and reference genes.

Gene of interest	Primer	Sequence (5'-3')	Tm (˚C)	% GC	Product size (bp)
Clock	*Clock*_qPCR_*F1*	CAG AAT TCA CAT CAA GGC ACA	53.4	42.9	188
	*Clock*_qPCR_*R1*	TGA GGT TTC CTC CCC TTT CT	55.6	50.0	
Cry1	*Cry1*_6F	CCT GCT TTC TGA CCA GAG G	55.3	57.8	113
	*Cry1*_7R	CCA CAT CCA ATT CCC AGA AG	53.4	50.0	
ARNT	*Bmal1*_7Fa	TGA CTG GGT ATG GCT AAG GA	57.6	55.0	119
	*Bmal1*_8Rq	GGC CTG CTG AAC CTT GTT GA	58.1	55.0	
Tim-like	*Timeout*_F	TGG GAA CAC AGA CAG GAA GAG	59.3	52.4	125
	*Timeout*_R	TGG ACT GTA GCA TCA TCG TCT G	59.9	50.0	
ROR/ HR3	*ROR*_6F	CCC ACG TAA ACC ACA TGA AA	53.1	45.0	125
	*ROR*_7R	TGA AGA ATC CCT TGC AAC CT	54.3	45.0	
aaNAT	*aaNAT*_F2	AGG ACG AAG CAG CCA CTT AC	57.2	55.0	214
	*aaNAT*_R2	CGT CGA CGC GAT TCT TTG AC	56.5	55.0	
18S	*Me*_for*	GTG CTC TTG ACT GAG TGT CTC G	57.4	54.5	116
	*Me*_rev*	CGA GGT CCT ATT CCA TTA TTC C	52.5	45.5	
EF1	*EF1α*_F†	CAC CAC GAG TCT CTC CCA GA	58.2	60.0	106
	EF1α_R†	GCT GTC ACC ACA GAC CAT TCC	58.2	57.1	
Tub	*TUB*_F†	TTG CAA CCA TCA AGA CCA AG	53.6	45.0	165
	*TUB*_R†	TGC AGA CGG GCT CTC TGT	58.0	61.1	

*Designed by Ciocan et al. (2011); † Designed by Cubero-Leon et al. (2012). Abbreviations: melting temperature, Tm; percentage guanine-cytosine content, % GC

3.2.6 qPCR assay optimisation

qPCR reactions were optimised for each target and reference gene to ensure accurate and efficient quantification according to the standards set out in the MIQE guidelines (Bustin et al., 2009). For each reaction, amplification plots were generated showing fluorescence (a proxy for qPCR product concentration) during successive

thermal cycles. The intersect between the amplification curve and the threshold level, which crosses the exponential phase of all reactions, generates a Cq value. The Cq value is therefore the cycle number at which the fluorescent signal is detected and is the raw data output used in relative quantification analyses. Cq values were assessed to confirm they occurred prior to 40 cycles – a cut-off point generally used to exclude low-efficiency reactions (Bustin et al., 2009).

qPCR reactions were set up as follows: 10 µL FastStart Universal SYBR Green Master (Rox) (Roche, UK), 7 µL molecular-grade water (Fisher Scientific, UK), 1 µL of each primer (Table 3.1) creating final concentrations ranging between 100 nM – 500 nM and 1 µL of cDNA (derived from 190 ng RNA). To determine the optimal primer concentrations of the genes of interest and the reference genes, primers were tested at final assay concentrations of 100 nM, 300 nM and 500 nM. Assays providing specific qPCR products at the lowest Cq value were selected for subsequent optimisation and were as follows: 100 nM (*Cry1*, *ARNT*, *EF1α*, *TUB*, *18S*), 300 nM (*Clock*, *Timeout*-like, *ROR/HR3*) or 500 nM (*aaNAT*).

Primer specificity was demonstrated by generating melt peak plots upon reaction completion. This was achieved by heating the qPCR products in 0.5 ºC increments from 60 ºC to 95 ºC to denature the dsDNA, causing a resultant decrease in fluorescence as the dye dissociates. Single peaks on the plots were indicative of a single qPCR product lacking contamination and undesirable secondary products. In addition, template-negative controls were performed for every primer pair to further confirm the absence of primer dimer formation and contamination. Results were checked using agarose gel electrophoresis on a 1% agarose TBE gel stained with GelRed™ Nucleic Acid Gel Stain (10,000X in water) (Biotium, Cambridge Bioscience, UK) (Section 2.2.9) and DNA sequence identity was confirmed using the

EZ-seq DNA Sanger sequencing service (Macrogen Europe, Amsterdam, The Netherlands) (Section 2.2.15).

All reactions were set up using the following plates and seals to standardise fluorescence reflection across samples: Hard-Shell® Low-Profile Thin-Wall 96-Well Skirted PCR Plates with white wells (BioRad, UK) and Microseal® 'B' Adhesive Seals (BioRad, UK). Reactions were performed on a CFX96 Real Time PCR Detection System (BioRad, Hemel Hempstead, UK) using the following thermal cycling conditions: 95 ºC for 2 min, followed by 45 cycles 95 ºC for 10 sec, 60 ºC for 1 min and 72 ºC for 1 min. Raw data, amplification plots and melt curve peaks were generated by the BioRad CFX Manager V1.6.541.1028 software.

3.2.7 Generation of standard curves to test qPCR efficiency

For each gene, primer efficiencies were tested by assessing qPCR product amplification over at least a 4X cDNA dilution range. Standard curve graphs of Cq value against log cDNA dilution were generated using Microsoft Office Excel 2007 and the slope of the line of best fit (y-intercept) was input into the qPCR Standard Curve Slope to Efficiency Calculator Tool (http://www.genomics.agilent.com/biocalculators/calcSlopeEfficiency.jsp?_requestid=851955), an online bioinformatics tool used to ascertain the primer amplification efficiency using the following equation: Efficiency = $-1+10^{(-1/slope)}$. Ideal primer efficiencies fall into the range of 90% to 110% (Taylor et al., 2010) and must be similar between the gene of interest and the reference gene (Livak and Schmittgen, 2001) i.e. both fall within this desirable range. Efficiencies greater than 100% can occur due to pipetting inaccuracies or presence of inhibitors.

3.2.8 Reference gene selection

Amplification data (Cq values) for the reference genes *EF1α*, *TUB* and *18S* were generated for 25% of the mussel samples (*n*=8 randomly selected from each time-point) using the optimised reaction conditions determined in this chapter. To test whether the reference genes exhibited stable expression levels across all time-points, the non-parametric Kruskal-Wallis test was performed in all cases using GraphPad InStat v3 (GraphPad Software Inc., La Jolla, USA), as the data showed unequal variance between groups. To ascertain which of the reference genes showed the most stable expression levels across treatments, and should therefore be selected for normalisation of this sample-set for future analyses, RefFinder (http://fulxie.0fees.us/?type=reference) (Xie et al., 2012) was used to rank the reference genes from most to least stable.

3.3 RESULTS

3.3.1 qPCR product amplification and primer specificity

qPCR products were successfully generated for the genes of interest and the reference genes as shown by the amplification plots (Figure 3.2). The presence of a single plot per reaction on both the amplification and melt peak graphs (Figure 3.3), in addition to single bands detected on the agarose gel (Figure 3.4), indicates successful, specific amplification. The absence of fluorescent signal in template-negative controls, run alongside the samples, also indicates the lack of secondary product formation. Melt peak plots for each amplified mRNA always showed the same temperature peak indicating gene-specificity of the primers; identical DNA sequences share the same length and guanine/cytosine content and therefore the same melting temperature. Finally, Sanger sequencing (EZ Seq, Macrogen Europe, The

Netherlands) and comparison of the obtained *M. edulis* sequences against the GenBank database confirmed that the amplicons were from the desired genes.

(a) *Clock* **(b) *Cry1*** **(c) *ARNT***

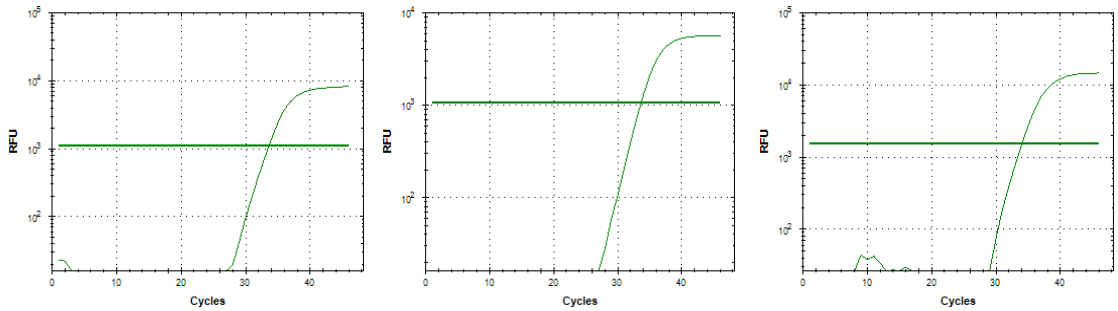

(d) *Timeout*-like **(e) *ROR/HR3*** **(f) *aaNAT***

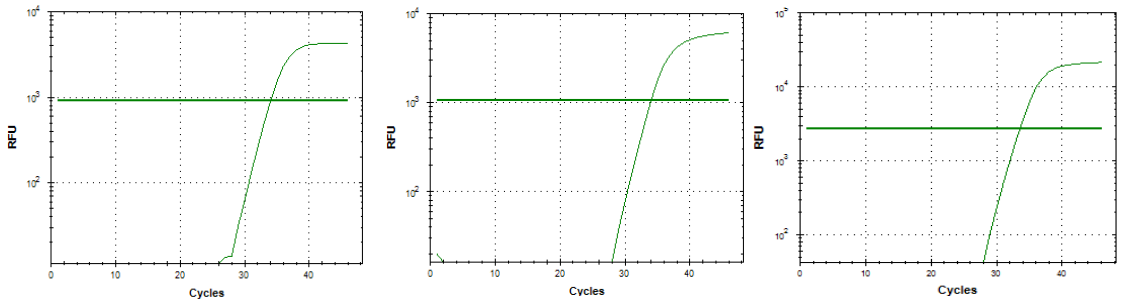

(g) *EF1a* **(h) *TUB*** **(i) *18S***

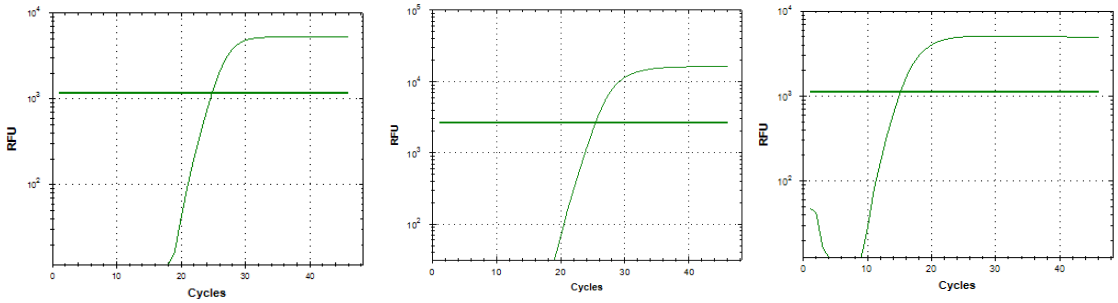

Figure 3.2 Representative results of cDNA amplification plots (log scale) generated from qPCR reactions containing *M. edulis* cDNA, FastStart Universal SYBR Green Master (Rox) (Roche, UK) and primers at either 100 nM (b), (c), (g), (h) and (i), 300 nM (a), (d) and (e), or 500 nM (f). Abbreviations: RFU, Relative Fluorescence Units.

(a) *Clock* **(b) *Cry1*** **(c) *ARNT***

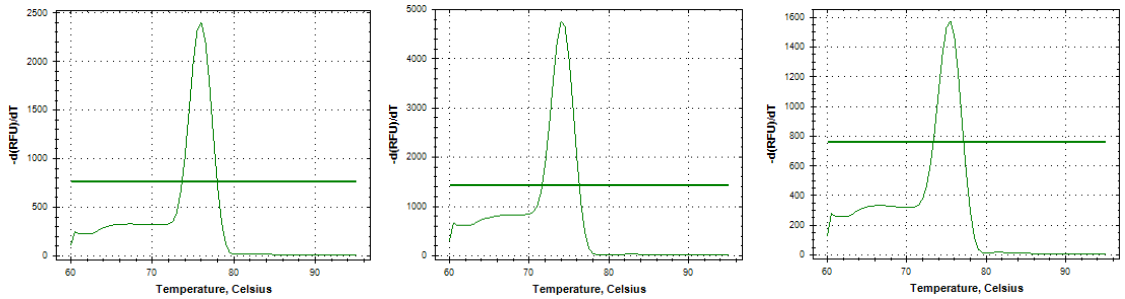

(d) *Timeout*-like **(e) *ROR/HR3*** **(f) *aaNAT***

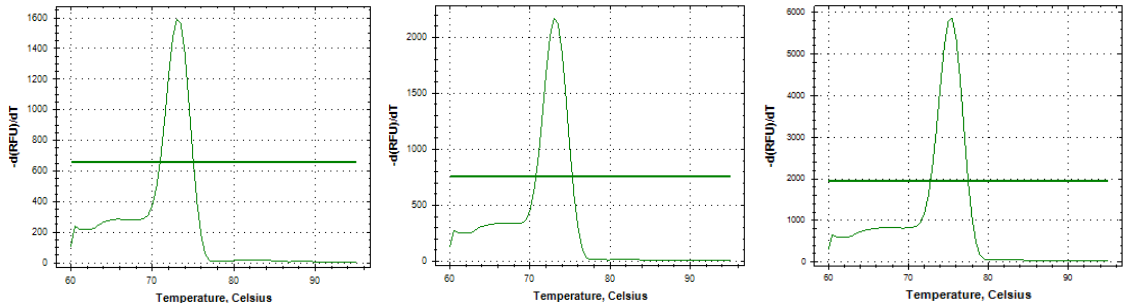

(g) *EF1a* **(h) *TUB*** **(i) *18S***

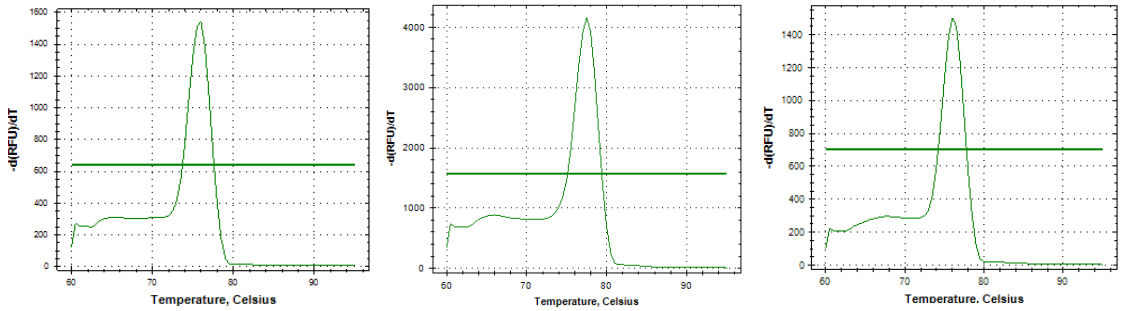

Figure 3.3 Representative results of melt peak plots generated from qPCR reactions containing *M. edulis* cDNA, FastStart Universal SYBR Green Master (Rox) (Roche, UK) and primers at either 100 nM (b), (c), (g), (h) and (i), 300 nM (a), (d) and (e), or 500 nM (f). Abbreviations: RFU, Relative Fluorescence Units.

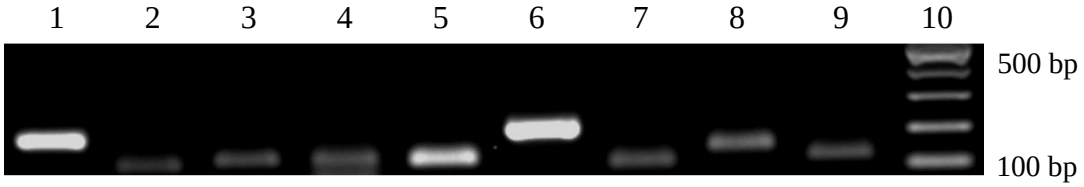

Figure 3.4 Gel image of 1% TBE agarose gel stained with GelRed™ Nucleic Acid Gel Stain (Biotium, Cambridge Bioscience, UK) showing 5 µL of qPCR product for the following genes: Lane 1, *Clock*; 2, *Cry1*; 3, *ARNT*; 4, *Tim*-like; 5, *ROR*/*HR3*; 6, *aaNAT*; 7, *EF1α*; 8, *TUB*; 9, *18S*; 10, GeneRuler 100 bp DNA Ladder (Thermo Fisher Scientific, UK).

3.3.2 Standard curves and amplification efficiencies

The standard curves for each gene show that there is a linear relationship between log cDNA dilution factor and Cq value (Figure 3.5). The R^2 values (which can range between 0 and 1) are all in close proximity to 1 (Table 3.2) indicating that cDNA dilution factor is a good predictor of Cq value as expected. This also indicates that there was a high standard of pipetting accuracy in the preparation of the qPCR reactions. All of the primer efficiencies fall into the desired 90% to 110% range (Table 3.2).

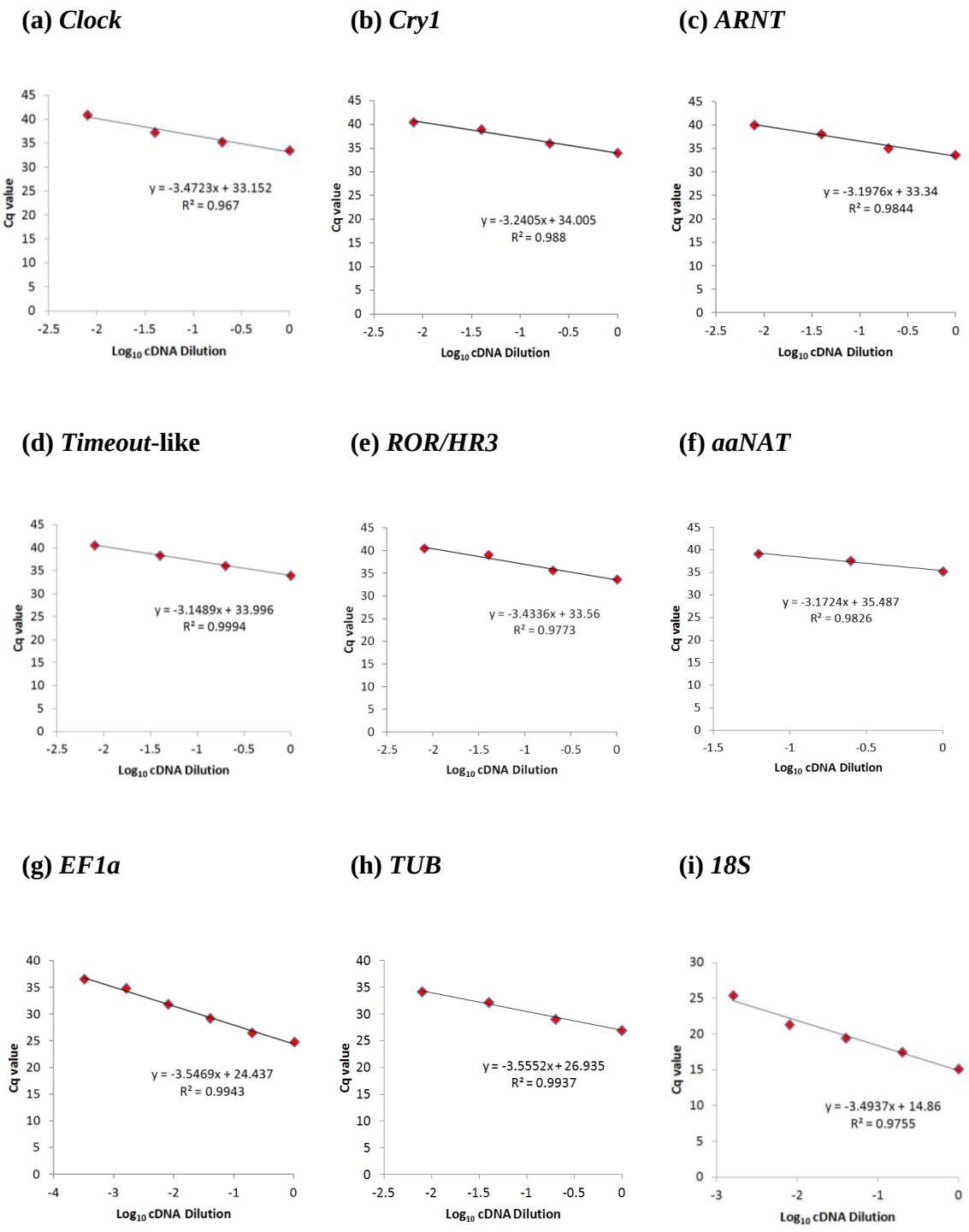

Figure 3.5 Standard curves showing qPCR amplification efficiency of *M. edulis* primers for different genes over a cDNA dilution series with R2 values displayed.

Table 3.2 R2 values of standard curve slopes from Figure 3.5 and the associated primer amplification efficiencies.

Category	Gene	Primers	Final primer concentration (nM)	R^2	Amplification efficiency (%)
Genes of interest	*Clock*	*Clock_qPCR*_F1 *Clock_qPCR*_R1	300	0.967	94.1
	Cry1	*Cry1*_ 6F *Cry1*_ 7R	100	0.988	103.5
	ARNT	*Bmal1*_7Fa *Bmal1*_8Rq	100	0.984	105.4
	Tim-like	*Timeout* F1 *Timeout* R1	300	0.999	107.8
	ROR/HR3	*ROR*_ 6F *ROR*_7R	300	0.977	95.5
	aaNAT	*aaNAT*_F2 *aaNAT*_R2	500	0.983	106.7
Reference genes	*EF1α*	*EF1α*_F *EF1α*_R	100	0.994	91.4
	TUB	*TUB*_F *TUB*_R	100	0.994	91.6
	18S	Me for Me rev	100	0.976	93.3

3.3.3 Reference gene selection

The comprehensive ranking of gene expression stability for *EF1α*, *TUB*, and *18S* generated by RefFinder (Xie et al., 2012) is shown in Figure 3.6. *EF1α* has the lowest geomean of ranking values and is therefore the most stable of the genes tested, whereas *TUB* has the highest value and is the least stable (Figure 3.6). Furthermore, for each gene, the Kolmogorov-Smirnov test indicated that the data were normally distributed, however the standard deviations of the groups (time-points) were significantly different for all three genes (*18S*: Bartlett statistic=29.952, p=0.0004; *EF1α*: Bartlett statistic=34.460, p<0.0001; *TUB*: Bartlett statistic=17.360, p=0.0434) so the non-parametric Kruskal-Wallis Test was performed in each case. Both *18S* (*KW*=15.368, p=0.0813) and *EF1α* (*KW*=11.239, p=0.2597) showed stable expression levels across time-points as no significant difference was detected. A significant difference between time-points was, however, detected for *TUB* (*KW*=22.529,

p=0.0073), indicating that it is not suitable as a reference gene for this sample set. As it is preferable for multiple reference genes to be used in combination (Bustin et al., 2009; Vandesompele et al, 2002), both *18S* and *EF1α* were selected for normalisation of gene expression data for this sample set.

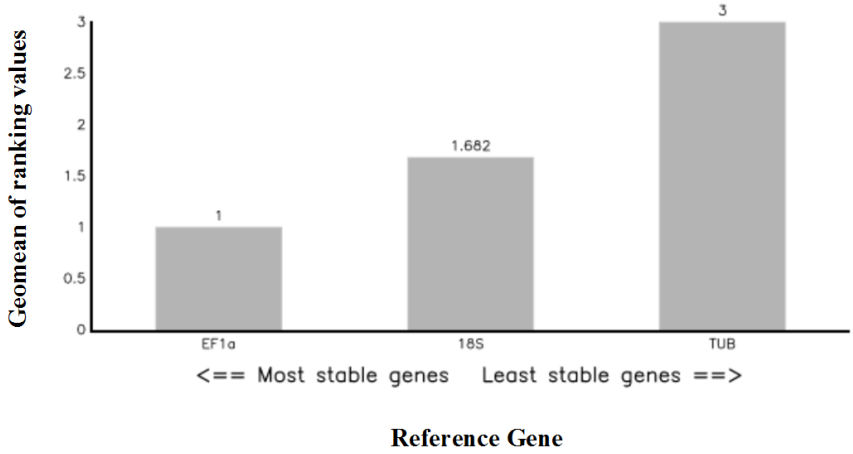

Figure 3.6 Comprehensive gene stability ranking of *EF1α*, *TUB*, and *18S* from a subset of seasonally-collected mussel samples (*n*=71) according to the geomean of ranking values assessed by RefFinder (Xie et al., 2012).

3.4 DISCUSSION

In this chapter, sequence-specific qPCR primers were designed, tested and optimised for the six *M. edulis* clock genes (*Clk*, *Cry1*, *ROR/HR3*, *Per* and *Rev-erb*) and clock-associated genes (*ARNT*, *Timeout*-like and *aaNAT*), and three reference genes (*EF1α*, *TUB*, and *18S*) using cDNA from a seasonally collected sample set. qPCR reactions were optimised for each primer pair to successfully amplify the genes of interest (Figure 3.2 to Figure 3.4) and primer specificity was further demonstrated by the lack of non-specific products present during melt peak generation (Figure 3.3) and by Sanger sequencing of qPCR products. Standard curves for all genes demonstrated that primer efficiencies were within the desired 90-110% range (Figure

3.5, Table 3.2) (Taylor et al., 2010; Bustin et al., 2009). The reference genes *EF1α* and *18S* were ranked the most stable combination out of the three tested (Figure 3.6) and, unlike *TUB*, they showed stable expression levels across all time-points (*18S* [*KW*=15.368, *p*=0.0813] and *EF1α* [*KW*=11.239, *p*=0.2597]). The geometric mean of *EF1α* and *18S* expression values will therefore be used for qPCR data normalisation of this sample-set in Chapter 4.

An important consideration of qPCR is that RNA concentration and quality are as high as possible and that approximately the same quantity of RNA is used per reaction (Bustin et al., 2009). To address these requirements, mussel tissue samples were stored appropriately by being immediately placed in RNA*later* stabilisation solution (Ambion, Life Technologies, USA) after dissection and then stored at -80 ^{o}C to preserve the RNA. Freeze-thaw cycles were avoided and the treatment of surfaces and equipment with RNase Away (Molecular Bioproducts, UK) helped to protect the samples from degradation from Ribonuclease (RNase) contamination. RNA integrity was assessed by performing agarose gel electrophoresis under denaturing conditions. However, contrary to many other phyla, the 28S fraction of mollusc RNA does not appear as a discreet band on denaturing formaldehyde agarose gels, even in high-quality samples, which makes this popular method of assessing RNA integrity less informative than in mammals (Barcia et al., 1997). RNA concentrations were quantified in randomised sample batches and a standardised concentration of 190 ng RNA was added to cDNA synthesis reactions to remove discrepancies in sample concentration (Bustin et al., 2009).

As the SYBR Green I technique was used, a caveat of which is that false positives may occur from the detection of any dsDNA present (Bustin et al., 2009), RNA was prepared using a DNase I incubation step to degrade both dsDNA and

ssDNA sources of contaminating genomic DNA. To further reduce the presence of false-positives, the gene-specific primers used in the qPCR reactions were optimised to amplify only single, specific products and to produce no secondary structures as demonstrated by the clean amplification plots, single melt peaks and single electrophoresis bands (Figure 3.2. to Figure 3.4). qPCR products were sequenced to confirm primer specificity. Furthermore, no fluorescence signals were detected from template-negative controls. These factors indicate that confounding factors such as secondary structure like primer dimers or sources of contamination did not contribute to the fluorescence detected from the optimised reactions.

Finally, a key requirement of the comparative Ct qPCR analysis method, which will be used to normalise relative expression data generated from this sample-set in the subsequent chapter, is that the primers for the genes of interest and the reference genes have an efficiency as close to 100% as possible (Taylor et al., 2010; Bustin et al., 2009; Livak and Schmittgen, 2001). This was demonstrated for all nine genes tested (Figure 3.5. and Table 3.2). The dynamic range over which *aaNAT* could be tested was slightly lower compared to the other genes as the Cq obtained for the undiluted cDNA sample was already quite late (>Cq 35) and the generally accepted maximal cut-off for reliable gene expression data is Cq 40 (Bustin et al., 2009). A final consideration for generating a full qPCR dataset for the seasonal mussel samples is that a minimum of three biological replicates and two technical replicates are recommended for qPCR (Taylor et al., 2010). This requirement will be met by analysing 30 individuals at each time-point and performing all qPCR reactions in duplicate.

3.5 CONCLUSION

qPCR is a powerful tool allowing the quantification of mRNA expression levels provided that the standardised MIQE Guidelines are followed. In this chapter, qPCR assays were developed and optimised for *M. edulis* clock genes (*Clk*, *Cry1*, *ARNT*, *ROR/HR3*, *Timeout*-like and *aaNAT*) on seasonally collected samples. Reference genes were selected and validated as stable for normalisation. In Chapter 4, this quantitative molecular approach is used as a tool to assess seasonal clock gene expression levels in the gonads of the seasonally reproductive *M. edulis* at different points of an annual cycle. The molecular clock mechanism is predicted to provide the link between environmental seasonal cues and biological rhythms.

Chapter 4

Influence of season on mRNA expression patterns of *M. edulis* circadian rhythm-related genes

4.1 INTRODUCTION

The natural changes in photoperiod and temperature that occur throughout the year are reliable environmental cues of season, which often act in conjunction in aquatic habitats (Numata and Udaka, 2010). The seasonal influences of these factors on molluscs are most commonly documented for reproductive activities such as growth, gametogenesis and oviposition (Numata and Udaka, 2010; Osada et al., 2007; Bohlken and Joosse, 1981; Seed, 1969) as many species undergo seasonal cycles of reproductive development. The effects of environmental factors, in particular photoperiod, temperature and food availability, on bivalve gametogenesis have been investigated in oysters (Maneiro et al., 2017; Fabioux et al., 2005; Chávez-Villalba et al., 2002; Li et al., 2000), scallops (Osada et al., 2007; Duinker et al., 2000; Saout et al., 1999; Martínez and Pérez, 2003), clams (Rodríguez-Rúa et al., 2003) and mussels (Dominguez et al., 2010; Fearman and Moltschaniwskyj, 2010; Galbraith and Vaughn, 2009; Pronker et al., 2008; Newell et al., 1982; Bayne et al., 1978; Seed, 1969). It is clear that timing and success of bivalve gametogenesis is influenced by a variety of exogenous and endogenous factors including photoperiod, temperature, food availability, genotype and neuroendocrine control (Gosling, 2005). For example, gradient increases in temperature and photoperiod resulted in higher percentages of

germinal cells in the oyster *Ostrea edulis* and longer photoperiod gradients resulted in greater total larval production (Maneiro et al., 2017). Gonad rebuilding was greater in spent *P. maximus* scallops kept under constant or increasing photoperiod regimes than under a natural decreasing regime (Duinker et al., 2000). Food availability and quality also influences gametogenesis as it is an energetically demanding process (Gosling, 2015; Galbraith and Vaughn, 2009; Pronker et al., 2008). The duration of conditioning, using optimal temperature and food supply, affected spawn number in *M. galloprovincialis*, though the effect of photoperiod requires further investigation (Dominguez et al., 2010). However, warm temperatures within the natural range can also reduce gametogenesis rates in the species as they manage their energy balance (Fearman and Moltschaniwskyj, 2010). Bivalves including mussels exhibit trade-offs between reproductive development and growth; greater growth rates are apparent in sterile triploids compared to fertile diploids undergoing seasonal gametogenesis (Payton et al., 2017c; Petes et al., 2008b; Brake et al., 2004).

In addition to environmental influences, bivalve reproductive development is controlled by neurohormones and steroids that affect gonad physiology (Gosling, 2015). For example, gonadotropin-releasing hormone (GnRH) triggers mitosis in primitive germ cells (Morishita et al., 2010) and serotonin is involved in diverse functions including oocyte maturation (Tanabe et al., 2006) and triggering spawning (Ram et al., 1993). The activity of neurosecretory cells in the cerebral, pedal and visceral ganglia of *M. edulis* coincides with reproductive development (de Zwann and Mathieu, 1992). Homologs of vertebrate sex steroids, and many of the genes encoding enzymes involved in their production from cholesterol, have also been identified in a number of bivalves including mussels (Blalock et al., 2018) and are generally accepted to be involved in reproductive development (Croll and Wang, 2007; Lafont and

Mathieu, 2007).

M. edulis have separate sexes and sexual maturity is reached within the first year (Duinker et al, 2008; Seed, 1969). The seasonal nature of reproductive development in the edible blue mussel *M. edulis* (Seed, 1969) leads to seasonal variation in both the recruitment of mussel spat (larval stages) and the value of adults, as the lower meat content of spawned mussels, and their shorter shelf life, makes them less desirable (Brake et al., 2004). As a result of the environmental influences on bivalve reproduction, the timing of seasonal gametogenesis in *M. edulis* varies both annually and geographically (Gosling, 2015; Chipperfield, 1953; Seed, 1976), as is the case for other bivalves including oysters (Zarnoch and Schreibman, 2012; Ruiz et al., 1992), clams (Kang et al., 2007; Laruelle et al., 1994) and scallops (DiBacco et al., 1995; MacDonald and Thompson, 1988). Mussel gametogenesis starts with the development of gametes in follicles, primarily in the mantle tissues (Lowe et al., 1982; Seed, 1976; Seed, 1969). In the UK, this generally commences in late autumn/winter with spawning usually occurring in the spring, often followed by redevelopment and additional spawning events under favourable local conditions (Chipperfield, 1953; Seed, 1969). However, geographic variation is apparent in the timing of gametogenesis as well as in the timing and frequency of spawning (Villalba, 1994; Newell et al., 1982; Bayne et al., 1976; Seed, 1976). For example, *M. edulis* collected from Anglesey, North Wales spawned once per year over a period of 3 years whereas a population from Plymouth, South England spawned at least twice a year over the same period (Lowe et al., 1982). Multiple spawning events in a year may produce consistent or variable numbers of spawned gametes (Rodhouse, 1984). Furthermore, even at the same location, differences in the timing of reproductive events can be observed due to the effects of microhabitat; in Killary Harbour in west Ireland wild

M. edulis spawn partially in early spring and fully in summer whereas two summer spawning events occur in rope-cultured mussels (Rodhouse et al., 1984). Variability in gametogenesis also occurs annually at the same site (Lowe et al., 1982; Seed, 1969). Mussels are therefore considered to have a flexible reproductive strategy in response to local environmental conditions (Gosling, 2015).

It has been well documented in other species that the circadian molecular clock mechanism can be entrained by environmental cues including light, temperature and food availability in order to maintain synchrony with external environmental cycles (Mohawk et al., 2012; Dubruille and Emery, 2008; Rensing and Ruoff, 2002). Though the clock mechanism is predominantly associated with the regulation of circadian rhythms, clock genes have been linked to photoperiodism in mammals (Bradshaw and Holzapfel, 2007; Tournier et al., 2003), fish (Herrero and Lepesant, 2014; Davie et al., 2009) and insects (Meuti et al., 2015; Pegoraro et al., 2014; Goto, 2013; Ikeno et al., 2010; Pavelka et al., 2003), suggesting involvement in longer-term seasonal rhythms, though further investigation is required (Danks, 2005). Photoperiod can act as a seasonal cue to inform biological time-keeping by influencing clock gene expression patterns resulting in differences in amplitude, phase, peak duration and rhythmicity (Benetta et al., 2019; Davie et al., 2009; Tournier et al., 2007; Goto and Denlinger, 2002). For example, seasonal differences in clock gene expression patterns are apparent in the pituitary of the sea bass *Dicentrarchus labrax* (Herrero and Lepesant, 2014) and photoperiod modulates the expression patterns of *Clock*, *Bmal1*, *Per2*, and *Cry2* in the brains of the Atlantic salmon *Salmo salar* (Davie et al., 2009). Photoperiod influences the expression of multiple clock genes in the suprachiasmatic nucleus (SCN) of the Syrian hamster *Mesocricetus auratus* in which the mammalian master circadian pacemaker is located (Tournier et al., 2003); effects on clock mRNA

expression include altered amplitude, phase and peak duration (Tournier et al., 2003). In addition, RNAi disruption of *Per* in the insect *Riptortus pedestris* leads to diapause aversion under a diapause-inducing photoperiod whereas the opposite is the case for *Cyc* RNAi under a diapause-averting photoperiod (Ikeno et al., 2010). Temperature is also known to affect different aspects of the molecular clock mechanism (Dubruille and Emery, 2008; Rensing and Ruoff, 2002), for example by affecting the prevalence of different clock gene isoforms in *Drosophila*, resulting in phase shifts of the clock (Helfrich-Förster et al., 2018).

No tissue type containing a "master clock" mechanism, such as the SCN in mammals (Mohawk et al., 2012), has been identified in bivalves to date. However, a peripheral tissue in which seasonal rhythms occur in *M. edulis* is the mantle tissue, which undergoes annual reproductive development (Seed, 1969). The extent to which circadian clock genes are involved in the regulation of such seasonal rhythms is unknown; seasonal differences in clock gene expression are yet to be investigated in molluscs and there are only a few studies in which daily patterns have been investigated, revealing oscillations of the following: *Cry1* and *RORβ* in the gills of *M. californianus* (Connor and Gracey, 2011), *Cry1* and *Cry2* in the head of the squid *E. scolopes* (Heath-Heckman et al., 2013), *Per* in the clock neurons of the sea snail *B. gouldiana* (Constance et al., 2002), *Cry1* in certain tissue types of the adductor muscle of *C. gigas* (Mat et al., 2016) and multiple clock genes in the gills of *C. gigas* (Perrigault and Tran, 2017). It is hypothesised that clock (*Clk, Cry1, ROR/HR3, Per* and *Rev-erb*) and clock-associated genes (*ARNT, Timeout*-like and *aaNAT*) will be expressed in *M. edulis* mantle tissue, a peripheral tissue that undergoes seasonal cycles of gametogenesis.

Phase shifts in the peaks of clock gene mRNA oscillations, which are commonly

entrained by light as a zeitgeber (Liu and Panda, 2017; Golombek and Rosenstein, 2010; Tomioka and Matsumoto, 2010; Hiebert et al., 2000), can shift between seasons in response to sunrise/sunset, and provide information on photoperiod length (Nunes and Saunders, 1999; Pittendrigh, 1960). If photoperiod is involved in the provisioning of seasonal information via the molecular clock mechanism in mussel mantles, clock mRNA expression may be expected to differ between winter (short photoperiod) and summer (long photoperiod), particularly at morning and evening time-points near the light/dark transitions. If light triggers clock gene expression, mRNA levels may peak sooner in the day than in winter as sunrise is earlier in summer. However, specific predictions of elevated or decreased gene expression at comparable time-points in different seasons provide a challenge as clock gene expression patterns vary between species (Tomioka and Matsumoto, 2015) and tissue type (Mat et al, 2016; Tomioka et al., 2012; Tobback et al., 2011), and photoperiod is known to affect multiple characteristics of their rhythms including amplitude, phase and peak duration (Benetta et al., 2019; Davie et al., 2009; Tournier et al., 2007; Goto and Denlinger, 2002). It is hypothesised that the expression levels of *M. edulis* clock and clock-associated genes will vary significantly at the same time of day between winter and summer, which exhibit short and long photoperiods respectively.

The aim of this chapter is to assess whether seasonal differences, encompassing natural photoperiod differences, influence expression patterns of circadian clock-associated genes in the reproductive tissues of blue mussels in the wild. It will be ascertained whether clock-associated genes are (1) expressed in the reproductive tissues (mantle) of both sexes, (2) show seasonal differences in expression patterns at the same time of day, and (3) show sex-specific expression patterns. To achieve this, male and female *M. edulis* from the same population were collected at comparable

daily time-points during winter and summer. Histological techniques were used to identify mussel sex and gametogenesis stage, and the qPCR assays optimised in Chapter 3 were used to quantify the expression of *Clock*, *Cry1*, *ARNT*, *Timeout*-like, *ROR*/*HR3* and *aaNAT*. Seasonal differences in mRNA expression levels at comparable daily time-points is indicative of a change in amplitude and/or a phase shift in the timing of peak gene expression, consistent with a photoperiodic response.

4.2 MATERIALS AND METHODS

4.2.1 Sample collection

Wild adult *M. edulis* were collected at low tide from the intertidal zone of Filey Bay, North Yorkshire, UK (54° 13' longitude and 0° 16' latitude) (Figure 3.1). In order to investigate the effects of seasonal photoperiod differences, sampling was conducted at the times of year when photoperiod difference was most pronounced; the winter and summer solstices are the shortest and longest days of the year respectively and the intervening equinoxes have effectively equal day and night lengths (Khavrus and Shelevytsky, 2010). As lunar cycles and tidal cycles can act as zeitgebers to entrain rhythms in some marine organisms (Tessmar-Raible et al., 2011; Naylor, 2010), sampling was conducted at the same time of the lunar month (new moon, spring tide phase) and at the same point in the tidal cycle (low tide) in all cases to standardise for these potentially confounding factors, whilst occurring as close to the solstices and equinoxes as possible. Sampling was carried out one day prior to and one day subsequent to the closest new moon to the winter (2014) and summer (2015) solstices and the spring and autumn equinoxes (2015). All sampling occurred within at least 13 days of a solstice or equinox (Dolby, 2014).

As photoperiod can affect the phase as well as the amplitude and total levels

of clock gene mRNA expression in vertebrates (Herrero and Lepesant, 2014; Davie et al., 2009; Tournier et al., 2007) and invertebrates (Benetta et al., 2019; Syrová et al., 2003; Goto and Denlinger, 2002), the sampling of multiple daily time-points allowed different points of the putative rhythmic cycle to be compared between season. To determine whether day length significantly affected *M. edulis* clock gene expression patterns, three time-points covering different times of day, were sampled during the winter and summer when seasonal differences in photoperiod are most extreme (7.5 hr in winter and 17 hr in summer). As the sample site could only be accessed during the two low tides per day, the following sample regime was adopted: three time-points were chosen for sampling in winter and summer, two of which were during early morning and evening low tides on the first day of sampling (20.12.14 in winter and 14.06.15 in summer), and the third was during the first low tide two days later (22.12.14 and 16.06.15 respectively) during the late morning (Figure 4.1). The two-day gap was sufficient for the timing of the low tide to shift enough for this third, different time-point to be sampled, with differences in daily photoperiod between the two days being negligible. n=30 individuals were sampled at each time-point. Finally, sampling was also conducted in the spring and autumn to confirm that the mantle tissue exhibits seasonal gametogenesis over the course of the year, demonstrating the relevance of this tissue type for this investigation into the effects of photoperiod on components of the molecular clock system. Likewise, in both the spring and autumn, sampling was performed during the early morning low tide (18.03.15 in spring and 11.09.15 in autumn) and two days later during the late morning (20.03.15 and 13.09.15 respectively) (Figure 4.1). Again, n=30 individuals were sampled at each time-point. The evening time-points were omitted at the equinoxes as multiple time-points were not required for seasonal histological investigation; equinox samples were not used

for gene expression analysis. In all cases, *n*=30 individuals were sampled at each time-point.

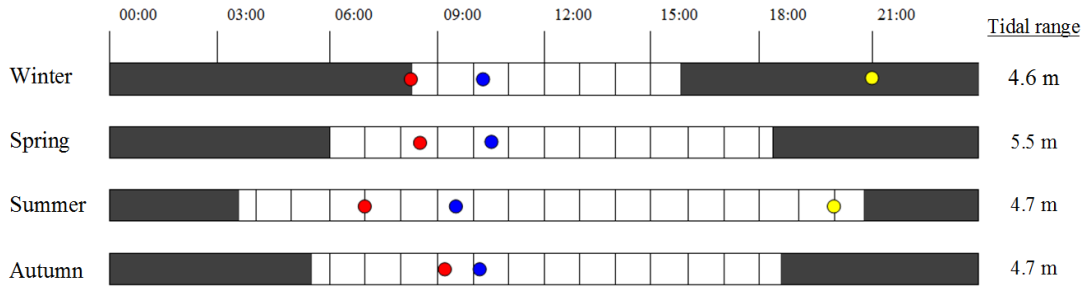

Figure 4.1 Diagram of mussel collection times from Filey Beach (during low tide) in each of the different seasons in relation to daylight hours (white areas) and darkness (shaded). Times are adjusted to Greenwich Mean Time (GMT). Early morning (red markers) and evening (yellow) were sampled on the same day and late morning (blue) was sampled two days later. *n*=30 individuals were sampled at each time-point.

After collection, the mussels were immediately taken to the laboratory for dissection. Mussel dissection and tissue storage conditions for both histological and molecular investigations are outlined in detail in Chapter 3 (Section 3.2.2). In all cases, mussel mantle tissue was sampled as this the tissue which undergoes seasonal cycles of reproductive gametogenesis (Seed, 1969). Early morning, late morning and evening time-points sampled at the winter and summer solstices (Figure 4.1), were used for gene expression analyses and mussels sampled in all four seasons were used for histological analyses to determine sex and gametogenesis stage.

4.2.2 Histology

4.2.2.1 Sample processing and wax embedding

Histological observations of the mantle tissue, containing the gonads in sexually developing mussels, are required to accurately assess sex (Petes et al., 2008a), and to determine the reproductive development stage. Histological examinations were

conducted on all mussel samples collected from all time-points from all four seasons (Figure 4.1). Mantle tissue samples, which were previously fixed in buffered 10% formalin solution (Sigma-Aldrich, Gillingham, UK) (Section 3.2.2.), were washed with 0.01M phosphate buffered saline (PBS) (Sigma Aldrich, Irvine, UK) for 15 min before being dehydrated in a series of ethanol (VWR, Lutterworth, UK) solutions as follows: 70% ethanol for 15 min, 90% for 15 min, 2 steps of 100% for 15 min, and finally 100% for 30 min. Clearing was performed to replace the alcohol with a miscible agent to allow wax infiltration; tissues were immersed in fresh aliquots of Histoclear II (National Diagnostics, UK) for 20 min and then overnight. The following day, two paraffin wax (VWR, UK) infiltration steps were performed, the first for 30 min and the second for 45 min. Samples were wax embedded using an EG 1160 Paraffin Wax Embedding Center (Leica Microsystems, Milton Keynes, UK) and left to set on the chilled work surface for 1 hr. A Shandon Finesse® Manual Rotary Microtome 325 (Thermo Scientific, UK) was used to cut 10 µm sections of wax-embedded tissue, which were then placed briefly in a water bath at 50 °C to warm the wax before being positioned on a microscope slide. Slides were dried overnight in a 37 °C oven to remove water and to allow removal of paraffin prior to staining.

4.2.2.2 Mayer's Haematoxylin and Eosin (H&E) Staining

Slides containing mussel mantle tissue sections were passed through the flame of a Bunsen burner to melt the paraffin wax and placed in Histoclear II (National Diagnostics, UK) for 10 min to clear. Samples were rehydrated by being placed for 3 min each in the following concentrations of ethanol: 100%, 95%, 75%, 45% and 25%. Samples were then placed in Mayer's Haematoxylin Solution (Sigma-Aldrich, UK) for 5 min to stain acidic structures, such as the nucleus a red/purple colour and a

"bluing" step was performed by rinsing samples in running tap water for 10 min to change the colouration to purple/blue to improve the contrast. Samples were then dehydrated by being placed for 2 min each in the following concentrations of ethanol: 25%, 45%, 75%, and 95%. Samples were counter-stained for 1 min in alcoholic eosin Y solution (Sigma-Aldrich, UK) which is an acidic dye that stains basic (acidophilic) structures, such as the cytoplasm and extracellular fibres, pink. Samples were then rinsed in 95% ethanol then 100% ethanol before being cleared in Histoclear II for 5 min. Finally, slides were mounted with DPX Mountant for histology (Sigma-Aldrich, UK) and left to set in the fume cupboard for 3 days.

4.2.2.3 Sex and gametogenesis stage determination

Mounted slides were viewed under a light microscope and both mussel sex and gametogenesis phase were assessed based on the "Scheme of Classification of Gonad Condition" described by Seed (1969) and summarised in Table 4.1. In this case, individuals were categorised as either developing (stages βI-IV), mature (stage βV), spawning (stages γIV-I), or resting/spawned (stage α0) (Table 4.1). Histological sex determination of resting/spawned mussels was not possible due to the absence of sexual structures. Photomicrographs were taken with the Nikon Eclipse 80i Advanced Research Microscope using Image Pro Premier software (Media Cybernetics, Marlow, UK).

Table 4.1 Brief summary of the "Scheme of Classification of Gonad Condition" proposed by Seed (1969) to identify arbitrary stages of gametogenesis for both sexes of blue mussel when microscopically examining stained sections of gonad tissue.

Category	Symbol	Stage	Brief Description of Gonads
Resting/ Spent	α	0	No sexual characteristics are present.
Developing	β	I	Gametogenesis has commenced within dense connective tissue but no spermatozoa or ova are present.
		II	The majority of each follicle contains gametes in the early stages of development with some mature gametes present.
		III	Approximately half of each follicle contains mature gametes and the volume of mantle tissue containing gonad tissue is approximately half that of mature individuals (βV).
		IV	The majority of each follicle now contains mature gametes but gametogenesis is still occurring.
		V	Fully ripe conditions have been reached.
Spawning	γ	IV	Spawning has commenced and density of gametes is less than in fully ripe individuals.
		III	Approximately half of each follicle has been emptied of mature gametes and a reduced area of gonad tissue is present in the mantle.
		II	The majority of each follicle is empty and still less area of the mantle is now comprised by gonad tissue.
		I	Lingering gametes are present and phagocytosis may often be observed.

4.2.3 Gene expression analysis

Gene expression was investigated in male and female *M. edulis* collected from early morning, late morning and evening time-points in winter 2014 and summer 2015. These samples were from the sample set which was optimised for qPCR analysis in Chapter 3.

4.2.3.1 Total RNA Isolation and quantification

The protocols and reagents used for total RNA isolation using the High Pure RNA Tissue Kit with DNase I treatment (Roche, UK) and RNA quantification using a Qubit 1.0 Fluorometer (Life Technologies) are described in detail in Chapter 3.

4.2.3.2 cDNA synthesis

The cDNA synthesis procedure using the Transcriptor High Fidelity cDNA Synthesis Kit (Roche, UK) with a standardised RNA concentration of 190 ng, which was used for all cDNA reactions, is described in detail in Section 3.2.4.

4.2.3.3 Primer design and qPCR optimisations

Details of primer design, reaction efficiencies and qPCR optimisations are detailed at length in Chapter 3 where the specificity and efficiency of all primers have been demonstrated.

4.2.3.4 qPCR amplification

qPCR reactions for the genes of interest (*Clk*, *Cry1*, *ARNT*, *ROR/HR3*, *Timeout*-like and *aaNAT*) and the validated reference genes (*18S* and *EF1*) were set up using the optimised conditions described in detail in Chapter 3. Reactions were performed in duplicate and melt-curves were generated for all samples. Template-negative controls for each gene were included on each plate.

4.2.3.5 Analysis of qPCR data

Amplification plots and melt peaks were checked for every reaction and only successful, specific reactions were used in subsequent analyses. For each sample, the mean Ct of the gene of interest duplicates was normalised with the geometric mean of the reference gene mean duplicates (*18S* and *EF1α*) using the $2^{-\Delta Ct}$ derivation of the comparative Ct method (Livak and Schmittgen, 2001; Schmittgen and Livak, 2008). This combination of reference genes (*18S* and *EF1α*) was determined to be the most

stable of the genes tested (*18S*, *EF1α* and *TUB*), and neither varied significantly across time-points (Section 3.3.3). Primer efficiency was tested in the previous chapter to be within the optimal range, where 2 in the equation represents a doubling of template with each cycle (Bio-Rad Laboratories, 2006). ΔCt was calculated from the mean values as follows: Ct gene of interest – Ct reference genes (Livak and Schmittgen, 2001). This version of the comparative Ct approach is appropriate for datasets where different individuals are sampled from each experimental group (Schmittgen and Livak, 2008). Calculations were performed in Microsoft Office Excel 2007, which was also used to display the data graphically. Statistical analysis was performed using GraphPad InStat v3 (GraphPad Software Inc., La Jolla, USA). Where data did not exhibit normality or equality of variance, the non-parametric Kruskal-Wallis test was performed and a p value of <0.05 was considered significant. Post hoc Dunn's Multiple Comparisons tests, appropriate for groups with unequal numbers of observations, were applied to biologically relevant comparisons (n=8-17). To test for seasonal differences, comparisons were made between equivalent time-points between winter and summer for males and females respectively (e.g. evening winter males vs evening summer males etc.). To test for daily differences, comparisons were made between daily time-points (early morning, late morning and evening) within each seasons for male and females respectively. Finally, to test for sex differences, male-female comparisons were performed at each individual time-point in both seasons. GraphPad InStat v3 automatically accounts for the number of comparisons using Dunn's test when calculating p values (GraphPad Software, Inc., 1990). Fold changes were calculated according to the $2^{-\Delta\Delta Ct}$ method (Schmittgen and Livak, 2008; Livak and Schmittgen, 2001).

4.3 RESULTS

4.3.1 Biometric data

Mean mussel shell length differed between seasons (Kruskal-Wallis $KW=14.893_{3(df)}$, $p=0.0019$); mussels collected in winter had a significantly longer shell length than those collected in both summer ($p<0.05$) and autumn ($p<0.01$), revealed by Dunn's Multiple Comparisons Tests (Figure 4.2). This difference, possibly due to predation (personal observation, 2015), this is not expected to be a confounding factor on the reproductive development or regulation of biological timing in these samples; *M. edulis* shell length has no effect on the timing of gonad development (Chipperfield, 1953) or the spawning period (Seed, 1969).

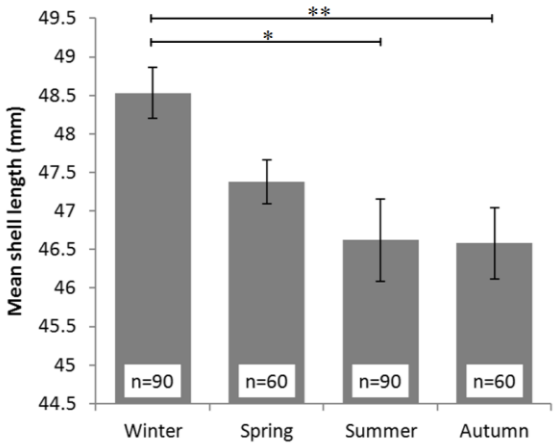

Figure 4.2 Mean shell length of mussels (± SEM) collected from four consecutive seasons commencing winter 2014. Significance detected by Kruskal-Wallis Test followed by Dunn's Multiple Comparisons Test; *denotes significance at the p<0.05 level and ** at the p<0.01 level.

In total, 300 mussels were sampled of which 34% were female, 46% were male, and 20% were resting/spawned (undetermined sex). No instances of hermaphrodism were recorded. The proportions of developing, mature, spawning and

resting/spawned individuals sampled from each season are shown in Figure 4.3 and representative photo micrographs of gonad tissue sections at these different stages of gametogenesis are shown in Figure 4.4.

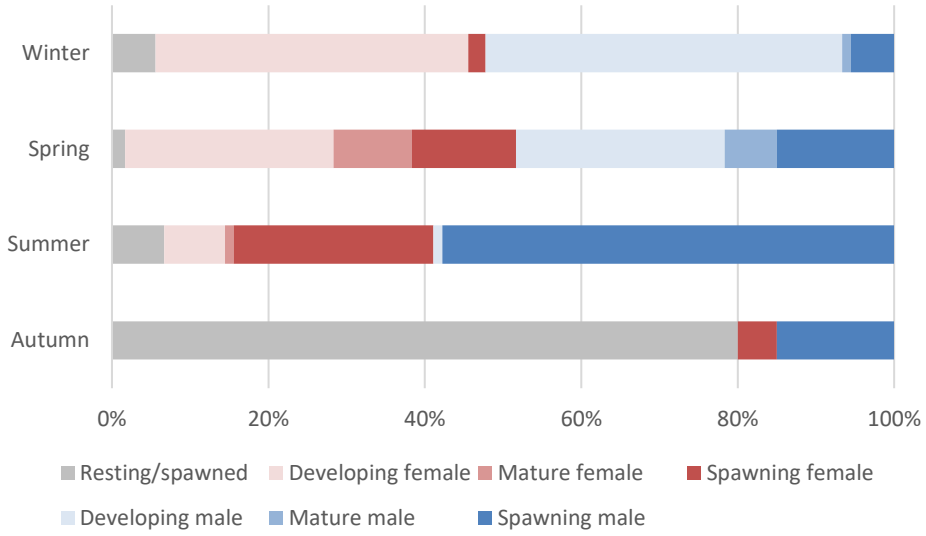

Figure 4.3 Sex and gametogenesis stages of *M. edulis* from Filey Beach, UK, during winter 2014 (*n*=90) and spring (*n*=60), summer (*n*=90) and autumn 2015 (*n*=60).

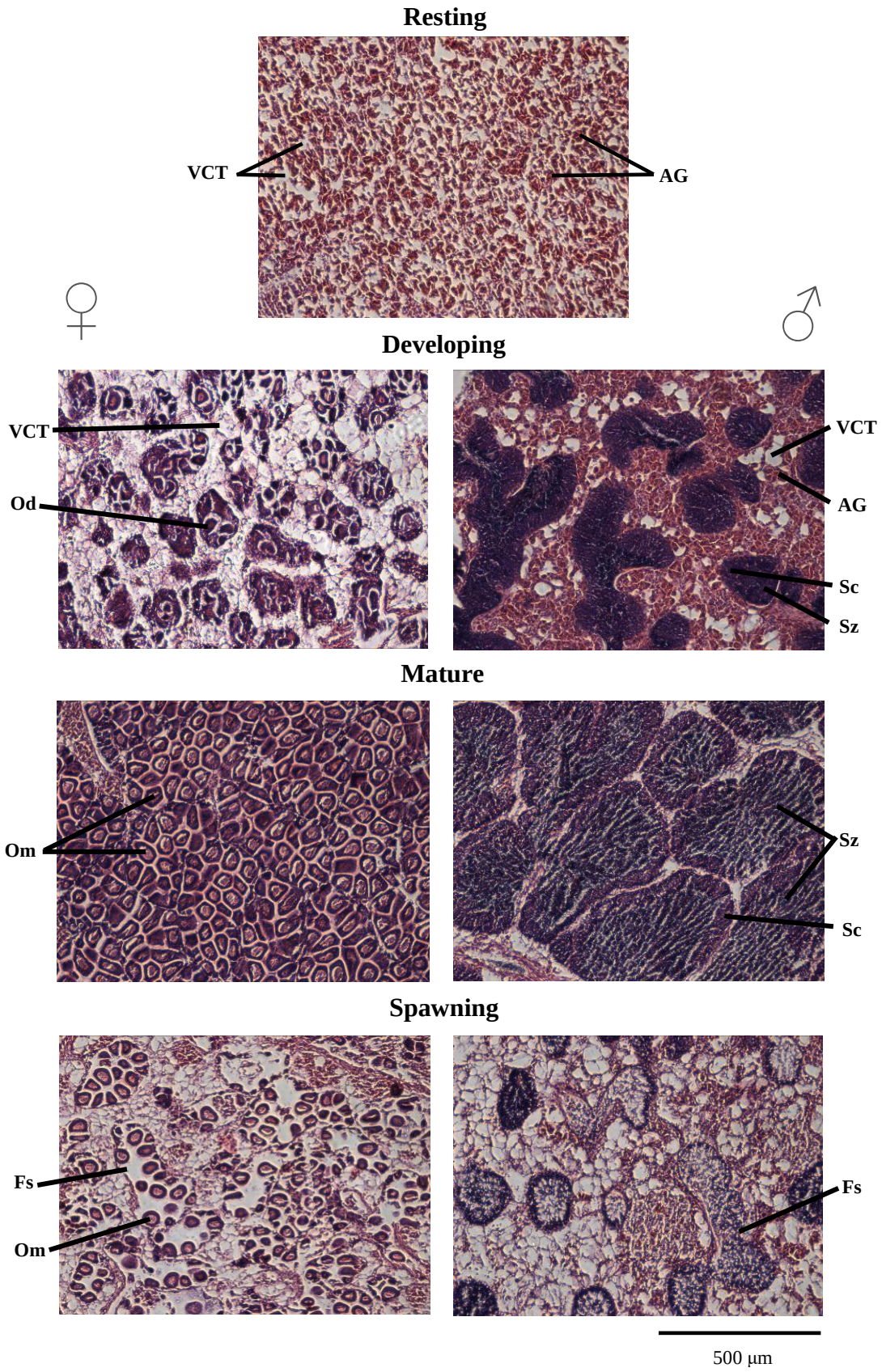

Figure 4.4 Photomicrographs of 10 µm *M. edulis* gonad sections at different stages of gametogenesis stained with Mayer's Haematoxylin and Eosin. Abbreviations: VCT, vesicular connective tissue cells; AG, adipogranular cells; Od, developing oocyte; Om, mature ova; Sc, spermatocytes; Sz, ripe spermatozoa; Fs, partially spawned follicles.

4.3.2 Seasonal gene expression patterns

Significant differences in gene expression were detected for five of the six genes investigated, as revealed by Kruskal-Wallis tests applied to all sampled time-points (n=8 to 17): *Clk* (KW=$53.915_{11(df)}$, p<0.0001), *Cry1* (KW=48.040_{11}, p<0.0001), *ARNT* (KW=25.043_{11}, p=0.0090), *ROR/HR3* (KW=50.303_{11}, p<0.0001) and *aaNAT* (KW=31.434_{11}, p=0.0009). No significant differences were detected between time-point or sex for *Timeout*-like expression (KW=4.178_{11}, p=0.9644) (Figure 4.5d).

Dunn's Multiple Comparisons tests, incorporating corrections for multiple comparisons (GraphPad Software, Inc., 1990), revealed seasonal differences in the expression of *Clk*, *Cry1* and *ROR/HR3* at equivalent time-points between winter and summer (Figure 4.5). Specifically, *Clk* expression was significantly higher in winter males in early morning than in summer males in both early (p<0.001) and late morning (p<0.001); both winter time-points were 3.4 fold lower than the summer time-point (Figure 4.5a). The expression of *Cry1* was also significantly higher in winter males from early morning compared to summer males from late morning (p<0.01); the latter was 3.8 fold lower (Figure 4.5b). The expression of *ROR/HR3* was significantly higher in early morning winter males than in early (p<0.001) and late morning (p<0.001) summer males, which were 4.3 and 3.9 fold lower respectively (Figure 4.5e). Results also indicated sex-specific differences in the expression of *Clk* and *Cry1* at individual time-points; *Clk* expression was significantly (2.2 fold) higher in females than males in late morning in the winter (p<0.05) and *Cry1* was significantly (6.0 fold) higher in females than males in late morning summer (p<0.001). A trend during the summer for greater *Cry1* expression in females was also present in early morning and evening, but was not significant. No significant differences between any of the pairs of groups tested were found for *ARNT* (Figure 4.5c) or *aaNAT* (Figure 4.5f).

(a) *Clk*

Male:

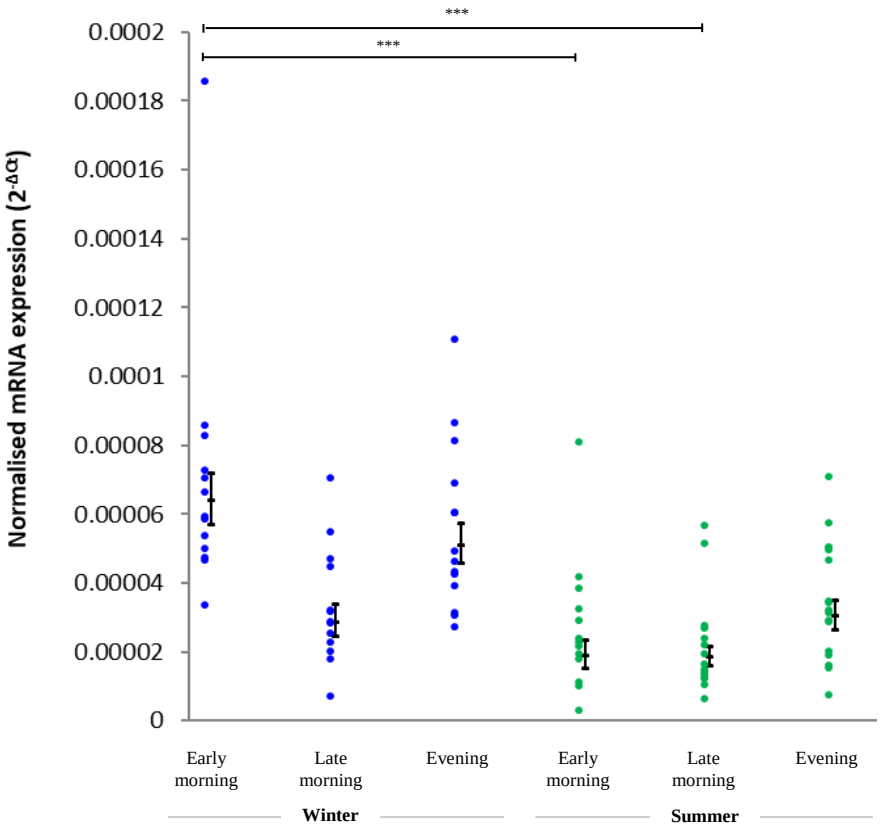

Female:

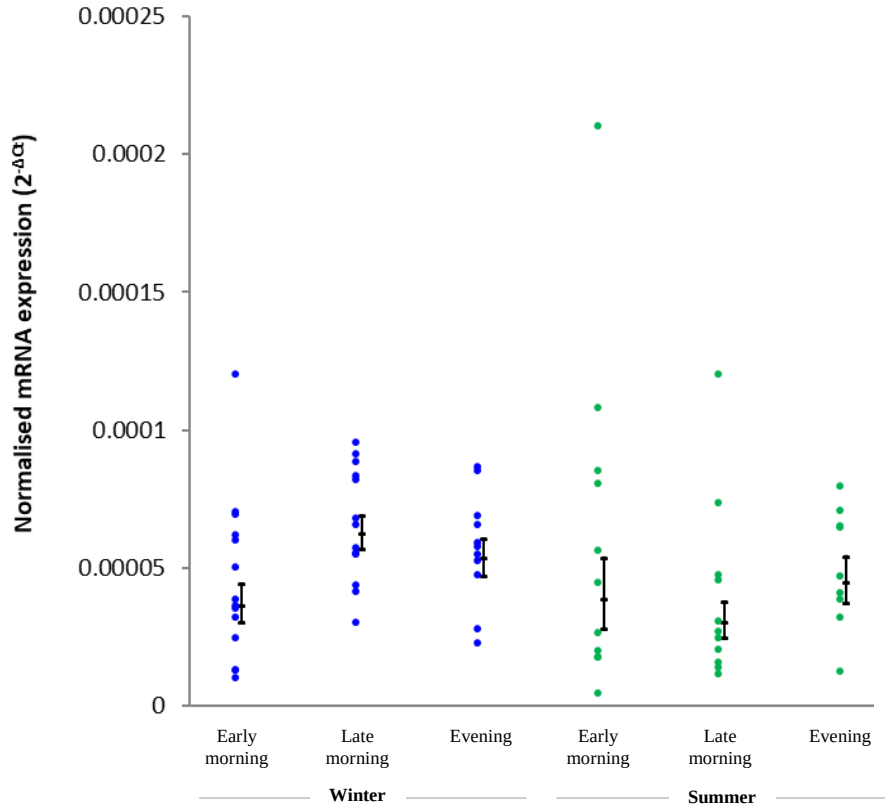

(b) *Cry1*

Male:

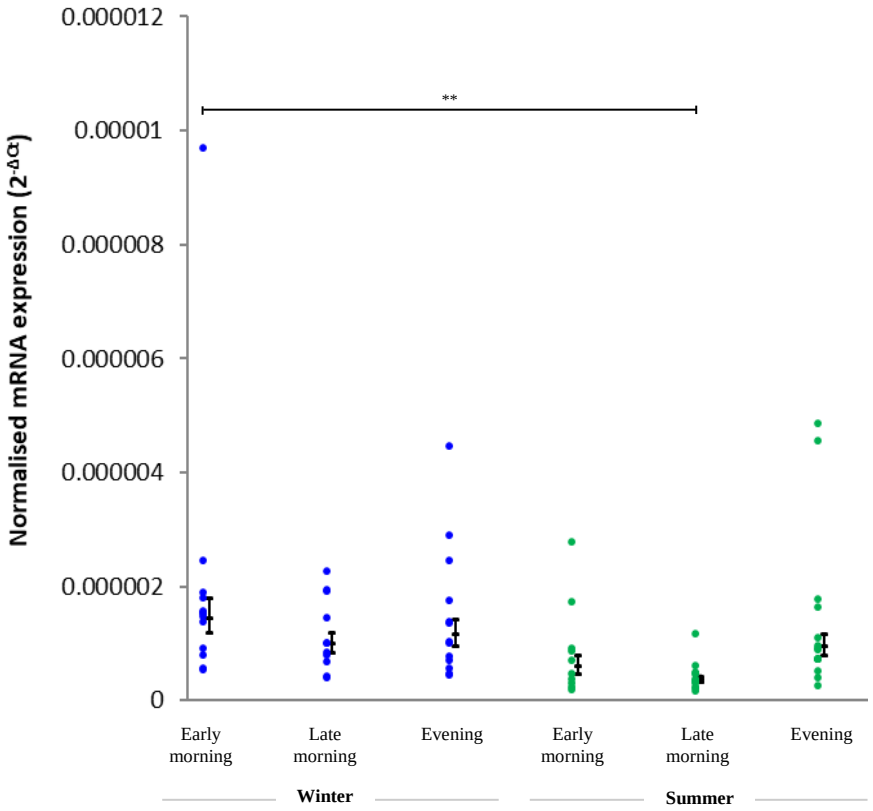

Female:

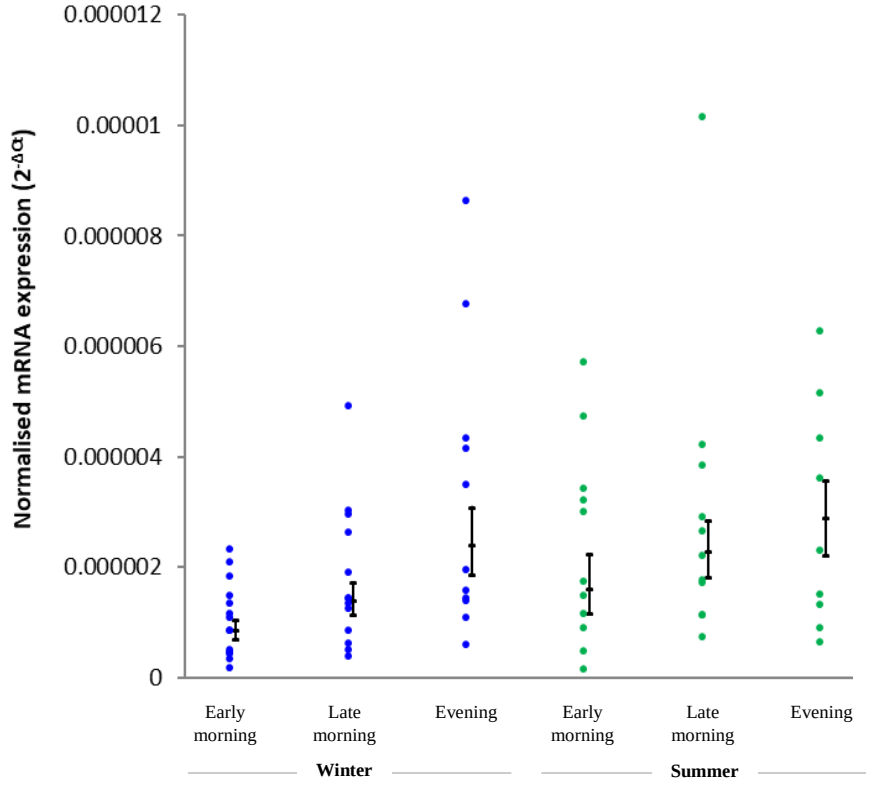

(c) *ARNT*

Male:

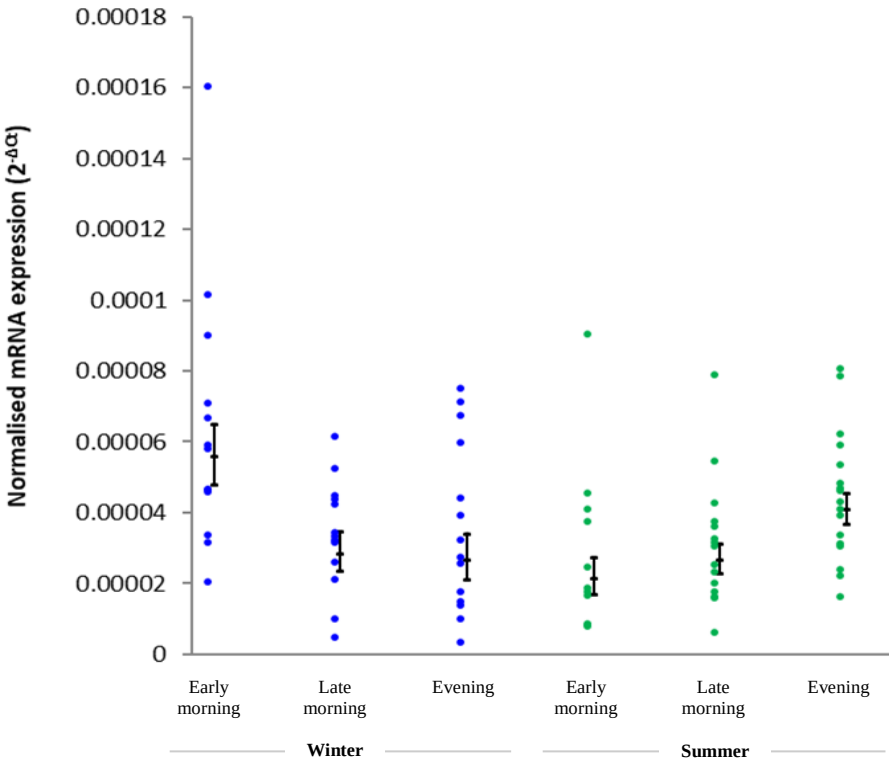

Female:

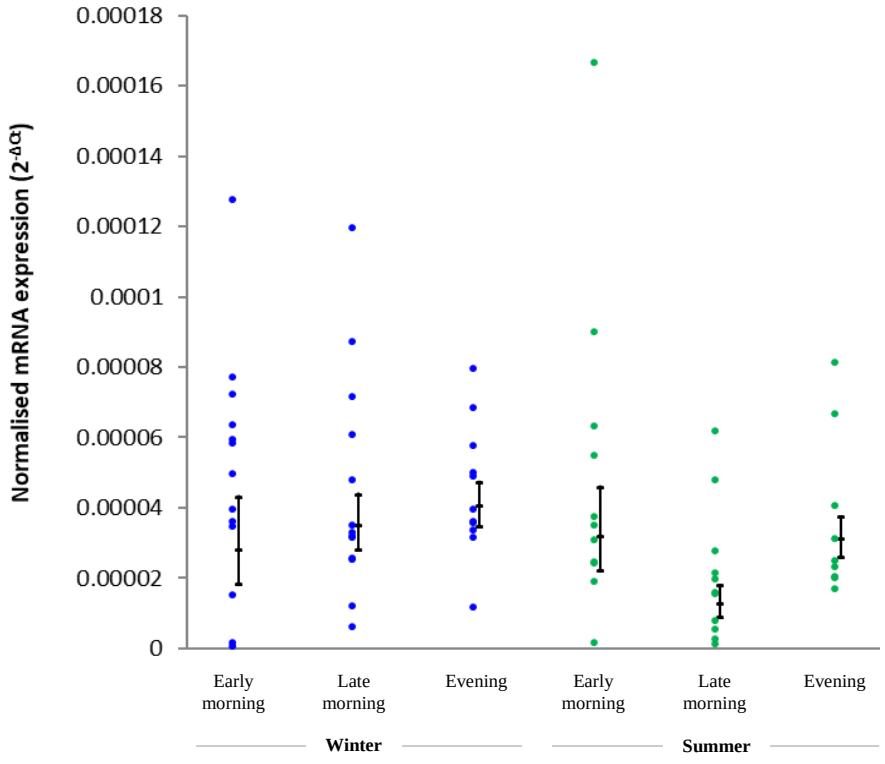

(d) *Timeout*-like

Male:

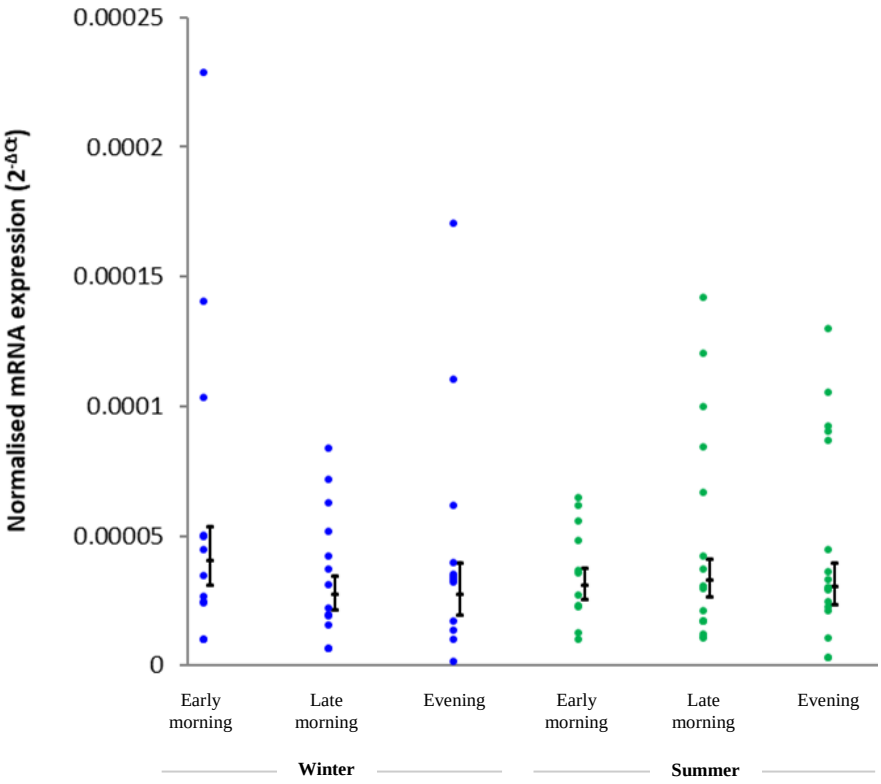

Female:

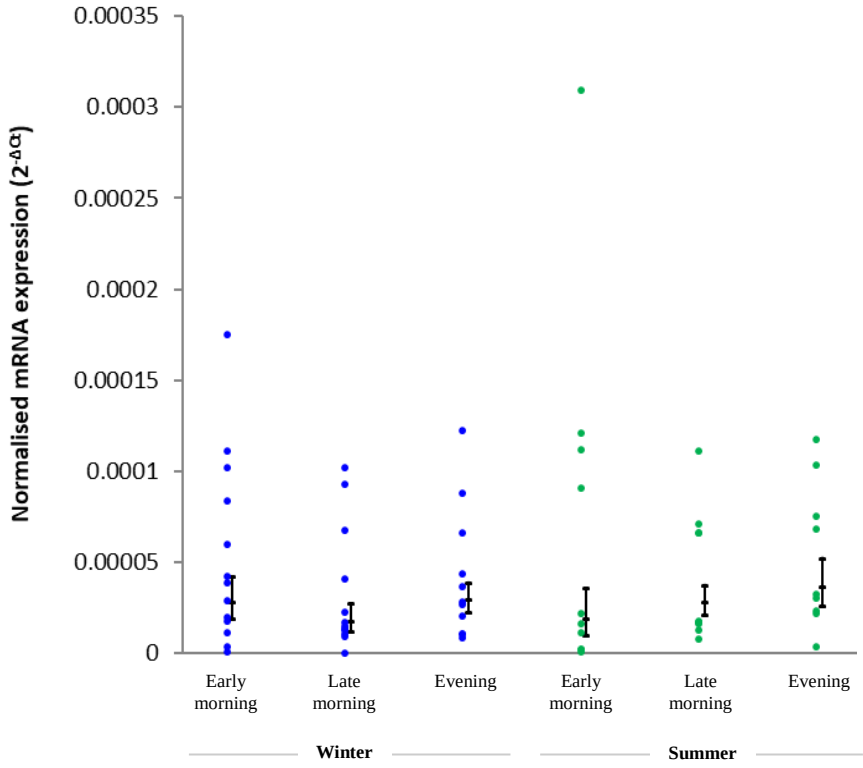

(e) *ROR/HR3*

Male:

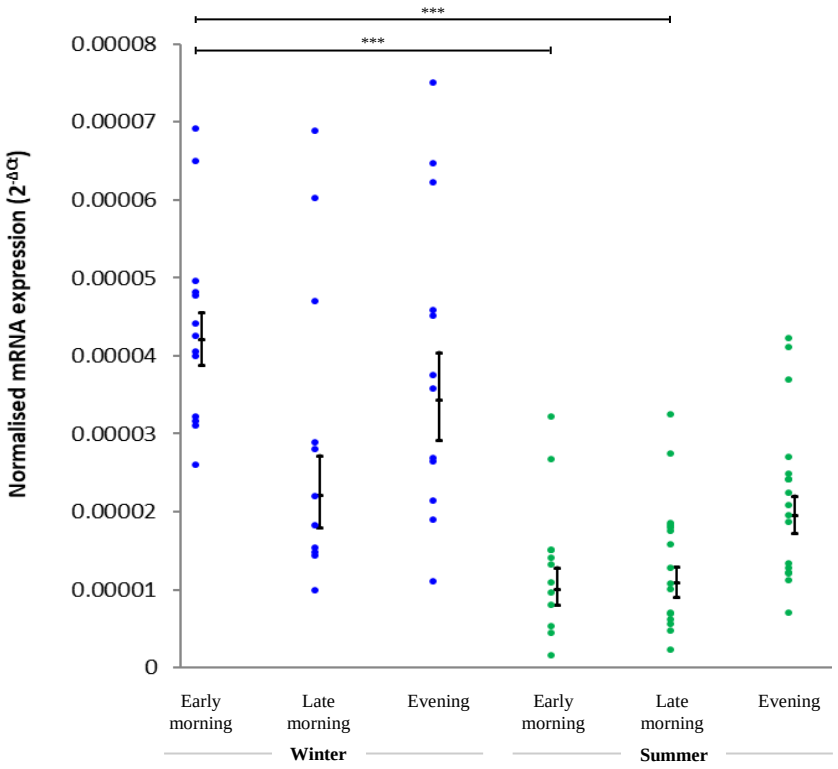

Female:

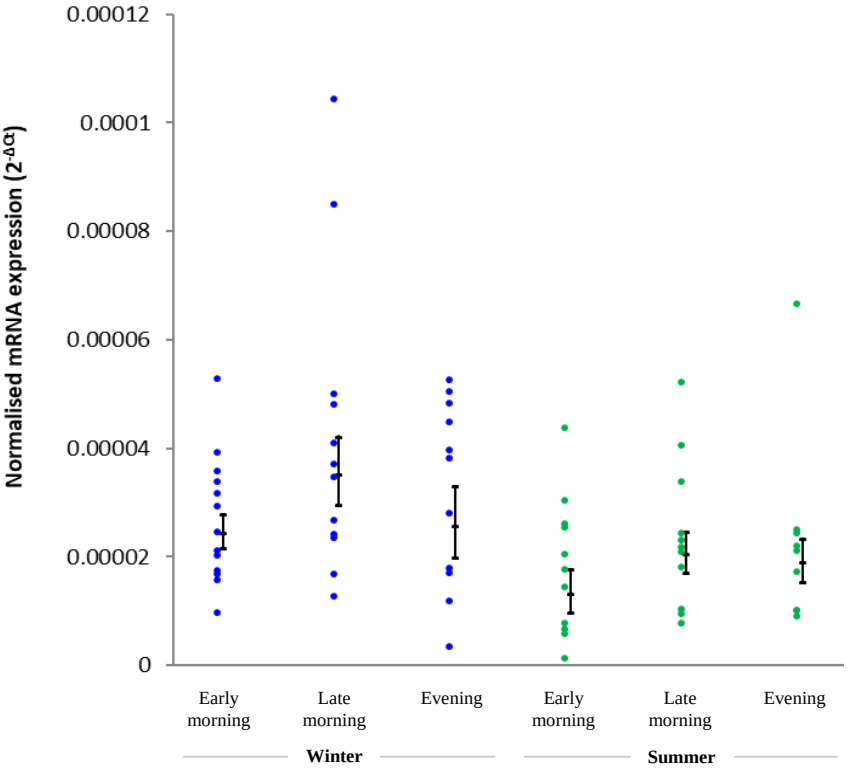

(f) *aaNAT*

Male:

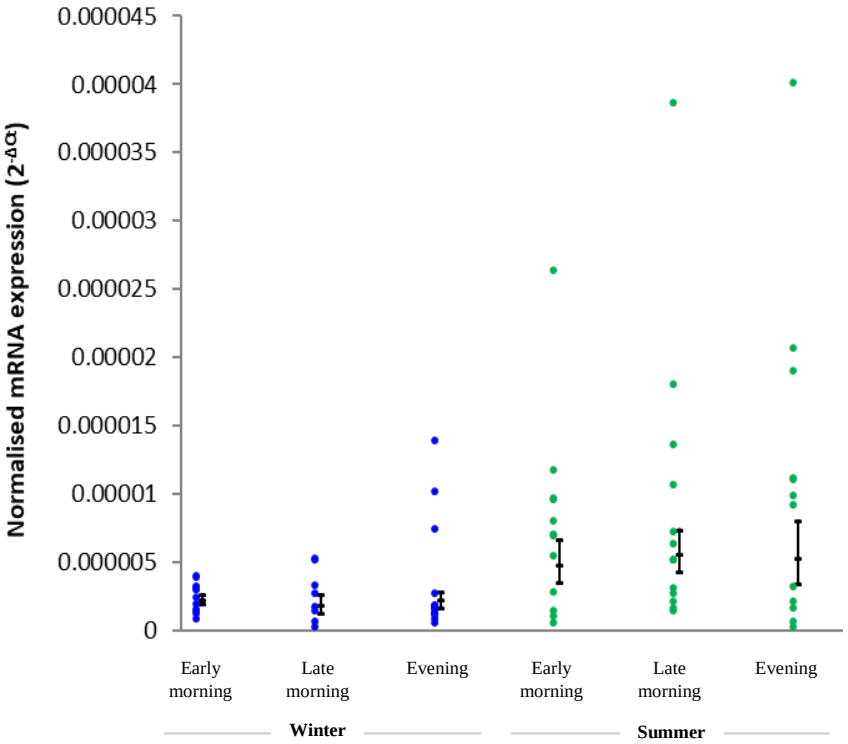

Female:

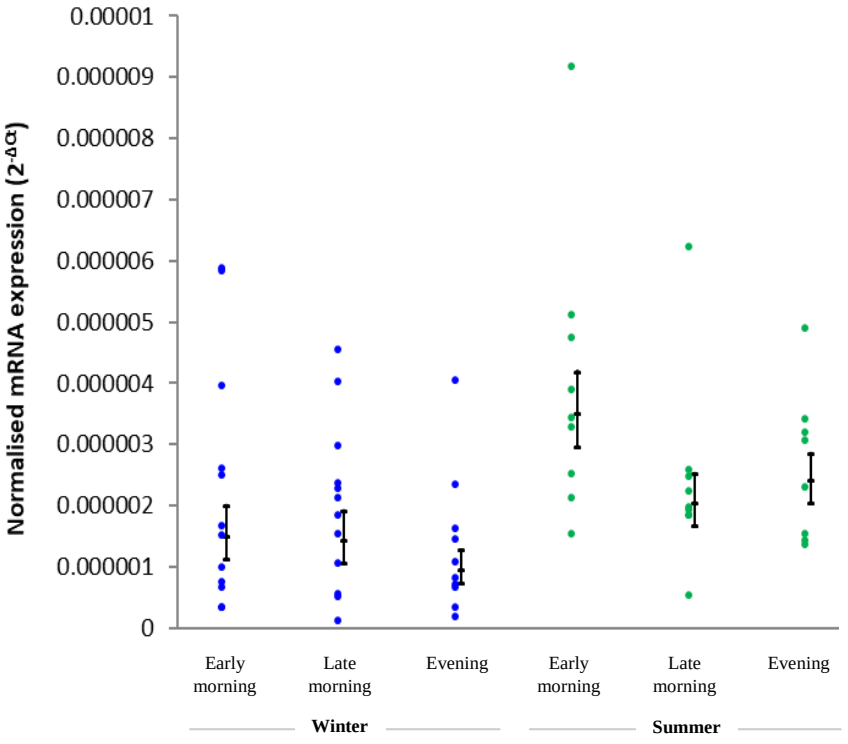

Figure 4.5 Daily and seasonal mRNA expression in *M. edulis* mantle tissue. Mean data ±SEM (black) with individual data-points (winter, blue; summer, green); *n*=8 to 17. Significance determined by Dunn's Multiple Comparisons Tests: * $p<0.05$, ** $p<0.01$ and *** $p<0.001$.

4.4 DISCUSSION

In this chapter, the expression of all six *M. edulis* clock (*Clk, Cry1*, *ROR/HR3*, *Per* and *Rev-erb*) and clock-associated genes (*ARNT, Timeout*-like and *aaNAT*) were detected in the gonads of both sexes, believed to be the first time their expression has been demonstrated in the reproductive tissues of a bivalve. Histological investigation showed seasonal progression of *M. edulis* gametogenesis commencing in winter for both sexes (Figure 4.3; Figure 4.4), confirming an annual biological rhythm in the mantle tissues used for gene expression, as expected (Seed, 1969). Statistically significant differences in mRNA expression levels were detected between winter and summer at the same time of day for males (*Clk*, *Cry1*, *ROR/HR3*) indicating a seasonal effect on gene expression (Figure 4.5a, b, and f). In addition, significant differences were also detected between sexes at individual time-points (*Clk* and *Cry1*), indicating sex-specific gene function/regulation (Figure 4.5a, b).

The expression of clock genes (*Clk, Cry1* and *ROR/HR3*) and clock-associated genes in *M. edulis* mantle tissue indicates the potential for a regulatory molecular clock-mechanism to exist in this peripheral tissue type, though circadian investigation is required. Such peripheral clocks have been documented in mammals (Mohawk and Green, 2012; Schibler et al., 2003), birds (Renthlei et al., 2019), fish (Whitmore et al., 1998) and insects (Tomioka et al., 2012), for example. The results of this chapter also revealed significant seasonal differences in the expression of *Clk, Cry1* and *ROR/HR3* at equivalent time-points between winter and summer; expression was significantly greater in winter males from early morning compared to summer males from early morning (*Clk* and *ROR/HR3*) and late morning (*Clk, Cry1, ROR/HR3*) (Figure 4.5a, b, f). These seasonal differences are consistent with the hypothesis that seasonal variables, such as photoperiod, influence the mRNA expression pattern of *M. edulis*

clock genes. Elevated expression of *Clk*, *Cry1* and *ROR*/*HR3* during the winter morning compared to the summer morning could indicate a change in expression amplitude, a phase shift in peak gene expression, and/or loss of clock mRNA rhythmicity between seasons. However, a greater number of sampling time-points over a 24 hr period in each season would be required to first ascertain circadian rhythmicity and then distinguish between these perturbations. Photoperiod has previously been shown to seasonally affect clock gene expression patterns resulting in differences in amplitude, phase, peak duration and rhythmicity (Benetta et al., 2019; Davie et al., 2009; Tournier et al., 2007; Goto and Denlinger, 2002). In the Atlantic salmon *S. salar*, *Cry2* is phase-delayed under long-day photoperiods, whereas this photoperiod induced arrhythmicity in *Clk*, *Bmal1*, and *Per2* compared to under a short-day photoperiod (Davie et al., 2009). In the sea bass *D. labrax*, *Clk*, *Bmal1*, *Per1* and *Cry1* showed diurnal variations in expression in summer, autumn and winter but not in the autumn (Herrero and Lepesant., 2014). In insects, the weak diurnal rhythm in *Clk* and *Per* expression under long days was lost under short days in the linden bug *P. apterus* (Syrová et al., 2003), and the expression of *Clk*, *Cry2*, *Per* and *Cyc* are influenced by photoperiod and the latitude from which the wasp *N. vitripennis* originates (Benetta et al., 2019). In the flesh fly *Sarcophaga crassipalpis*, the timing of the scotophase (dark period) shifts peak *Per* expression, and long day length dampened the amplitude of *Tim* mRNA expression (Goto and Denlinger, 2002). Finally, in the hamster *C. cricetus*, the levels of *Clk* mRNA in the SCN were reduced under short days, and the expression of *Bmal1* became arrhythmic (Tournier et al., 2007). The work in this chapter is the first time seasonal clock mRNA expression has been investigated in a mollusc.

Clk, in addition to being an integral component of the circadian molecular

clock mechanism (Young, 2000), is required to prevent reproductive defects (Beaver et al., 2002; Miller et al., 2004) and avoid potentially lethal effects (Tobback et al., 2011). In addition, *Clk* RNAi disruption in the insect *R. pedestris* suppressed photoperiodic ovarian development (Ikeno et al., 2013). *Clk* expression was significantly higher in the testes and ovaries of the locust *Schistocerca gregariai* compared to non-reproductive tissues (Tobback et al., 2011). However, even among insects, *Clk* mRNA expression can be either circadian or constant depending on the species (Tomioka and Matsumoto, 2015) and the tissue type (Whitmore et al., 1998). This is also the case for bivalves where constant *Clk* expression was apparent in *M. californianus* gills (Connor and Gracey, 2011) whereas diurnal variation has recently been observed in the gills of *C. gigas* (Perrigault and Tran, 2017). In this chapter, early morning winter males had significantly greater *Clk* expression than early and late morning summer males (Figure 4.5a); expression was reduced 3.4 fold in each case. *Clk* expression patterns are also known to be influenced by day length in fish, which is also the case for the other clock genes *Bmal1*, *Per2* and *Cry2* (Davie et al. 2009; Herrero and Lepesant 2014).

M. edulis Cry1 bears sequence similarities to other invertebrate Type I cryptochromes, which encode photoreceptors sensitive to blue light (see Chapter 2). *Cry1* exhibits a daily expression pattern in *M. californianus* (Connor and Gracey 2011) in addition to other bivalves (Perrigault and Tran 2017; Mat et al. 2016) and was found to exhibit seasonal mRNA expression differences herein. Expression was significantly lower (3.8 fold) in summer males from late morning than winter males from early and late morning (Figure 4.5b). Furthermore, two instances of sex-specific differences in expression at the same time-point were found in the case of *Clk* and *Cry1*; *Clk* expression was significantly higher (2.2 fold) in late morning winter females

compared to males (Figure 4.5a), and *Cry1* expression was significantly higher (6.0 fold) in late morning summer females than males (Figure 4.5b). This suggests sex-specific clock function and/or regulation. Differential regulation of the gene between sexes under the same environmental conditions suggests a sex-specific function of *Cry1* in mussel gonads. *Cry1* expression in *M. edulis* gonad tissue from both sexes contrasts with the absence of *Cry1* expression detected in the ovarian tissues of *Drosophila* (Rush et al., 2006). The expression of vertebrate *Cry1* is much higher in the ovary of the amphibian *Xenopus tropicalis* than in other tissue types (Kubo et al. 2010), and functional mammalian-type *Cry* expression is thought to be a requirement for photoperiodic ovarian development in the insect *R. pedestris* (Ikeno et al., 2011b). The gene also appears to have non-cyclic clock-independent roles in mouse oocyte development (Amano et al., 2009) and spermatogenesis (Alvarez et al., 2003).

ROR acts as a core clock gene in mammals (Jetten et al., 2001) and *RORβ* is required for vision and reproductive success (André et al., 1998). *HR3*, the invertebrate ortholog, is also involved in regulating rhythms along with *E75/Rev-Erb* in some species; *HR3* disruption impacts the expression of *Cyc*, *Tim* and *Clk* in the insect *Thermobia domestica* (Kamae et al., 2014). *HR3* has additional roles in moulting and embryogenesis (Carney et al., 1997). *ROR* exhibits a circadian pattern of mRNA expression in the mussel *M. californianus* (Connor and Gracey, 2011) and seasonal expression differences were found in *M. edulis* herein (Figure 4.5e). *ROR/HR3* expression was significantly higher in males from early morning in the winter compared to males from early and late morning in the summer (4.3 and 3.9 fold lower than winter respectively) (Figure 4.5e). *ROR/HR3* has previously been investigated in reproductive tissues of other species. In the mosquito *Aedes aegypti HR3* is expressed in fat bodies and ovaries and appears to be involved in the regulation

of ecdysone-triggered vitellogenin response (Kapitskaya et al., 2000) and both *HR3* and E75/*Rev-Erb* are required for vitellogenesis and oogenesis in the beetle *Ribolium castaneum* (Xu et al., 2010). In mice, *RORA* expression is differentially regulated by male and female hormones, with testosterone exhibiting negative feedback and estradiol exhibiting positive feedback (Sarachana et al., 2011). Mouse *RORA* was also found to regulate the transcription of the enzyme aromatase which catalyses estrogen biosynthesis from testosterone (Sarachana et al., 2011). Aromatase activity has previously been detected in bivalves using an aromatase assay approach (Matsumoto et al., 1997) and with immunohistochemistry using anti-human P450 aromatase antibodies (Prisco et al., 2017; Rosati et al., 2019). Though a molluscan homolog of the *CYP19* gene that encodes aromatase is yet to be identified (Liu et al., 2017), homologs of many of the other vertebrate steroidogenesis genes have now been identified in *M. edulis* (Blalock et al., 2018), though interactions with ROR/HR3 remain to be investigated.

No significant differences in mRNA expression were detected between time-point or between sex for *ARNT*, *Timeout*-like and *aaNAT* (Figure 4.5c, d, and f). This may reflect their putative functions as clock-associated genes, involved in interactions with clock components, rather than acting as core molecular clock components. *M. edulis ARNT* shares most sequence similarity with *ARNT/TANGO* rather than the closely related gene *ARNTL/CYC/BMAL1* (see Chapter 2). The latter is involved in the core clock mechanism of vertebrates and invertebrates (Young, 2000) and is required for mammalian reproductive development (Alvarez et al., 2008) and insect photoperiodic response (Ikeno et al., 2011a). However, like ARNTL/BMAL1, mammalian ARNT1 and 2 can dimerise with the protein encoded by the melatonin-activated NPAS4 gene creating a herterodimer which triggers *Cry1* expression, linking

ARNT to circadian regulation (West et al., 2013). Dimerisation with other binding partners means ARNT/TANGO is involved in a variety of other processes including neural development (Kewley et al., 2004; Sonnenfeld et al., 1997), estrogen receptor transcription (Brunnberg et al., 2003), and response to hypoxia and xenobiotics (Kewley et al., 2004). Gene knockout of either of the two mammalian forms of *ARNT* result in death in mice embryos, further emphasising its developmental importance (Kewley et al., 2004). The function of *ARNT* is not yet know in molluscs.

Tim is a core insect clock gene involved in light-mediated reactions (Peschel et al., 2009), whereas its paralog *Timeout* is involved in chromosome cohesion (Benna et al., 2010) and mediating the effects of damage to the replication fork during DNA synthesis (Errico and Costanzo, 2010). However, *Timeout* mRNA is expressed in a circadian pattern in some insects (Tomioka and Matsumoto, 2015) and its function has been linked to light entrainment of the clock in *Drosophila* (Benna et al., 2010). Conversely rhythmic expression of *Timeout* was not apparent in the sea anemone *N. vectensis* (Reitzel et al., 2010). Similarly, mammalian *Tim*, the ortholog of *Timeout* (Gotter, 2006), does not have a circadian rhythm in the brains of mice (Koike et al., 1998), however a *Tim* isoform interacts with the clock mechanism in the brains of rats (Barnes et al., 2003). *Tim* is yet to be isolated from mussels, and the function of *Timeout*-like requires further investigation.

Finally, *M. edulis aaNAT*, encoding the non-vertebrate type (NV-aaNAT) also did not vary significantly between the time-points tested or between males and females at the same time-point (Figure 4.5f). Though the vertebrate type VT-aaNAT catalyses the rate limiting step of circadian melatonin production (Klein, 2007), and the insect type (iaaNAT) links the circadian and photoperiodic systems (Hiragaki et al., 2015; Mohamed et al., 2014), it is unclear whether the more ancestral NV-aaNAT is involved

in processes beyond neurotransmission and detoxification (Pavlicek et al., 2010). However, among cnidaria aaNAT appears to regulate rhythmic melatonin production in the gonads of the sea star *E. brasiliensis* (Peres et al., 2014) and though melatonin does not rhythmically cycle in the sea pansy *R. köllikeri*, a seasonal correlation was found between gonad maturation and melatonin increase, suggesting a potential role as a seasonal messenger (Mechawar and Anctil, 1997). Rhythmic melatonin content has also been previously detected in molluscs (Abran et al., 1994; Blanc et al., 2003; Muñoz et al., 2011) though the function requires further investigation.

Finally, as *M. edulis* were sampled from the wild for this experiment, the seasonal differences in mRNA expression observed may be caused by many seasonal cues such as photoperiod, temperature, food availability and social cues (Paul et al., 2008). Photoperiod, an important seasonal cue in multiple taxa (Denlinger, 2009) including molluscs (Numata and Udaka, 2010; Bohlken and Joosse, 1981) varied between 7.5 hr in winter and 17 hr in summer (Figure 4.1) however no data collection was performed for non-photoperiodic seasonal cues like temperature, which would be required to confirm seasonal patterns in these variables. Furthermore, additional investigation is required to establish whether the expression of *M. edulis* clock genes exhibit rhythmic circadian patterns. Though no daily variation in mRNA expression was discovered for any of the genes analysed, a greater sampling frequency over a 24 hr period is required to capture such circadian changes. Sampling in this field experiment was constrained by natural tidal cycles and was designed to capture seasonal differences rather than diurnal variation in expression, which was the focus of a laboratory-based exposure experiment in Chapter 5.

4.5 CONCLUSIONS

mRNA expression of all six clock and clock-associated genes was detected in the mantle tissue of both sexes, indicating the potential for a peripheral molecular clock mechanism to be present. Seasonal clock mRNA expression differences indicate that seasonal environmental changes impact upon molecular clock components as a possible mechanism of providing seasonal cues to inform rhythmic biological processes. Differential *Clk* and *Cry1* expression between males and females indicates sex-specific regulation and/or function. Investigation into the 24 hr expression patterns of *M. edulis* clock genes will provide further insights into the molecular-level regulation of biological timekeeping in this species, which will be addressed in Chapter 5.

Chapter 5

Effect of light and temperature cycles on circadian rhythm-related genes in *M. edulis* under laboratory conditions

5.1 INTRODUCTION

Circadian rhythms are endogenously regulated on a molecular level by a circadian clock mechanism. As discussed in previous chapters, this negative feedback system comprises interactions between clock genes and their proteins, which regulate their own expression throughout a 24 hr cycle (Allada et al., 2001; Young and Kay, 2001). Though these endogenous interactions can persist in the absence of external stimuli, synchronisation (entrainment) between internal molecular rhythms and external environmental cycles e.g. light and temperature, is an essential feature of circadian rhythms (Golombek and Rosenstein, 2010; Dubruille and Emery, 2008; Rensing and Ruoff, 2002) considered to confer adaptive advantage (Vaze and Sharma, 2013).

Clock genes play a vital role in regulating endogenous biological rhythms in diverse phyla (Hardin, 2005; Allada et al., 2001; Young and Kay, 2001; Young, 2000), however the mechanisms underpinning the timekeeping ability of molluscs are an understudied aspect of their biology. The few studies to date in which clock genes have been characterised in molluscs are as follows: cephalopods (Heath-Heckman et al., 2013), gastropods (Cook et al., 2018; Duback et al., 2018; Schnytzer et al., 2018; Bao et al., 2017; Constance et al., 2002), and bivalves (Schnytzer et al., 2018;

Perrigault and Tran, 2017; Sun et al., 2016; Pairett and Serb, 2013; Connor and Gracey, 2011). Clock genes, and those with clock-associated functions, have also been isolated from the blue mussel in this thesis (see Chapters 2 to 4). Rhythmic biological processes occurring in this commercially important genus (*Mytilus*) include valve movements with circadian (Gnyubkin, 2010; Robson et al., 2010; Wilson et al., 2005; Ameyaw-Akumfi and Naylor, 1987) and ultradian periodicities (Rodland et al., 2006), circatidal cell renewal (Zaldibar et al., 2004), seasonal sexual development (Seed, 1969), and rhythmic gene expression where circadian periodicity is more prevalent than tidal (Connor and Gracey, 2011). The rhythmic expression of molluscan clock genes includes *Cry1* and *ROR* which exhibit circadian expression in *M. californianus* gills (Connor and Gracey, 2011). In the head of the squid *E. scolopes* *Cry1* and *Cry2* are also rhythmically expressed (Heath-Heckman et al., 2013). In the clock neurons of sea snail *B. gouldiana*, *Per* is rhythmically expressed under light/dark cycles but does not oscillate in constant darkness (Constance et al., 2002). Only weak oscillations or constant expression were detected for clock genes in the limpet *Cellana rota* (Schnytzer et al., 2018) whereas the expression cycles of numerous oyster clock genes indicate endogenous circadian activity in *C. gigas* (Perrigault and Tran, 2017; Mat et al., 2016). It is yet to be ascertained whether the molecular circadian clock of the blue mussel is endogenous in nature – an important aspect of the chronobiology of the species, pertaining to the regulation of multiple physiological and behavioural rhythms.

Temperature compensation is another key feature of circadian rhythms, meaning that their endogenous ~24 hr period is able to be maintained over a range of constant temperatures (Ruoff, 2004; Rensing et al., 2001). Despite this, the function of the molecular clock mechanism can be both directly and indirectly affected by

temperature changes, that are either pulses or periodic, by influencing input pathways, molecular interactions, phase shifts, amplitude and entrainment (Rensing and Ruoff, 2002). In addition, rhythms can be entrained by temperature cues in both invertebrates and vertebrates (Waite et al., 2017; Glaser and Stanewsky, 2005; Lahiri et al., 2005) with daily temperature cycles of just 1-2 °C able to entrain ectotherms (Rensing and Ruoff, 2002). Thermocycles modulate clock gene expression in mosquitos, with temperature and light sensitivity of clock components varying between species (Rivas et al., 2018). In molluscs, temperature pulses can disrupt gene expression rhythms as some tidal and circadian transcripts in *M. californianus* lose their rhythmicity following experimental heating events (Connor and Gracey, 2011), however the effect of thermocycles on the clock gene activity of bivalves is not known. In Chapter 4, it was revealed that intertidal mussels exposed to natural seasons, encompassing shifts in photoperiod, show differences in clock gene (*Clk*, *Cry1*, *ROR/HR3*) expression between seasons however the relative importance of light and temperature are yet to be investigated.

The purpose of this chapter was to investigate whether *M. edulis* clock genes (1) show variation in mRNA expression under cycling light/dark conditions simulating day/night, (2) show persistent endogenous rhythmicity in the absence of light and (3) are influenced by diurnal thermocycles in the absence of light. It was hypothesised that diurnal clock gene expression occurs in *M. edulis* under LD conditions and persists under DD, indicative of endogenous regulation. It was also hypothesised that temperature cycles can modulate clock gene expression patterns. For this purpose, a laboratory-based experiment was performed using hypothetical lighting and temperature regimes to investigate the effect of diurnal light and temperature cycles on clock mRNA expression patterns. In addition to the clock genes (*Clock*, *Cry1*,

ROR/HR3) and clock-associated genes (*ARNT*, *Timeout*-like, *aaNAT*) isolated and discussed at length in previous chapters, two additional clock genes were also targeted: *Period* (*Per*) and *Rev-erb/NR1D1*. The endogenous nature of blue mussel clock mRNA expression is revealed for the first time herein. This work is also the first investigation into the effect of temperature, in particular diurnal temperature cycles, on the molecular clock mechanism of a bivalve.

5.2 MATERIALS AND METHODS

5.2.1 Mussel collection and laboratory acclimation

Wild, adult *M. edulis* (mean length (mm) ± SEM: 40.53 ± 0.25, *n*=498) were collected from the rocky shore intertidal zone at Filey Beach, North Yorkshire, UK (54° 13' longitude and 0° 16' latitude) during low tide on the evening of 24.11.16, which was 5 days before the new moon lunar phase. Mussels were transferred to the laboratory on the same day and divided into 9 independent glass tanks (*n*=56 each) containing 30 L of 35 ppt artificial seawater (Tropic Marin, Germany). Mussels were kept constantly submerged and each tank was aerated by two air stones to maintain water quality (Figure 5.1).

Figure 5.1 Photo of 3 of the 9 tanks of *M. edulis* used in the exposure experiment.

Mussels were acclimated to laboratory conditions for 10 days. It is important that organisms being examined for their rhythmic activities are maintained in experimental conditions for over a week before being assessed, as rhythms exhibited initially are those which were entrained by the source habitat (Robson et al., 2010; Kim et al., 1999). During the acclimation period, water temperature was maintained at 9.7 ± 0.4 °C (mean ± SD) in a climate-controlled room and a light regime of 10 hrs light/14 hrs dark was chosen, in accordance with a previous study on bivalves in which daily and tidal activity, in addition to *Cry1* expression rhythms, were investigated in *C. gigas* (Mat et al., 2016). This lighting regime was not selected to replicate a particular time of year, but was used an artificial setup to investigate the effect of LD and DD on clock gene expression patterns in a controlled experimental environment. Throughout both the acclimation and experimental periods, 50% water changes, using 35 ppt artificial seawater (Tropic Marin, Germany) pre-chilled to acclimation/experimental temperature as appropriate, were conducted on alternate days. Mussels were fed daily with PhytoGreen-M suspension (Brightwell Aquatics, UK) containing 10 – 15 µm *Tetraselmis* sp. phytoplankton added to a final concentration of ~0.43 million cells per ml, as per manufacturer's instructions. Half-tank water changes, conducted at irregular times to avoid introducing a regular tidal cue, ensured mussels remained constantly submerged, removing the effect of emersion as a potential zeitgeber (Mat et al., 2016). Similarly, feeding times were irregular to reduce the likelihood of food acting as a zeitgeber (Robson et al., 2010). Physical properties of the seawater were monitored daily using an "ama-digit ad 15th Electronic Thermometer" (Amarell Electronic, Kreuzwertheim, Germany), a 3510 pH Meter (Jenway, Bibby Scientific Limited, Stone, UK) and a V2 salinity refractometer (TMC, UK). Water parameters in the tanks did not require adjusting during the acclimation

or experiments periods.

5.2.2 Experimental treatments and sampling

After the acclimation period, 3 tanks of mussels per room (*n*=56 in each tank) were concurrently exposed to one of the following conditions in independent climate/light-controlled rooms: 10:14 hr light/dark cycles at constant 9 °C temperature (LD), constant darkness at 9 °C (DD) or constant darkness with thermocycles of 10:14 hr thermophase:cryophase differing by 3.6 ± 0.2 °C where 9 °C was the cryophase (DDTC). Light and temperature conditions were hypothetical regimes and are summarised in Figure 5.2.

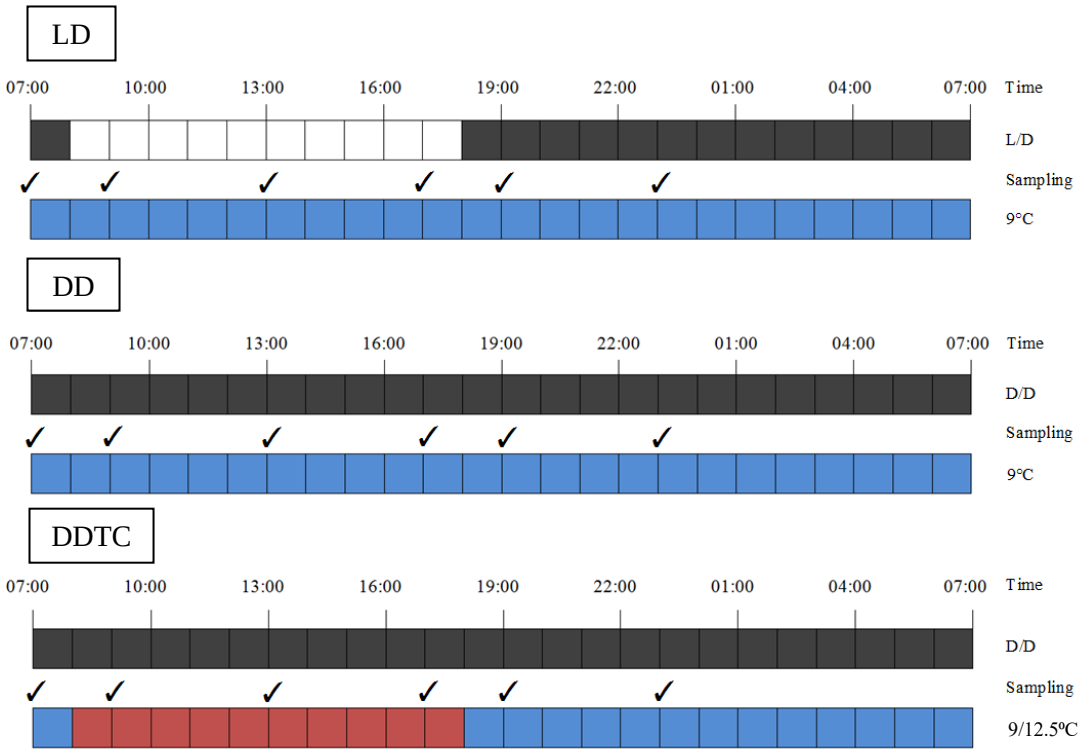

Figure 5.2 Treatment conditions and sampling regime for circadian mussel exposure experiment. Ticks represent sampling times. Abbreviations: LD, light/dark; DD, dark/dark; DDTC, dark/dark temperature cycles.

Light intensity was measured with a Hi 97500 Portable Luxmeter (Hanna Instruments Ltd, Leighton Buzzard, UK) and was 500 lux during the LD light phase (photophase) and 0 lux during the dark phase (scotophase), DD and DDTC. Water changes during dark periods were performed using a dim red LED headlamp (3 lux) to minimise light disturbance as much as possible. Water temperature was measured with a ama-digit ad 15th Electronic Thermometer (Amarell Electronic, Kreuzwertheim, Germany) and was as follows (mean ± SD): 9.7 °C ± 0.5 in LD and DD, 10.1 °C ± 0.4 at the end of DDTC cryophase, and 13.7 °C ± 0.4 at the end of DDTC thermophase. Temperature cycles were created by controlling the ambient air temperature resulting in a gradual change in water temperature. There was a 3.6 ± 0.2 °C (mean ± SD) difference between cryophase and thermophase which is within the range of naturally occurring day/night sea surface temperature variation occurring in different locations around the world (Kawai and Wada, 2007) such as the 3 °C diurnal variation in SST recorded off northern Japan (Sakaida et al. (2000). However, diurnal sea surface temperature (SST) measurements were not collected at the Filey Bay sampling site so the thermocycles used herein are an artificial experimental condition. The duration of the cryophase and thermophase were chosen to match the respective durations of the dark and light periods in the LD treatment. Salinity was measured using a V2 salinity refractometer (TMC, UK) and was 35.4 ± 0.6 ppt across all tanks and pH was measured using a 3510 pH Meter (Jenway, Bibby Scientific Limited, Stone, UK) and was 7.8 ± 0.1.

For all treatments, mussels were sampled at zeitgeber/circadian times ZT 23 (7 am), ZT 1 (9 am), ZT 5 (1 pm), ZT 9 (5 pm), ZT 11 (7 pm) and ZT 15 (11 pm) where ZT 0 (8 am) was lights on and ZT 10 (6 pm) was lights off in the control treatment, and temperature up and temperature down in the thermocycles treatment

Figure 5.2. These time-points were chosen based on Mat et al. (2016) which is designed to strategically sample different points of the putative rhythm: sampling is targeted to time-points before and after each zeitgeber transition (e.g. lights on, lights off) in addition to 5 hr after each transition. Exposure duration was 13 days for the control and thermocycles treatment, and 14 days for constant darkness treatment as the large sample sizes made it impractical to dissect all mussels on the same day. Mussel shell lengths were measured the longest dimension prior to dissection. At each of the 6 sampling time-points, tissue from the mantle, foot, posterior adductor muscle and gill was dissected (Figure 5.3) from *n*=28 mussels from each treatment and stored in 1 mL RNA*later* solution (Ambion, Life Technologies, USA) at -20 °C for molecular work. Mantle tissue was also collected from each individual and stored for histological and chemical analyses described in Section 3.2.2. Mantle tissue was also collected at sampling points ZT 23 (7 am) and ZT 9 (5 pm) from all treatments, and stored in TRI Reagent® at -20 °C to preserve proteins.

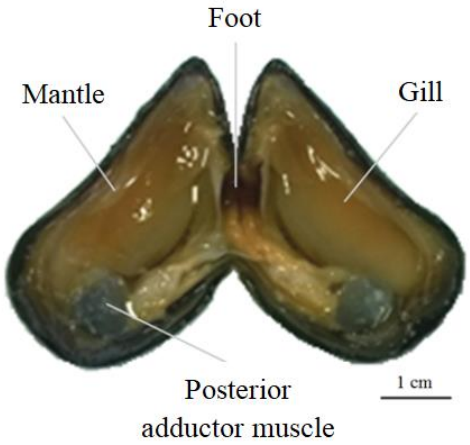

Figure 5.3 Photo of a mussel which has been cut open with the tissues dissected labelled

5.2.3 Histology

To assess mussel sex, histology was performed on formalin-preserved mantle tissue samples using ethanol dehydration, paraffin wax embedding, microtome

sectioning and H&E staining as previously described (Section 4.2.2).

5.2.4 Total RNA isolation and quantification

Male mussels (*n*=7-9) were randomly selected from each time-point from each of the 3 treatments for molecular work. Male mussels were selected for investigation as males previously showed significant seasonal differences for a number for clock genes (*Clk, Cry1*, *ROR/HR3*) at equivalent times of day suggesting a potential involvement in the regulation of biological timekeeping (see Chapter 4). Samples were randomised and analysed blind. In each case, total RNA was extracted from ~10 mg mantle tissue using the High Pure RNA Tissue Kit reagents (Roche, UK) including DNase I treatment as previously described (Section 2.2.2.). RNA concentrations were measured using the Qubit 1.0 Fluorometer (Life Technologies, UK) (Section 2.2.3.).

5.2.5 cDNA synthesis

cDNA was synthesised using the Precision Nanoscript2 Reverse Transcription Kit (PrimerDesign, Southampton, UK). Each reaction contained 180 ng RNA, 1 µL random nonamer (9 bp oligonucleotide) primer mix and RNase/DNase free water to a total volume of 10 µL. Samples were incubated at 65 °C for 5 min, before being placed immediately on ice. The following reagents were added: 5 µL NanoScript2 4x RT reaction buffer, 1 µL dNTP mix (10 mM each), 3 µL RNase/DNase free water and 1 µL of 160 U/µl NanoScript2 reverse transcriptase enzyme. Samples were mixed and centrifuged prior to incubation at 25 °C for 5 min, 42 °C for 20 min and 75 °C for 10 min. Samples were stored at -20 °C.

5.2.6 Isolation and characterisation of *Per* and *Rev-erb*

In addition to the clock and clock-associated genes isolated in the previous chapters (*Clk*, *Cry1*, *ARNT*, *Tim*-like, *ROR*/*HR3* and *aaNAT*), two other clock genes, *Per* and *Rev-erb* which are involved in core clock interactions in diverse phyla (Kamae et al., 2014; Guillaumond et al., 2005; Young and Kay, 2001; Zeng et al., 1996), were isolated herein so a wider range of clock genes could be investigated. An alignment of *Per* sequences from the scallop *Mizuhopecten yessoensis* (Genbank accession XM_021519834.1) and the oyster *C. gigas* (JH816853.1) was created from which degenerate primers were designed (Table 5.1). PCR conditions, using 1 µL of *M. edulis* cDNA, were as follows: 2.5 µL Fisher BioReagent 10× Taq Buffer A, 0.5 µL dNTP mix (40 mM), 0.5 µL of each 10 µM primer, 0.25 µL of 5U/µL Fisher BioReagents™ Taq DNA Polymerase, 0.5 µL $MgCl_2$ (25 mM), and molecular-grade water (Fisher Scientific, UK) to a total volume of 25 µL. Thermal cycling conditions were 94 °C for 2 min, followed by 35 cycles of 94 °C for 30 sec, 45 °C for 30 sec and 72 °C for 30 sec, with a final extension of 72 °C for 2 min. A second PCR was performed under the same conditions using 5 µL of the original PCR product and the band obtained from electrophoresis was purified from the gel with the Macherey Nagel NucleoSpin Gel and PCR Clean-up Kit (Fisher Scientific, UK) and eluted in 20 µL 5 mM Tris/HCl buffer.

Table 5.1 Primers used for isolating partial *M. edulis* clock gene sequences.

Target gene	Primer	Sequence (5'-3')	Predicted amplicon size (bp)
Per	ecPER_F3	AAG ACA GAA TGG TCC AGT TTT A	~551-626
	ecPER_R5	ACC TT**K** GTA CTG CT**M** CCA AA	
Rev-erb	E75_F1	CTA GCG GCT TCC ACT ATG GG	463
	E75_R2	GGG TCT CTG GCA AGT TGG G	

Degenerate nucleotides shown in bold

Primers for *Rev-erb* (Table 5.1) were designed based on the *M. galloprovincialis Rev-erb* sequence (Raingeard et al., 2013) and were tested on 1 µL of *M. edulis* cDNA with the following PCR reagents: 5 µL 5X Herculase II Reaction Buffer (Agilent Technologies, UK), 0.5 µL dNTP mix (40 mM), 0.5 µL of each primer (10 µM), 0.25 µL Herculase II Fusion DNA Polymerase (Agilent Technologies) and molecular-grade water (Fisher Scientific, UK) to a total volume of 25 µL. Thermal cycling conditions were 94 °C for 5 min, followed by 35 cycles of 94 °C for 30 sec, 55 °C for 30 sec and 72 °C for 30 sec, with a final extension of 72 °C for 5 min. PCR products for both genes were separated on 1% agarose TBE gels stained with Gel Red Nucleic Acid Gel Stain (Cambridge Bioscience, Cambridge, UK) and were sequenced using the EZ Seq Sanger sequencing service (Macrogen Europe, Amsterdam, The Netherlands). Resulting sequences were manually edited and aligned with BioEdit (Version 7.0.9.0).

To confirm sequence identities, blastn/blastx searches were performed against the NCBI GenBank database (https://blast.ncbi.nlm.nih.gov/Blast.cgi) and multiple species amino acid sequence alignments were created for PER and REV-ERB using Clustal Omega (https://www.ebi.ac.uk/Tools/msa/clustalo/). Phylogenetic trees using maximum likelihood analysis were generated using MEGA7 version 7.0 (Kumar et al., 2016). The Jones-Taylor-Thornton (JTT) model and the Nearest Neighbour Interchange (NNI) method for heuristic searches were used, with support for the tree indicated by bootstrap values from 1000 replicates displayed on the nodes.

5.2.7 qPCR optimisation and amplification

Real-time qPCR reactions were optimised and performed for the following *M. edulis* target genes: *Clk*, *Cry1*, *ROR/HR3*, *Per*, *Rev-erb*, *ARNT*, *Timeout*-like and

aaNAT, in addition to reference genes *18S* and *EF1* assessed as stable in previous *M. edulis* qPCR experiments (Chapter 4, Cubero-Leon et al., 2012; Ciocan et al., 2011) and their geometric mean expression did not vary significantly between groups ($KW=27.199_{17}$, $p=0.0552$). The qPCR primers, which are detailed in Table 5.2, were designed using the Primer-BLAST tool (http://www.ncbi.nlm.nih.gov/tools/primer-blast/). qPCR assays were performed using 10 µL PrecisionPLUS 2X qPCR MasterMix with SYBR Green for the ICycler (PrimerDesign, UK) combined with 7 µL molecular-grade water, 2 µL primer mix and 1 µL 1:2 diluted cDNA (derived from 180 ng RNA). Optimised final primer concentrations were 100 nM for the genes of interest and 50 nM for the reference genes and standard curves confirmed primer efficiencies of 90-110% in line with the MIQE guidelines (Taylor et al., 2010; Bustin et al., 2009). qPCR reactions were performed in duplicate on a CFX96 Real Time PCR Detection System (Bio-Rad, Hemel Hempstead, UK) and thermal cycling conditions were as follows: 95 °C for 2 min, followed by 40 cycles of 95 °C for 10 sec, 60 °C for 1 min and 72 °C for 1 min. Negative controls were included on each plate for all primer pairs and melt peaks were generated for all samples upon reaction completion to confirm primer specificity, lack of contamination and absence of primer dimers. Agarose gel electrophoresis was used to confirm the presence of single PCR products for assays and no amplification in template-negative controls.

Table 5.2 Primers used for qPCR amplification of *M. edulis* genes with primer melting temperatures (Tm), percentage guanine-cytosine content (% GC) and qPCR product sizes shown.

Gene of interest	Primer	Sequence (5'-3')	Tm (˚C)	% GC	Size of product (bp)
Clk	*Clock*_qPCR_F3	GCA GAA TTC ACA TCA AGG CAC A	56.1	45.5	115
	*Clock*_qPCR_R3	AGT CAT ACC CAG ACG TCC CT	57.4	55.0	
Cry1	*Cry1*_ qPCR_F2	GTC TGT CAG GAG GTT CCA CTG	57.2	57.1	85
	*Cry1*_ qPCR_R2	ACA GGT CAA AGC ATC TGG CT	56.9	50.0	
ARNT	*ARNT*.qPCR.F3	CAG CAG GTG CCC CTA CTT AT	56.8	55.0	117
	ARNT.qPCR.R3	CAG GCG GCC ATA TAA CTG GT	57.3	55.0	
Timeout-like	*Timeout*_F3	ATG TTC AGG GAA CAG AAC CCA	56.3	47.6	107
	*Timeout*_R3	TCC TGC TCT CTA ACC ATC TCC	55.6	52.4	
ROR/ HR3	*ROR*_qPCR_F1	AGA GAC GCT GTG AAG TTT GGT	56.6	47.6	117
	*ROR*_qPCR_R1	GCC TGT CGG TGA TGT TGG AT	57.7	55.0	
aaNAT	*aaNAT*_F2	AGG ACG AAG CAG CCA CTT AC	57.2	55.0	214
	*aaNAT*_R2	CGT CGA CGC GAT TCT TTG AC	56.5	55.0	
Per	*Per*_qPCR_F1	TCA TCA GAC AAG AGA AGC GGG	56.7	52.4	92
	*Per*_qPCR_R1	GGA ATG TCG ACT CCA AAA TCA GG	55.9	47.8	
Rev-erb	*E75*_F5	AGT TGG TAT GTC CAG GGA TGC	57.0	52.4	107
	*E75*_R5	GGT TCA CCT GAG TCT GAC AGT	56.4	52.4	
EF1a	*EF1a*_F5	GAT GGG TTG GTA CAA GGG GT	57.0	55.0	119
	*EF1a*_R5	GGA GAG CTT TGT CTG TGG GT	57.1	55.0	
18S	*18S*_F4	TGA CTC AAC ACG GGA AAA C	52.9	47.4	120
	*18S*_R4	GAC AAA TCG CTC CAC CAA C	54.2	52.6	

5.2.8 Analysis of qPCR data

RT-qPCR data of mRNA expression of the genes of interest (*Clk*, *Cry1*, *ROR/HR3*, *Per*, *Rev-erb*, *ARNT*, *Timeout*-like and *aaNAT*) at each of the 6 time-points from LD, DD and DDTC, were normalised to the geometric mean of the reference genes (*18S* and *EF1*) and presented graphically using Microsoft Excel. Statistical analyses were performed in GraphPad InStat v3 on the normalised expression values to compare the 6 time-points for each treatment respectively to test for significant diurnal variation in each treatment. Significance was assessed for each treatment either by One-way Analysis of Variance (ANOVA) followed by the post hoc Tukey-Kramer Multiple Comparisons Test when significance ($p<0.05$) was detected, or by the non-parametric Kruskal-Wallis test, when the Bartlett's test detected unequal variance, followed by the post-hoc Dunn's Multiple Comparisons Test when significant differences were found ($p<0.05$). The GraphPad InStat v3 software used incorporates corrections for multiple comparisons using post hoc tests (GraphPad Software, Inc., 1990). mRNA expression was considered rhythmic when significant variation was detected across the 6 time points assessed.

5.3 RESULTS

5.3.1 Isolation of *Per* and *Rev-erb*

The top three sequence matches to *M. edulis Per* and *Rev-erb* on the NCBI sequence database revealed by blastn (nucleotide database) and blastx (protein database) searches are summarised in Table 5.3. A partial 575 bp *Per* sequence was isolated from *M. edulis* (GenBank Accession MH836580) which conceptually translates to an amino acid sequence sharing 41% similarity with a period-like isoform from the oyster *Crassostrea virginica* (XP_022345656.1) and 38% with period from

the sea snail *B. gouldiana* (AAK97374.1). *Per* was then identified in *M. galloprovincialis* by comparing the *M. edulis Per* sequence against the transcriptome database generated by Moreira et al. (2005); a 96% similarity match was obtained with a 3,360 bp sequence (Unigene27326). A PAS domain and Period C terminal region was identified in the PER multiple-species amino acid alignment which indicated relatively low sequence homology even among bivalves (Figure 5.4), as has been noted previously for other bivalve species (Pairett and Serb, 2013). A phylogenetic tree, constructed using the longer of the two *Mytilus* PER sequences identified (*M. galloprovincialis*), showed grouping of *Mytilus* PER with other mollusc sequences, including bivalves, and closer relationships to other invertebrate sequences compared to vertebrates (Figure 5.5).

A 427 bp partial *Rev-erb/NR1D1* sequence (MH748543) was also isolated which, when conceptually translated, shared 96% amino acid similarity with both *M. galloprovincialis NR1D1* (ABU89807.2) and *NR1D2* (ABU89808.2) and 72% similarity with *C. gigas NR1D* (AHV90297.1) (Table 5.3). A DNA-binding domain of REV-ERB receptor-like was found in the multiple-species amino acid sequence alignment (Figure 5.6) and phylogenetic analysis grouped *Mytilus* PER among other bivalve PER sequences (Figure 5.5).

Table 5.3 Summary of top blastn (nucleotide) and blastx (protein) GenBank database search results, all of which are molluscs. Query cover is the percentage coverage of the *M. edulis* query sequence which overlaps the database hit sequence, and ident is the percentage of matches within the coverage area.

***M. edulis* sequence**		**Species**	**Gene**	**GenBank Accession Number**	**Query Cover (%)**	**Ident (%)**
Per (575 bp) **MH836580**	Blastn	*M. yessoensis*	*Period* homolog 2-like	**XM_021519834.1**	14	84
		Tochuina tetraquetra	*Period*	**MG427049.1**	14	80
		B. gouldiana	*Period*	**AF353619.1**	23	78
	Blastx	*C. virginica*	PER-like isoform X2	**XP_022345656.1**	99	41
		C. gigas	PER	**AQM57604.1**	99	39
		B. gouldiana	PER	**AAK97374.1**	98	38
Rev-erb (427 bp) **MH748543**	Blastn	*M. galloprovincialis*	*NR1D2*	**EF644355.2**	99	96
		M. galloprovincialis	*NR1D1*	**EF644354.2**	99	96
		M. galloprovincialis	*NR1DΔ*	**EF644353.2**	42	99
	Blastx	*M. galloprovincialis*	NR1D2	**ABU89808.2**	99	96
		M. galloprovincialis	NR1D1	**ABU89807.2**	99	96
		C. gigas	NR1D	**AHV90297.1**	99	73

PER

```
M.edulis                ------------------------------------------------------------ 0
M.galloprovincialis     RH*TLIFRGICGKNYILKFIILYSNVIPNRKNKMFTKVYDIRT*FSNMDNQKFIDSTYGS 58
M.yessoensis            ---------------------------------------------MACEPDSNYGS 11
C.virginica             ---------------------------------------------MEECFVSDSTYGS 13

M.edulis                ------------------------------------------------------------ 0
M.galloprovincialis     FS-GFISSNSSSYSMSLSDSEFPEEPPSTSGCSSDFAH--STTQKDKRKERLKQYLRQLK 115
M.yessoensis            YCLSTVQSSSSSISMSLNESDLVEDQPSTSGCSSEQPYTKKLALRKSRKEQVKRYLKELK 71
C.virginica             LK-SGMQDSSSSFSMSLSGSDTFEDQPSTSGCSSDMTH------KEKRKSRVKQYLRQLK 66

M.edulis                ------------------------------------------------------------ 0
M.galloprovincialis     QIVNPATESGAHVSTLGALRHVINSIQKNKEDEKNVSSERCISICSTSE-----SEVEMN 170
M.yessoensis            GLVVQP---SGNLGTLSALQQVVDTFKQIKEEKELSSK---LAKQENEFNLPFDEQNDLN 125
C.virginica             AMVPPSSGKKGKMGTLSALQHVIGSLQKIQEEKDKSQLASCDALTEELDNSLFDKENQLN 126

M.edulis                ------------------------------------------------------------ 0
M.galloprovincialis     ILSLKAVDDLQILVSTKGLKIVQVSPSLKKILGYPVDS-WIGRELTSFLHRKDVVTVNSS 229
M.yessoensis            SVCLNHEEALFFTLRYPDLNIGAVSKNITDVLGYPEPDYLVGRDICNFVHKKDIVTMNSS 185
C.virginica             AQVLKLEETVHMVLTVNELSVLKVSENITSVLGYPVDS-WVNRSIGHFVHKKDIVTINTS 185

M.edulis                ------------------------------------------------------------ 0
M.galloprovincialis     YVLDDADKFDTNLN--FSIKFDEDGNATSEPPKKVLYCRLRHYKSL-KSGFNLEK-KDQY 285
M.yessoensis            MSVHQEMR----DEDGLSSSDNNEGEGRFQIQKKLFYFRLRKYKVL-TGGFSLSSKETEF 240
C.virginica             LNIDAEEPVQLTDYDDSSMESKNTEGGKASHIRKKFFFRIRNYKGLQQSGFSLMK-PDRF 244

M.edulis                ------------------------------------------------------------ 0
M.galloprovincialis     TSFQASVSMKKFNSD----------------KFKPKQFLLLECQPLNSAYNGNWSEMTTE 329
M.yessoensis            QTFQATVAQQPNVSD-------------PTHKKKNKLSVVLKCVPMRSAYESEK----LQ 283
C.virginica             TTVQASMVVGYYNERKQGDSPNSSSSSSGESTHRRRKCIFLDCVPLRSLYNIEN--VQLD 302
                                                                  PAS Domain
M.edulis                ------------------------------------------------------------ 0
M.galloprovincialis     KKTFGTRHSLFCSYTYIHPNAIPLLGYLPQDMVGMSIFDFYHPEEFEQLYNIYRQVVTSK 389
M.yessoensis            NMTFSTRHSLFCSYSHIDSKAIPLLGFLPQDIVGMSIFDFYHPDDIELLYGIYQQVVNTE 343
C.virginica             NQTFYMRHTIYCSYSYMHPNAIPLLGYLPQDMNGMSIFDFYHRDDTETLYNIYKRIIASK 362

M.edulis                ------------------LIYKTERSSFINPWSKRLEFIIGQHTVIKGPQNIDVFSPPPR 42
M.galloprovincialis     GTTISSPKIRFRTHNGDWIYVKTEWSSFINPWSKRLEFIIGQHTVIKGPQNIDVFSPPPR 449
M.yessoensis            TVPFESPPFRFRVRNGAWVYVKTEWSRFVNPWSHRLEFVIGQHTVIKGPTRKNIFGQMLN 403
C.virginica             GTTFRSKPIRLRTRNGDWLTVETEWSSFANPWSHRLEFIIGQHRVLKPPTDRDVFSEADR 422
                                      :  :** * * ****:****:**** *:* *   ::*.   .

M.edulis                QECIAEEPEQYHKNLRLIRKLLLQPVVDEARTVALNIVEEPTEDVSVSPSPDGDXEETSI 102
M.galloprovincialis     QECIAEEPEQYHKNLRLIRKLLLQPVVDEARTVALNIVEEPIEDVSVSPTPDGDTEEISI 509
M.yessoensis            QNVNVNLSDNLARLKQMIRDLLLKPLVSVQIATPNQTIEKHRLNEE-WTDPDGPVKEHSI 462
C.virginica             PSMIPQLSDQQQKLQQKIRQMLLEPVSEEKAAVLH----EPRTDSSDDQKTLEETEKVTK 478
                         .   :  ::  :  : **.:**:*: .   :.      :   : .         :: :

M.edulis                -------RTQEAKKKLXSAT--XNEQCNEILDDNLSGTYEQLSYTNNIKRFLMSQPKTY- 152
M.galloprovincialis     -------RTQEAKKKLQSAT--RNEQCNEILDDNLSGTYEQLSYTNNIKRFLMSQPKTY- 559
M.yessoensis            T----------------Y--VDDSNASSSVSTNRETLSYDHLNYTSNIKRFLLSQKNTIY 504
C.virginica             KSKQQTEKTAERKESLQSTESLGGNSLPNFPEHESSMAYEQLNYANSIKRYLMSQQKTY- 537
                                          .:   ..  .. : :*::*.*:..***:*:** :*

M.edulis                SSSSDKRSGNDSYTDDSNAID----SDEVPDFGVDIPYPKPPS----------------- 191
M.galloprovincialis     SSSSDKRSGNDSYTDDSNAID----SDEVPDFGVDIPYPKPPSFCSSTKVLVSEKEDM-- 613
M.yessoensis            SPFSEKKSASSTEEE------QHESSSCDSLLEVDISVPMPPSFGSSTKVLLSEQEREES 558
C.virginica             SSSSEKKTTSEEETDTPCTISTTEEEASDAEFEVDISVPKPPSFGSSTKVLLSEQEQRED 597
                        *  *:*:: ..   :          .     : ***  * ***

M.yessoensis            GVAVFTLLDSDMATQPKNITTVPQSSRPNSPSYVMGKEVEPKVHVQQDKGMFSLMSLTQE 618
C.virginica             VASSPAHQIEDNTE---DTTTFPGVLA---PPLMA---PPPPV---ESPDTRKLVTLTHD 645
M.edulis                ------------------------------------------------------------ 191
M.galloprovincialis     -VPSPSCQTEEIGE---ETSREAQINL---------------L---PIQEANVLMSLTQE 651
```

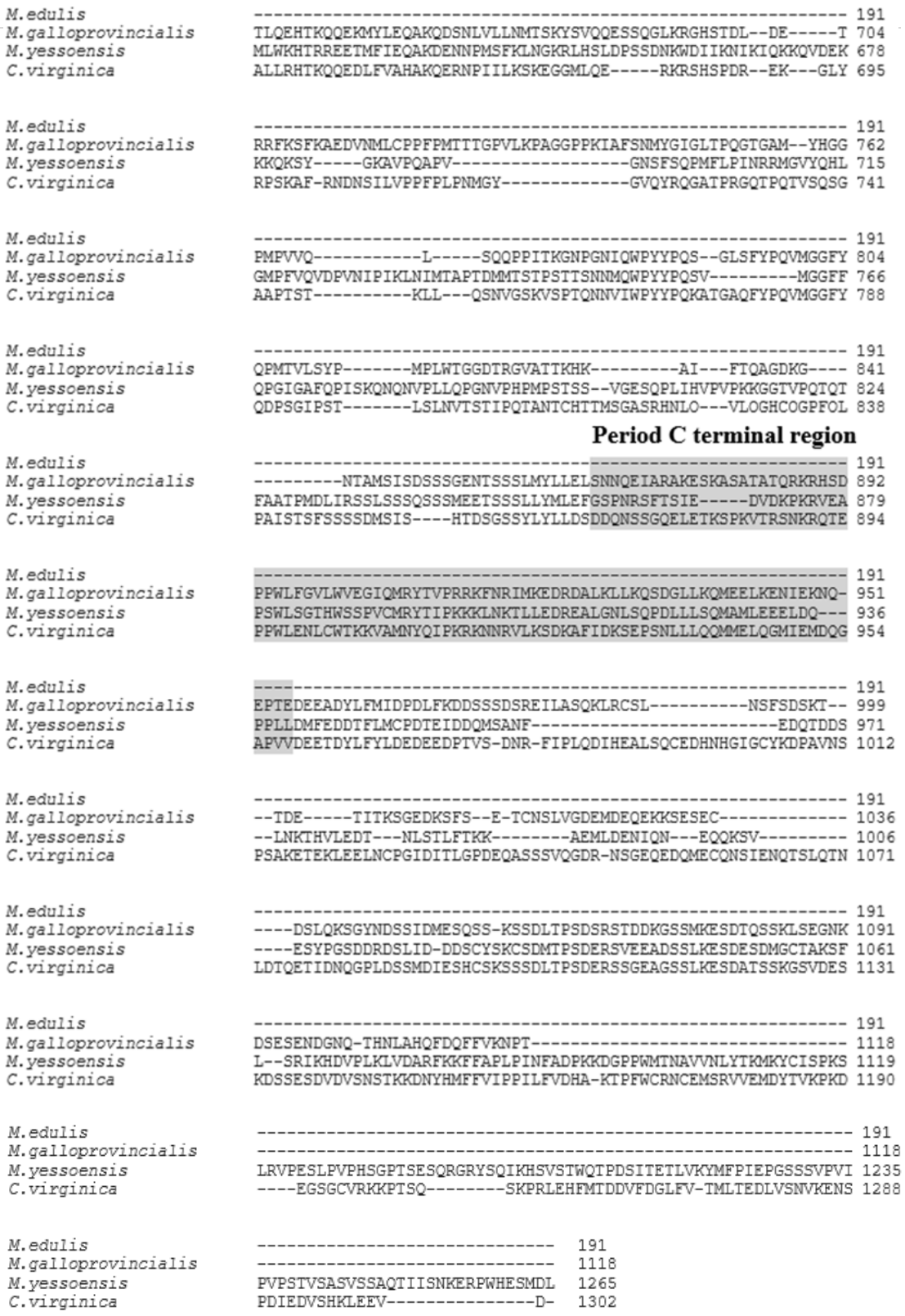

Figure 5.4 Multiple species amino acid alignment of partial *M. edulis* PER (MH836580) aligned with PER (Unigene27326) from *M. galloprovincialis* (Moreira et al., 2005), period circadian protein-like isoform X2 from the oyster *C. virginica* (XP_022345656.1) and a period homolog from the scallop *M. yessoensis* (XP_021375509.1). Symbols represent the following: dashes, alignment gaps; asterisks, homology; colons, conserved amino acid substitutions (similar chemical properties); full stops, semi-conserved amino acid substitutions (similar conformation). Functional protein domains are shaded/ labelled.

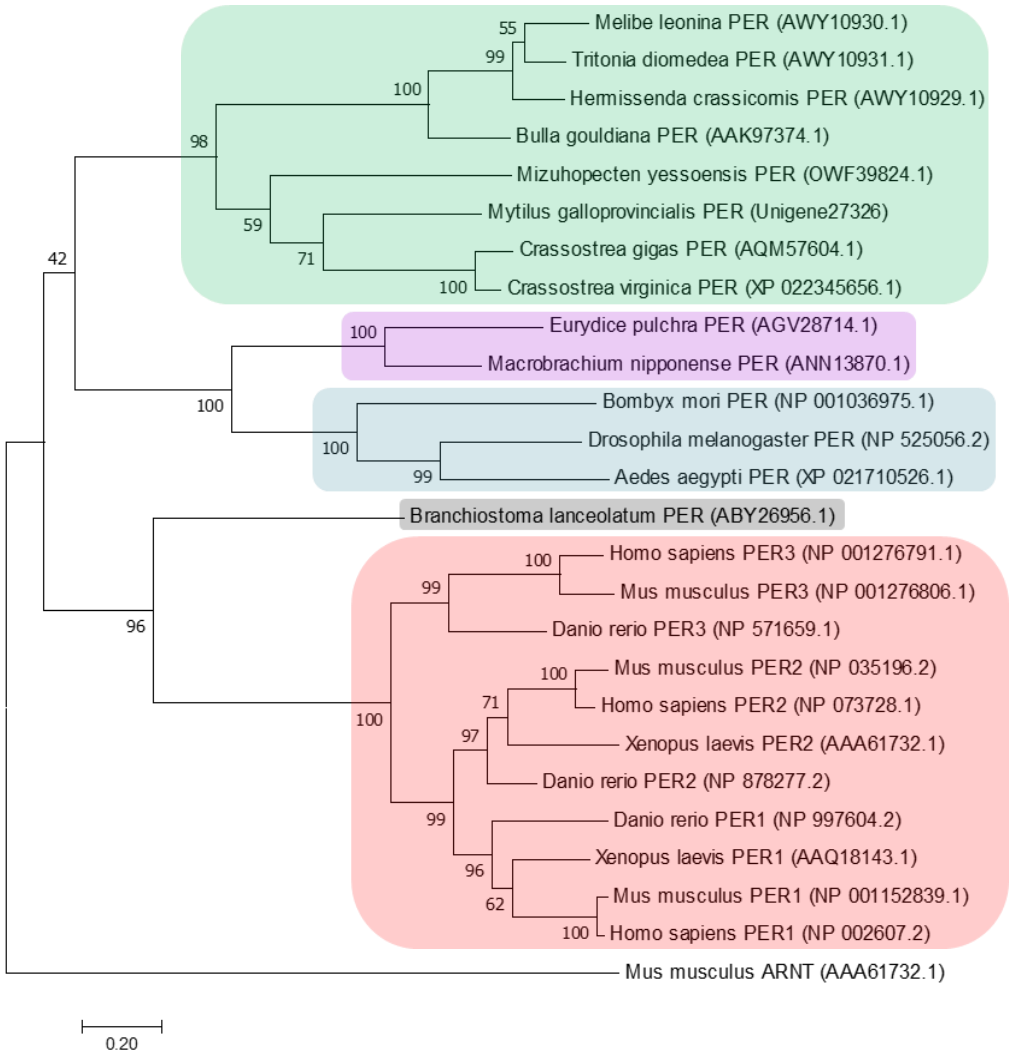

Figure 5.5 Phylogenetic tree of PER amino acid sequences (455 amino acid positions, gaps eliminated) using the Maximum Likelihood method based on the Jones-Taylor-Thornton model, conducted in MEGA7. Percentages displayed on branches are from 1000 bootstrap replicates. Branches are to scale with lengths measured in number of substitutions per site. Shaded boxes show PER from molluscs, green; crustaceans, purple; insects, blue; lancelet, grey; vertebrates, red. The tree was rooted with mouse ARNT as the outgroup.

REV-ERB

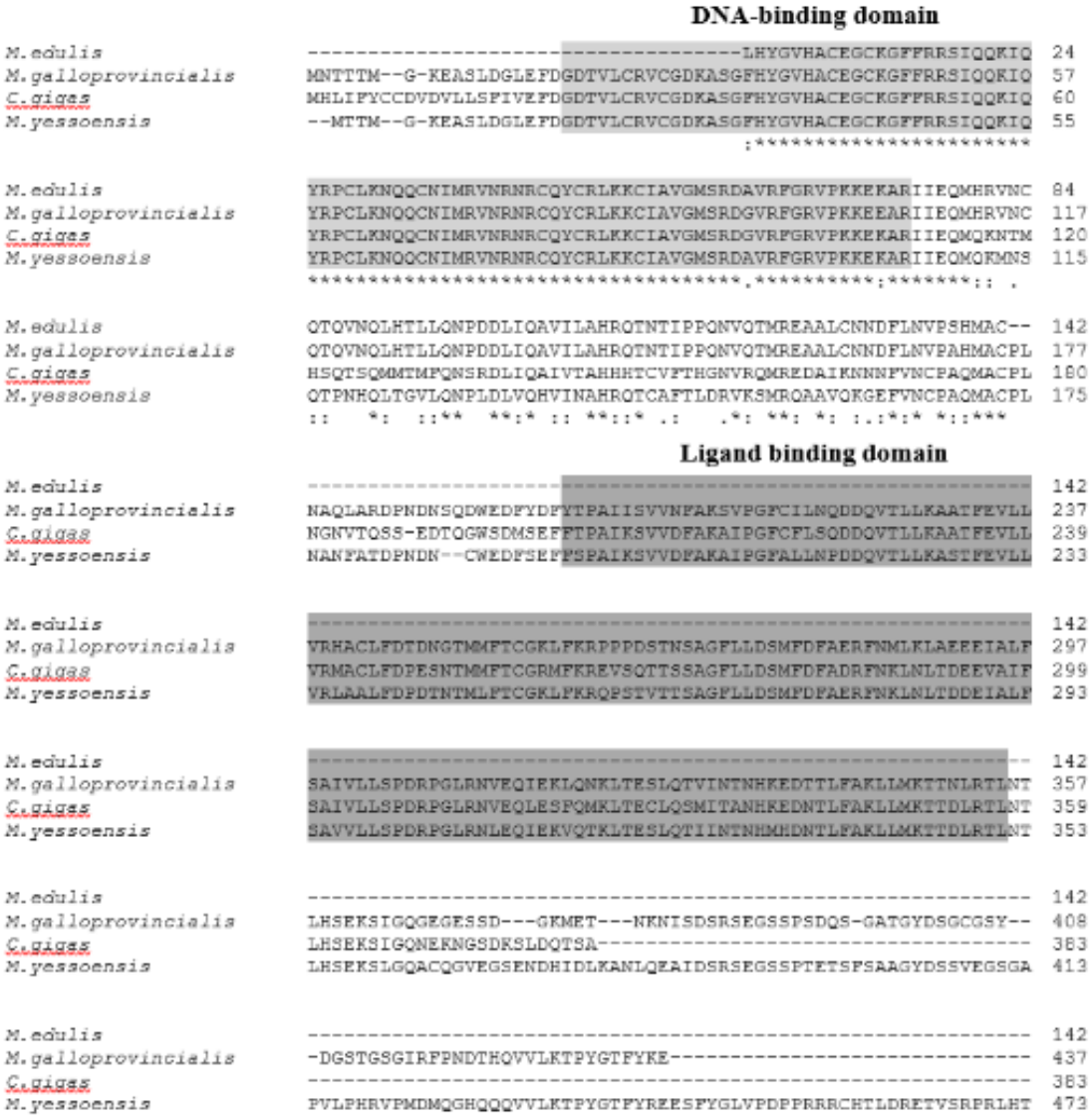

Figure 5.6 Multiple species amino acid alignment of partial *M. edulis* REV-ERB (Accession MH748543) aligned with mussel *M. galloprovincialis* REV-ERB (ABU89807.2), oyster *C. gigas* REV-ERB (AHV90297.1) and scallop *M. yessoensis* E75 (OWF42026.1). Symbols represent the following: dashes, alignment gaps; asterisks, homology; colons, conserved amino acid substitutions (similar chemical properties); full stops, semi-conserved amino acid substitutions (similar conformation). Functional protein domains are shaded and labelled. The 3' end of the alignment is cropped.

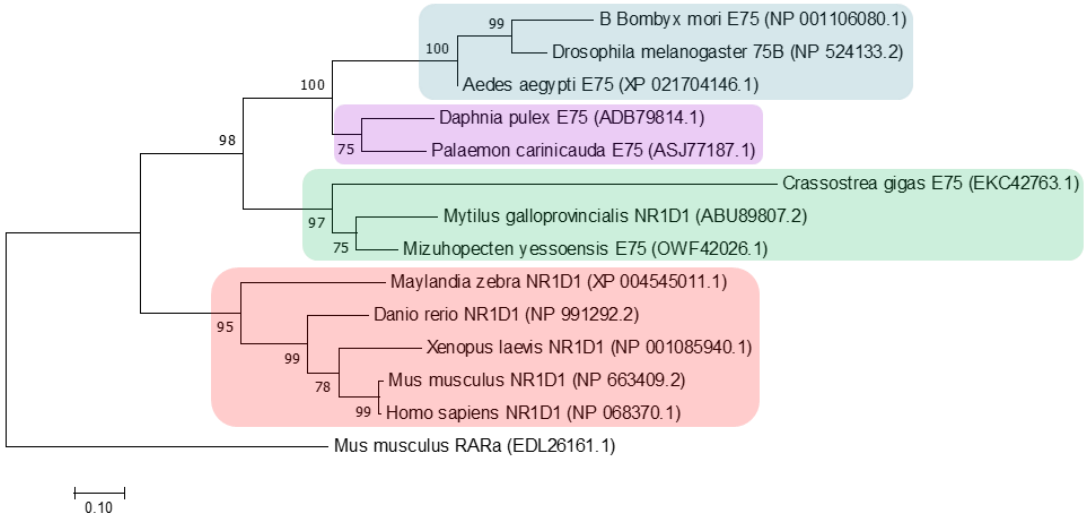

Figure 5.7 Phylogenetic tree of REV-ERB/NR1D1/E75 amino acid sequences (329 amino acid positions, gaps eliminated) using the Maximum Likelihood method based on the Jones-Taylor-Thornton model, conducted in MEGA7. Percentages displayed on branches are from 1000 bootstrap replicates. Branches are to scale with lengths measured in number of substitutions per site. Shaded boxes represent molluscs, green; crustaceans, purple; insects, blue; vertebrates, red. The tree was rooted with mouse RARa as the outgroup.

5.3.2 qPCR product amplification and primer specificity

qPCR products were successfully generated for the eight genes of interest and two reference genes as demonstrated by the single curves on the amplification plots (Figure 5.8), single melt peaks (Figure 5.9) and single bands detected via agarose gel electrophoresis (Figure 5.10), indicative of specific qPCR products with no primer dimers or sources of contamination. Likewise, no fluorescent signal was detected in the template-negative controls (Figure 5.10).

(a) *Clk*

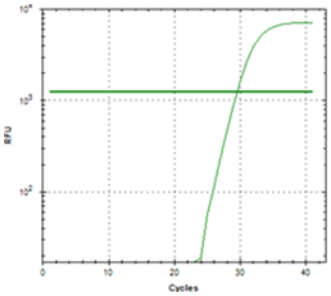

(b) *Cry1*

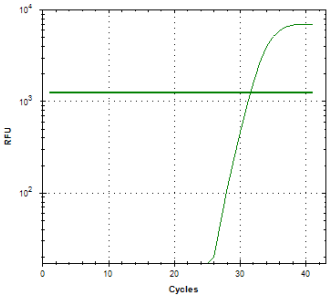

(c) *ARNT*

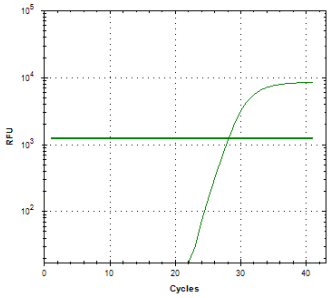

(d) *Timeout-like*

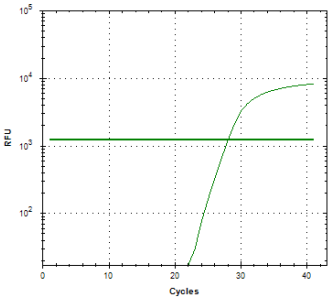

(e) *ROR/HR3*

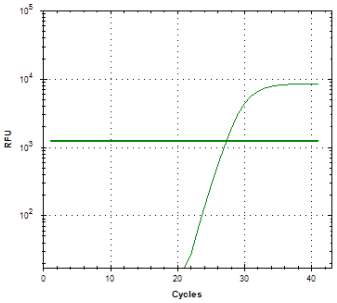

(f) *aaNAT*

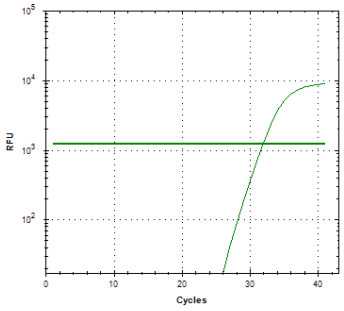

(g) *Per*

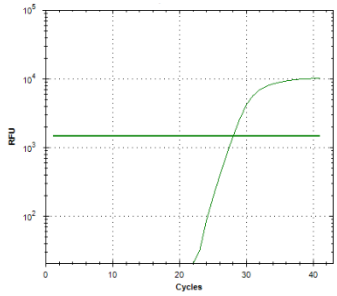

(h) *Rev-erb*

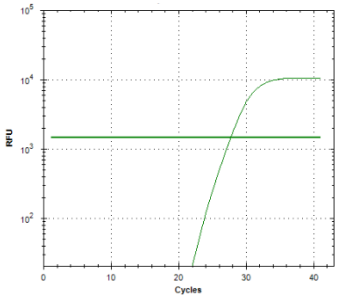

(i) *EF1a*

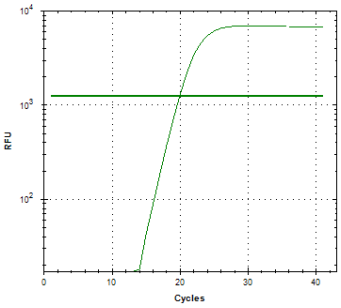

(j) *18S*

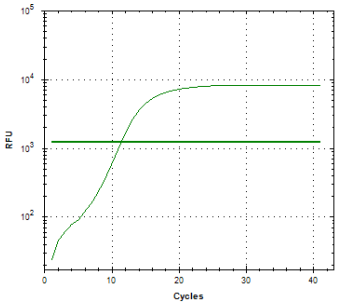

Figure 5.8 Representative results of cDNA amplification plots (log scale) generated from qPCR reactions containing *M. edulis* cDNA, PrecisionPLUS 2x qPCR MasterMix with SYBR Green for the ICycler (PrimerDesign, UK) and primers at either 100 nM (a) to (h) or 50 nM (i) and (j). Abbreviations: RFU, Relative Fluorescence Units.

(a) *Clk*

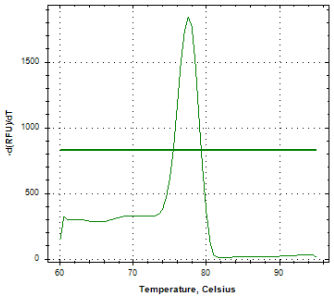

(b) *Cry1*

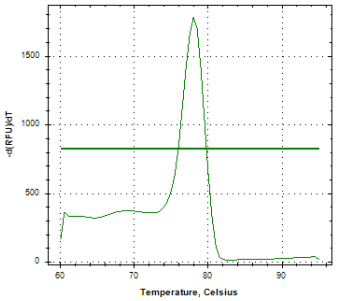

(c) *ARNT*

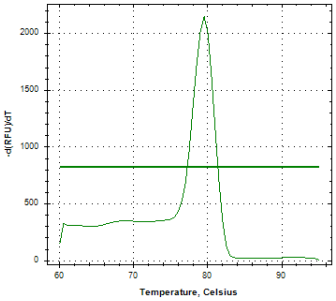

(d) *Timeout-like*

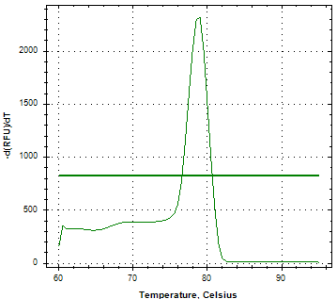

(e) *ROR/HR3*

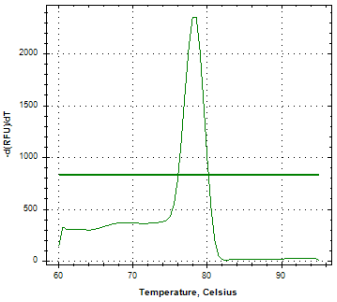

(f) *aaNAT*

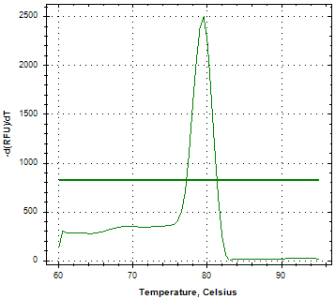

(g) *Per*

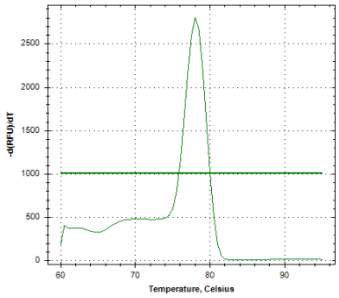

(h) *Rev-erb*

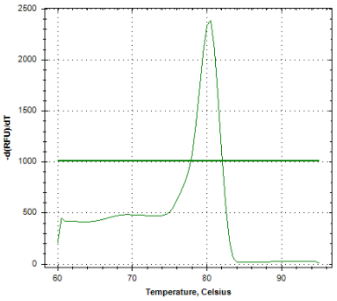

(i) *EF1a*

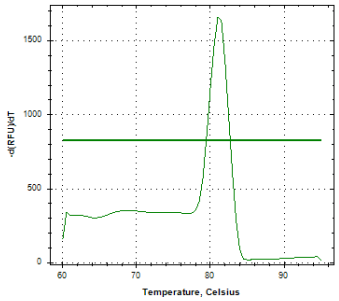

(j) *18S*

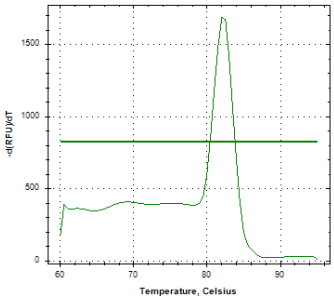

Figure 5.9 Representative results of melt peak plots generated from qPCR reactions containing *M. edulis* cDNA, PrecisionPLUS 2X qPCR MasterMix with SYBR Green for the ICycler (PrimerDesign, UK) and primers at either 100 nM (a) to (h) or 50 nM (i) and (j). Abbreviations: RFU, Relative Fluorescence Units.

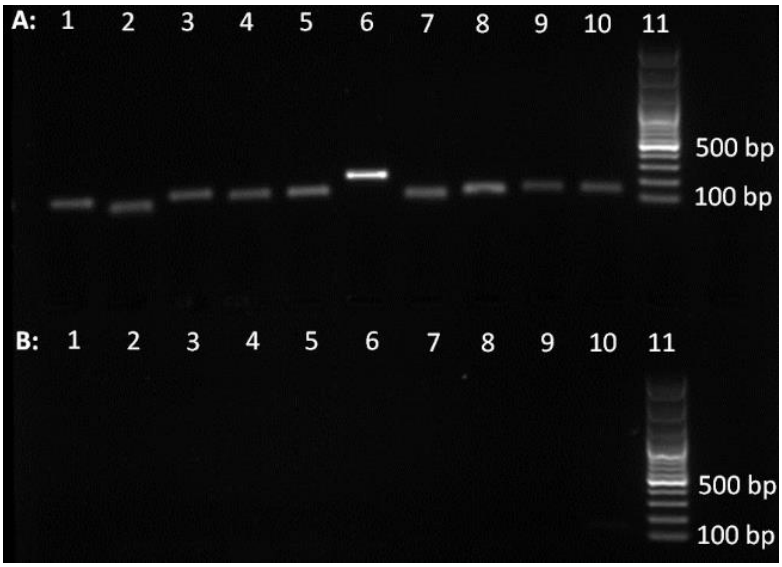

Figure 5.10 1% TBE agarose gel stained with GelRed™ Nucleic Acid Gel Stain (Biotium, Cambridge Bioscience, UK) showing 5 µL of qPCR product (row A) and equivalent negative controls (row B) as follows: Lane 1, *Clk*; 2, *Cry1*; 3, *ARNT*; 4, *Timeout*-like; 5, *ROR/HR3*; 6, *aaNAT*; 7, *Per*; 8, *Rev-erb*; 9, *EF1α*; 10, *18S*; 11, GeneRuler 100 bp DNA Ladder (Thermo Fisher Scientific, UK).

5.3.3 Standard curves and amplification efficiencies

The standard curves generated for each gene demonstrate a linear relationship between log cDNA dilution factor and Cq value (Figure 5.11). The R^2 values of the standard curves are all in close proximity to 1 (Table 5.4) showing good correlation between cDNA dilution factor and Cq value, indicative of an accurately prepared efficient reaction. The primer efficiencies all fall within or in close proximity to the desired 90% to 110% range (Table 5.4).

Table 5.4 Parameters of the standard curves produced from optimised primer pairs

Category	Gene	Primers	Final primer concentration (nM)	R^2	Amplification efficiency (%)
Genes of interest	*Clk*	*Clock*_qPCR_F3 *Clock*_qPCR_R3	100	0.9417	112.33
	Cry1	*Cry1*_ qPCR_F2 *Cry1_qPCR_R2*	100	0.9949	103.85
	ARNT	*ARNT*_qPCR_F3 *ARNT*_qPCR_R3	100	0.9995	95.03
	Timeout-like	*Timeout*_F3 *Timeout*_R3	100	0.9897	90.63
	ROR/HR3	*ROR*_qPCR_F1 *ROR*_qPCR_R1	100	0.9729	103.54
	aaNAT	*aaNAT*_F2 *aaNAT*_R2	100	0.9688	90.63
	Per	*Per*_qPCR_F1 *Per*_qPCR_R1	100	0.9765	107.42
	Rev-erb	*E75_F5* *E75_R5*	100	0.9487	101.22
Reference genes	*EF1α*	*EF1a*_F5 *EF1a*_R5	50	0.9946	91.64
	18S	*18S*_F4 *18S*_R4	50	0.9992	103.85

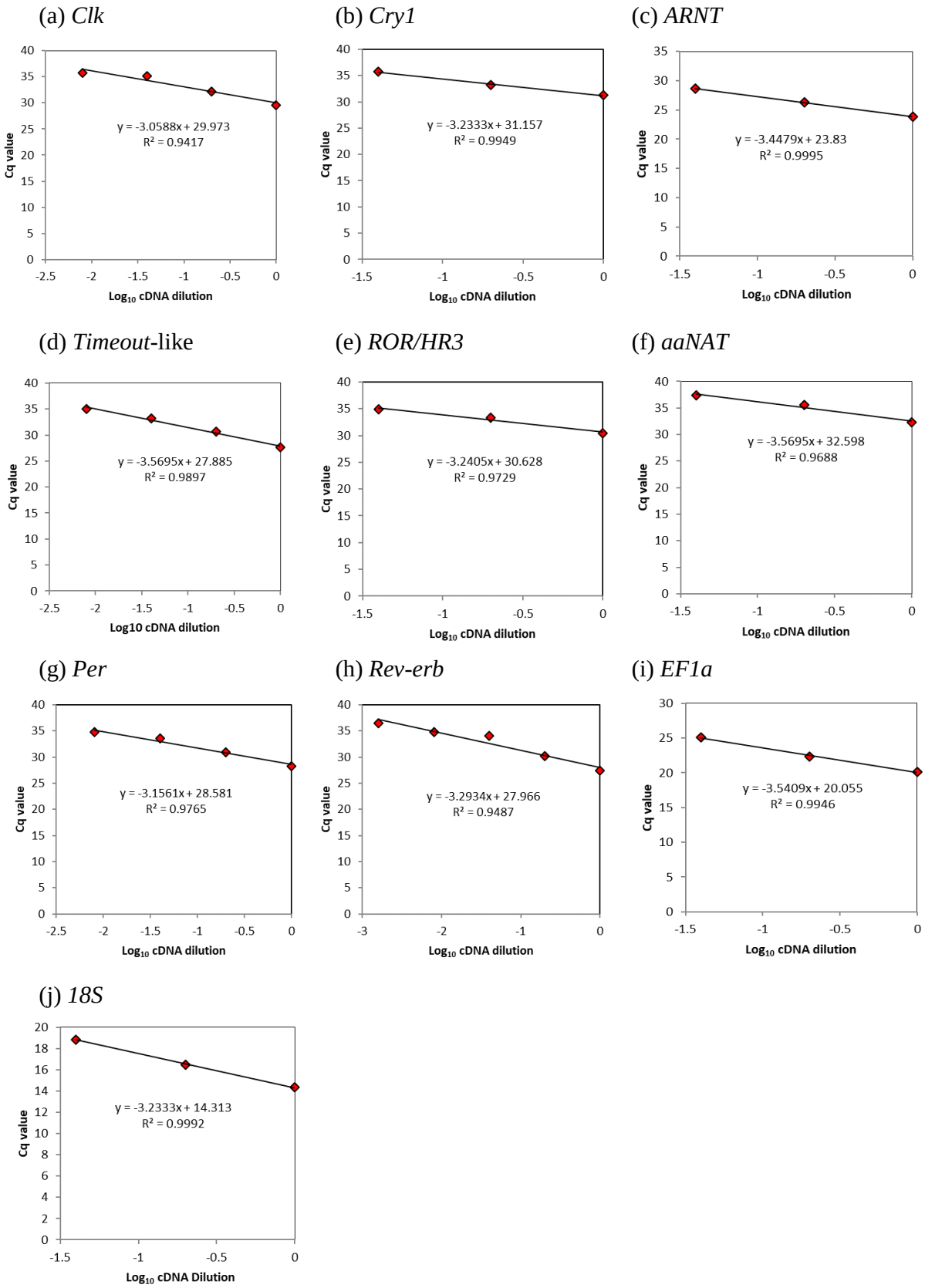

Figure 5.11 Standard curves showing qPCR amplification efficiency of *M. edulis* primers for different genes over a cDNA dilution series with R^2 values displayed.

5.3.4 Rhythmic expression of clock genes under LD and DD

After acclimation, *M. edulis* were concurrently exposed to either 10:14 hr light/dark cycles (LD) or constant darkness (DD) for 12 days so the expression patterns of clock and clock-associated genes could be investigated. Under LD, all five of the canonical clock genes investigated (*Clk*, *Cry1*, *ROR/HR3*, *Per* and *Rev-erb*) exhibited significant daily variation in mRNA expression levels (Figure 5.12, Figure 5.13 Table 5.5). Expression levels in LD tended to increase significantly after lights on at zeitgeber time 0 (ZT 0), decreasing by the end of the photophase at ZT 9, with some cases, *Cry1* in particular, showing a second peak in expression at the beginning of the dark period at ZT11 (Figure 5.12 and Figure 5.13). For all five of these clock genes, significant circadian variation in expression was also apparent in the absence of light under DD, indicative of endogenous regulation (Figure 5.12, Figure 5.13, and Table 5.5). Different patterns were apparent for the clock-associated genes *ARNT*, *Timeout*-like and *aaNAT*. Though *ARNT* mRNA expression was not significant under LD, there was significant variation under DD with increases in expression at the start of the subjective day and night respectively (Figure 5.12, Figure 5.13, and Table 5.5). Significant variation in *Timeout*-like expression was detected under both LD and DD, peaking at ZT16 during the LD scotophase, and peaking during both the subjective day and night under DD (Figure 5.12, Figure 5.13, and Table 5.5). Conversely, expression of *aaNAT* was constant under both LD and DD (Table 5.5).

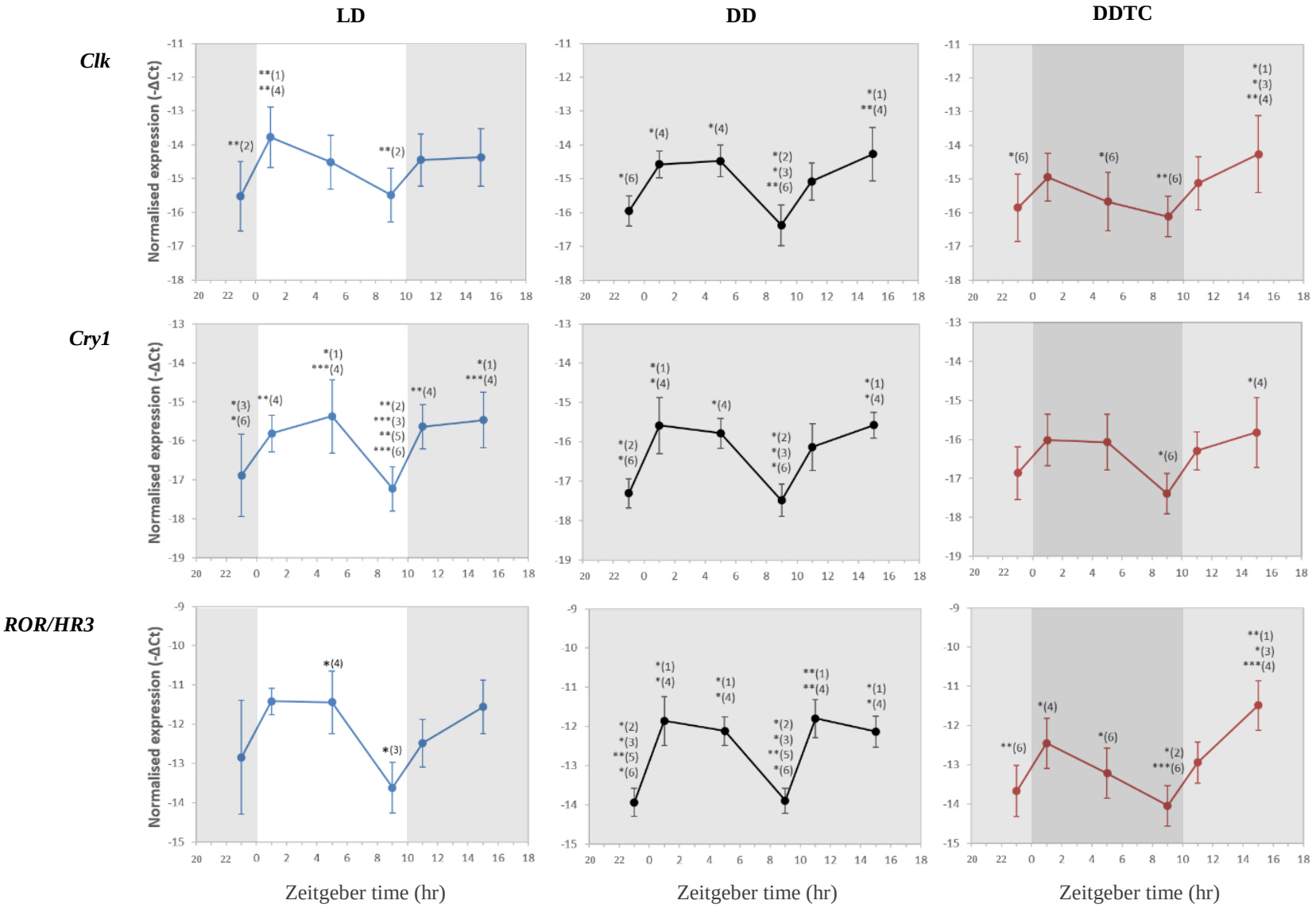
LD
DD
DDTC
Clk
Cry1
ROR/HR3
Normalised expression (-ΔCt)
Zeitgeber time (hr)
Zeitgeber time (hr)
Zeitgeber time (hr)

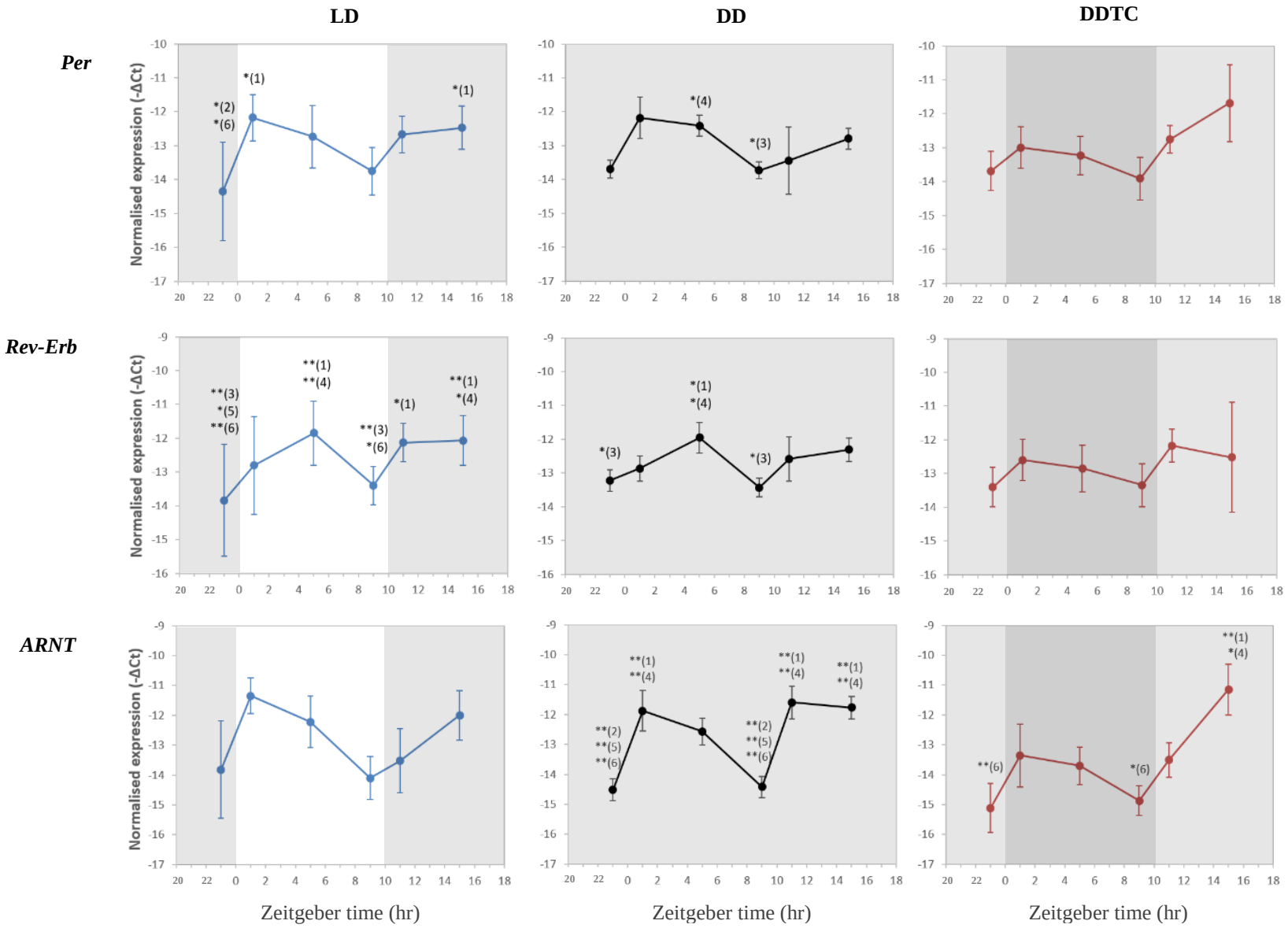
LD
DD
DDTC
Per
Rev-Erb
ARNT
Normalised expression (-ΔCt)
Zeitgeber time (hr)
Zeitgeber time (hr)
Zeitgeber time (hr)

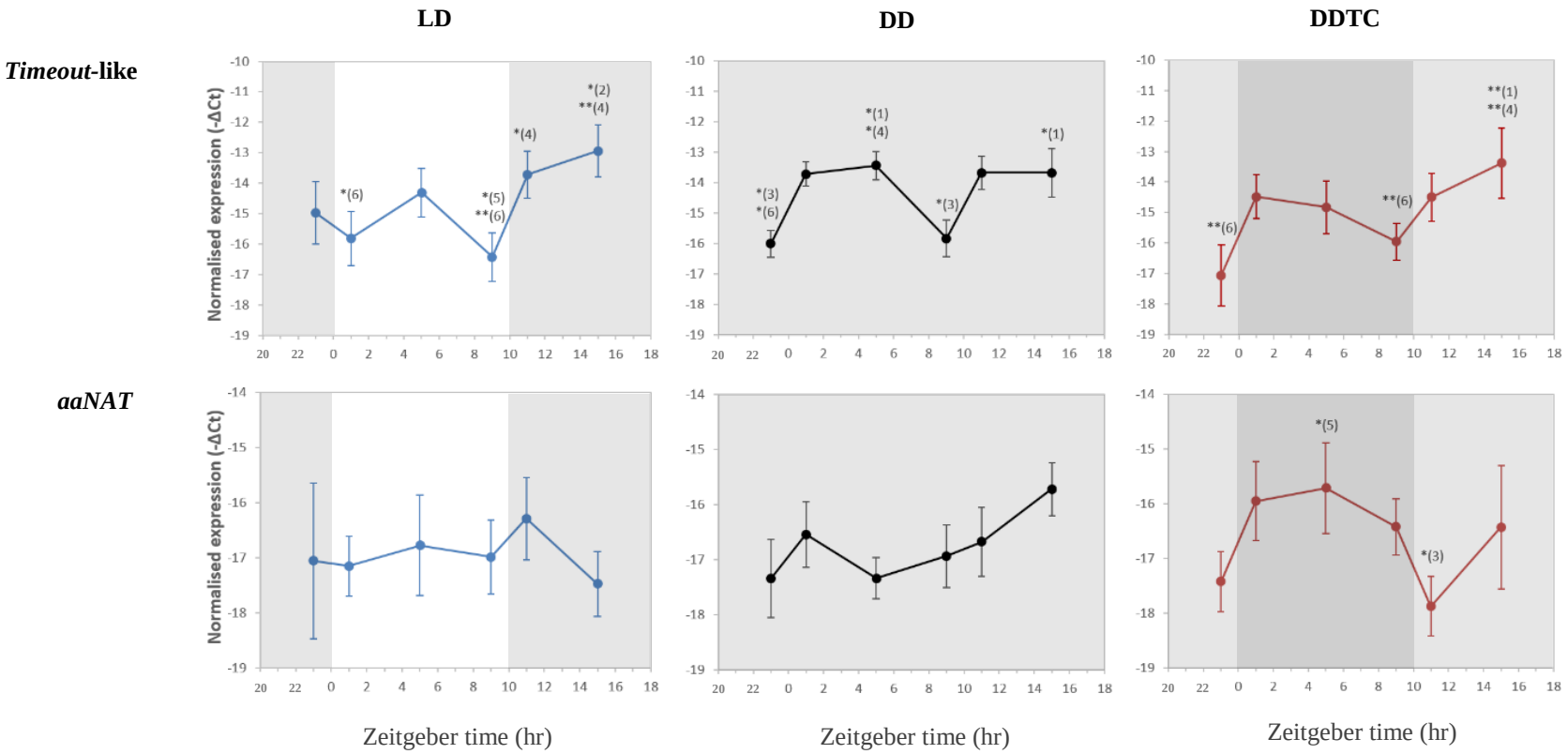

Figure 5.12 Influence of photocycles and thermocycles on the daily variation of mRNA expression of clock and clock-associated genes in *M. edulis* male mantle tissue, normalised to *18S* and *EF1* reference genes. Mean data are plotted ±SEM; *n*=5-9. Significance denoted by * $p < 0.05$, ** $p < 0.01$ and *** $p < 0.001$ with adjacent numbers referring to time-points as follows: (1) ZT 23, (2) ZT 1, (3) ZT 5, (4) ZT 9, (5) ZT 11 and (6) ZT 15. ZT 0 (8 am GMT) was lights on and ZT 10 (6 pm) was lights off in LD, and temperature up and temperature down respectively in DDTC. Abbreviations: LD, light/dark; DD, dark/dark; DDTC, dark/dark with ~3.5 °C thermocycles. Unshaded areas represent photophase, light shading represents darkness and heavy shading represents a thermophase (warm phase) during darkness.

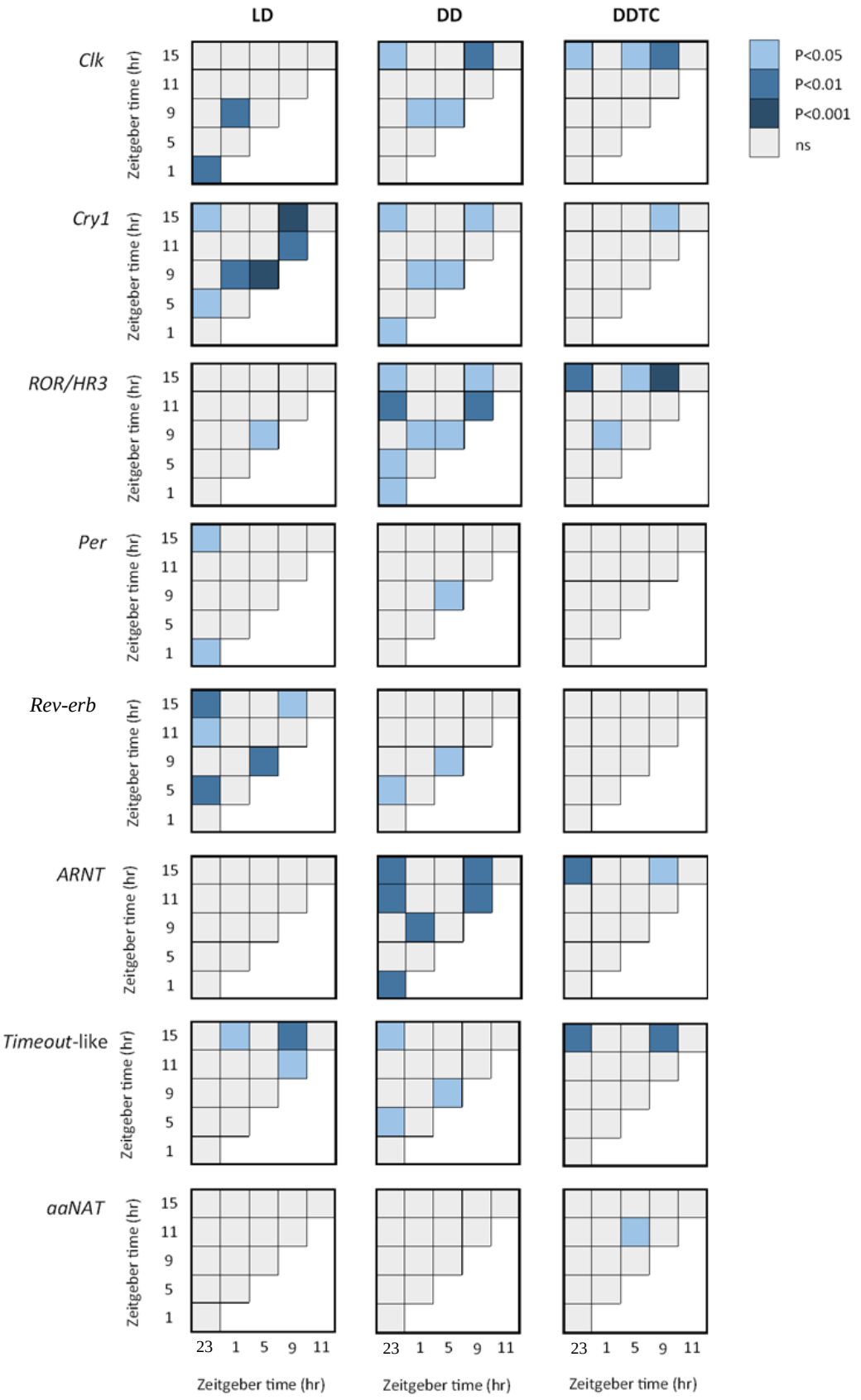

Figure 5.13 Relative expression heat maps showing time-points where mRNA expression (normalised to *18S* and *EF1*) significantly differed for each gene revealed by Tukey-Kramer Multiple Comparisons Tests following ANOVA or Dunn's Multiple Comparisons Tests following Kruskal-Wallis. *n*=5-9 per grid square.

Table 5.5 Statistical analysis of the effect of diurnal light and temperature cycles on *M. edulis* clock mRNAs.

	LD		**DD**		**DDTC**	
Gene	Test statistic	*p*	Test statistic	*p*	Test statistic	*p*
Clk	$F = 5.341_{5,40}$	0.0007	$F = 4.720_{5,41}$	0.0017	$F = 4.620_{5,40}$	0.0020
Cry1	$F = 8.257_{5,39}$	<0.0001	$F = 4.731_{5,41}$	0.0017	$F = 3.245_{5,40}$	0.0149
ROR/ HR3	$F = 3.014_{5,40}$	0.0211	$F = 6.042_{5,41}$	0.0003	$F = 5.407_{5,39}$	0.0007
Per	$F = 4.171_{5,38}$	0.0041	$KW = 16.549_{5}$	0.0054	$KW = 14.846_{5}$	0.0110
Rev-erb	$F = 6.173_{5,38}$	0.0003	$F = 3.747_{5,38}$	0.0074	$F = 2.368_{5,37}$	0.0583 **(ns)**
ARNT	$F = 1.870_{5,40}$	0.1213 **(ns)**	$F = 7.279_{5,41}$	<0.0001	$KW = 18.617_{5}$	0.0023
Timeout-like	$F = 5.332_{5,38}$	0.0008	$KW = 21.943_{5}$	0.0005	$KW = 20.267_{5}$	0.0011
aaNAT	$F = 0.398_{5,39}$	0.8471 **(ns)**	$F = 1.911_{5,41}$	0.1133 **(ns)**	$F = 2.787_{5,40}$	0.0299

One-way analysis of variance (ANOVA), with degrees of freedom shown in subscript after F value. Kruskal-Wallis Test (Nonparametric ANOVA) with degrees of freedom shown after KW statistic. Significant differences are shaded. Abbreviations: LD, light/dark; DD, dark/dark; DDTC, dark/dark with ~3.5 °C thermocycles; ns, not significant.

5.3.5 Expression of clock genes under DDTC

In addition to LD and DD exposures, the mRNA expression patterns of the clock and clock-associated genes were also investigated in mussels exposed to ~3.5 ºC temperature cycles in constant darkness (DDTC). Four of the five clock genes, *Clk*, *Cry1*, *ROR/HR3* and *Per* showed significant diurnal variation in expression under DDTC as was the case under LD and DD, however the application of thermocycles resulted in a loss of significant rhythmicity for *Rev-erb* (Figure 5.12, Figure 5.13, and Table 5.5). Thermocycles had different effects on the expression patterns of clock-associated genes *ARNT*, *Timeout*-like and *aaNAT*. For *ARNT* and *Timeout*-like, significant differences in diurnal expression were apparent, with peak expression occurring in the cryophase in both cases Figure 5.12 and Figure 5.13). Thermocycles significantly modulated the constant expression of *aaNAT* exhibited under both LD

and DD; the mid thermophase was when mRNA expression peaked, whereas it was lowest immediately after the cryophase transition (Figure 5.12 and Figure 5.13).

5.4 DISCUSSION

Predicting and responding to upcoming changes in the environment is an adaptive trait (Vaze and Sharma, 2013), however little is known about the relationship between environmental cycles and biological rhythms in molluscs. In this chapter, sequences of clock genes *Per* and *Rev-erb* were isolated for the first time from *M. edulis*, and mRNA expression of these and the previously characterised genes (*Clk*, *Cry1*, *ROR/HR3*, *ARNT*, *Timeout*-like, *aaNAT*) were investigated under light/dark (LD), constant darkness (DD) and diurnal temperature cycles of 3.6 °C (DDTC). The results showed endogenous clock gene expression, indicated by daily variation under LD which persisted under DD, and revealed some instances of gene expression patterns being significantly modulated by temperature cycles.

5.4.1 Isolation of *Per* and *Rev-erb*

Per is involved in core clock interactions in diverse phyla; PER forms a complex with TIM in *Drosophila* (Zeng et al., 1996) and with a non-light sensitive cryptochrome protein, CRY, in mice (Young and Kay, 2001). Although as many as three versions of *Per* occur in vertebrates, only one homolog is present in molluscs (Sun et al., 2016; Constance et al., 2002). A 575 bp *Per* sequence (MH836580) was isolated from *M. edulis* herein (Table 5.3) allowing the subsequent identification of a 3.3 Kb *Per* from *M. galloprovincialis* transcriptome data (Moreira et al., 2005) which shared 96% similarity. Identifications were further confirmed by a multiple-species amino acid alignment, revealing characteristic PAS and Period C domains (Figure 5.4)

and a phylogenetic tree that grouped mollusc PER sequences together (Figure 5.5), though *Per* is a divergent gene with low sequence homology between species (Pairett and Serb, 2013).

Rev-erb is also a canonical clock gene in many species. *Rev-erb* negatively regulates *ROR* expression in mammals, comprising the second interlocked feedback loop of the molecular clock mechanism (Guillaumond et al., 2005). Similar roles are played by the respective invertebrate homologs *HR3* and *E75* in some insects (Kamae et al., 2014). A 427 bp *Rev-erb* sequence (MH748543) was isolated from *M. edulis* in this chapter which shared a high degree of sequence similarity with other bivalve *Rev-erb* sequences (Table 5.3) and *Mytilus* sequences contain characteristic DNA-binding and ligand-binding domains (Figure 5.6) as well as grouping together phylogenetically with other mollusc REV-ERB sequences (Figure 5.7).

5.4.2 Effect of photocycles and darkness on clock mRNA expression

Significant differences in mRNA expression were found across the 6 time-points under LD cycles for the five clock genes *Clk*, *Cry1*, *ROR/HR3*, *Per* and *Rev-erb* as well as for *Timeout*-like (Figure 5.12; Figure 5.13; Table 5.5). These significant expression variations also persisted under DD, a feature consistent with endogenous circadian control (Figure 5.12; Figure 5.13; Table 5.5). There are relatively few other studies to date in which the molecular timekeeping ability of molluscs have been investigated. Among bivalves, *M. californianus* kept in LD cycles under a tidal regime exhibited a circadian pattern of *Cry1* and *ROR* expression in the gills, whereas *Clk* and *Bmal* were constant (Connor and Gracey, 2011). A number of clock genes were expressed diurnally under LD in the gills of the oyster *C. gigas* and were modulated by DD: *Clk*, *Cry1*, *Cry2*, *Per*, *Rev-Erb*, *Bmal*, *Tim*, *pCry* and *6-4photolyase* (Perrigault

and Tran, 2017). In the adductor muscle of *C. gigas*, *Cry1* expression could be entrained by LD and tidal cycles respectively, however oscillations only persisted under DD in the case of the latter (Mat et al., 2016). In the same species, RNA interference of *Clk* has been shown to disrupt the expression of *Cry1*, *Per*, *Rev-erb* and *Bmal* (Payton et al., 2017a). Among gastropods, the clock genes investigated in the limpet *Cellana rota* did not oscillate significantly in wild animals under natural intertidal conditions (Schnytzer et al., 2018). Significant diurnal expression of *Clk*, *Per* and two *cryptochrome* genes (photosensitive and non-photosensitive) were, however, apparent in the brain of nudibranch mollusc *Melibe leonina* (Duback et al., 2018). Rhythmic *Per* expression also occurred in the eye neurons of the marine gastropod *B. gouldiana* under LD, but not DD, however expression was constant under both conditions in the gut and head ganglia (Constance et al., 2002). Finally in the cephalopod *E. scolopes*, *Cry1* and *Cry2* oscillate diurnally in the head and the former is also rhythmic in the light organ in synchrony with luminescence from bacterial symbionts (Heath-Heckman et al., 2013).

In this chapter, *M. edulis* clock genes generally increased in expression around the dark to light transition at ZT 0 (Figure 5.12; Figure 5.13; Table 5.5). This pattern is consistent with clock gene expression patterns in *C. gigas* gills in the spring/summer when oysters exhibit diurnal activity (Perrigault and Tran, 2017), whereas at least *Cry1* shifts to peak during the scotophase (dark phase) when they are nocturnal during the winter months (Tran et al., 2015; Mat et al., 2012). The second peaks in expression apparent herein during the subjective night for a number of *M. edulis* genes under LD (*Cry1* and *Rev-erb*) and DD (*Cry1*, *Clk* and *ROR*) suggest a possible ultradian (<24 hr) rhythm. Night-time expression peaks are also apparent in the brain of the nudibranch *M. leonine* (Duback et al., 2018). As is the case in other organisms, it

appears that clock expression patterns in molluscs vary between species and tissue type (Mat et al., 2016; Heath-Heckman et al., 2013) as different circadian clocks are present and active on a cellular level in numerous tissue types (Tomioka et al., 2012).

Different responses to light regimes were exhibited by the *M. edulis* clock-associated genes *ARNT*, *Timeout*-like and *aaNAT*. *ARNT* expression showed a trend under both LD and DD however only the latter was significant (Figure 5.12; Figure 5.13; Table 5.5). ARNT, which is a bHLH-PAS protein like BMAL1, is able to dimerise with the melatonin-activated protein NPAS4 to trigger expression of *Cry1* in mammals (West et al., 2013). As was the case for the clock genes, *M. edulis Timeout*-like expression varied significantly under both LD and DD (Figure 5.12; Figure 5.13; Table 5.5), which indicates clock-control. Peak *Timeout*-like expression under LD was during the dark phase (scotophase) at ZT 15 whereas no circadian pattern was apparent for the gene in the sea anemone *Nematostella vectensis* (Reitzel et al., 2010). *Timeout* functions in light entrainment in *Drosophila* (Benna et al., 2010) and its ortholog, mammalian-type *Timeless*, has also been linked to vertebrate clock function in addition to other non-circadian roles (Gotter, 2006; Barnes et al., 2003). Conversely, *aaNAT* did not appear to be under circadian control as constant expression was observed under both LD and DD, despite its involvement in rhythmic melatonin synthesis in mammals (Klein, 2007) and certain invertebrates (Peres et al., 2014).

The present work on blue mussels is consistent with previously proposed hypothetical models of the molecular clock mechanism in molluscs, which include genes and putative interactions integral to both vertebrate and invertebrate systems (Perrigault and Tran, 2017; Sun et al., 2016). Further investigation into clock mRNA expression patterns over two consecutive days would show whether the significant variation in expression observed herein can be confirmed as rhythmic and whether the

periodicity is circadian (24 hr) or ultradian (e.g. 12.4 hr tidal cycles) in nature.

5.4.3 Effect of thermocycles on clock mRNA expression

Episodes of temperature stress affect gene expression patterns in *Mytilus* by elevating and repressing groups of genes (Lockwood et al., 2015) and by disrupting gene rhythmicity (Connor and Gracey, 2011). However, the impact of diurnal temperature cycles on the molluscan circadian clock is unknown. Circadian clocks are temperature compensated so the period of the rhythm is effectively constant over a range of temperatures (Sweeney and Hastings, 1960). Temperature cycles, however, can act as a zeitgeber to entrain the phase of the clock in organisms inhabiting terrestrial and aquatic environments (Glaser and Stanewsky, 2005; Lahiri et al., 2005; Rensing and Ruoff, 2002).

The expression patterns of two genes were modulated by thermocycles in this experiment. Thermocycles eliminated the significant variation in *Rev-erb* expression that was apparent under both LD and DD (Figure 5.12; Figure 5.13; Table 5.5). *Rev-erb* is also expressed in an endogenous circadian manner in *C. gigas* in which it has been hypothesised to be a core clock gene (Perrigault and Tran, 2017). Aside from a role in the clock mechanism, *Rev-erb* is also involved in moulting, metamorphosis and reproduction in other invertebrates (Cruz et al., 2012; Hannas et al., 2010). If the circadian-expressed gene *Rev-erba* is deleted in mice, normal rhythms of body temperature are disrupted and cold tolerance is altered (Gerhart-Hines et al., 2013). The oscillation amplitude of *Rev-erb* has shown to be affected by another type of stressor in *C. gigas*; the toxin producing algae *Alexandrium minutum*, which also abolishes the day/night difference in expression of *Clk*, *Cry1*, *Per* and *Tim1*, with a corresponding lack of nocturnality observed in valve opening duration (Payton et al.,

2017b). Disruption of clock gene rhythmicity, such as for *Rev-erb* herein, could therefore affect diverse biological processes. The timing of the clock gene-protein interactions comprising the molecular clock mechanism affects the timing of the expression of multiple clock-controlled genes, thereby having knock-on effects on downstream physiological and behavioural processes (Bozek et al., 2009; Harmer et al., 2001; McDonald and Rosbash, 2001; Zhang et al., 2009).

Thermocycles had the opposite effect on *aaNAT*, in that a significant difference in expression was triggered by DDTC, whereas constant levels were observed under both LD and DD (Figure 5.12; Figure 5.13; Table 5.5). This suggests a clock-independent biochemical response to temperature, consistent with the proposed function of the non-vertebrate gene in functions such as detoxification (Pavlicek et al., 2010), whereas the vertebrate version is integral to rhythmic melatonin synthesis (Klein, 2007). Although the rhythmic production of melatonin does occur in molluscs, potential links to timekeeping ability are not yet known.

The other mussel clock genes investigated (*Clk*, *Cry1*, *ROR/HR3* and *Per*) exhibited significant circadian expression under all three experimental conditions (LD, DD and DDTC) indicating that temperature cycles did not ablate gene expression oscillations (Figure 5.12; Figure 5.13; Table 5.5). The clock-associated gene *ARNT* also showed significant variation in expression under DD and DDTC (Figure 5.12; Figure 5.13; Table 5.5). *ARNT*, which is also called hypoxia-inducible factor (HIF)-1β, is involved in the cellular signalling response to pollutants via the aryl hydrocarbon receptor (AhR) pathway, in addition to mediation of hypoxia via the hypoxia-inducible (HIF) pathway (Mandl and Depping, 2014). In the sea snail *Haliotis diversicolor*, a 3 °C warming event did not affect the expression of *ARNT*/*HIF-1β* in the gills and hemocyctes, however *HIF-1α*, which encodes a protein which heterodimerises with

HIF-1β, was elevated (Cai et al., 2014). HIF-1α is linked to the circadian regulation via binding to the promoter regions of clock genes such as *Cry1, Per1, Per2* and (Peek et al., 2017; Egg et al., 2013).

Studies on *Drosophila* reveal further effects of temperature on circadian systems; alternative 3' splicing in the untranslated region of *Per* is boosted under low temperatures with short photoperiods, whereas high temperatures enhance this phenomenon in *Tim* (Helfrich-Förster et al., 2018; Dubruille and Emery, 2008; Majercak et al., 2004). Phase advancement of the clock therefore occurs at low temperatures due to the combined effect of quicker *Per* accumulation and abundance of TIM isoforms with a greater affinity for CRY (Helfrich-Förster et al., 2018). Thermocycles also act as a zeitgeber for PER and TIM entrainment under constant light, with the oscillations lost when temperature is also constant (Glaser and Stanewsky, 2005). Many aspects of the molecular circadian clock are therefore impacted upon by temperature cycles from gene expression and epigenetic influences to protein stability (Stevenson, 2018; Rensing and Ruoff, 2002) and species differences in clock temperature sensitivity is thought to have resulted in geographic radiations (Helfrich-Förster et al., 2018; Rivas et al., 2018). Functional studies are required to help clarify further aspects of bivalve clock organisation.

5.4.4 Conclusions

This chapter investigated the effect of diurnal light and temperature cycles on clock mRNA expression to establish the influence of environmental factors on the molecular basis of *M. edulis* circadian timing. In conclusion, expression of the canonical clock genes (*Clk, Cry1, ROR/HR3, Per* and *Rev-erb*) varied in an endogenous manner consistent with endogenous control. Temperature cycles

modulated the significantly variable expression pattern of *Rev-erb* to constant levels and conversely triggered significant diurnal variation in *aaNAT* expression that was otherwise constant. Further studies are needed to fully characterise the molecular interactions comprising the clock mechanism of mussels, but clock genes clearly play an important role in regulating biological timekeeping in marine bivalves.

Chapter 6

Identification of seasonally expressed mRNAs using a global transcriptomic approach

6.1 INTRODUCTION

Seasonality, the regular annual recurrence of a pattern, influences almost all ecosystems by encompassing a variety of factors such as light, temperature, precipitation, and resource availability. Environmental cycles influence biotic physiological responses. For example, in bivalves, physiological and behavioural processes that vary throughout the year include gametogenesis (Rodríguez-Rúa et al., 2003; Duinker et al., 2000; Seed, 1969), larval recruitment (Broitman et al., 2008), feeding and absorption rates (Cranford and Hill, 1999), biochemical composition (Khan et al., 2006; Pazos et al., 1997), metabolism (Banni et al., 2011; Mao et al., 2006), growth rates (Khan et al., 2006), byssal thread attachment strength (Moeser and Carrington, 2006), immune parameters (Duchemin et al., 2007) and thermal tolerance (Chapple et al., 1998). In addition to being dependent on both exogenous and endogenous parameters, many of these seasonally variable processes are interlinked. For example, there is a trade-off between reproductive development and growth, demonstrated by sterile triploid bivalves with greater growth rates than their fecund diploid conspecifics (Payton et al., 2017c; Brake et al., 2004).

Seasonal effects are apparent on a molecular level; seasonal mRNA expression differences have been investigated in bivalves including clams (de Sousa et al., 2014),

oysters (Dheilly et al., 2012), scallops (Boutet et al., 2008) and mussels (Banni et al., 2011; Ciocan et al., 2011). Sex, followed by gonadal development stage, were the two factors explaining the majority of the variation in gonad gene expression in a microarray study on the European clam *Ruditapes decussates* (de Sousa et al., 2014). Transcriptomic profiles of gonadal development have also been created for the mussel *M. galloprovincialis* (Banni et al., 2011) and the scallop *Argopecten purpuratus* (Boutet et al., 2008) revealing sex-specific and maturation-specific patterns of expression. Investigation into seasonal gene expression of a non-reproductive tissue in female *M. galloprovincialis* which underwent gametogenesis in the field, showed differences in genes involved in metabolism, stress response and immunity (Banni et al., 2011). These previous studies used samples encompassing reproductive stage differences linked to seasonal change, often with the aim of identifying markers for gametogenesis (Dheilly et al., 2012; Ciocan et al., 2011; Boutet et al., 2008). In contrast, this chapter aims to identify seasonal gene expression differences in blue mussel gonads for which sex and gametogenesis stage are not contributing factors. The purpose was to identify genes involved in the input (detection of environmental cues e.g. photoreception) and regulation (e.g. components of the molecular clock system) of the timekeeping system as opposed to outputs (physiological/behavioural biological rhythms e.g. gametogenesis). This approach was used as a means to potentially identify seasonally expressed genes which may have an involvement in the regulation of time keeping, based on known functions in other species.

Suppression Subtractive Hybridisation (SSH) is a molecular technique allowing the identification of mRNAs that are differentially expressed between a pair of sample sets. The approach involves the creation of two cDNA libraries, each from a different mRNA population, which are combined allowing hybridisation;

unhybridised cDNAs are equalised, enriched and amplified so mRNAs differing in their expression between the two populations may be identified. This technique, though relatively complex and time-consuming, is beneficial for discovering new genes and is good alternative to gene expression profiling when microarrays are unavailable (Farrell, 2010). SSH has successfully been applied in previous bivalve studies to identify differentially expressed genes according to gonadal development stage (Ciocan et al., 2011), tissue type (Craft et al., 2010), in response to exposure to various pollutants (de Cerio et al., 2013; Ciocan et al., 2011; Yang et al., 2012), and in healthy and intersex bivalves (Ciocan et al., 2012).

In contrast to the gene targeted strategy used in previous chapters, the aim of this chapter is to use SSH as a global approach to identify novel seasonal *M. edulis* genes which may have links to the molecular clock mechanism. This includes genes involved in the provisioning of seasonal information, components of the molecular clock mechanism and clock-controlled output genes (CCGs). To achieve this, gametogenesis stage, lunar phase, tidal phase and sampling time, were all standardised whereas factors including photoperiod and temperature regime, two of the most common zeitgebers in rhythm entrainment, varied naturally between seasons. Seasonal comparisons were performed for males and females respectively to identify genes differentially expressed between winter and spring/summer. The identification of novel genes exhibiting seasonal expression differences will aid in the understanding of the molecular mechanisms underpinning essential rhythmic processes in *M. edulis* and help provide a foundation from which the impacts of environmental change can be predicted.

6.2 MATERIALS AND METHODS

6.2.1 Sampling and selection of mussels

Sexually developing female M. edulis at gametogenesis stages βII to βIII (Figure 6.1) were selected from the seasonally collected mussels described in detail in Chapter 3. Females were selected at random from the summer late morning and winter late morning time-points (n=7 each). For the males, sexually developing individuals at gametogenesis stages βIII to βIV (Figure 6.1) were selected from late morning in winter and late morning in spring (n=6 each). Winter and summer exhibit the most extreme discrepancy in photoperiod (10 hr) and were therefore chosen for comparison of female mussels. For males, a comparison between winter and spring was performed instead (4.5 hr photoperiod difference), as the late stages of gametogenesis predominant in summer would not have allowed for standardisation of gametogenesis stage between seasons.

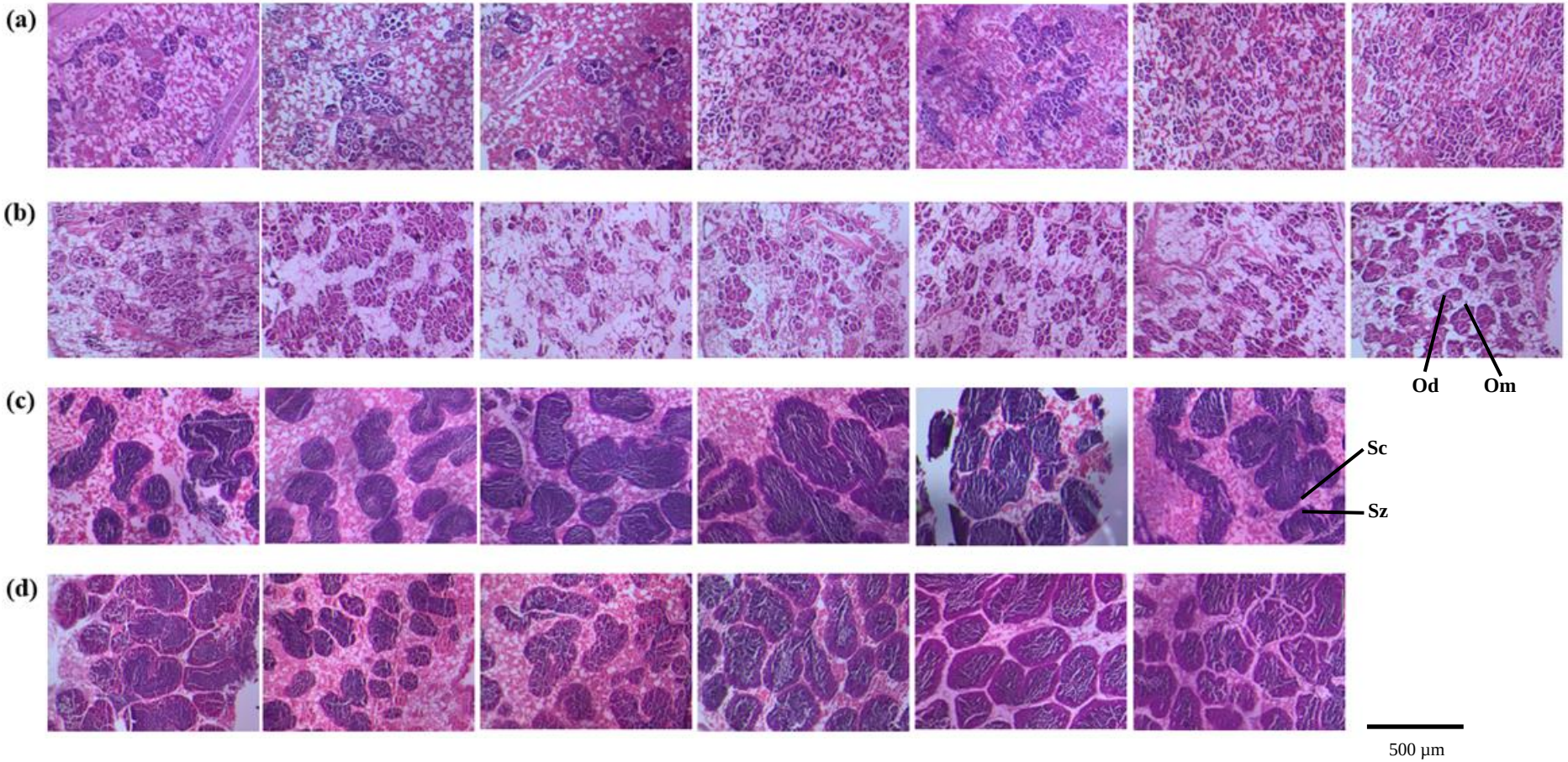

Figure 6.1 Photomicrographs of H&E stained *M. edulis* gonad sections. Females at gametogenesis stages βII and βIII (Seed, 1969) sampled from late morning at the (a) winter solstice 2014 and (b) summer solstice 2015 and males at gametogenesis stages βIII to βIV (Seed, 1969) sampled from late morning at the (c) winter solstice 2014 and (d) spring equinox 2015. Abbreviations: Od, developing oocyte; Om, mature ova; Sc, spermatocytes; Sz, ripe spermatozoa.

6.2.2 Total RNA extraction and quantification

Total RNA was extracted using the High Pure RNA Tissue Kit (Roche, UK) (Section 2.2.2) and quantified using the Qubit 1.0 Fluorometer (Life Technologies, UK) (Section 2.2.3). RNA integrity was checked on a 1% formaldehyde agarose denaturing RNA gel containing 0.15 ug/mL ethidium bromide (Life Technologies, Paisley, UK) (Section 2.2.4). RNA from each treatment was pooled so each sample was represented at an equal concentration in each total 2.5 µg RNA pool (females: 357.1 ng, *n*=7; males: 416.7 ng, *n*=6).

6.2.3 RNA precipitation

Each of the four RNA pools was ethanol precipitated to concentrate the RNA in a lower volume prior to cDNA synthesis. Sterile 3M sodium acetate solution (adjusted to pH 5.3 with glacial acetic acid) (Fisher Scientific, UK) was combined with RNA and 4 °C absolute ethanol (VWR Chemicals, UK) in the following ratio: 0.1:1:2. Samples were incubated at -80 °C for 30 min and centrifuged at 20,000 x *g* for 20 min before carefully removing as much supernatant possible without disturbing the pellet. The sample was dried using a Concentrator 5301 (Eppendorf, UK) until all residual liquid was removed (approx. 10 min). The pellet was dissolved in 3.5 µL molecular-grade water (Fisher Scientific, UK) and stored at -20 °C. RNA concentrations were measured as previously described and confirmed to be between 100 – 200 ng/µL before proceeding to SMARTer™ PCR cDNA Synthesis.

6.2.4 SMARTer™ PCR cDNA Synthesis

The SMARTer™ PCR cDNA Synthesis Kit (Clontech, Saint-Germain-en-Laye, France) was used for first-strand cDNA synthesis following the manufacturer's

guidelines. This method preferentially generates complete cDNA sequences over partial sequences, avoiding the underrepresentation of 5' sequence ends which may otherwise occur (Clontech, France). For each sample, 3 µL RNA (approx. 500 ng) was mixed with 1 µL 3'SMART CDS Primer IIA and 0.5 µL deionized water, before being heated at 72 °C for 3 min and then 42 °C for 2 min. The following reagents from the kit were then added: 0.25 µL RNase Inhibitor (40 U/µL), 2 µL 5X First Strand Buffer (250 mM Tris-HCl [pH 8.3], 375 mM KCl and 30 mM $MgCl_2$), 0.25 µL DTT (100 mM), 1 µL dNTP mix (10 mM each), 1 µL SMARTer II A oligonucleotide and 1 µL SMARTscribe™ Reverse Transcriptase (100 U/µL). After being gently mixed and briefly centrifuged, samples were heated to 42 °C for 90 min followed by 70 °C for 10 min. Finally, 40 µL TE buffer (10 mM Tris-HCl [pH 7.5] and 0.1 mM EDTA, Agilent Technologies, UK) were added to each sample before being stored at -20 °C. A control reaction was also performed alongside the other samples, using Control Mouse Liver Total RNA (1 µg/µL).

6.2.5 cDNA Amplification by Long Distance (LD) PCR

LD PCR was used to generate double-stranded (ds) cDNA by combining 30 µL of the first-strand cDNA described in the previous section with 222 µL deionised water, 30 µL 10X cDNA PCR Reaction Buffer, 6 µL 50X dNTP mix (10 mM each), 5' PCR Primer II A (12 µM) and 50X Advantage cDNA Polymerase Mix (containing KlenTaq-1 DNA polymerase, a proofreading polymerase and TaqStart® Antibody for hotstart reactions) (Clontech, France). In order to determine the optimal cycle number required for the reaction, the samples were placed in a pre-heated thermal cycler and subjected to the following program: 95 °C for 1 min and then 15 cycles of 95 °C for 15 sec, 65 °C for 30 sec and 68 °C for 6 min. Afterwards, 275 µL was temporarily

stored at 4 °C and the remaining 25 µL was subjected to further thermal cycles as previously described, with 5 µL volume being removed after every 3 cycles until no further volume remained. This allowed samples subjected to the following number of cycles to be analysed together on a 1% TAE agarose gel containing 0.15 ug/mL ethidium Bromide (Invitrogen, UK): 15, 18, 21, 24, 27 and 30 cycles. The optimal cycle number was one cycle before the cycle giving the strongest signal on the gel. The sample previously set aside at 4 °C was then run for the additional cycles required to reach this optimum stage. All samples were then stored at -20 °C. Again, the control mouse liver sample from the kit was also analysed alongside the other samples.

6.2.6 Column Chromatography

Column Chromatography was used to purify the cDNA from impurities including proteins, enzymes, nucleotides, salts and solvents. Prior to commencing, 7 µL of the ds cDNA from the optimised LD PCR reactions was set aside to be run on a gel as a control for comparative purposes. The remainder of the sample (approx. 250 µL) was purified and concentrated using CHROMA SPIN +TE-1000 columns (Clontech, France) according to the manufacturer's instructions. Briefly, the procedure involved combining equal volumes of sample and phenol:chloroform:isoamyl alcohol 25:24:1 (Sigma-Aldrich, UK) and centrifuging at 20,000 x *g* for 10 min to separate the upper aqueous phase. This phase was mixed with 700 µL n-butanol (Fisher Scientific. UK), centrifuged at 20,000 x *g* for 1 min and the upper n-butanol organic layer was discarded. A CHROMA SPIN+TE-1000 column, containing a resin matrix in sterile TE buffer (10 mM Tris-HCl [pH 8.0], 1 mM EDTA), was prepared by allowing gravity to drain the buffer inside it. 150 mL of filter sterilised 1X TNE buffer (10 mM Tris Base, 1 mM EDTA, 200 mM NaCl,

adjusted to pH 7.4 with concentrated HCl) was added to the column and completely drained. The flow-through was discarded. The sample was then carefully pipetted onto the surface of the gel matrix and a further 4 steps of adding 1X TNE buffer were then performed, each time collecting the eluate in a clean tube; the following buffer volumes were used: 25 µL, 150 µL, 320 µL, and 75 µL. To confirm the success of the procedure, 10 µL of the final and the penultimate eluates (which contain the purified cDNA) were run alongside 3 µL of the LD PCR sample set aside at the beginning, on a 1% TAE gel containing 0.15 ug/mL ethidium bromide. Both eluates were then combined prior to RsaI digestion.

6.2.7 RsaI Digestion

Chromatography-purified cDNA was digested using the restriction enzyme RsaI (which cuts GT-AC sites) to produce shorter cDNA fragments with the blunt ends required for future adaptor ligation. All but 10 µL of the sample was combined with 36 µL RsaI restriction buffer (100 mM Bis Tris Propane-HCl (pH 7.0), 100 mM $MgCl_2$, 1 mM DTT) and 1.5 µL RsaI (10 units/µL), mixed well and incubated at 37 °C for 3 hr. A positive control containing 1 µL lambda (λ) DNA (454 µg/mL) (Promega, Southampton. UK), 0.5 µL RsaI enzyme, 2 µL RsaI restriction buffer and 16.5 µL molecular-grade water (Fisher Scientific, UK) was also prepared, along with a negative control of 1 µL λ DNA and 19 µL water. To confirm success, the 10 µL of undigested cDNA was run on a 1% TAE gel containing 0.15 ug/mL ethidium bromide, as was the same volume of digested cDNA, positive control and negative control.

6.2.8 Purification of digested cDNA

Following RsaI digestion, cDNA was purified using the NucleoSpin® Gel and

PCR Clean-up Kit (Macherey Nagel, UK) according to the manufacturer's instructions and eluting in a final volume of 15 µL NE Buffer (5 mM Tris/HCl, pH 8.5). This technique is summarised in Section 2.2.10. cDNA concentration was then measured using a fluorometer (Section 2.2.11) and where concentrations were in excess of 300 ng/µL, they were diluted to this concentration using molecular-grade water (Fisher Scientific, UK) according to the manufacturer's recommendations.

6.2.9 Adaptor Ligation

In order to ligate adaptors to the cDNA, 1 µL cDNA from each sample was first diluted with 5 µL molecular-grade water (Fisher Scientific, UK) and 2 µL of the dilution was mixed with 2 µL Adaptor 1 (10 µM) and 2 µL Adaptor 2R (10 µM) respectively. A control reaction was set up in the same manner, using a mixture of 1 µL control DNA (3 ng/µL; Hae III-digested bacteriophage ΦX174 DNA) (Clontech, France) with 5 µL ΦX174/ Hae III (150 ng/mL) (Fisher Scientific, UK). To each mixture, the following reagents were added: 3 µL sterile water, 2 µL 5X Ligation Buffer (250 mM Tris-HCl (pH 7.8), 50 mM $MgCl_2$, 10 mM DTT and 0.25 mM BSA) and 1 µL T4 DNA Ligase (400 units/µL; contains 3 mM ATP). 2 µL from each reaction was then combined together in a third tube to created unsubtracted controls and all reactions were incubated at 16 °C overnight. To stop the reactions and inactivate the ligase, 1 µL 20X EDTA/glycogen mix (200 mM EDTA; 1 mg/mL glycogen) was added and reactions were heated at 72 °C for 5 min. Finally, 1 µL of each unsubtracted control was diluted in 1 µL sterile water (for Section 6.2.10.3) and all tubes were frozen at -20 °C.

Analysis of the ligation reaction was assessed by PCR on the control cDNA sample using 1 µL gene-specific primers for the *Glycerol-3-Phosphate*

Dehydrogenase gene (10 µM G3PDH3' and G3PDH5') (Clontech, France) together and using the same volume of G3PDH3' paired with Primer 1 (10 µM) (which anneals to the adaptor) in PCR reactions containing the following: 1 µL adaptor-ligated cDNA diluted 200X, 18.5 µL molecular-grade water, 2.5 µL 10X cDNA PCR Reaction Buffer, 0.5 µL dNTP mix (10 mM each) and 0.5 µL 50X Advantage cDNA Polymerase Mix (Clontech, France). Samples were heated at 75 °C for 5 min, 94 °C for 30 sec, and then subjected to 40 cycles of 94 °C for 10 sec, 65 °C for 30 sec, and 68 °C for 2.5 min before being cooled to 4 °C. 5 µL of each sample was visualised on a 2% agarose TAE ethidium bromide gel. The stages involved in adaptor ligation, and subsequent hybridisation and PCR, are summarised in Figure 6.2.

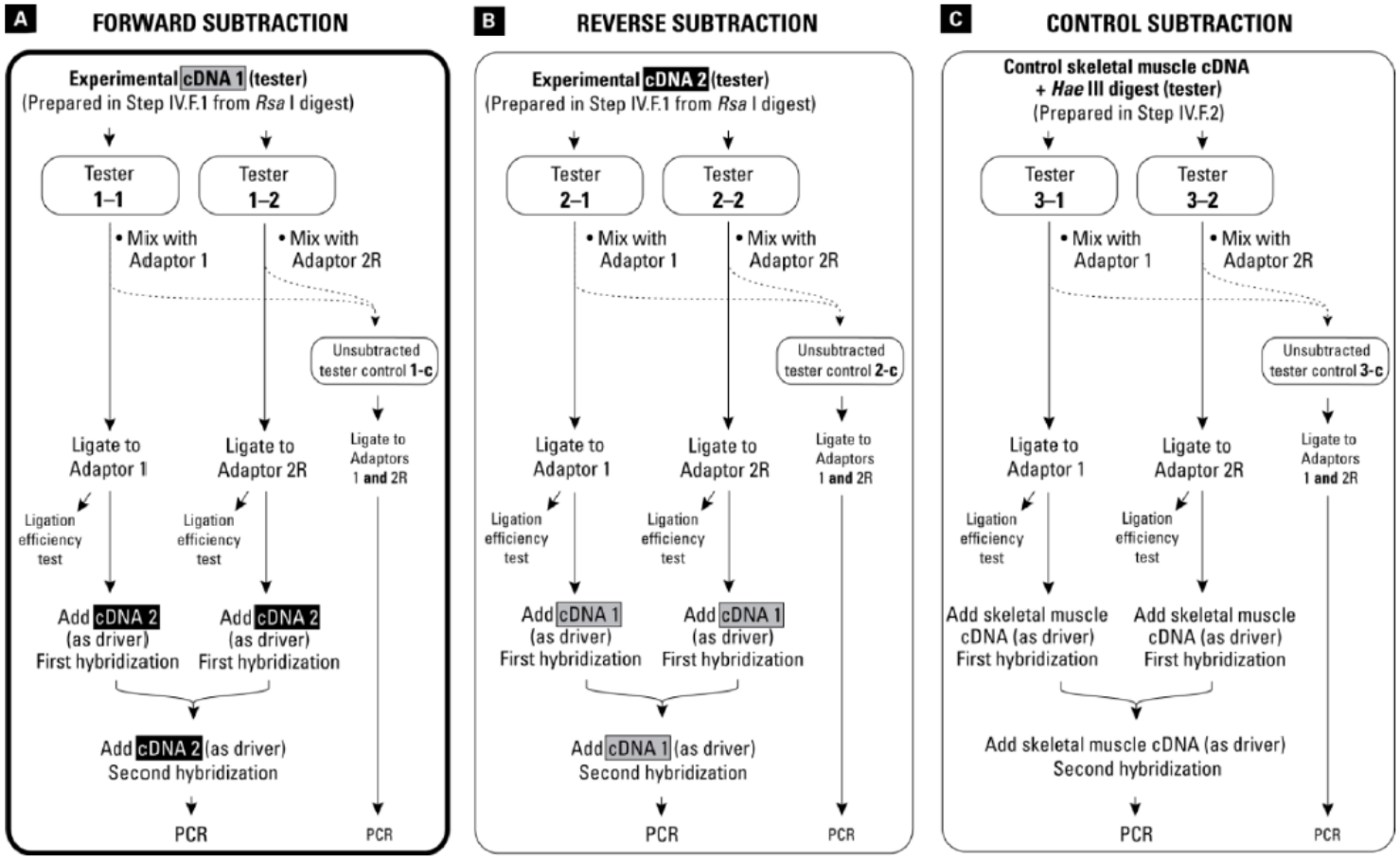

Figure 6.2 Diagram summarising adaptor ligation, hybridisation and PCR stages of the SSH experiment. A. Forward subtraction summarises the main experiment. B. Reverse subtraction uses the tester as the driver and vice versa, allowing differential screening. C. Control subtraction uses control skeletal muscle cDNA (Source: SelectTM cDNA Subtraction Kit User Manual, Clontech).

6.2.10 Suppression Subtractive Hybridization (SSH)

6.2.10.1 First hybridisation

The first hybridisation reaction was performed by mixing 1.5 µL of each adaptor-ligated tester sample (Adaptor 1-ligated Tester and Adaptor 2R-ligated Tester) with 1 µL 4X Hybridisation Buffer (contents undisclosed by manufacturer) at room temperature, and 1.5 µL of purified RsaI-digested Driver cDNA (Section 6.2.8). Samples were briefly centrifuged, incubated at 98 °C for 1.5 min, and then incubated at 68 °C for 6 hr.

6.2.10.2 Second hybridisation

The second hybridisation involved mixing 1 µL of each purified RsaI-digested cDNA with 1 µL 4X Hybridisation Buffer and 2 µL sterile water and heating the samples at 98 °C for 1.5 min. Each sample was then simultaneously combined with the corresponding two adaptor-ligated tester cDNA samples generated in the first hybridisation step (Section 6.2.10.1) and heated at 68 °C overnight. Samples were then diluted with 200 µL Dilution Buffer (20 mM HEPES pH 8.3, 50 mM NaCl, and 0.2 mM EDTA pH 8.0) and heated to 68 °C for 7 min before being stored at -20 °C.

6.2.10.3 Primary and secondary PCR amplification

Primary PCR reactions were set up using 1 µL of either the 200X diluted subtracted cDNA (Section 6.2.10.2) or 1 µL of the unsubtracted controls diluted in 1 mL sterile water (Section 6.2.9) and the following reagents: 19.5 µL sterile water, 2.5 µL 10X cDNA PCR Reaction Buffer, 0.5 µL dNTP mix (10 mM each), 1 µL PCR Primer 1 (10 µM) and 0.5 µL 50X Advantage cDNA Polymerase Mix (Clontech,

France). The following thermal cycling parameters were used: 95 °C for 5 min, 94 °C for 25 followed by 32 cycles of 94 °C for 10 sec, 66 °C for 30 sec, and 72 °C for 1.5 min, before being cooled to 4 °C. 8 µL of each sample was checked on a 2% agarose TAE ethidium bromide gel.

Secondary PCR products were prepared by diluting 3 µL of the primary PCR products in 27 µL sterile water. 1 µL of each dilution was then combined with the same reagents and volumes used for the primary PCR, with the exception that 1 µL Nested PCR Primer 1 (10 µM) and Nested PCR Primer 2R (10 µM) replaced PCR Primer 1, and the sterile water volume was reduced by 1 µL. The thermal cycling conditions were: 12 cycles of 94 °C for 10 sec, 68 °C for 30 sec, and 72 °C for 1.5 min.

6.2.11 Agarose gel electrophoresis and purification of DNA bands

8 µL of each secondary PCR product (Section 6.2.10.3) was run on a 2% agarose TAE ethidium bromide gel. The lanes on the gel containing the resulting bands/smears were cut into two pieces, one containing larger fragments than the other. Each gel section was purified using the NucleoSpin® Gel and PCR Clean-up Kit (Macherey Nagel, UK) according to the manufacturer's instructions (Section 2.2.10) and DNA was eluted in a final volume of 20 µL Buffer NE (5 mM Tris/HCl, pH 8.5).

6.2.12 Preparation of chemically competent *E. coli*

Chemically competent *E. coli* were produced to be used as host cells for the cloning of DNA from the SSH experiment. An LB agar plate (30 µg/mL streptomycin) was streaked with MAX Efficiency® DH10B™ *E. coli* cells (Invitrogen, UK) under aseptic conditions and incubated overnight at 37 ºC. A single colony was

used to inoculate 5 mL LB broth (10 µg/mL streptomycin), which was placed in a shaking incubator overnight at 37 ^{o}C and 200 rpm. 200 mL of LB broth (10 µg/mL streptomycin) pre-heated to 37 ^{o}C was added to the sample which was returned to the incubator under the same conditions until the optical density (OD_{600}) was at 0.5 to obtain cells in the mid-log phase of growth. After 5 min of being chilled on ice, the cells were pelleted by centrifuging at 4 ^{o}C for 15 min at 4000 x *g*. After the supernatant was removed, 80 mL Transformation Buffer I (TfbI) (30 mM potassium acetate, 10 mM rubidium chloride, 50 mM manganese chloride, 15% volume per volume glycerol; pH 5.8, filter sterilised) was added and the cells were resuspended. The sample was then incubated for 10 min on ice. Another centrifugation step was performed as previously described, the supernatant was discarded and the pellet was very gently resuspended in 8 mL Transformation Buffer II (TfbII) (10 mM MOPs, 75 mM calcium chloride, 10 mM rubidium chloride and 15% volume per volume glycerol; pH 6.5, filter sterilised). The cells were incubated on ice for 20 min and aliquots of 50 µL chemically competent cells were snap-frozen in liquid nitrogen and stored at -80 ^{o}C.

6.2.13 Cloning PCR products and gel-extracted DNA

Cloning reactions were performed using The Original TA Cloning Kit with pCR® 2.1 Vector (Life Technologies, UK) and chemically competent MAX Efficiency® DH10B™ *E. coli* cells (Life Technologies, UK) (Section 6.2.12). Ligation reactions using the secondary PCR products from the SSH reaction (Section 6.2.10.3) were set up as follows: 1.5 µL of PCR product, 0.25 µL sterile water, 0.25 µL 5X T4 DNA Ligase Buffer (250 mM Tris-HCl pH 7.6, 50 mM $MgCl_2$, 5 mM ATP, 5 mM DTT, 25% (w/v) polyethylene glycol-8000) , 0.5 µL pCR® 2.1 Vector (25 ng/µL in

10mM Tris-HCl, 1 mM EDTA pH 8.0) and 0.5 µL ExpressLink™ T4 DNA ligase (5 U/µL). Ligation reactions were incubated at 14 ^{o}C overnight then 2 µL was combined with 50 µL chemically competent MAX Efficiency® DH10B™ *E. coli* cells (Invitrogen, UK) and the mixture was incubated on ice for 30 min. Cells were transformed by performing a heat shock step in water bath at 42 ^{o}C for 75 sec, immediately cooling on ice for 2 min and adding 250 µL room temperature sterile LB broth (100 µg/mL ampicillin). Samples were incubated in a shaking incubator at 37 ^{o}C and 200 rpm for 1 hr and 50 µL was spread on a pre-warmed LB agar plate (100 µg/mL ampicillin) which had already been spread with 40 µL 20 mg/mL X-gal (in DMSO) for blue/white screening. After overnight incubation at 37 ^{o}C, individual successfully transformed white colonies were used to inoculate 5 mL aliquots of LB broth (100 µg/mL ampicillin), which were incubated overnight at 37 ^{o}C and 200 rpm. Cell pellets were created by centrifuging the overnight cultures for 5 min at 20,000 x *g* and removing the supernatant. Pellets were frozen at -80 ^{o}C.

6.2.14 Screening and purification of plasmids

To further confirm the presence of an insert in the vector and to ascertain its size, a cell pellet of transformed *E. coli* from 1 mL overnight culture was resuspended in 200 µL molecular-grade water and heated to 99 ^{o}C to rupture the cells. A PCR reaction was performed using 1 µL of this sample, 8.06 µL molecular-grade water (Fisher Scientific, UK), 0.25 µL 40 mM dNTPs (Fisher Scientific, UK), 0.19 µL Expand High Fidelity^{PLUS} Enzyme Blend (5 U/µL, containing a mixture of Taq polymerase and a proofreading polymerase) (Roche, UK), 2.5 µL Expand High Fidelity^{PLUS} Reaction Buffer 5X containing 7.5 mM $MgCl_2$ (Roche, UK) and 0.25 µL each of primers M13R (5'-CAG GAA ACA GCT ATG AC-3') and M13F (5'-GTA

AAA CGA CGG CCA GT-3') (IDT, Belgium) which were both at 100 pmol/ µL concentration. The thermal cycling conditions were as follows: 94 ^{o}C for 2 min, followed by 35 cycles of 94 ^{o}C for 30 sec, 50 ^{o}C for 30 sec and 72 ^{o}C for 1 min, and finally cycle at 72 ^{o}C for 7 min. Agarose gel electrophoresis was performed; PCR products of 183 bp lacked inserts in the vector, whereas larger bands were indicative of success.

The Nucleospin Plasmid DNA purification Kit (Machery-Nagel, UK) was used to purify plasmids containing inserts from pelleted *E. coli* derived from an aliquot 2 mL overnight culture. The manufacturer's instructions were performed as follows: cells were resuspended in 250 µL Buffer A1(containing RNase A) to induce lysis and then mixed with 250 µL Buffer A2 (containing 0.2 – 2% sodium hydroxide) and left at room temperature for up to 5 min until the lysate cleared in order to free the plasmid DNA from the cell. 300 µL Buffer A3 (containing guanidine hydrochloride) was then added to neutralise the sample pH, followed by centrifugation at 11,000 x *g* for 5 min to obtain a cleared lysate. The sample was bound to the silica membrane of a Nucleospin Plasmid column by adding the sample and centrifuging at 11,000 x *g* for 1 min. After the supernatant was discarded, the sample was washed with 500 µL Buffer AW (containing guanidine hydrochloride and isopropanol) then 600 µL Buffer A4 with a centrifugation step of 11,000 x *g* for 1 min after each. The membrane was dried by centrifuging at the same speed for 2 min and finally the sample was eluted by adding 50 µL Buffer AE (5 mM Tris/HCl, pH 8.5), incubating at room temperature for 1 min and centrifuging at 11,000 x *g* for 1 min. Purified plasmid DNA was then stored at -20 ^{o}C.

6.2.15 Sequencing and sequence identification

Plasmids were sequenced by sending 9.75 µL of purified plasmid DNA and 0.25 µL of either primer M13R (100 pmol/µL) or primer M13F (100 pmol/µL) to the EZ-seq DNA Sanger sequencing service (Macrogen Europe, Amsterdam, The Netherlands). Bioedit (version 7.2.5) was used to check and edit the sequences and to remove vector and adaptor sequences from the ends. Sequences were identified using BLAST searches (blastn and blastx algorithms) to compare them against the nucleotide and protein sequence databases on the NCBI website (http://blast.ncbi.nlm.nih.gov/Blast.cgi). The E value of each match indicates its reliability as it represents the number of matches with a similar score to arise by random chance. Therefore, the closer the value to zero, the better the match.

6.2.16 qPCR validation of SSH results

A total of 6 genes with a range of different functions (Figure 6.3; Figure 6.4) were selected from across the 4 cDNA libraries for qPCR validation as follows: for females *Pyridoxal kinase* (*PDXK*), which was up-regulated in the summer samples compared to the winter, and *Nucleolar GTP-binding protein 1* (*GTPBP1-like*), *ATP-binding cassette sub-family E member 1* (*ABCE1*) and *Neuroplastin-like* which showed the opposite pattern, were selected. For the males, *NADH dehydrogenase subunit 4* (*ND4*), which was up-regulated in the spring compared to the winter, and *Eukaryotic Initiation Factor 4A-like* (*eIF-4A-like*), which showed the opposite pattern, were chosen. qPCR primers were designed using Primer-BLAST (http://www.ncbi.nlm.nih.gov/tools/primer-blast/) (Table 6.1). Primers for the references genes *18S* and *EF1a* (Table 6.1) were previously validated for their suitability for normalisation on this seasonal sample set (Chapter 3). qPCR was

performed on the same samples used for SSH along with the following number of additional samples (from the appropriate gametogenesis stages) to increase the sample number: summer females (*n*=2), winter females (*n*=4), winter males (*n*=3) and spring males (*n*=2). All reactions were performed in duplicate using the same reagents, thermal cycling conditions and equipment described in detail in Chapter 3.

Table 6.1 Primers used for qPCR validation of SSH experiment

Target Gene	Primer	Sequence 5'-3'	% GC	Amplicon Size (bp)
For qPCR on females				
PDXK	PK_F1	ACA CCA AAC CAG TAC GAA GC	50.0	83
	PK_R1	AGA TCG TCC ATT GCC AGC AG	55.0	
GTPBP1-like	GTP_F1	GCC ATT AAA GGT TTG TTG GCG A	45.5	131
	GTP_R1	GCT CTG GCC CAT CTT AGA GC	60.0	
ABCE1	ABCE1_F	AAC TGT CGC ACT GTT CCT TGA	47.6	108
	ABCE1_R	GCT GGC AGG AAA ATT AGC CC	55.0	
Neuroplastin	Neuro_F	ACC ATT AAA GGC ACC GGT TGA	47.6	92
	Neuro_R	ATG TGG GTG CCA AGC TCT AC	55.0	
For qPCR on males				
ND4	NADH_F1	AGC CAC CAC AGA CTT ATG GC	55.0	99
	NADH_R1	CTT ATG AGG GGT GAG CGA GC	60.0	
eIF-4A-like	EIF_F1	GAA TCG TCC ACC TCT GCC AA	55.0	88
	EIF_R1	TGT ACA GCA GGT TTC ACT CGT	47.6	
Reference genes				
18S	Me for	GTG CTC TTG ACT GAG TGT CTC G	54.5	116
	Me rev	CGA GGT CCT ATT CCA TTA TTC C	45.5	
EF1a	EF1a_F	CAC CAC GAG TCT CTC CCA GA	60.0	106
	EF1a_R	GCT GTC ACC ACA GAC CAT TCC	57.1	

6.2.17 Statistical analysis

Statistical analyses were performed in GraphPad InStat v3 (GraphPad Software Inc., La Jolla, USA) on mussel shell length data and mRNA expression data from the qPCR validation of the SSH experiments. The datasets were assessed for

normality and homogeneity of variance, followed by either an unpaired t-test or, in cases where a significant difference between the standard deviations was evident, a Mann-Whitney Test. In all cases, statistical significance was accepted at the $p<0.05$ level. Graphs were created in Microsoft Office Excel 2007.

6.3 RESULTS

6.3.1 Biometric measurements

The average shell lengths for the mussels used in the SSH and qPCR experiments are shown in Table 6.2. No significant difference was detected in shell length between female mussels selected from winter and summer (unpaired t-test: $t(18)=1.406$, $p=0.177$). No difference in shell length was apparent for male samples between winter and spring either (Mann-Whitney Test: $U=25.5$, $p=0.321$).

Table 6.2 Biometric data for average mussel shell length with the standard deviation (SD) and standard error (SEM).

Sex	Season	*n*=	Length (mm)	SD	SEM
Female	Winter	11	49.8	4.4	1.3
	Summer	9	46.9	4.9	1.6
Male	Winter	9	49.8	3.7	1.2
	Spring	8	48.3	1.5	0.5

6.3.2 SSH Analysis

A total of 40 clones containing successfully ligated plasmids were sequenced from the pooled female SSH samples and compared to the NCBI sequence database using blastx and blastn searches: 37.5% matched to sequences with known identities

and function (Figure 6.3; Table 6.3), 12.5% matched to unnamed sequences, 7.5% produced no matches and 42.5% were duplicate sequences. For the SSH experiment on male mussels, a total of 18 ligated plasmids were sequenced: 27.7% matched to sequences with known identities and function (Figure 6.4; Table 6.4), 5.5% matched to unnamed sequences, 27.7% had no database matches and 38.8% were duplicate sequences. Of the successfully identified sequences, the majority of matches were to molluscs (Table 6.3; Table 6.4).

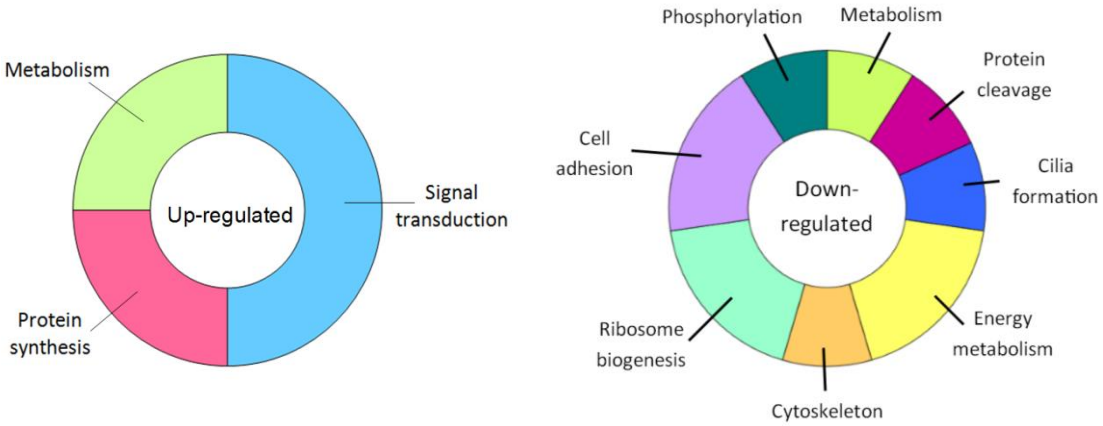

Figure 6.3 Functional categories of mRNAs identified by SSH as potentially up-regulated (left; *n*=4) or down-regulated (right; *n*=11) in female *M. edulis* mantle tissue in summer compared to winter.

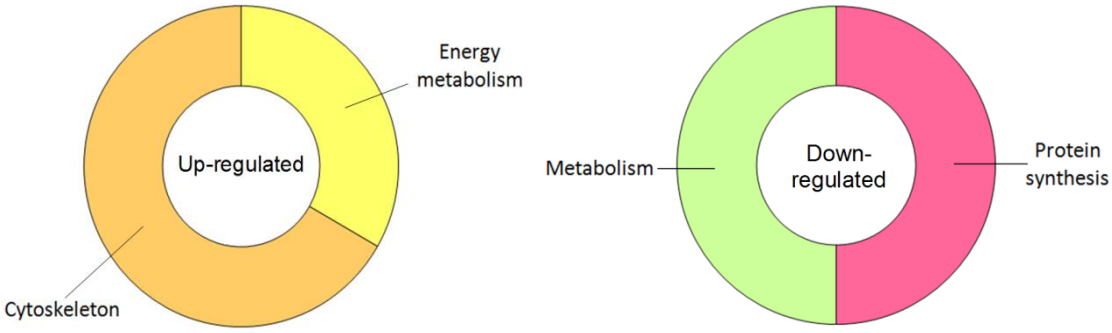

Figure 6.4 Functional categories of mRNAs identified by SSH as potentially up-regulated (left; *n*=3) or down-regulated (right; *n*=2) transcripts in male *M. edulis* mantle tissue in spring compared to winter.

Table 6.3 mRNAs indicated by SSH to be potentially differentially expressed in the gonads of female *M. edulis,* at sexual development stages βII to βIII, sampled at the winter and summer solstices. *denotes result from blastn nucleotide search, all other results are from a blastx search.

Clone accession number	Length (bp)	Identity	Species match	Result accession number	e-value	Function	Reference(s)
Up-regulated in female summer solstice samples (compared to winter solstice)							
Signal transduction							
JZ970419	222	**Heat shock protein 90** (*HSP90-1*)	*M. galloprovincialis*	CAJ85741.1	2e-29	- Molecular chaperone - Signal transduction - Circadian clock interactions with BMAL1	Picard, 2002 Zhao et al., 2011 Schneider et al., 2014
JZ970427	274	**Calmodulin (CaM)** (*calmodulin*)	*Lymnaea stagnalis*	ABB85281.1	6e-11	- Calcium-activated signal transduction - Biomineralisation - Phototransduction	Van Eldik et al., 1998 Li et al., 2004 Hardie, 2001
Metabolic function							
JZ970420	776	**Pyridoxal kinase-like** (*PDXK)*	*Lottia gigantea*	XP_009054441.1	3e-117	- Transferase enzyme involved in vitamin B_6 metabolism	Schibler 2005
Protein synthesis							
N/A	592	**16S (mitochondrial rRNA)***	*M. trossulus*	KU925349.1	0.0	- Mitochondrial ribosomal RNA involved in protein synthesis	Taanman, 1999

Down-regulated in female summer solstice samples (compared to winter solstice)							
Cell adhesion							
JZ970421	534	**Neuroplastin-like**	*C. gigas*	XP_011450189.1	9e-20	- Immunoglobulin superfamily (IgSF) transmembrane protein involved in cell adhesion and cell-cell recognition	Owczarek and Berezin, 2012
MH359088	609	**Hemicentin-like**	*Mizuhopecten yessoensis*	XP_021370012.1	1e-16	- Cellular adhesion - Mitotic cytokinesis - Retinal function	Xu et al., 2013
Ribosome biogenesis							
JZ970422	545	**Nucleolar GTP-binding protein 1-like** (*GTPBP1-like*)	*Lingula anatina*	XP_013398687.1	5e-112	- Ribosome biogenesis - Linked to circadian rhythm regulation by enabling *aaNAT* degradation	Woo et al., 2011
JZ970426	1004	**ATP-binding cassette sub-family E member 1** (*ABCE1*)	*C. gigas*	XP_011449756.1	0.0	- Initiation of translation - Ribosome biogenesis and recycling	Pisarev et al., 2010
Energetic metabolism							
JZ970423	679	**ATP synthase lipid-binding protein, mitochondrial-like**	*Biomphalaria glabrata*	XP_013066447.1	2e-41	- Subunit of an enzyme catalysing adenosine triphosphate (ATP) synthesis (Electron transport chain/ energy metabolism)	De Grassi et al., 2006
N/A	459	**Cytochrome c oxidase subunit II** (*COX2*)	*M. trossulus*	ADE05891.1	9e-53	- Subunit of an enzyme involved in the mitochondrial electron transport chain/ energy metabolism	García-Horsman et al., 1994

Cytoskeleton							
JZ970424	1033	**Alpha tubulin** (*alpha-tubulin*)	*B. floridae*	XP_002601443.1	0.0	- Microtubule formation: - Cytoskeleton - Chromosome separation - Cilia/flagella structure	Keeling and Doolittle, 1996
JZ970428	540	**Centrosomal protein of 131 kDa-like (5-azacytidine induced protein 1)** (*CEP131*)	*C. gigas*	EKC38807.1	2e-16	- Cilia formation	Hall et al., 2013
Protein cleavage							
JZ970425	338	**Mitochondrial-processing peptidase subunit beta-like (β-MPP)**	*Saimiri boliviensis boliviensis*	XP_010349997.1	4e-62	- Subunit of an enzyme that cleaves targeting signals from mitochondrial proteins	Gakh et al., 2002
Metabolism							
JZ970429	421	**Chitinase/ chitotriosidase-like**	*Mytilus coruscus*	AHC08445.2	3e-64	- Enzyme involved in chitin metabolism - Biomineralisation	Weiss and Schönitzer, 2006 Banni et al., 2011
Phosphorylation							
MH359089	724	**Dual specificity testis-specific protein kinase 1-like** (*TESK1*)	*Mizuhopecten yessoensis*	XP_021367571.1	3e-30	- Phosphorylation - Spermatogenesis role in males	Meng et al., 2014

Table 6.4 mRNAs indicated by SSH to be potentially differentially expressed in male gonads (stage βIII to βIV) at the winter solstice and spring equinox.

Clone accession number	**Length (bp)**	**Identity** (based on blastx searches)	**Species match**	**Result accession number**	**e-value**	**Function**	**Reference(s)**
Up-regulated in male spring equinox samples (compared to winter solstice)							
Energetic metabolism							
N/A	1018	**NADH dehydrogenase subunit 4** (*ND4*)	*M. edulis*	AAV68419.1	4e-154	- Mitochondrial electron transport chain	Craft et al., 2010
Cytoskeleton organisation							
JZ970430	328	**Beta tubulin** (*beta-tubulin*)	*Parascolymia vitiensis*	BAD11697.1	2e-75	- Microtubule formation: - Cytoskeleton - Chromosome separation - Cilia/flagella structure	Keeling and Doolittle, 1996
JZ970431	434	**Actin**	*Cyrenoida floridana*	AAS20336.1	1e-99	- Microfilament formation: - Cytoskeleton - Cell contraction - Cell motility	Mitchison and Cramer, 1996
Down-regulated in male spring equinox samples (compared to winter solstice)							
Protein synthesis							
JZ970432	979	**Eukaryotic Initiation Factor 4A-like** (*eIF-4A-like*)	*C. gigas*	XP_011421890.1	3e-142	- Helicase involved in protein synthesis by binding mRNA to ribosome	Andreou and Klostermeier, 2013
Metabolism							
JZ970433	915	**Chitinase/ chitotriosidase-like**	*M. galloprovincialis*	AKS48199.1	8e-84	- Enzyme involved in chitin metabolism - Biomineralisation	Weiss and Schönitzer, 2006 Banni et al., 2011

6.3.3 qPCR validation of SSH

Six cDNA transcripts identified as potentially differentially expressed from the SSH experiments were selected for validation using qPCR to confirm the results. In females: the up-regulated *PDXK* and down-regulated *GTPBP1-like*, *ABCE1* and *Neuroplastin-like* transcripts. In males: the up-regulated *ND4* and down-regulated *eIF-4A-like*. Primer concentrations, R^2 values and primer efficiencies for the optimised reactions are displayed in Table 6.5 and the standard curves are shown in Figure 6.5. Though qPCR on all genes showed the expected trends based on the SSH results, only the mRNA expression of *GTPBP1-like* was significant between seasons with a significantly lower expression in summer than winter (Mann-Whitney: U= 23.0, p=0.0465) (Figure 6.6).

Table 6.5 Final primer concentrations for qPCR with R^2 values and amplification efficiencies.

Target Gene	Forward primer	Reverse primer	Final primer concentration (nM)	R^2	Efficiency (%)
mRNA isolation from female mussels					
PDXK	PK_F1	PK_R1	300	0.9607	98.6
GTPBP1-like	GTP_F1	GTP_R1	200	0.9968	93.2
ABCE1	ABCE1_F	ABCE1_R	300	0.9699	105.68
Neuroplastin	Neuro_F	Neuro_R	300	0.9998	98.03
mRNA isolation from male mussels					
ND4	NADH_F1	NADH_R1	300	0.9925	94.0
eIF-4A-like	EIF_F1	EIF_R1	300	0.9977	90.3

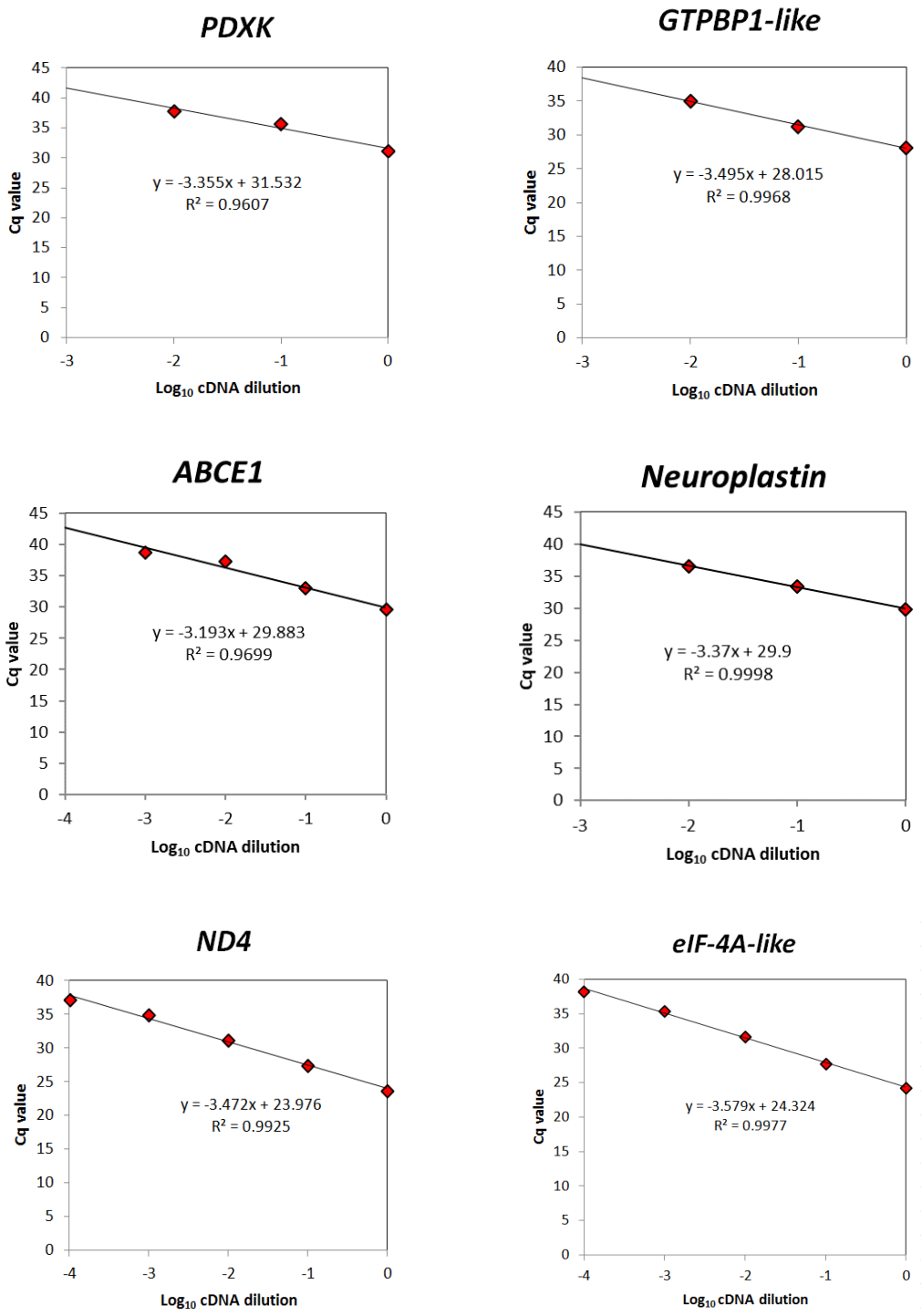

Figure 6.5 Standard curves showing qPCR amplification over a dilution series of *M. edulis* cDNA with R^2 values displayed.

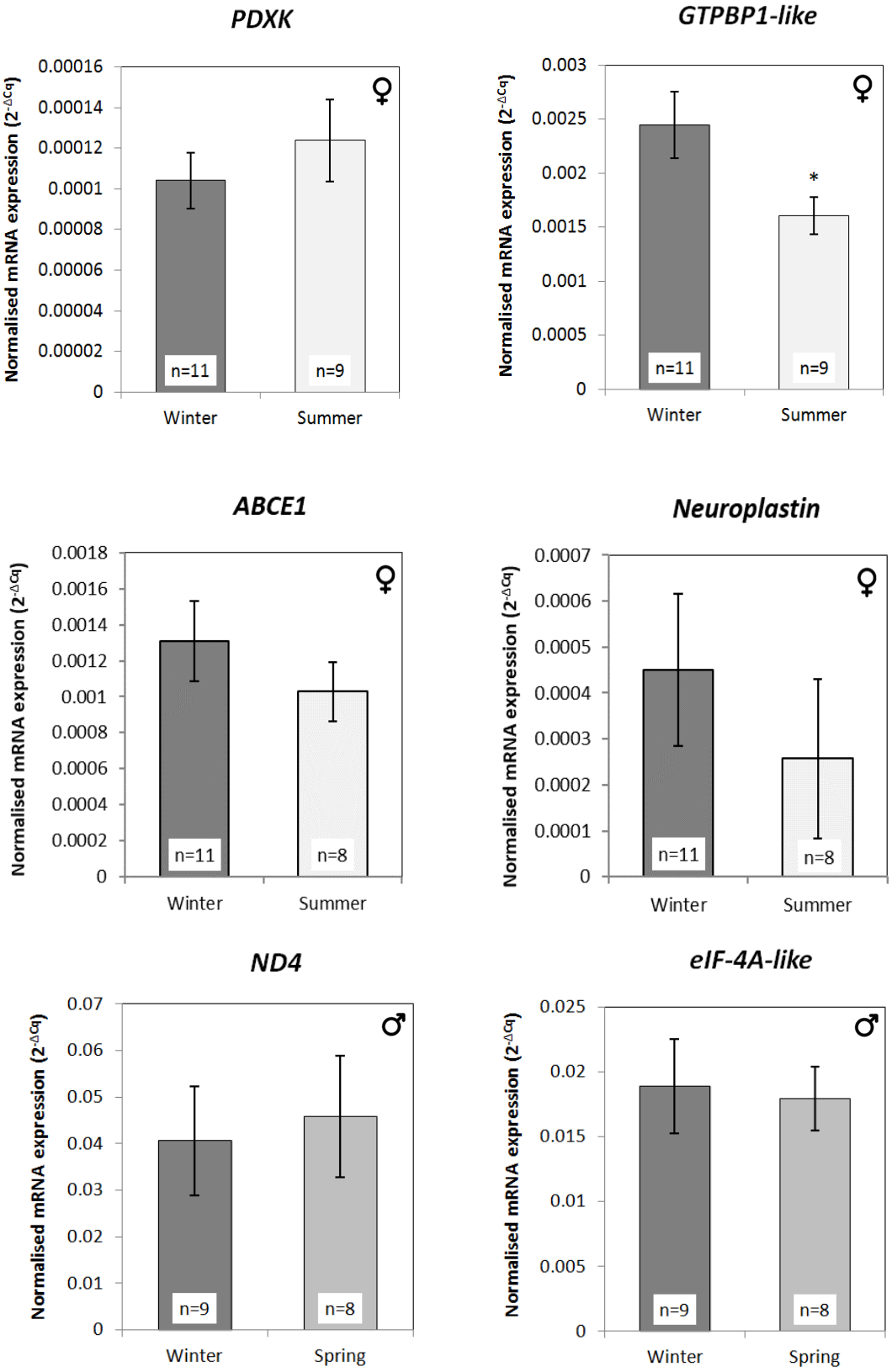

Figure 6.6 mRNA expression of transcripts identified by SSH as potentially differentially expressed between seasons in female (*PDXK*, *GTPBP1-like*, *ABCE1*, *Neuroplastin*) and male (*ND4*, *eIF-4A-like*) *M. edulis* gonads. Mean data ±SEM. Units are arbitrary. *denotes significance at $p<0.05$.

6.4 DISCUSSION

In this chapter, *M. edulis* cDNA libraries allowed the identification of genes that were indicated by SSH to be potentially up-regulated or down-regulated in their mRNA expression between wild-caught winter and summer females, and between winter and spring males respectively. The success rates for the identification of novel cDNA sequences were 31.7% in the female experiment and 27.7% for males, which are consistent with the 22-53% success rate from other such bivalve experiments (de Cerio et al., 2013; Ciocan et al., 2012; Ciocan et al., 2011; Yang et al., 2012). Identification rates are at this level as sequences cannot be identified if they match to unnamed sequences or fail to match to known sequences. Furthermore, duplicate sequences obtained during cloning were not counted as novel transcripts. Differentially expressed transcripts were identified from both cDNA libraries for each sex, with a total of n=15 identified from the female SSH experiment comparing winter and summer (Table 6.3) and n=5 from the male experiment comparing winter and spring (Table 6.4). A winter/summer comparison could not be made for males as *M. edulis* seasonal sexual development constrained the number of samples obtained at the appropriate stage of gametogenesis. Gametogenesis was controlled for, rather than investigated as part of the experimental design, as it is an output of a biological rhythm, and the goal of this investigation was to identify genes that may be involved in environmental detection and the regulatory molecular timekeeping mechanism (Figure 1.7). Similarly, a greater sample number would be beneficial in detecting significance in mRNA expression differences, but the same constraint was applicable.

As only one of the six genes selected for qPCR validation confirmed significant seasonal differences (*GTPBP1-like*) (Figure 6.6), the SSH results cannot be considered fully validated. As a result, the identified genes cannot be confirmed herein as

showing significant seasonal differences in expression levels and further evidence is required. Nonetheless, a number of the genes isolated in this chapter show possible links with the regulation of biological timekeeping based on the literature, and have potential to be used as candidate genes in future investigations into seasonality in mussels.

6.4.1 mRNA expression in females

Four mRNAs suggested by SSH to be potentially up-regulated in female mantle tissue in summer compared to winter, had functions in signal transduction (*HSP90-1*, *calmodulin*), metabolic enzymatic processes (*PDXK*) and protein synthesis (*16S*) (Figure 6.3; Table 6.3). Several potentially down-regulated transcripts (*n*=11) were also identified which were involved cell adhesion (*Neuroplastin-like*, *hemicentin*), ribosome biogenesis (*GTPBP1-like*, *ABCE1*), energy metabolism (*ATP synthase lipid-binding protein, mitochondrial-like*; *MT-CO2*), cytoskeleton function (*alpha-tubulin*), cilia formation (*CEP131*), protein cleavage (*β-MPP*), phosphorylation reactions (*TESK1*) and metabolism (*Chitinase/ chitotriosidase-like*) (Figure 6.3; Table 6.3). A number of these genes encode proteins that interact with elements of the molecular clock mechanism (HSP90, CaM, GTPBP1).

6.4.1.1 Potentially up-regulated SSH transcripts (summer vs. winter)

Heat shock protein 90 (HSP90) is a highly abundant chaperone protein that maintains the folding, regulation and integrity of cytosolic proteins (Picard, 2002). Stress conditions in bivalves, including thermal stress, can trigger up-regulation of heat shock genes including *HSP90* (Park et al., 2015; Banni et al., 2011), resulting in a greater protein abundance (Tomanek and Zuzow, 2010). *HSP90* expression is

diurnal in *M. californianus* with elevated levels triggered by low tide (Connor and Gracey, 2011). Expression is also elevated in thermally stressed *C. gigas* with a generally greater increase in summer (Farcy et al, 2008), consistent with the findings herein. With regards to the mammalian circadian clock, HSP90 maintains BMAL1 protein levels such that its inhibition disrupts interlinked clock components, resulting in disturbances to the rhythm, phase and amplitude (Schneider et al., 2014). HSP90 is also involved in vertebrate ovarian development via its estrogen receptor (ER) binding role upstream of vitellogenesis, a function possibly occurring in the crustacean *Macrobrachium nipponense* as expression varies with ovarian development, peaking during vitellogenesis (Zhao et al., 2011).

HSP90 interacts with calmodulin (Calcium-Modulated Protein; CaM) (Picard, 2002), which was also up-regulated herein. CaM is a ubiquitous, multi-functional messenger protein activated by calcium binding. Pertaining to the circadian clock, CaM is involved in *Drosophila* phototransduction, the sensory perception of light (Hardie, 2001). Furthermore, calcium-dependent binding of melatonin to CaM on the oocyte membranes of the amphibian *Xenopus laevis* suggests a potential rhythmic mechanism for the synchronisation of cellular processes (Romero et al., 1998). Phototransduction genes, including *CaM*, have previously been documented in the mantle/eyes of various scallop and oyster species (Sun et al., 2016; Li et al., 2004) and CaM regulation of calcium metabolism is integral to bivalve shell formation as calcium carbonate crystals are the most prevalent component (Li et al., 2004). CaM up-regulation in summer females may therefore indicate a seasonal elevation in calcium metabolism.

Also up-regulated was *pyridoxal kinase*-like (*PDXK*), encoding an enzyme integral to vitamin B6 metabolism which catalyses the conversion of pyridoxal to the

bioactive form of vitamin B6, pyridoxal 5'-phosphate (PLP), an essential coenzyme in multiple enzymatic metabolic processes (Yang et al., 1996). In peripheral tissues, some proline- and acid-rich basic leucine zipper transcription factors (PAR bZip) are regulated by the clock mechanism and their regulation of *PDXK* results in its cyclic expression causing rhythmicity in downstream metabolic reactions (Schibler 2005). An increase in *PDXK* expression in the summer could therefore indicate elevated levels of vitamin B_6 metabolism.

Finally, eukaryotic 16S is a mitochondrially encoded rRNA (mt-rRNA) molecule encoded by *MT-RNR2* in humans, which is involved in mitochondrial gene expression (Taanman, 1999). 16S has previously been found to be differentially expressed in male *M. edulis* gonads at different stages of gametogenesis (Ciocan et al., 2011) and now this study indicates a seasonal difference in female gonads at the same (developing) stage of gametogenesis, with upregulation occurring in summer. Conversely, elevated temperatures resulted in down-regulation of 16S in the clam *Ruditapes decussates* (Velez et al., 2017).

6.4.1.2 Potentially down-regulated SSH transcripts (summer vs. winter)

A transcript encoding a neuroplastin-like protein was identified by SSH as down-regulated in summer females compared to winter. Neuroplastin (encoded by *NPTN*) belongs to the Ig superfamily (IgSF) of proteins. Its isoforms have signalling and cellular adhesion functions and are involved in maintenance of the nervous system (Owczarek and Berezin, 2012). *Hemicentin*-like, which also encodes an IgSF protein involved in cellular adhesion and mitotic cytokinesis (Xu et al., 2013), was also downregulated. Conversely, an RNA-Seq experiment on the clam *R. philippinarum* found *Hemicentin* to be downregulated in the gills in response to cold temperature

stress, though qPCR validation was inconclusive (Nie et al., 2016).

Nucleolar guanosine-triphosphate-binding protein 1-like (*GTPBP1*) was validated by qPCR as being significantly down-regulated in female mussels from the summer, where photoperiod was greatest (Figure 6.6). GTPBP1 is a post-transcriptional regulator of mRNA quantity and quality as it regulates mRNA degradation (Woo et al., 2011). In mammals, GTPBP1 plays a role in circadian rhythm regulation by forming part of a protein complex which binds to *aaNAT* mRNA facilitating its degradation (Woo et al., 2011); both proteins are expressed in a circadian manner in the rat pineal gland, peaking during the night, which regulates nocturnal melatonin production (Woo et al., 2011). The relationship between *aaNAT* and circadian regulation is less clear in invertebrates (Peres et al., 2014; Mohamed et al., 2014) though mussel *aaNAT* was found to be constantly expressed under LD conditions in the previous chapter. Another down-regulated gene involved in ribosome biogenesis was ATP-binding cassette sub-family E member 1 (ABCE1), also known as RNase L inhibitor (RLI) or HP68, which is a protein with wide-ranging biological roles in regulating protein translation, ribosome recycling, cell division, anti-apoptosis and mammalian viral infection (Tian et al., 2012).

ATP synthase lipid-binding protein mitochondrial-like is a subunit of the enzyme ATP synthase that is required for the formation of adenosine triphosphate (ATP) involved in energy transfer. It is associated with the mitochondrial electron transfer chain, as is the case for Cytochrome C oxidase subunit II (MT-CO2), the second subunit of cytochrome C oxidase. Transcripts encoding both of these proteins were down-regulated in *M. edulis* in summer, potentially indicative of a reduction in energy metabolism.

Also identified was alpha-tubulin, part of a subfamily of globular proteins

belonging to the tubulin superfamily. Heterodimerisation between alpha- and beta-tubulins leads to the formation of microtubules, essential components of the cellular cytoskeleton, which are also involved in chromosome separation and play a structural role in cilia and flagella (Keeling and Doolittle, 1996). Another down-regulated transcript also required for cilia formation and function is *Centrosomal protein of 131 kDa* (*CEP131/AZI1*) (Hall et al., 2013; Wilkinson et al., 2009). Cilia have important roles in bivalves including particle filtration (food and pseudofaeces), respiration and oocyte transportation through the gonoducts (Gosling, 2015; Tanabe et al., 2010). Downregulation of these genes in female gonads could indicate a reduced ability of these cilia-dependent processes in individuals developing in the summer. Genes involved in ciliary function were also down regulated as part of the CO_2 stress response in the Sydney rock oyster *Saccostrea glomerata* (Ertl et al., 2016).

A transcript encoding the Mitochondrial-processing peptidase (MPP) subunit beta-like was also down-regulated in summer. The two sub-units comprising the enzyme are α-MPP and β-MPP (Gakh et al., 2002). MPP cleaves pre-sequences off nuclear-encoded proteins, which, although essential for translocation of such proteins into the mitochondria, may later obstruct further sorting, and protein folding so are consequently removed (Gakh et al., 2002). This suggests that mitochondrial biosynthesis activities in the gonads of female *M. edulis* could be lower in the summer.

A transcript encoding the serine/threonine kinase Dual specificity testis-specific protein kinase 1 (*TESK1*) was down-regulated. This enzyme catalyses phosphorylation reactions and is particularly noted for its importance in spermatogenesis in males, although it is also expressed in other tissues including the brain, liver and kidneys, with lower levels detected in female gonads (Meng et al., 2014).

Finally, chitinases are enzymes that degrade chitin, a structurally important biopolymer present in numerous organisms, including in the larval and adult shells of bivalves (Weiss and Schönitzer, 2006; Gosling, 2015). For example, elevated CO_2 triggered the down regulation of both chitinase and chitin synthase in the oyster *S. glomerata* as part of a switch to chitin modification processes as opposed to synthesis/degradation (Ertl et al., 2016). In addition to being involved in shell-remodelling processes, chitinases are used by bivalves to digest chitin in consumed algae (Yang et al., 2015) and in host defence against pathogens containing chitin (Okada et al., 2013). Chitin metabolism genes were up-regulated in *M. galloprovincialis* digestive glands in the summer but also down-regulated in the mantle of females with the progression of gametogenesis (Banni et al., 2011). A chitinase gene has also been implicated in early embryonic development in *C. gigas* (Badariotti et al., 2007). This chapter reveals seasonal downregulation between winter and summer of *Chitinase/chitotriosidase-like* in the mantles of female *M. edulis* at the same gametogenesis stage. This could therefore indicate seasonal differences in chitin shell modification processes (Ertl et al., 2016), food availability/composition (Yang et al., 2015), and/or host pathogen defence (Okada et al., 2013), though further investigation is required.

6.4.2 mRNA expression in males

Three mRNA transcripts were identified as up-regulated in male mantle tissue in spring compared to winter, with functions in cytoskeleton processes (*beta-tubulin*, *actin*) and the electron transport chain (*ND4*) (Figure 6.4; Table 6.4). The two down-regulated transcripts encoded a helicase involved in protein synthesis (*eIF-4A-like*) and an enzyme involved in chitin metabolism (*chitinase/chitotriosidase-like*) (Figure

6.4; Table 6.4).

6.4.2.1 Potentially up-regulated SSH transcripts (spring vs. winter)

Up-regulation of tubulin family genes occurs with the progression of male gamete development in *M. galloprovincialis* (Banni et al., 2011); however, this chapter reveals the up-regulation of *beta-tubulin* in male *M. edulis* in spring compared to winter despite individuals being at the same stage of gametogenesis. The function of tubulin subunits in microtubule formation was discussed in the previous section. Another key component of cytoskeleton formation and function which was upregulated was *actin*, encoding an essentially ubiquitous protein in eukaryotic cells; one of its multi-functional roles is in the formation of microfilaments involved processes such as cell contraction and motility (Mitchison and Cramer, 1996). Isoforms of *actin* and *alpha-tubulin* have been shown to be up-regulated in response to elevated temperatures in *M. galloprovincialis* and *M. trossulus* respectively, where the effect of temperature stress on cytoskeleton gene expression profiles appears to be species-specific, relating to whether the species is cold- or warm-adapted (Tomanek and Zuzow, 2010). Altered expression of *beta-tubulin* and *actin* transcripts has also been reported in mussels that have undergone CO_2 stress (Ertl et al., 2016). Actin is often used as a reference gene in qPCR reactions however this seasonal expression difference reinforces previous concerns over the suitability of the gene for this purpose in *M. edulis* (Jarque et al., 2014; Cubero-Leon et al., 2012).

ND4 is a mitochondrial gene encoding NADH dehydrogenase subunit 4 which is a subunit of the enzyme NADH dehydrogenase (ubiquinone) also known as Complex I, a key component of the mitochondrial electron transport chain. Compared to other mitochondrial mRNAs, expression levels of *ND4* are high in *M.*

galloprovincialis and levels vary with tissue type (Craft et al., 2010). Up-regulation of this gene between winter and spring is indicative of seasonal changes in expression profiles of genes relating to energy metabolism in *M. edulis*.

6.4.2.2 Potentially down-regulated SSH transcripts (spring vs. winter)

Eukaryotic Initiation Factor 4A-like (*eIF-4A*) is a helicase-encoding gene that was down-regulated in spring males compared to winter. eIF-4A unwinds RNA secondary structures and is involved in translation initiation (Andreou and Klostermeier, 2013). Other closely related eukaryotic initiation factors have been up-regulated in *S. glomerata* in response to elevated CO_2 levels, as were chitin metabolism-related genes including chitinase (Ertl et al., 2016). As previously discussed for female *M. edulis*, a chitinase/chitotriosidase-like in males was also found to be more abundant in the winter. These results may be indicative of a stress response to natural seasonal change (Ertl et al., 2016; Okada et al., 2013) or relate to food availability/composition (Yang et al., 2015).

6.4.3 Limitations and alternative approaches

Results generated by SSH require post-validation with a second method to confirm differential expression (Farrell, 2010). Of the six genes selected herein for qPCR validation of the SSH results, only *GTPBP1-like* showed a significant difference in expression between season, confirming that expression was significantly higher in females in winter than in summer (Figure 6.6). No significant seasonal differences were detected using qPCR on *PDXK*, *ABCE1*, *neuroplastin*, *ND4* and *eIF-4A-like*. Low sample number was a constraint; the seasonal reproductive development of *M. edulis* limited the number of individuals that were at the same stage of gametogenesis

in both seasons. Further qPCR validation using a larger sample set is therefore required to lend support to the unvalidated seasonal gene expression differences indicated by SSH and to determine the robustness of the SSH results.

Alternative approaches that can be applied to assess seasonal transcriptomic changes include gene expression profiling using DNA microarrays. This popular approach can capture the expression of thousands of genes simultaneously however, unlike SSH, advance knowledge of the target sequences is required (Baldi and Hatfield, 2011). Microarrays have previously been used to investigate seasonal transcriptomic profiles in different bivalve species (de Sousa et al., 2014; Dheilly et al., 2012; Banni et al., 2011). A more modern approach is RNA-Seq, which allows relative quantification of RNA between two or more groups using next generation sequencing technology (Zhao et al., 2014). Though it is more costly, RNA-Seq has a broader dynamic range than microarrays and does not rely on pre-designed probes (Zhao et al., 2014). RNA-Seq has recently used to investigate the seasonal transcriptomes of the planktonic sea snail *Limacina helicina antarctica*, providing molecular-level insights into their seasonal maturation and growth (Johnson et al., 2019).

6.5 CONCLUSIONS

The aim of this chapter was to identify blue mussel genes that were differentially expressed between seasons as a means to identify genes with known clock-related functions in other speices, such as provisioning of seasonal information, participation in core clock interactions, and CCGs. The mRNAs revealed by SSH herein allowed the isolation of transcripts involved in functions including signal transduction, metabolism, protein synthesis, cytoskeleton function, cell adhesion and

cilia formation. Of particular relevance to mussel chronobiology, were genes encoding proteins with roles in phototransduction (*CaM*), those which interact with components of the molecular clock mechanism (*HSP90-1, CaM, GTPBP1*), and those involved in the melatonin synthesis pathway (*GTPBP1*). With the exception of *GTPBP1*, qPCR was not successful in validating the SSH results. Further investigation is required in the future to ascertain seasonality of the isolated transcripts. However, this work still contributes toward the little known mechanisms of blue mussel biorhythm entrainment by revealing potentially interesting genes meriting further investigation in the context of clock-associated functioning.

Chapter 7

General Discussion

This thesis provides novel insights into the molecular basis of biological timekeeping in the blue mussel by characterising clock genes, determining their activity over daily and seasonal timeframes, and identifying seasonal genes with clock-associated functions meriting further investigation. The contribution of this work to the fields of marine chronobiology and intertidal ecology will be discussed, as will its wider relevance to potential climate change impacts on marine biorhythms. The main findings of this thesis will be summarised, making reference to the aims outlined in Chapter 1. Future experiments will be proposed to broaden our understanding of bivalve chronobiology by addressing current gaps in the knowledge. This research is particularly relevant in the context of a changing climate; the impacts of elevated temperature and the implications of decoupled environmental cues on the timing and success of *M. edulis* gametogenesis will be discussed in the final section of this chapter.

7.1 Relevance and contribution to the field

Despite the ubiquitous nature of biological rhythms and their widespread influence on virtually all the major biological processes, chronobiology is an under-studied aspect of bivalve ecology. This is despite the fact that many edible bivalves, such as blue mussels, are both ecologically (Gutiérrez et al., 2003) and commercially important (FAO, 2018). Of particular relevance is the seasonal gametogenesis cycle

of *M. edulis*, which results in annual variation in the condition of adults, and the availability of mussel spat (Domínguez et al., 2010). Regulation of blue mussel biorhythms, in particular those regulating seasonal reproductive development, and investigating the environmental cues influencing their timing, has wide reaching relevance to both natural and aquacultural settings. Therefore the main objectives of this thesis were to isolate and characterise genes and proteins comprising the molecular clock mechanism, explore the effects of photoperiod, temperature cycles and season on clock gene expression, and to identify seasonal genes with clock-associated functions or involvement in infradian rhythms. This thesis advances our understanding of how biological rhythms are regulated in *M. edulis* by isolating a number of clock genes and examining how environmental factors including light and temperature modulate their expression on a daily and seasonal basis.

The molecular clock mechanism governing biorhythm regulation is particularly well characterised in mammals and insects (Mohawk et al., 2012; Dubruille and Emery, 2008; Hardin, 2005), but when this thesis began in 2014, there were few studies in which bivalve clock components had been isolated (Pairett and Serb, 2013; Zhang et al., 2012; Connor and Gracey, 2011). This thesis has expanded upon this knowledge by isolating and characterising sequences from number of clock genes (*Clk*, *Cry1*, *ROR/HR3*, *Per* and *Rev-erb*) (Chapter 2 and 5), clock-associated genes (*ARNT*, *Timeout*-like and *aaNAT*), and putative clock proteins (CLK and TIM) (Chapter 2) from *M. edulis* for the first time. qPCR assays were developed in line with the MIQE guidelines (Bustin et al., 2009) as a quantitative tool to investigate the mRNA expression of these genes in *M. edulis* and*18S* and *EF1* were validated as stable reference genes for normalisation (Chapter 3).

Diurnal clock gene oscillations are known to be integral to circadian regulation

(Allada et al., 2001; Young, 2000) and light and temperature cycles are predominant zeitgebers in many circadian systems (Mohawk et al., 2012; Dubruille and Emery, 2008; Rensing and Ruoff, 2002). Though Connor and Gracey (2011) had investigated the diurnal transcriptomes of *M. californianus* over a tidal/circadian cycle, revealing rhythmic diurnal expression of *Cry1* and *RORβ*, it remained to be investigated whether this clock gene expression was in direct response to light/dark cycles or as a result of endogenous circadian regulation. This thesis filled this gap in the knowledge by investigating the mRNA expression patterns of a number of clock and clock-associated genes over a diurnal time-frame under LD and DD laboratory conditions, revealing significant expression variations consistent with endogenous regulation (Chapter 5). As summarised in Figure 7.1, significant variation in mRNA expression was apparent for *Clk*, *Cry1*, *ROR/HR3*, *Per*, *Rev-erb* and *Timeout*-like over 24 hr under LD, which in each case persisted under DD indicative of endogenous circadian control.

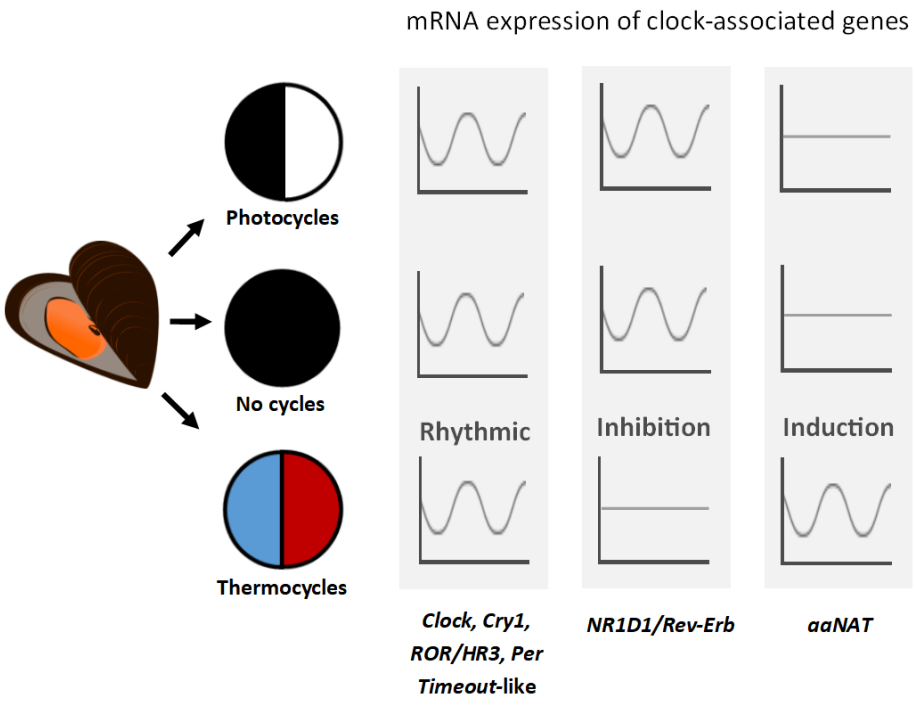

Figure 7.1 Diagram summarising the effect of light and temperature cycles on the expression of *M. edulis* clock genes in the laboratory-based experiment conducted in Chapter 6.

Recent studies have begun to emerge that have characterised clock genes in other bivalve species (Sun et al., 2016) and have also investigated their expression over diurnal timeframes (Schnytzer et al., 2018; Perrigault and Tran, 2017). This highlights bivalve chronobiology as a growing area of research, relevant to understanding the temporal dynamics of complex intertidal environments, which are often considered to present early signs of the impacts of climate change (Helmuth et al., 2006b).

Understanding the influence of environmental factors like light and temperature on mussel seasonal reproduction is required to provide a deeper understanding about the ecology of the species and is also useful to inform broodstock conditioning in aquacultural settings (Domínguez et al., 2010; Fabioux et al., 2005). This thesis further expanded our knowledge of bivalve chronobiology by exploring beyond circadian timeframes. To investigate the potential for the clock mechanism to be influenced by seasons, encompassing natural biotic and abiotic factors including different photoperiods, winter/summer differences in clock mRNA expression patterns were investigated (Chapter 4). Seasonal progression results in photoperiod differences at high latitudes, which can affect the clock expression patterns of aquatic (Herrero and Lepesant, 2014; Davie et al., 2009) and terrestrial organisms (Benetta et al., 2019; Tournier et al., 2003). This thesis revealed seasonal differences in mussel clock gene expression; in particular *Clk*, *Cry1* and *ROR/HR3* were differentially expressed in male mussels between summer and winter at equivalent daily time points (Chapter 4), potentially indicating a similar response to photoperiod, though mussels were investigated *in situ* under the influence of various combined environmental factors. This suggests that seasonal environmental cues can modulate the activity of clock components. Furthermore, for the first time in a bivalve, expression levels of

M. edulis clock genes were examined in both sexes. It was found that a significant difference in *Cry1* and *Clk* expression occurred between sexes at a single time-point in the summer and winter respectively (Chapter 4). This could indicate a sex-specific oscillator-independent function of these genes in *M. edulis* gonads, such as the roles played by *Cry1* in gametogenesis in both sexes in mice (Amano et al. 2009; Alvarez et al., 2003) or sexual dimorphism in circadian timing such as differences in sleep-arousal systems (Bailey and Silver, 2014) and liver metabolism in mice (Bur et al., 2009).

This thesis also identified a number of new candidate genes meriting further investigation in terms of seasonal response (Chapter 6). This includes those with putative involvement in the clock mechanism such as *GTPBP1*, involved in the circadian regulation of mammalian *aaNAT* expression (Woo et al., 2011), *HSP90*, involved in maintaining BMAL1 protein levels (Schneider et al., 2014), and *CAM*, involved in phototransduction in *Drosophila* (Hardie, 2001) Though there appears to be overlap between the circadian regulatory system and the photoperiodic response in other invertebrates (Bradshaw and Holzapfel, 2007; Pavelka et al., 2003), the extent to which the two are linked remains unclear (Goto, 2012) and the molecular basis of insect photoperiodism, for example, is yet to be established (Denlinger et al., 2017; Bradshaw and Holzapfel, 2010).

Another novel aspect of this work was the investigation into the ability of temperature cycles to modulate circadian expression patterns of mussel clock genes (Chapter 5). The rhythmic characteristics of the molecular clock mechanism can be affected by pulse or periodic temperature changes in plants, fungi, invertebrates and vertebrates (Rensing and Ruoff, 2002). This includes temperature acting as a zeitgeber for entrainment; for example, temperature can synchronise the molecular clock of

Drosophila (Glaser and Stanewsky, 2005) and zebrafish *Danio rerio* (Lahiri et al., 2005), and can entrain larval release in the mud crab *Dyspanopeus sayi* (Waite et al., 2017). Here it was found that temperature cycles abolish the significant variation in *M. edulis* clock gene *Rev-erb* mRNA expression over a daily timeframe to constant levels, whereas significant diurnal variation is induced in the otherwise constant expression of the non-circadian clock-associated gene *aaNAT* (Figure 7.1) (Chapter 5). This foundation can be built upon by future studies to ascertain further direct and indirect effects of temperature change on the *M. edulis* clock, including whether temperature acts as a zeitgeber in the species. This is important because establishing the sensitivity of the clock to environmental temperature cues is of wider relevance to studies investigating the impacts of environmental temperature change on coastal ecosystems.

It is clear that a greater consideration of chronobiology is required in marine biology experiments in general and for several reasons as follows (Mat, 2018). Mussel transcriptomes vary temporally across diurnal (Connor and Gracey, 2011; Gracey et al., 2008) and annual (Chapter 6; Banni et al., 2011) timeframes, as well as across spatial scales (Place, 2008). Blue mussels are widely used as bioindicator species of environmental pollution (Rittschof and McClellan-Green, 2005; O'Connor, 2002) however seasonality is known to be a confounding factor of some molecular biomarkers used to measure these effects (Jarque et al., 2014). It is therefore important that experiments consider and allow for parameters that may act as zeitgebers such as photoperiod, temperature and feeding cycles, which will be impacted upon by factors such as location, season and the time of day the experiment/sampling is conducted (Mat, 2018).

Sex and reproductive stage influence the transcriptomes of bivalve gonad

tissues (de Sousa et al., 2014; Dheilly et al., 2012; Ciocan et al., 2011; Boutet et al., 2008), and even the transcriptomes of non-reproductive tissues (Banni et al., 2011), highlighting the importance of determining these parameters in mRNA expression studies. For example, *M. edulis* show varying degrees of susceptibility to endocrine disrupting chemicals at different stages of seasonal gametogenesis (Ciocan et al., 2010). Furthermore, this thesis indicates that the *M. edulis* gonad transcriptome may vary between seasons even in individuals of the same sex at the same stage of gametogenesis (Chapter 6), indicative of seasonal effects. In addition to considering the effects of these factors on the expression of candidate genes, it is also clearly important that the reference genes used to normalise gene expression data are optimised and validated as stably expressed across the specific treatment groups of each individual experiment to generate accurate, reliable data (Chapter 3; Cubero-Leon, 2012).

This thesis provides novel insights into the regulation of blue mussel biological rhythms, detailing novel aspects of their chronobiology, which has wide-reaching relevance to the ecology of the species and diverse applications that utilise this important bivalve. This research provides a foundation upon which future investigations into bivalve chronobiology can build upon. Suggestions for further research are discussed below.

7.2 Future work

7.2.1 Identifying other components of the clock

Despite the valuable contribution of this thesis in isolating clock and clock-associated genes, as well as putative clock proteins, from blue mussels for the first time, further components of the molecular clock mechanism remain undiscovered.

Cry1 was isolated in herein, however additional cryptochrome genes may also be present in mussels as two are present in the squid *E. scolopes* (*escry1* and *escry2*) (Heath-Heckman et al., 2013), three in the oyster *C. gigas* (*CgCry1*, *CgCry2* and *CgpCry*) (Perrigault and Tran, 2017) and three in the scallop *P. yessoensis* (*Cry*, *Cry1* and *Cry2*) (Sun et al., 2016). Similarly, *Timeout-like* was isolated from blue mussels herein but it is likely that *Tim* may also exist in the species as both *Tim* and *Timeout* are present in the oyster *C. gigas* (GenBank accessions EKC41755.1 and XP_011441580.1) and the limpet *L. gigantean* (Reitzel et al., 2010). Furthermore, both *ARNT/TANGO* and *ARNTL/CYC/BMAL1* have also been isolated from *C. gigas* (XP_011419459.1; Perrigault and Tran, 2017) suggesting *M. edulis* *ARNTL/CYC/BMAL1* may also exist. Targeted gene isolation, using the recently available sequence information from other bivalves may prove successful in identifying *M. edulis* homologs.

The protein isolation approach used herein, testing cross-species reactivity of human clock antibodies, led to the isolation of blue mussel proteins consistent with the predicted molecular weights of CLOCK and TIMELESS (Figure 4.6). There is further scope for testing commercially available *Drosophila* antibodies against *M. edulis* in the same manner. For example, PER antibodies designed for insects have proven effective in isolating PER from the crustacean *Daphnia pulex* (Bernatowicz et al., 2016) and the sea snail *B. gouldiana* (Constance et al., 2002), as well as detecting CRY in the crayfish *Procambarus clarkia* (Fanjul-Moles et al., 2004). However, it would be most effective to design and develop species-specific *M. edulis* clock protein antibodies as has previously been done for *E. scolopes* CRY1 (Heath-Heckman et al., 2013). Clock protein isolation would allow subsequent quantification, for example by using a loading control such as Glyceraldehyde-3-phosphate dehydrogenase

(GAPDH) with Western blotting to perform relative comparisons between protein expression in different treatments, or by developing specific ELISA assays. It could then be established whether clock protein levels follow the same temporal patterns as their mRNA expression patterns, as both post-transcriptional and post-translational modifications are essential to clock function (Kojima et al., 2011; Gallego and Virshup, 2007).

Further investigation into mussel phototransduction genes would also be beneficial in widening our understanding of the molecular mechanisms of light perception in this species. A number of phototransduction genes including opsin, rhodopsin and G-proteins have been discovered in scallops and oysters (Sun et al., 2016; Pairett and Serb, 2013) which could provide interesting candidate genes for investigation in mussels. At present, studies generating transcriptome data for mussels, for example using microarrays and next generation sequencing, provide a valuable molecular genetic tool in identifying novel genes and detecting large-scale patterns in gene expression variation. For example, a recent study performing whole-genome sequencing on *M. galloprovincialis* has contributed to the available genomic resources available for mussels (Murgarella et al., 2016).

7.2.2 Function of clock components and oscillations

To determine the functional importance of *M. edulis* clock genes, the effects of clock gene disruption could be measured on other aspects of circadian regulation. Links between clock gene expression and organismal response have been revealed by RNA interference (RNAi), which suppresses the expression of specific target mRNAs allowing the knock-on effects to be investigated. For example, the effects of *Per* RNAi performed on the wasp *N. vitripennis* were measured on both a molecular level,

revealing altered expression of other clock genes, and on a whole-organism level, revealing delayed diapause (Benetta et al., 2019). Similarly, in the insect *R. pedestris*, RNAi of *Per* and *Cyc* disrupts diapause (Ikeno et al., 2011a) and *Clk* RNAi disrupts the circadian rhythm of cuticle deposition and normal photoperiodic ovarian development (Ikeno et al., 2013). *Tim*-knockdown in *S. gregaria* females has been shown to result in a detrimental effect on the number of progeny produced (Tobback et al., 2011) and *Drosophila Tim* is involved in the nocturnal upregulation of phagocytosis (Stone et al., 2012; Lee and Edery, 2008). Furthermore, both *Tim* and *Timeout*/*Tim2* knockout/disruption cause embryonic lethality in mice (Gotter et al., 2000), worms (Chan et al., 2003) and *Drosophila* (Benna et al., 2010). *Clk* function is also required to avoid potentially lethal effects in the desert locust *S. gregaria* (Tobback et al., 2011) and prevent reproductive defects in *Drosophila* (Beaver et al., 2002) and rats (Miller et al., 2004). Similarly, *HR3* expressed in the fat bodies and ovaries of the mosquito *A. aegypti* is involved in the regulation of ecdysone-triggered vitellogenin response (Kapitskaya et al., 2000), and both *HR3* and E75/*Rev-Erb* are required for vitellogenesis and oogenesis in the beetle *R. castaneum* (Xu et al., 2010).

Pertaining to bivalves, a non-invasive RNAi method which disrupted *Clk* expression in the oyster *C. gigas* has recently been shown to affect the expression of *Cry1*, *Per*, *Rev-erb* and *Bmal* (Payton et al., 2017a). Results also suggested that such disruption of the *C. gigas* clock could modify the bioaccumulation rate of the paralytic shellfish toxin saxitoxin and that this physiological output also varied with ploidy; triploid oysters (commonly used in aquaculture) were more sensitive to the interference than diploids (Payton et al., 2017a). This non-invasive RNAi approach could be applied to *M. edulis* clock genes to provide insights into gene function and whether their oscillations are essential for circadian rhythms.

M. edulis CRY1, identified herein, groups phylogenetically with insect-type CRY1 sequences based on sequence similarity (Figure 2.5). *Drosophila Cry1* acts as a blue-light photoreceptor, which facilitates the light-induced degradation of TIM (Peschel et al., 2009), whereas the mammalian form is not light sensitive and acts as a core clock component (Zhang and Kay, 2010). The light responsiveness of cryptochrome has been investigated in *Drosophila* by experimenting upon *Cry*-null mutants (Fogle et al., 2001) however, in non-model organisms, exposure experiments on wild type individuals under different light spectra have also been informative regarding *Cry* blue-light sensitivity. In the cnidarian *N. vectensis*, upregulation of two *Cry* genes has been discovered under light regimes incorporating blue-light (Reitzel et al., 2010). Alternatively, a photosensitive assay can be performed by expressing *Cry* genes in *Drosophila* Schneider 2 (S2) cells, in which degradation of CRY in response to light can be investigated (Zhu et al., 2005). These approaches could be used to establish the effects of light spectra on *M. edulis Cry1* and its protein to provide insights into their circadian functions.

Finally, binding partners of bivalve clock proteins have been hypothesised to include PER-TIM and CLK-BMAL/CYC binding (Perrigault and Tran, 2017; Sun et al., 2016), analogous to the *Drosophila* system. This may also be applicable to *M. edulis*, but is yet to be confirmed in bivalves. In *N. vectensis*, heterodimerisation between CLOCK and CYCLE has been evidenced by co-immunoprecipitation, whereas CLOCK did not bind with ARNTL (Reitzel et al., 2010). Again, this approach could be used to determine clock protein binding partners in *M. edulis* and to provide more information on post-translational aspects of circadian regulation. A more complete picture of the molecular clock system will allow subsequent exploration of how the system may be linked to other biochemical networks and

pathways.

7.2.3 Master clocks and peripheral clocks

Circadian rhythms can be sustained on the level of tissues and individual cells (Tomioka et al., 2012; Welsh et al., 2004; Plautz et al., 1997). Clock gene expression patterns are tissue-specific (Whitmore et al., 1998; Tomioka et al., 2012; Tobback et al., 2011; Kubo et al., 2010) and the synchronisation of clocks operating in different cells and tissues is necessary to coordinate large-scale rhythms in many species (Welsh et al., 2004; Reppert and Weaver, 2002). This is achieved by the "master clock" located in the mammalian SCN and in the ventro-lateral neurons of *Drosophila* (Mohawk et al., 2012; Tomioka et al., 2012), however it is unknown whether a similar central clock exists in bivalves.

Tissue types from which molluscan clock genes have been isolated include the gills (Perrigault and Tran, 2017; Connor and Gracey, 2011) eyes (Pairett and Serb, 2013; Constance et al., 2002), adductor muscle (Mat et al., 2016), and mantle tissue (Sun et al., 2016). Further studies investigating the clock mechanism in different tissues of *M. edulis* would complement the research in this thesis on the mantle tissues. It would be particularly interesting to investigate the eyes and cerebral ganglion of mussels which are perhaps the most likely candidates to house a master clock, if present. Light can both directly and indirectly entrain clocks with or without the requirement of ocular phototransduction (Tomioka et al., 2012; Whitmore et al., 2000). The role of the eyes in circadian clock rhythmicity has been investigated in marine gastropods, implicating ocular pacemakers in the circadian activity of *Aplysia* and *Bulla* (Block and Wallace, 1982), whereas extra-ocular pacemakers play a predominant role in the clockwork of the closely related *Bursatella* (Naylor, 2010).

M. edulis develop photosensitive eyespots as larvae which are retained into adulthood as cephalic eyes (Morton, 2001; Rosen, 1977). The route of photoperiod detection requires clarification, though extra-ocular detection is suspected to play a role (Northrop, 2000; Rosen, 1977).

In situ hybridisation (ISH), using labelled RNA probes, allows target mRNA expression to be localised within cells, tissues embryos and larvae, providing information about the spatial and temporal distribution of target genes. The application of ISH to *M. edulis* could therefore localise clock mRNA expression to different adult tissues and allow comparisons to be made. Furthermore, investigating *M. edulis* clock gene activity at different stages of development is likely to prove informative as the mobile, planktonic, larval stages occupy a distinct niche to the sessile, benthic adults. Mussel larvae are known to exhibit either positive or negative responses to light depending on development stage (Bayne, 1964), however any links to clock mechanism are presently unknown. Clock expression patterns have previously been shown to vary with embryo age and larval development stages in the sponge *Amphimedon queenslandica* (Jindrich et al., 2017) and the sea anemone *N. vectensis* (Peres et al., 2014). For example, after *A. queenslandica* larvae emerge from the adult, *Cry2* expression becomes more widespread and is no longer predominant only in the photosensitive cells of the pigment ring (Jindrich et al., 2017). The chronobiology of larval life stages of marine bivalves is an understudied aspect of their ecology requiring further research focus.

7.2.4 Genomics and proteomics

The circadian clock exerts influence on diverse molecular, cellular, and organismal processes via the action of multiple CCGs (Doherty and Kay, 2010; Bozek

et al., 2009; Zhang et al., 2009; Harmer et al., 2001; McDonald and Rosbash, 2001). Rhythmic organismal processes have been documented in bivalves (Table 1.1), such as circadian siphon extension (feeding proxy) in the clam *P. philippinarum* (Houki et al., 2015), circatidal stomach epithelial renewal in *M. galloprovincialis* (Zaldibar et al., 2004), and circadian and ultradian shell gape in *M. edulis* (Ameyaw-Akumfi and Naylor, 1987) and *C.gigas* (Mat et al., 2016; Mat et al., 2012), however the connections between molecular-level clock regulation and whole organism/population-level responses require further investigation. Few studies have investigated the activity of clock genes as well as organismal responses in bivalves. *Cry1* expression was found to shift to peak during the dark phase of LD cycles when *C. gigas* are nocturnal during the winter (Tran et al., 2015; Mat et al., 2012). In the same species, a number of other clock genes were isolated and characterised over LD and DD cycles in oysters in which valve activity was found to be circadian (Perrigault and Tran, 2017).

At present, genomics and proteomics resources for mussels are relatively scarce. Pertaining to chronobiology, studies using microarray technology have revealed daily (Connor and Gracey, 2011), tidal (Connor and Gracey, 2011) and seasonal transcriptomic variations (Banni et al., 2011) in *Mytilus* spp gene expression. Investigations have also revealed temperature-dependent changes in expression in *Mytilus* spp. transcriptomes in response to acute heat stress with shared, as well as species-specific, transcript responses between *M. galloprovincialis* and *M. trossulus* (Lockwood et al., 2010). Furthermore, tidal and, to a lesser extent circadian, transcripts can lose periodicity following elevated temperature at low tide (Connor and Gracey, 2011). Transcriptomic responses to another stressor, salinity, also showed instances of significant changes in *Mytilus* spp. gene expression, some of which were

species-specific (Lockwood and Somero, 2011). However, microarrays require knowledge of sequences *a priori* and can have issues with probe performance (Zhao et al., 2014). Advances in transcriptomics technology have led to the development next-generation sequencing (NGS), also known as high-throughput sequencing. NGS has recently given insights into the composition and structure of the genome of *M. galloprovincialis,* predicting over 10,000 putative genes (Murgarella et al., 2016).

The RNA-Seq approach uses NGS to detect RNA presence and quantity, allowing whole transcriptome sequencing and large-scale mRNA quantification at a higher resolution and over a greater dynamic range (Martin and Wang, 2011). Comparative transcriptomics using RNA-Seq have allowed comparison of expression profiles from different *M. galloprovincialis* tissues types (Moreira et al., 2015) and revealed tissue-specific differences in response to toxins (Prego-Faraldo et al., 2018). RNA-Seq has also recently allowed transcriptome comparisons between different species of the *Mytilus* species complex revealing candidate genes representing multiple molecular functions including mitochondrial activity, gametogenesis, reactive oxygen species (ROS) production and ATP reserves (Knöbel et al., 2020; Romero et al., 2019). Application of the RNA-Seq approach to mussel samples collected over a range of different timescales would generate a large amount of comparative sequence data, which would provide further insights into their chronobiology. Studies that investigate such transcriptome responses to zeitgeber cycles, whilst measuring organismal responses in tandem, would help to integrate the molecular clock with biological processes operating on a whole-organism scale.

The work in this thesis focused on clock mRNA expression however post-transcriptional and post-translational modifications are also an essential aspect of circadian regulation (Millius et al., 2019; Kojima et al., 2011; Gallego and Virshup,

2007). Although mRNA expression is often used as a proxy for the presence of a protein, there is not a necessarily a strict correlation between mRNA abundance and protein abundance (Payne, 2015). This is due to various complex mechanisms including the influence of micro RNAs, discrepancies in the rates of synthesis/decay, and differences in the phase and/or amplitude of their oscillations (Payne, 2015). Techniques to investigate protein abundance include nanoflow chromatography with high-resolution tandem mass spectrometry, allowing rapid and high-sensitivity quantification of proteins (Vogel and Marcotte, 2012). This approach could be used to investigate rhythmic protein abundances in mussels in the future.

7.2.5 Lunar influences

The effects of light and temperature on *M. edulis* clock genes were main focus of this thesis as the majority of the rhythmic transcriptome of the closely related *M. californianus* is predominantly circadian in nature, even in an intertidal environment (Connor and Gracey, 2011). However, intertidal zones are dynamic environments where multiple other factors can also act as environmental cues. The changing transcriptomes of *M. californianus* over a tidal cycle show at least four different physiological states, the timing and magnitude of which are affected by height on the shore and microhabitat characteristics (Gracey et al., 2008). Rhythms with tidal periodicities in bivalves include the renewal of epithelial cells in the stomach of *M. edulis* under subtidal conditions (Zaldibar et al., 2004) and circatidal value movements in subtidal *C. gigas* in situ (Tran et al., 2011) though not under laboratory conditions (Mat et al., 2012). Endogenous circatidal rhythms of locomotion have also been identified in various mobile species of gastropod (Schnytzer et al., 2018; Vanagt et al., 2008; Petpiroon and Morgan, 1983; Zann, 1973). In terms of the environmental cues

able to entrain tidal rhythms, research on marine crustaceans has revealed that zeitgebers include hydrostatic pressure, temperature, salinity and wave action/mechanical agitation (Naylor, 2010). It is possible that these factors may also act as tidal cues for bivalves such as *M. edulis* which contain a number of mechanoreceptors including a pair of statocycts for gravity detection/orientation (Bayne, 1971), various superficial mechanoreceptors (Murakami and Machemer, 1982; LaCourse and Northrop, 1978), and a pair of abdominal sense organs thought to detect water currents and water-borne vibrations (Zhadan, 2005; Haszprunar, 1985; Haszprunar, 1983). For all organisms, the molecular mechanisms of tidal clocks, and their relationship with the circadian system require further investigation (Tessmar-Raible et al., 2011). Rhythmic clock genes were only found to cycle with a circadian, rather than tidal, periodicity in the gills of *C. gigas* (Perrigault and Tran, 2017) and *M. californianus* (Connor and Gracey, 2011). *Cry1* is circadian under LD in adductor muscle tissues of *C. gigas*, though it cycles with tidal periodicity under tidal conditions in constant darkness (Mat et al., 2016). There is scope to explore whether the clockwork of *M. edulis* exhibits circatidal periodicities in different tissue types under tidal regimes.

Moonlight is also able to influence bivalve behaviour. *C. gigas* can detect moonlight and sense whether it is increasing or decreasing throughout the lunar cycle, modulating their valve opening behaviour to have a greater amplitude at third compared to first quarter moons, despite similar illumination levels (Payton and Tran, 2019). It is not yet known whether this behaviour is a direct response or under endogenous control, like the entrainment of the annelid *Platynereis dumerilii* circalunar clock by moonlight (Hauenschild, 1960), though it is clear that even low levels of nocturnal light can trigger a behavioural response. The influence of

moonlight on mussel biorhythms remains to be investigated beyond conflicting reports of lunar spawning (Korringa, 1947. It is clear that intertidal organisms are exposed to multiple environmental cycles and there is further scope to determine their relative importance to different rhythmic biological processes.

7.3 Implications of climate change

Global mean surface temperatures are predicted to increase between 0.3 °C and 0.7 °C by 2035 with sea levels rising and the oceans continuing to become warmer and more acidic (IPCC, 2014). Impacts on marine ecosystems are diverse, including changes in ocean productivity, species distributions, community structure/composition, population dynamics and disease prevalence (Zippay and Helmuth, 2012; Jones et al., 2010; Hoegh-Guldberg and Bruno, 2010; Harley et al., 2006; Helmuth et al., 2006b). Effects on *Mytilus* distribution include poleward range contractions as a result of extensive mortality at the southern limits caused by high summer temperatures (Jones et al., 2010). However, mussel beds experience thermal heterogeneity on a microhabitat level due to shading/sheltering resulting from variation in substrate orientation and angle (Zippay and Helmuth, 2012) so body temperatures occur in geographical mosaics rather than clear latitudinal gradients (Helmuth et al., 2006a). Changes on small spatial and temporal scales can therefore have large population-level effects (Westerbom et al., 2019).

Episodes of elevated temperature, where mussel body temperature increased by 7 °C, disrupted the rhythmic transcriptome of *M. californianus*, causing loss of periodicity in numerous circadian and tidally expressed transcripts lasting a number of hours after the event (Connor and Gracey, 2011). Endogenously regulated circadian rhythms are temperature compensated so the phase remains relatively stable over a

range of temperatures in plants, vertebrates and invertebrates (Sweeney and Hastings, 1960) however diurnal temperature cycles can entrain rhythms in diverse organisms including invertebrates such as insects (Glaser and Stanewsky, 2005) and arthropods (Rensing and Ruoff, 2002) and were also shown to disrupt the otherwise rhythmic cycling of clock gene *Rev-erb* in the gonads of male mussels herein (Figure 5.13). Further studies investigating temperature, particularly as a zeitgeber, are required to clarify the role of this environmental variable in the circadian regulation of marine mussels.

In terms of reproductive development, both temperature and photoperiod are important cues for marine bivalve gametogenesis (Domínguez et al., 2010; Fabioux et al., 2005; Saout et al., 1999; Paulet and Boucher., 1991). For example, gametogenesis in *C. gigas* can be advanced or delayed under different coupled photoperiod and temperature regimes (Fabioux et al., 2005). Food supply is also required for mussel reproductive success, with a greater number of gametes produced under conditions of favourable food supply (Domínguez et al., 2010; Kang et al., 2000), with different algal diets resulting in different levels of fecundity and spawning success (Pronker et al., 2008). Mussels exhibit a plastic response to environmental stress, balancing trade-offs between stress response and reproduction (Petes et al., 2008b). In *M. californianus*, accelerated mass spawning with slower regeneration was found to occur on the relatively high stress upper shore (lower food availability and higher temperatures), whereas potentially less risky "dribble spawning" was apparent under the less stressful conditions of the lower shore throughout the year (Petes et al., 2008b). Mussels that are thermally stressed or starved are not able to develop mature gametes and experience a decline in dry weight, experiencing reductions in protein and carbohydrate content (Bayne and Thompson, 1970). Elevated water temperatures and

limited food supply also affect post-spawned adult *M. edulis*, leading to decreased byssal thread attachment strength and increased mortality (Clements et al., 2018). Furthermore, sex inversion in *M. galloprovincialis* has been recorded under starvation conditions in post-spawned females, impacting upon sex ratios (Chelyadina et al., 2018). Marine invertebrates using environmental cues to synchronise reproductive development, including mussels, will be impacted by the decoupling of temperature, photoperiod and food availability as a result of climate change (Petes et al., 2008b; Lawrence and Soame, 2004). Detrimental impacts on reproductive success could include incomplete gametogenesis, spawning failure or spawning at an unfavourable time, which would impact upon larval survival and recruitment with ramifications for higher trophic levels (Lawrence and Soame, 2004). Intertidal mussels can inhabit niches close to the limits of their physiological tolerances (Múgica et al., 2015) so the disruption of biological rhythms or phase shifts in the timing of environmental cues and stressors could therefore have serious physiological consequences. Determining the interaction between temperature and other environmental stressors, whether additive, synergistic or antagonistic (Crain et al., 2008) and investigating the sensitivity, acclimatisation and local adaptation of mussels is needed to predict the direct and indirect effects of climate change on this genus (Zippay and Helmuth, 2012).

7.4 General conclusion

Despite the wide-reaching importance of rhythmic biological processes, the molecular mechanisms regulating timekeeping ability of marine bivalves are little understood. Bivalve chronobiology is an emerging area of research. This thesis outlines the first investigation into the molecular clock mechanism of the

commercially and ecologically important blue mussel *M. edulis*. Novel insights into the chronobiology of the species were revealed by isolating and characterising clock genes, revealing the endogenous nature of their oscillations, and demonstrating the ability of temperature cycles to modulate clock and clock-associated gene expression. Investigations also uncovered sex and seasonal differences in clock gene expression patterns and revealed other putative seasonal genes meriting further investigation. Key areas for future research include further characterisation of the components and function of the mussel molecular clock mechanism, ascertaining the importance of clock function at different stages of larval and sexual development, and exploring the importance of and interaction between different zeitgebers in the context of dynamic intertidal environments influenced by environmental change. A greater depth of understanding in bivalve chronobiology is not only relevant from an ecological perspective, but also to aquacultural broodstock conditioning, environmental biomonitoring, and investigations into the impacts of environmental change. Rhythmic biological processes are at risk of disruption if environmental cues become desynchronised, leading to potentially serious physiological and ecological implications.

References

Abran, D., Anctil, M., and Ali, M. A., 1994. Melatonin activity rhythms in eyes and cerebral ganglia of *Aplysia californica*. *General and Comparative Endocrinology, 96*(2), 215-222.

Allada, R. and Chung, B.Y., 2010. Circadian organisation of behavior and physiology in *Drosophila*. *Annual Review of Physiology 17*(72), 605-624.

Allada, R., Emery, P., Takahashi, J.S. and Rosbash, M., 2001. Stopping time: the genetics of fly and mouse circadian clocks. *Annual Review of Neuroscience 24*(1), 1091-1119.

Allada, R., White, N.E., So, W.V., Hall, J.C. and Rosbash, M., 1998. A mutant *Drosophila* homolog of mammalian *clock* disrupts circadian rhythms and transcription of *period* and *timeless*. *Cell 93*(5), 791-804.

Alvarez, J.D., Chen, D., Storer, E. and Sehgal, A., 2003. Non-cyclic and developmental stage-specific expression of circadian clock proteins during murine spermatogenesis. *Biology of Reproduction, 69*(1), 81-91.

Alvarez, J., Hansen, A., Ord, T., Bebas, P., Chappell, P.E., Giebultowicz, J.M., Williams, C., Moss, S. and Sehgal, A., 2008. The circadian clock protein BMAL1 is necessary for fertility and proper testosterone production in mice. *Journal of Biological Rhythms, 23*(1), 26-36.

Amano, T., Matsushita, A., Hatanaka, Y., Watanabe, T., Oishi, K., Ishida, N., Anzai, M., Mitani, T., Kato, H., Kishigami, S. and Saeki, K., 2009. Expression and functional analyses of circadian genes in mouse oocytes and preimplantation embryos: Cry1 is involved in the meiotic process independently of circadian clock regulation. *Biology of Reproduction*, *80*(3), 473-483.

Ameyaw-Akumfi, C. and Naylor, E., 1987. Temporal patterns of shell-gape in *Mytilus edulis*. *Marine Biology*, *95*(2), 237-242.

Andreazzoli, M. and Angeloni, D., 2017. The Amphibian Clock System. In *Biological Timekeeping: Clocks, Rhythms and Behaviour* (pp. 211-222). Springer, New Delhi.

Andreou, A.Z. and Klostermeier, D., 2013. The DEAD-box helicase eIF4A: paradigm or the odd one out? *RNA Biology*, *10*(1), 19-32.

André, E., Gawlas, K., Steinmayr, M. and Becker-André, M., 1998. A novel isoform of the orphan nuclear receptor RORβ is specifically expressed in pineal gland and retina. *Gene*, *216*(2), 277-283.

Ansart, A., Vernon, P. and Daguzan, J., 2001. Photoperiod is the main cue that triggers supercooling ability in the land snail, *Helix aspersa* (Gastropoda: Helicidae). *Cryobiology*, *42*(4), 266-273.

Aschoff, J., 1960, January. *Exogenous and endogenous components in circadian rhythms*. In Cold Spring Harbor symposia on quantitative biology (Vol. 25, 11-28). Cold Spring Harbor Laboratory Press.

Aschoff, J., 1981. A survey on biological rhythms. In *Biological Rhythms*. Springer, Boston, MA, 3-10.

Bachleitner, W., Kempinger, L., Wülbeck, C., Rieger, D. and Helfrich-Förster, C., 2007. Moonlight shifts the endogenous clock of *Drosophila melanogaster*. *Proceedings of the National Academy of Sciences USA*, *104*(9), 3538-3543.

Badariotti, F., Thuau, R., Lelong, C., Dubos, M.P. and Favrel, P., 2007. Characterization of an atypical family 18 chitinase from the oyster *Crassostrea gigas*: evidence for a role in early development and immunity. *Developmental & Comparative Immunology*, *31*(6), 559-570.

Bailey, M. and Silver, R., 2014. Sex differences in circadian timing systems: implications for disease. *Frontiers in Neuroendocrinology*, *35*(1), 111-139.

Baldi, P. and Hatfield, G.W., 2011. *DNA microarrays and gene expression: from experiments to data analysis and modeling*. Cambridge university press.

Banni, M., Negri, A., Mignone, F., Boussetta, H., Viarengo, A. and Dondero, F., 2011. Gene expression rhythms in the mussel *Mytilus galloprovincialis* (Lam.) across an annual cycle. *PLOS One*, *6*(5), e18904.

Bao, Y., Xu, F. and Shimeld, S.M., 2017. Phylogenetics of lophotrochozoan bHLH genes and the evolution of lineage-specific gene duplicates. *Genome Biology and Evolution*, *9*(4), 869-886.

Barcia, R., Lopez-García, J.M., and Ramos-Martínez, J.I., 1997. The 28S fraction of rRNA in molluscs displays electrophoretic behaviour different from that of mammal cells. *IUBMB Life*, *42*(6), 1089-1092.

Barnes, J.W., Tischkau, S.A., Barnes, J.A., Mitchell, J.W., Burgoon, P.W., Hickok, J. R., and Gillette, M.U., 2003. Requirement of mammalian *Timeless* for circadian rhythmicity. *Science*, *302*(5644), 439-442.

Bayne, B.L., 1964a. Primary and secondary settlement in *Mytilus edulis* L. (Mollusca). *Journal of Animal Ecology 33*(3), 513-523.

Bayne, B.L., 1964b. The responses of the larvae of *Mytilus edulis* L. to light and to gravity. *Oikos*, *15*, 162-174.

Bayne, B.L., 1971. Some morphological changes that occur at the metamorphosis of the larvae of *Mytilus edulis*. In *The Fourth European Marine Biology Symposium* (259-280). Cambridge University Press.

Bayne, B.L. ed. 1976. *Marine mussels: their ecology and physiology* (Vol. 10).

Cambridge University Press.

Bayne, B.L., Holland, D.L., Moore, M.N., Lowe, D.M. and Widdows, J., 1978. Further studies on the effects of stress in the adult on the eggs of *Mytilus edulis*. *Journal of the Marine Biological Association of the United Kingdom*, *58*(4), 825-841.

Bayne, B.L. and Thompson, R.J., 1970. Some physiological consequences of keeping *Mytilus edulis* in the laboratory. *Helgoländer Wissenschaftliche Meeresuntersuchungen*, *20*(1), 526.

Beaver, L.M., Gvakharia, B.O., Vollintine, T.S., Hege, D.M., Stanewsky, R. and Giebultowicz, J.M., 2002. Loss of circadian clock function decreases reproductive fitness in males of *Drosophila melanogaster*. *Proceedings of the National Academy of Sciences*, USA, *99*(4), 2134-2139.

Beaver, L.M., Hooven, L.A., Butcher, S.M., Krishnan, N., Sherman, K.A., Chow, E.S.Y. and Giebultowicz, J.M., 2010. Circadian clock regulates response to pesticides in *Drosophila* via conserved Pdp1 pathway. *Toxicological Sciences, 115*(2), 513-520.

Beaver, L.M., Rush, B.L., Gvakharia, B.O. and Giebultowicz, J.M., 2003. Noncircadian regulation and function of clock genes *period* and *timeless* in oogenesis of *Drosophila melanogaster*. *Journal of Biological Rhythms*, *18*(6), 463-472.

Bebas, P., Cymborowski, B. and Giebultowicz, J.M., 2001. Circadian rhythm of sperm release in males of the cotton leafworm, *Spodoptera littoralis*: in vivo and in vitro studies. *Journal of Insect Physiology*, *47*(8), 859-866.

Beck, S.D. ed., 2012. *Insect photoperiodism*. Elsevier.

Beersma, D.G.M. and Gordijn, M.C.M., 2007. Circadian control of the sleep-wake cycle. *Physiology and Behavior, 90*, 190-195.

Benetta, E.D., Beukeboom, L.W. and Zande, L.V.D., 2019. Adaptive differences in circadian clock gene expression patterns and photoperiodic diapause induction in *Nasonia vitripennis*. *The American Naturalist*, *193*(6), 881-896.

Beninger, P.G., Donval, A. and Le Pennec, M., 1995. The osphradium in *Placopecten magellanicus* and *Pecten maximus* (Bivalvia, Pectinidae): histology, ultrastructure, and implications for spawning synchronisation. *Marine Biology*, *123*(1), 121-129.

Benitez-King, G. and Anton-Tay, F., 1993. Calmodulin mediates melatonin cytoskeletal effects. *Experientia*, *49*(8), 635-641.

Benito, J., Hoxha, V., Lama, C., Lazareva, A. A., Ferveur, J. F., Hardin, P. E., and Dauwalder, B., 2010. The circadian output gene takeout is regulated by *Pdp1ε*. *Proceedings of the National Academy of Sciences USA*, *107*(6), 2544-2549.

Benna, C., Bonaccorsi, S., Wülbeck, C., Helfrich-Förster, C., Gatti, M., Kyriacou, C.P., Costa, R. and Sandrelli, F., 2010. *Drosophila timeless2* is required for chromosome stability and circadian photoreception. *Current Biology*, *20*(4), 346-352.

Bentley, G.E., 2010. Photoperiodism and reproduction in birds. In: RJ Nelson, DL Denlinger, DE Somers, eds 2010. *Photoperiodism: The Biological Calendar*; Oxford University Press: Oxford, UK, 420-445.

Bernatowicz, P.P., Kotwica-Rolinska, J., Joachimiak, E., Sikora, A., Polanska, M.A., Pijanowska, J. and Bębas, P., 2016. Temporal expression of the clock genes in the water flea *Daphnia pulex* (Crustacea: Cladocera). *Journal of Experimental Zoology Part A: Ecological Genetics and Physiology*, *325*(4), 233-254.

Bertolucci, C., Frigato, E. and Foà, A., 2017. The reptilian clock system: Circadian clock, extraretinal photoreception, and clock-dependent celestial compass orientation mechanisms in reptiles. In *Biological Timekeeping: Clocks, Rhythms and Behaviour*. Springer, New Delhi, 223-239.

Bignell, J.P., Dodge, M.J., Feist, S.W., Lyons, B., Martin, P.D., Taylor, N.G.H., Stone, D., Travalent, L. and Stentiford, G.D., 2008. Mussel histopathology: effects of season, disease and species. *Aquatic Biology*, *2*(1), 1-15.

Bio-Rad Laboratories, Inc. 2006. Real-Time PCR Applications Guide.

Blalock, B.J., Robinson, W.E., Loguinov, A., Vulpe, C.D., Krick, K.S. and Poynton, H.C., 2018. Transcriptomic and Network Analyses Reveal Mechanistic-Based Biomarkers of Endocrine Disruption in the Marine Mussel, *Mytilus edulis*. *Environmental Science & Technology*, *52*(16), 9419-9430.

Blanc, A., Vivien-Roels, B., Pévet, P., Attia, J. and Buisson, B., 2003. Melatonin and 5-methoxytryptophol (5-ML) in nervous and/or neurosensory structures of a gastropod mollusc (*Helix aspersa maxima*): synthesis and diurnal rhythms. *General and Comparative Endocrinology 131*(2), 168-175.

Block, G.D. and Wallace, S.F., 1982. Localization of a circadian pacemaker in the eye of a mollusc, *Bulla*. *Science*, *217*(4555), 155-157.

Block, G.D., Khalsa, S.B.S., McMahon, D.G., Michel, S. and Guesz, M., 1993. Biological clocks in the retina: cellular mechanisms of biological timekeeping. In *International Review of Cytology* (Vol. 146, 83-144). Academic Press.

Boettcher, K.J., Ruby, E.G. and McFall-Ngai, M.J., 1996. Bioluminescence in the symbiotic squid *Euprymna scolopes* is controlled by a daily biological rhythm. *Journal of Comparative Physiology A*, *179*(1), 65-73.

Bohlken, S. and Joosse, J., 1981. The effect of photoperiod on female reproductive activity and growth of the freshwater pulmonate snail *Lymnaea stagnalis* kept under laboratory breeding conditions. *International Journal of Invertebrate Reproduction*, *4*(4), 213-222.

Borg, B., 2010. Photoperiodism in fishes. In: RJ Nelson, DL Denlinger, DE Somers, eds. *Photoperiodism: The Biological Calendar*, Oxford University Press: Oxford, UK, 371-398.

Boutet, I., Moraga, D., Marinovic, L., Obreque, J. and Chavez-Crooker, P., 2008. Characterization of reproduction-specific genes in a marine bivalve mollusc: influence of maturation stage and sex on mRNA expression. *Gene*, *407*(1-2), 130-138.

Bozek, K., Relógio, A., Kielbasa, S.M., Heine, M., Dame, C., Kramer, A. and Herzel, H., 2009. Regulation of clock-controlled genes in mammals. *PloS one*, *4*(3), e4882.

Bradshaw, W.E. and Holzapfel, C.M., 2007. Evolution of animal photoperiodism. *Annual Review of Ecology, Evolution and Systematics*, *38*, 1-25.

Bradshaw, W.E. and Holzapfel, C.M., 2010. What season is it anyway? Circadian tracking vs. photoperiodic anticipation in insects. *Journal of Biological Rhythms*, *25*(3), 155-165.

Brady, A.K., Snyder, K.A. and Vize, P.D., 2011. Circadian cycles of gene expression in the coral, *Acropora millepora*. *PloS one*, *6*(9).

Brake, J., Davidson, J. and Davis, J., 2004. Field observations on growth, gametogenesis, and sex ratio of triploid and diploid *Mytilus edulis*. *Aquaculture*, *236*(1-4), 179-191.

Breese, W.P., Millemann, R.E. and Dimick, R.E., 1963. Stimulation of spawning in the mussels, *Mytilus edulis* Linnaeus and *Mytilus californianus* Conrad, by Kraft mill effluent. *The Biological Bulletin*, *125*(2), 197-205.

Broitman, B.R., Blanchette, C.A., Menge, B.A., Lubchenco, J., Krenz, C., Foley, M., Raimondi, P.T., Lohse, D. and Gaines, S.D., 2008. Spatial and temporal patterns of invertebrate recruitment along the west coast of the United States. *Ecological Monographs*, *78*(3), 403-421.

Brunnberg, S., Pettersson, K., Rydin, E., Matthews, J., Hanberg, A. and Pongratz, I., 2003. The basic helix–loop–helix–PAS protein ARNT functions as a potent coactivator of estrogen receptor-dependent transcription. *Proceedings of the National Academy of Sciences, USA 100*(11), 6517-6522.

Bur, I.M., Cohen-Solal, A.M., Carmignac, D., Abecassis, P.Y., Chauvet, N., Martin, A.O., Van Der Horst, G.T., Robinson, I.C., Maurel, P., Mollard, P. and Bonnefont, X., 2009. The circadian clock components CRY1 and CRY2 are necessary to sustain sex dimorphism in mouse liver metabolism. *Journal of Biological Chemistry*, *284*(14), 9066-9073.

Bustin, S. A., Benes, V., Garson, J. A., Hellemans, J., Huggett, J., Kubista, M., Mueller, R., Nolan, T., Pfaffl, M.W., Shipley, G.L., Vandesompele, J. and Wittwer, C. T., 2009. The MIQE guidelines: minimum information for publication of quantitative real-time PCR experiments. *Clinical Chemistry*, *55*(4), 611-622.

Butler, R. A., Kelley, M. L., Olberding, K. E., Gardner, G. R. and Van Beneden, R. J., 2004. Aryl hydrocarbon receptor (AhR)-independent effects of 2, 3, 7, 8-tetrachlorodibenzo-p-dioxin (TCDD) on softshell clam (*Mya arenaria*) reproductive

tissue. *Comparative Biochemistry and Physiology Part C, Toxicology & Pharmacology*, *138*(3), 375-381.

Cai, X., Huang, Y., Zhang, X., Wang, S., Zou, Z., Wang, G., Wang, Y. and Zhang, Z., 2014. Cloning, characterization, hypoxia and heat shock response of hypoxia inducible factor-1 (HIF-1) from the small abalone *Haliotis diversicolor*. *Gene*, *534*(2), 256-264.

Carney, G.E., Wade, A.A., Sapra, R., Goldstein, E.S. and Bender, M., 1997. *DHR3*, an ecdysone-inducible early-late gene encoding a *Drosophila* nuclear receptor, is required for embryogenesis. *Proceedings of the National Academy of Sciences USA*, 94, 12024-12029.

Cashmore, A.R., Jarillo, J.A., Wu, Y.J. and Liu, D., 1999. Cryptochromes: blue light receptors for plants and animals. *Science*, *284*(5415), 760-765.

Cassone, V.M., 2014. Avian circadian organization: a chorus of clocks. *Frontiers in Neuroendocrinology*, *35*(1), 76-88.

Cazaméa-Catalan, D., Besseau, L., Falcón, J. and Magnanou, E., 2014. The Timing of timezyme diversification in vertebrates. *PloS One*, *9*(12), e112380.

Cermakian, N. and Sassone-Corsi, P., 2000. Multilevel regulation of the circadian clock. *Nature Reviews Molecular Cell Biology*, *1*, 59-67.

Chan, R.C., Chan, A., Jeon, M., Wu, T.F., Pasqualone, D., Rougvie, A.E., and Meyer, B.J., 2003. Chromosome cohesion is regulated by a clock gene paralogue TIM-1. *Nature*, *423*(6943), 1002-1009.

Chapple, J.P., Smerdon, G.R., Berry, R.J. and Hawkins, A.J., 1998. Seasonal changes in stress-70 protein levels reflect thermal tolerance in the marine bivalve *Mytilus edulis* L. *Journal of Experimental Marine Biology and Ecology*, *229*(1), 53-68.

Chávez-Villalba, J., Barret, J., Mingant, C., Cochard, J.C. and Le Pennec, M., 2002. Autumn conditioning of the oyster *Crassostrea gigas*: a new approach. *Aquaculture*, *210*(1-4), 171-186.

Chelyadina, N., Pospelova, N., Popov, M., Smyrnova, L., Kharchuk, I. and Ryabushko, V., 2018. Sex inversion in cultivated mussels *Mytilus galloprovincialis* Lam. (Crimea, Black Sea) under influence of external environmental factors. *Ecologica Montenegrina*, *19*, 26-31.

Chipperfield, P.N., 1953. Observations on the breeding and settlement of *Mytilus edulis* (L.) in British waters. *Journal of the Marine Biological Association of the United Kingdom*, *32*(02), 449-476.

Ciocan, C.M., Cubero-Leon, E., Minier, C. and Rotchell, J.M., 2011. Identification of reproduction-specific genes associated with maturation and estrogen exposure in a marine bivalve *Mytilus edulis*. *PLoS One 6*(7), e22326.

Ciocan, C.M., Cubero-Leon, E., Peck, M.R., Langston, W.J., Pope, N., Minier, C. and Rotchell, J.M., 2012. Intersex in *Scrobicularia plana*: transcriptomic analysis reveals novel genes involved in endocrine disruption. *Environmental Science & Technology*, *46*(23), 12936-12942.

Ciocan, C. M., Cubero-Leon, E., Puinean, A. M., Hill, E. M., Minier, C., Osada, M., Fenlon, K. and Rotchell, J. M., 2010. Effects of estrogen exposure in mussels, *Mytilus edulis*, at different stages of gametogenesis. *Environmental Pollution*, *158*(9), 2977-2984.

Clements, J.C., Hicks, C., Tremblay, R. and Comeau, L.A., 2018. Elevated seawater temperature, not p CO2, negatively affects post-spawning adult mussels (*Mytilus edulis*) under food limitation. *Conservation Physiology*, *6*(1), cox078.

Cobb, C.S., Pope, S.K. and Williamson, R., 1995. Circadian rhythms to light-dark cycles in the lesser octopus, *Eledone clrrhosa*. *Marine & Freshwater Behaviour & Physiology 26*(1), 47-57.

Cohen, S.E. and Golden, S.S., 2015. Circadian rhythms in cyanobacteria. *Microbiology and Molecular Biology Reviews*, *79*(4), 373-385.

Connor, K.M. and Gracey, A.Y., 2011. Circadian cycles are the dominant transcriptional rhythm in the intertidal mussel *Mytilus californianus*. *Proceedings of the National Academy of Sciences USA, 108*(38), 16110-16115.

Constance, C. M., Green, C. B., Tei, H. and Block, G. D., 2002. *Bulla gouldiana* period exhibits unique regulation at the mRNA and protein levels. *Journal of Biological Rhythms*, *17*(5), 413-427.

Cook, G.M., Gruen, A.E., Morris, J., Pankey, M.S., Senatore, A., Katz, P.S., Watson III, W.H. and Newcomb, J.M., 2018. Sequences of circadian clock proteins in the nudibranch molluscs *Hermissenda crassicornis*, *Melibe leonina*, and *Tritonia diomedea*. *The Biological Bulletin*, *234*(3), 207-218.

Costa, R., Peixoto, A.A., Barbujani, G. and Kyriacou, C.P., 1992. A latitudinal cline in a Drosophila clock gene. *Proceedings of the Royal Society of London. Series B: Biological Sciences*, *250*(1327), 43-49.

Couper, J. M. and Leise, E. M., 1996. Serotonin injections induce metamorphosis in larvae of the gastropod mollusc *Ilyanassa obsoleta*. *The Biological Bulletin*, *191*(2), 178-186.

Craft, J.A., Gilbert, J.A., Temperton, B., Dempsey, K.E., Ashelford, K., Tiwari, B., Hutchinson, T.H. and Chipman, J.K., 2010. Pyrosequencing of *Mytilus galloprovincialis* cDNAs: tissue-specific expression patterns. *PLoS One*, *5*(1), e8875.

Cragg, S.M. and Nott, J.A., 1977. The ultrastructure of the statocysts in the pediveliger larvae of *Pecten maximus* (L.) (Bivalvia). *Journal of Experimental Marine Biology and Ecology*, *27*(1), 23-36.

Crain, C.M., Kroeker, K. and Halpern, B.S., 2008. Interactive and cumulative effects of multiple human stressors in marine systems. *Ecology Letters*, *11*(12), 1304-1315.

Cranford, P.J. and Hill, P.S., 1999. Seasonal variation in food utilization by the suspension-feeding bivalve molluscs *Mytilus edulis* and *Placopecten magellanicus*. *Marine Ecology Progress Series*, *190*, 223-239.

Croll, R.P. and Wang, C., 2007. Possible roles of sex steroids in the control of reproduction in bivalve molluscs. *Aquaculture*, *272*(1-4), 76-86.

Cruz, J., Mane-Padros, D., Zou, Z. and Raikhel, A.S., 2012. Distinct roles of isoforms of the heme-liganded nuclear receptor E75, an insect ortholog of the vertebrate Rev-erb, in mosquito reproduction. *Molecular and Cellular Endocrinology*, *349*(2), 262-271.

Cubero-Leon, E., Ciocan, C. M., Minier, C. and Rotchell, J. M., 2012. Reference gene selection for qPCR in mussel, *Mytilus edulis*, during gametogenesis and exogenous estrogen exposure. *Environmental Science and Pollution Research*, *19*(7), 2728-2733.

Danks, H.V., 2005. How similar are daily and seasonal biological clocks? *Journal of Insect Physiology, 51,* 609-619.

Dardente, H., Wyse, C.A., Birnie, M.J., Dupré, S.M., Loudon, A.S., Lincoln, G.A. and Hazlerigg, D.G., 2010. A molecular switch for photoperiod responsiveness in mammals. *Current Biology*, *20*(24), 2193-2198.

Darlington, T.K., Wager-Smith, K., Ceriani, M.F., Staknis, D., Gekakis, N., Steeves, T.D., Weitz, C.J., Takahashi, J.S. and Kay, S.A., 1998. Closing the circadian loop: CLOCK-induced transcription of its own inhibitors per and tim. *Science*, *280*(5369), 1599-1603.

Davie, A., Minghetti, M. and Migaud, H., 2009. Seasonal variations in clock-gene expression in Atlantic salmon (*Salmo salar*). *Chronobiology International*, *26*(3), 379-395.

Dawson, A., King, V.M., Bentley, G.E. and Ball, G.F., 2001. Photoperiodic control of seasonality in birds. *Journal of Biological Rhythms*, *16*(4), 365-380.

Dawson, A. and Sharp, P.J., 2007. Photorefractoriness in birds—photoperiodic and non-photoperiodic control. *General and Comparative Endocrinology*, *153*(1-3), 378-384.

de Cerio, O.D., Hands, E., Humble, J., Cajaraville, M.P., Craft, J.A. and Cancio, I., 2013. Construction and characterization of a forward subtracted library of blue mussels *Mytilus edulis* for the identification of gene transcription signatures and biomarkers of styrene exposure. *Marine Pollution Bulletin*, *71*(1-2), 230-239.

De Grassi, A., Lanave, C. and Saccone, C., 2006. Evolution of ATP synthase subunit c and cytochrome c gene families in selected Metazoan classes. *Gene*, *371*(2), 224-233.

De Lange, R. P. J., Joosse, J. and Van Minnen, J., 1998. Multi-messenger innervation of the male sexual system of *Lymnaea stagnalis*. *Journal of Comparative Neurology*, *390*(4), 564-577.

de Sousa, J.T., Milan, M., Bargelloni, L., Pauletto, M., Matias, D., Joaquim, S., Matias, A.M., Quillien, V., Leitão, A. and Huvet, A., 2014. A microarray-based analysis of gametogenesis in two Portuguese populations of the European clam *Ruditapes decussatus*. *PLoS One*, *9*(3), e92202.

de Zwann, A. and Mathieu, M., 1992. Cellular biochemistry and endocrinology. In: *The Mussel Mytilus: Ecology, Physiology, Genetics and Culture* (ed E. M. Gosling), 223-307. Elsevier science Publishers B. V., Amsterdam.

DeCoursey, P.J., 2004. The behavioral ecology and evolution of biological timing systems. In: J.C. Dunlap, J.J. Loros, & P.J. DeCoursey (Eds.), *Chronobiology: Biological timekeeping*. Sinauer Associates, 27-65.

DeCoursey, P.J., Walker, J.K. and Smith, S.A., 2000. A circadian pacemaker in free-living chipmunks: essential for survival? J*ournal of Comparative Physiology A*, *186*(2), 169-180.

Denlinger, D.L., 1986. Dormancy in tropical insects. *Annual Review of Entomology*, *31*(1), 239-264.

Denlinger, D.L., 2009. Overview. In: Nelson, R.J., Denlinger, D.L., and Somers, D.E. 2009. *Photoperiodism: The Biological Calendar*. Oxford University Press, 165-172

Denlinger, D.L., Hahn, D.A., Merlin, C., Holzapfel, C.M. and Bradshaw, W.E., 2017. Keeping time without a spine: what can the insect clock teach us about seasonal adaptation? *Philosophical Transactions of the Royal Society B: Biological Sciences*, *372*(1734), 20160257.

Dheilly, N.M., Lelong, C., Huvet, A., Kellner, K., Dubos, M.P., Riviere, G., Boudry, P. and Favrel, P., 2012. Gametogenesis in the Pacific oyster *Crassostrea gigas*: a microarrays-based analysis identifies sex and stage specific genes. *PloS One*, *7*(5), e36353.

DiBacco, C., 1994. Reproductive cycle of the giant sea scallop, Placopecten magellanicus (Gmelin), on northeastern Georges Bank, 1597.

Dixit, A.S. and Singh, N.S., 2011. Photoperiod as a proximate factor in control of seasonality in the subtropical male Tree Sparrow, *Passer montanus*. *Frontiers in Zoology*, 8(1), doi:10.1186/1742-9994-8-1

Dodd, A.N., Kusakina, J., Hall, A., Gould, P.D. and Hanaoka, M., 2014. The circadian regulation of photosynthesis. *Photosynthesis Research*, *119*(1-2), 181-190.

Dodd, A.N., Salathia, N., Hall, A., Kévei, E., Tóth, R., Nagy, F., Hibberd, J.M., Millar, A.J. and Webb, A.A., 2005. Plant circadian clocks increase photosynthesis, growth,

survival, and competitive advantage. *Science*, *309*(5734), 630-633.

Doherty, C.J. and Kay, S.A., 2010. Circadian control of global gene expression patterns. *Annual Review of Genetics*, *44*, 419-444.

Dolby, D., 2014. *Filey Bay Tide Times*, viewed December 2014, <https://www.tidetimes.org.uk/filey-bay-tide-times>.

Dolezel, D., 2015. Photoperiodic time measurement in insects. *Current Opinion in Insect Science*, *7*, 98-103.

Domínguez, L., Villalba, A. and Fuentes, J., 2010. Effects of photoperiod and the duration of conditioning of gametogenesis and spawning of the mussel *Mytilus galloprovincialis* (Lamarck). *Aquaculture Research, 41*, e807-e818 doi: 10.1111/j.1365-2109.2010.02601.x

Duback, V.E., Pankey, M.S., Thomas, R.I., Huyck, T.L., Mbarani, I.M., Bernier, K.R., Cook, G.M., O'Dowd, C.A., Newcomb, J.M. and Watson III, W.H., 2018. Localization and expression of putative circadian clock transcripts in the brain of the nudibranch *Melibe leonina*. *Comparative Biochemistry and Physiology Part A: Molecular & Integrative Physiology*, *223*, 52-59.

Dubruille, R. and Emery, P., 2008. A plastic clock: how circadian rhythms respond to environmental cues in *Drosophila*. *Molecular Neurobiology, 38*, 129-145.

Duchemin, M.B., Fournier, M. and Auffret, M., 2007. Seasonal variations of immune parameters in diploid and triploid Pacific oysters, *Crassostrea gigas* (Thunberg). *Aquaculture*, *264*(1-4), 73-81.

Dudley, T.E., DiNardo, L.A. and Glass, J.D., 1998. Endogenous regulation of serotonin release in the hamster suprachiasmatic nucleus. *Journal of Neuroscience*, *18*(13), 5045-5052.

Duinker, A., Håland, L., Hovgaard, P. and Mortensen, S., 2008. Gonad development and spawning in one and two year old mussels (*Mytilus edulis*) from Western Norway. *Journal of the Marine Biological Association of the United Kingdom*, *88*(7), 1465-1473.

Duinker, A., Saout, C. and Paulet, Y. M., 2000. Effect of photoperiod on conditioning of the great scallop. *Aquaculture International*, *7*(6), 449-457.

Dunlap, J.C., 1999. Molecular bases for circadian clocks. *Cell*, *96*(2), 271-290.

Dunlap, J.C. and Loros, J.J., 2006. How fungi keep time: circadian system in Neurospora and other fungi. *Current Opinion in Microbiology*, *9*(6), 579-587.

Dunlap, J.C., Loros, J.J. and DeCoursey, P.J., 2004. *Chronobiology: biological timekeeping*. Sinauer Associates.

Eelderink-Chen, Z., Mazzotta, G., Sturre, M., Bosman, J., Roenneberg, T. and

Merrow, M., 2010. A circadian clock in *Saccharomyces cerevisiae*. *Proceedings of the National Academy of Sciences USA, 107*(5), 2043-2047.

Egg, M., Köblitz, L., Hirayama, J., Schwerte, T., Folterbauer, C., Kurz, A., Fiechtner, B., Möst, M., Salvenmoser, W., Sassone-Corsi, P. and Pelster, B., 2013. Linking oxygen to time: the bidirectional interaction between the hypoxic signaling pathway and the circadian clock. *Chronobiology International*, *30*(4), 510-529.

Ellers, O., 1995. Discrimination among wave-generated sounds by a swash-riding clam. *The Biological Bulletin*, *189*(2), 128-137.

Engelen, E., Janssens, R. C., Yagita, K., Smits, V. A., van der Horst, G. T. and Tamanini, F., 2013. Mammalian TIMELESS is involved in period determination and DNA damage-dependent phase advancing of the circadian clock. *PloS One*, *8*(2), e56623.

Ennos, A.R., 2007. *Statistical and data handling skills in biology*. Pearson Education.

Errico, A. and Costanzo, V., 2010. Differences in the DNA replication of unicellular eukaryotes and metazoans: known unknowns. *EMBO Reports*, *11*(4), 270-278.

Ertl, N.G., O'Connor, W.A., Wiegand, A.N. and Elizur, A., 2016. Molecular analysis of the Sydney rock oyster (*Saccostrea glomerata*) CO_2 stress response. *Climate Change Responses*, *3*(1), 6.

Escamilla-Chimal, E.G., Velázquez-Amado, R.M., Fiordelisio, T. and Fanjul-Moles, M.L., 2010. Putative pacemakers of crayfish show clock proteins interlocked with circadian oscillations. *Journal of Experimental Biology*, *213*(21), 3723-3733.

Fabioux, C., Huvet, A., Le Souchu, P., Le Pennec, M. and Pouvreau, S., 2005. Temperature and photoperiod drive *Crassostrea gigas* reproductive internal clock. *Aquaculture*, *250*(1-2), 458-470.

Falcón, J., Coon, S.L., Besseau, L., Cazaméa-Catalan, D., Fuentès, M., Magnanou, E., Paulin, C., Boeuf, G., Sauzet, S., Jørgensen, E.H., Mazan, S., Wolf, Y.I., Koonin, E.V., Steinbach, P.J., Hyodo, S. and Klein, D.C., 2014. Drastic neofunctionalization associated with evolution of the timezyme AANAT 500 Mya. *Proceedings of the National Academy of Sciences USA*, *111*(1), 314-319.

Fanjul-Moles, M.L., Escamilla-Chimal, E.G., Gloria-Soria, A. and Hernández-Herrera, G., 2004. The crayfish *Procambarus clarkii* CRY shows daily and circadian variation. *Journal of Experimental Biology*, *207*(9), 1453-1460.

Farcy, É., Voiseux, C., Lebel, J.M. and Fiévet, B., 2009. Transcriptional expression levels of cell stress marker genes in the Pacific oyster *Crassostrea gigas* exposed to acute thermal stress. *Cell Stress and Chaperones*, *14*(4), 371-380.

Farner, D.S., 1961. Comparative physiology: photoperiodicity. *Annual Review of Physiology*, *23*(1), 71-96.

Farrell, R.E., 2010. Non-Array Methods for Global Analysis of Gene Expression. In: Farrell, R.E. ed. 2010. *RNA Methodologies, A Laboratory Guide for Isolation and Characterization*, 4th edition, 515-538.

Morton, B., 2001. The evolution of eyes in the Bivalvia. In: Gibson, R.N., Barnes, M. and Atkinson, R.J.A. eds. 2001. *Oceanography and Marine Biology, An Annual Review*, Volume 39: An Annual Review, *39*, 165-205.

Farrington, J.W., Tripp, B.W., Tanabe, S., Subramanian, A., Sericano, J.L., Wade, T.L. and Knap, A.H., 2016. Edward D. Goldberg's proposal of "the mussel watch": reflections after 40 years. *Marine Pollution Bulletin*, *110*(1), 501-510.

Fearman, J. and Moltschaniwskyj, N.A., 2010. Warmer temperatures reduce rates of gametogenesis in temperate mussels, *Mytilus galloprovincialis*. *Aquaculture*, *305*(1-4), 20-25.

Fenske, M.P. and Imaizumi, T., 2016. Circadian rhythms in floral scent emission. *Frontiers in Plant Science*, 7, 462.

Field, I.A., 1922. *Biology and Economic Value of the Sea Mussel Mytilus Edulis* (No. 922). US Government Printing Office.

Fogle, K.J., Parson, K.G., Dahm, N.A. and Holmes, T.C., 2011. Cryptochrome is a blue-light sensor that regulates neuronal firing rate. *Science*, *331*(6023), 1409-1413.

Fong, P.P. and Pearse, J.S., 1992. Evidence for a programmed circannual life cycle modulated by increasing daylengths in *Neanthes limnicola* (Polychaeta: Nereidae) from central California. *The Biological Bulletin*, *182*(3), 289-297.

Food and Agriculture Organization of the United Nations (FAO)., 2018. Global aquaculture production online query. http://www.fao.org/fishery/statistics/global-aquaculture-production/query/en

Food and Agriculture Organization of the United Nations (FAO), Fisheries and Aquaculture Department., 2017. *Cultured Aquatic Species Information Programme: Mytilus edulis (Linnaeus, 1758).* [Online] Available at: <http://www.fao.org/fishery/culturedspecies/Mytilus_edulis/en> [Accessed 13 February 2017].

Food and Agriculture Organization of the United Nations (FAO). (2016) Global aquaculture production online query. http://www.fao.org/fishery/topic/16140/en

Forsythe, W.C., Rykiel Jr, E.J., Stahl, R.S., Wu, H.I. and Schoolfield, R.M., 1995. A model comparison for daylength as a function of latitude and day of year. *Ecological Modelling*, *80*(1), 87-95.

Foulkes, N. S., Borjigin, J., Snyder, S. H. and Snyder, S. H., 1997. Rhythmic transcription: the molecular basis of circadian melatonin synthesis. *Trends in Neurosciences*, *20*(10), 487-492.

Gakh, O., Cavadini, P. and Isaya, G., 2002. Mitochondrial processing peptidases. *Biochimica et Biophysica Acta (BBA)-Molecular Cell Research*, *1592*(1), 63-77.

Galbraith, H.S. and Vaughn, C.C., 2009. Temperature and food interact to influence gamete development in freshwater mussels. *Hydrobiologia*, *636*(1), 35-47.

Gallego, M. and Virshup, D.M., 2007. Post-translational modifications regulate the ticking of the circadian clock. *Nature Reviews Molecular Cell Biology*, *8*(2), 139-148.

García-Horsman, J.A., Barquera, B., Rumbley, J., Ma, J. and Gennis, R.B., 1994. The superfamily of heme-copper respiratory oxidases. *Journal of Bacteriology*, *176*(18), 5587.

Gardner, M.J., Hubbard, K.E., Hotta, C.T., Dodd, A.N. and Webb, A.A., 2006. How plants tell the time. *Biochemical Journal*, *397*(1), 15-24.

Garcia-March, J.R., Jiménez, S., Sanchis, M.A., Monleon, S., Lees, J., Surge, D. and Tena-Medialdea, J., 2016. In situ biomonitoring shows seasonal patterns and environmentally mediated gaping activity in the bivalve, *Pinna nobilis*. *Marine Biology*, *163*(2), 29.

Gehring, W. and Rosbash, M., 2003. The coevolution of blue-light photoreception and circadian rhythms. *Journal of Molecular Evolution*, *57*(1), S286-S289.

Gekakis, N., Staknis, D., Nguyen, H.B., Davis, F.C., Wilsbacher, L.D., King, D.P., Takahashi, J.S. and Weitz, C.J., 1998. Role of the CLOCK protein in the mammalian circadian mechanism. *Science*, *280*(5369), 1564-1569.

Gerhart-Hines, Z., Feng, D., Emmett, M.J., Everett, L.J., Loro, E., Briggs, E.R., Bugge, A., Hou, C., Ferrara, C., Seale, P. and Pryma, D.A., 2013. The nuclear receptor Rev-erbα controls circadian thermogenic plasticity. *Nature*, *503*(7476), 410.

Giguère, V., Tini, M., Flock, G., Ong, E., Evans, R.M. and Otulakowski, G., 1994. Isoform-specific amino-terminal domains dictate DNA-binding properties of RORα, a novel family of orphan hormone nuclear receptors. *Genes and Development, 8*, 538-553.

Glaser, F.T. and Stanewsky, R., 2005. Temperature synchronization of the *Drosophila* circadian clock. *Current Biology*, *15*(15), 1352-1363.

Gnocchi, D. and Bruscalupi, G., 2017. Circadian rhythms and hormonal homeostasis: pathophysiological implications. *Biology*, *6*(1), 10-30.

Gnyubkin, V.F., 2010. The circadian rhythms of valve movements in the mussel *Mytilus galloprovincialis*. *Russian Journal of Marine Biology, 36*(6), 419-428.

Golden, S.S., Ishiura, M., Johnson, C.H. and Kondo, T., 1997. Cyanobacterial circadian rhythms. *Annual Review of Plant Biology*, *48*(1), 327-354.

Golombek, D.A. and Rosenstein, R.E., 2010. Physiology of circadian entrainment.

Physiological Reviews, *90*(3), 1063-1102.

Gosling, E., 2015. Marine bivalve molluscs. John Wiley & Sons.

Goto, S.G., 2013. Roles of circadian clock genes in insect photoperiodism. *Entomological Science*, *16*(1), 1-16.

Goto, S.G. and Denlinger, D.L., 2002. Short-day and long-day expression patterns of genes involved in the flesh fly clock mechanism: period, timeless, cycle and cryptochrome. *Journal of Insect Physiology*, *48*(8), 803-816.

Gotter, A.L., 2006. A Timeless debate: resolving TIM's noncircadian roles with possible clock function. *Neuroreport*, *17*(12), 1229-1233.

Gotter, A. L., Manganaro, T., Weaver, D.R., Kolakowski, L.F., Possidente, B., Sriram, S., MacLaughlin, D.T. and Reppert, S.M., 2000. A time-less function for mouse *timeless*. *Nature Neuroscience*, *3*, 755-756.

Gotter, A. L., Suppa, C. and Emanuel, B.S., 2007. Mammalian TIMELESS and Tipin are evolutionarily conserved replication fork-associated factors. *Journal of Molecular Biology*, *366*(1), 36-52.

Grabek, K.R. and Chabot, C.C., 2012. Daily rhythms of PERIOD protein in the eyestalk of the American lobster, *Homarus americanus*. *Marine and Freshwater Behaviour and Physiology*, *45*(4), 269-279.

Gracey, A.Y., Chaney, M.L., Boomhower, J.P., Tyburczy, W.R., Connor, K. and Somero, G.N., 2008. Rhythms of gene expression in a fluctuating intertidal environment. *Current Biology*, *18*(19), 1501-1507.

GraphPad Software, Inc., 1990. *The InStat guide to choosing and interpreting statistical tests. A manual for GraphPad InStat Version 3*. GraphPad Software, Inc. San Diego, USA.

Gray, D.R. and Hodgson, A.N., 1999. Endogenous rhythms of locomotor activity in the high-shore limpet, *Helcion pectunculus* (Patellogastropoda). *Animal Behaviour*, *57*(2), 387-391.

Griffin, E.A., Staknis, D. and Weitz, C.J., 1999. Light-independent role of CRY1 and CRY2 in the mammalian circadian clock. *Science*, *286*(5440), 768-771.

Guillaumond, F., Dardente, H., Giguère, V. and Cermakian, N., 2005. Differential control of *Bmal1* circadian transcription by REV-ERB and ROR nuclear receptors. *Journal of Biological Rhythms*, *20*(5), 391-403.

Gusev, O.A. and Golubev, A.I., 2001. Tide-associated biological rhythms of some white sea littoral invertebrates. *Advances in Space Research*, *28*(4), 613-615.

Gutiérrez, J.L., Jones, C.G., Strayer, D.L. and Iribarne, O.O., 2003. Mollusks as ecosystem engineers: the role of shell production in aquatic habitats. *Oikos*, *101*(1),

79-90.

Gwinner, E., 2012. *Circannual rhythms: endogenous annual clocks in the organization of seasonal processes* (Vol. 18). Springer Science & Business Media.

Gwinner, E., 1996. Circadian and circannual programmes in avian migration. *The Journal of Experimental Biology*, *199*, 39-49.

Gwinner, E. and Brandstatter, R., 2001. Complex bird clocks. *Philosophical Transactions of the Royal Society of London. Series B: Biological Sciences*, *356*(1415), 1801-1810.

Häfker, N.S., Meyer, B., Last, K.S., Pond, D.W., Hüppe, L. and Teschke, M., 2017. Circadian clock involvement in zooplankton diel vertical migration. *Current Biology*, *27*(14), 2194-2201.

Hall, E.A., Keighren, M., Ford, M.J., Davey, T., Jarman, A.P., Smith, L.B., Jackson, I.J. and Mill, P., 2013. Acute versus chronic loss of mammalian Azi1/Cep131 results in distinct ciliary phenotypes. *PLoS Genetics*, *9*(12), e1003928.

Hannas, B.R. and LeBlanc, G.A., 2010. Expression and ecdysteroid responsiveness of the nuclear receptors HR3 and E75 in the crustacean *Daphnia magna*. *Molecular and Cellular Endocrinology*, *315*(1), 208-218.

Hannas, B.R., Wang, Y.H., Baldwin, W.S., Li, Y., Wallace, A.D. and LeBlanc, G.A., 2010. Interactions of the crustacean nuclear receptors HR3 and E75 in the regulation of gene transcription. *General and Comparative Endocrinology*, *167*(2), 268-278.

Hardege, J.D., Ram, J.L. and Bentley, M.G., 1997. Activation of spawning in zebra mussels by algae-, cryptomonad-, and gamete-associated factors. *Experimental Biology Online*, *2*(2), 1-9.

Hardie, R.C., 2001. Phototransduction in *Drosophila* melanogaster. *Journal of Experimental Biology*, *204*(20), 3403-3409.

Hardin, P.E., 2005. The circadian timekeeping system of *Drosophila*. *Current Biology 15*(17), R714-R722.

Hardin, P.E., Hall, J.C. and Rosbash, M., 1990. Feedback of the *Drosophila* period gene product on circadian rhythm cycling of its messenger RNA levels. *Nature 343*, 536-540.

Harley, C.D., Randall Hughes, A., Hultgren, K.M., Miner, B.G., Sorte, C. J., Thornber, C.S., Rodriguez, L.F., Tomanek, L. and Williams, S.L. (2006). The impacts of climate change in coastal marine systems. *Ecology Letters*, *9*(2), 228-241.

Harmer, S.L., Panda, S. and Kay, S.A., 2001. Molecular bases of circadian rhythms. *Annual Review of Cell and Developmental Biology*, *17*(1), 215-253.

Haszprunar, G., 1983. Comparative analysis of the abdominal sense organs of

Pteriomorpha (Bivalvia). *Journal of Molluscan Studies*, Suppl, 12(A), 47-50.

Haszprunar, G., 1985. The fine structure of the abdominal sense organs of Pteriomorpha (Mollusca, Bivalvia). *Journal of Molluscan Studies, 51*(3), 315-319.

Haszprunar, G., 1987. The fine morphology of the osphradial sense organs of the Mollusca. III. Placophora and Bivalvia. *Philosophical Transactions of the Royal Society of London. B, Biological Sciences*, *315*(1169), 37-61.

Hauenschild, C., 1960, January. Lunar periodicity. In *Cold Spring Harbor Symposia on Quantitative Biology* (Vol. 25, 491-497). Cold Spring Harbor Laboratory Press.

Haug, M.F., Gesemann, M., Lazović, V. and Neuhauss, S.C., 2015. Eumetazoan cryptochrome phylogeny and evolution. *Genome Biology and Evolution*, *7*(2), 601-619.

Heath-Heckman, E. A., Peyer, S. M., Whistler, C. A., Apicella, M. A., Goldman, W. E. and McFall-Ngai, M. J., 2013. Bacterial bioluminescence regulates expression of a host cryptochrome gene in the squid-vibrio symbiosis. *MBio*, *4*(2), e00167-13.

Helfrich-Förster, C., 2006. The neural basis of *Drosophila*'s circadian clock. *Sleep and Biological Rhythms*, *4*(3), 224-234.

Helfrich-Förster, C., Bertolini, E. and Menegazzi, P., 2018. Flies as models for circadian clock adaptation to environmental challenges. *European Journal of Neuroscience*, *51*(1), 166-181.

Helm, B., Ben-Shlomo, R., Sheriff, M.J., Hut, R.A., Foster, R., Barnes, B.M. and Dominoni, D., 2013. Annual rhythms that underlie phenology: biological time-keeping meets environmental change. *Proceedings of the Royal Society B: Biological Sciences*, *280*(1765), 20130016.

Helmuth, B., Broitman, B. R., Blanchette, C. A., Gilman, S., Halpin, P., Harley, C. D., O'Donnell, M.J., Hofmann, G.E., Menge, B. and Strickland, D. (2006a). Mosaic patterns of thermal stress in the rocky intertidal zone: implications for climate change. *Ecological Monographs*, *76*(4), 461-479.

Helmuth, B., Mieszkowska, N., Moore, P., and Hawkins, S. J. (2006b). Living on the edge of two changing worlds: forecasting the responses of rocky intertidal ecosystems to climate change. *Annual Review of Ecology, Evolution, and Systematics*, *37*, 373-404.

Herrero, M.J. and Lepesant, J.M., 2014. Daily and seasonal expression of clock genes in the pituitary of the European sea bass (*Dicentrarchus labrax*). *General and Comparative Endocrinology*, *208*, 30-38.

Hiebert, S.M., Thomas, E.M., Lee, T.M., Pelz, K.M., Yellon, S.M. and Zucker, I., 2000. Photic entrainment of circannual rhythms in golden-mantled ground squirrels: role of the pineal gland. *Journal of Biological Rhythms*, *15*(2), 126-134.

Hiragaki, S., Suzuki, T., Mohamed, A.A. and Takeda, M., 2015. Structures and functions of insect arylalkylamine N-acetyltransferase (iaaNAT); a key enzyme for physiological and behavioral switch in arthropods. *Frontiers in Physiology*, *6*, 113.

Hirayama, J. and Sassone-Corsi, P., 2005. Structural and functional features of transcription factors controlling the circadian clock. *Current Opinion in Genetics and Development 15*, 548–556.

Hoegh-Guldberg, O., and Bruno, J.F. (2010). The impact of climate change on the world's marine ecosystems. *Science*, *328*(5985), 1523-1528.

Hommay, G., Kienlen, J.C., Gertz, C. and Hill, A., 2001. Growth and reproduction of the slug *Limax valentianus* Firussac in experimental conditions. *Journal of Molluscan Studies*, *67*(2), 191-207.

Houki, S., Kawamura, T., Irie, T., Won, N.I. and Watanabe, Y., 2015. The daily cycle of siphon extension behavior in the Manila clam controlled by endogenous rhythm. *Fisheries Science*, *81*(3), 453-461.

Hruz, T., Wyss, M., Docquier, M., Pfaffl, M.W., Masanetz, S., Borghi, L., Verbrugghe, P., Kalaydjieva, L., Bleuler, S., Laule, O. and Descombes, P., 2011. RefGenes: identification of reliable and condition specific reference genes for RT-qPCR data normalization. *BMC Genomics*, *12*(1), 156.

Ikeno, T., Ishikawa, K., Numata, H. and Goto, S.G., 2013. Circadian clock gene Clock is involved in the photoperiodic response of the bean bug *Riptortus pedestris*. *Physiological Entomology*, *38*(2), 57-162.

Ikeno, T., Numata, H. and Goto, S.G., 2011a. Circadian clock genes period and cycle regulate photoperiodic diapause in the bean bug *Riptortus pedestris* males. *Journal of Insect Physiology*, *57*(7), 935-938.

Ikeno, T., Numata, H. and Goto, S.G., 2011b. Photoperiodic response requires mammalian-type cryptochrome in the bean bug *Riptortus pedestris*. *Biochemical and Biophysical Research Communications*, *410*(3), 394-397.

Ikeno, T., Tanaka, S.I., Numata, H. and Goto, S.G., 2010. Photoperiodic diapause under the control of circadian clock genes in an insect. *BMC Biology*, *8*(1), 116.

Inoue, K., Waite, J. H., Matsuoka, M., Odo, S., and Harayama, S., 1995. Interspecific variations in adhesive protein sequences of *Mytilus edulis*, *M. galloprovincialis*, and *M. trossulus*. *The Biological Bulletin*, *189*(3), 370-375.

IPCC (2014): *Climate Change 2014: Synthesis Report*. Contribution of Working Groups I, II and III to the Fifth Assessment Report of the Intergovernmental Panel on Climate Change [Core Writing Team, R.K. Pachauri and L.A. Meyer (eds.)]. IPCC, Geneva, Switzerland, 151.

Izawa, N., Suzuki, T., Watanabe, M. and Takeda, M., 2009. Characterization of arylalkylamine *N*-acetyltransferase (AANAT) activities and action spectrum for

suppression in the band-legged cricket, *Dianemobius nigrofasciatus* (Orthoptera: Gryllidae). *Comparative Biochemistry and Physiology Part B: Biochemistry and Molecular Biology*, *152*(4), 346-351.

Jacklet, J.W., 1969. Circadian rhythm of optic nerve impulses recorded in darkness from isolated eye of *Aplysia*. *Science*, *164*(3879), 562-563.

Jarque, S., Prats, E., Olivares, A., Casado, M., Ramón, M. and Piña, B., 2014. Seasonal variations of gene expression biomarkers in *Mytilus galloprovincialis* cultured populations: Temperature, oxidative stress and reproductive cycle as major modulators. *Science of the Total Environment*, *499*, 363-372.

Jetten, A.M. and Ueda, E., 2001. The ROR nuclear orphan receptor subfamily: critical regulators of multiple biological processes. *Progress in Nucleic Acid Research and Molecular Biology*, *69*, 205-247.

Jindrich, K., Roper, K.E., Lemon, S., Degnan, B.M., Reitzel, A.M. and Degnan, S.M., 2017. Origin of the Animal Circadian Clock: Diurnal and Light-Entrained Gene Expression in the Sponge *Amphimedon queenslandica*. *Frontiers in Marine Science*, *4*, 327.

JNCC, 2016a. *Joint Nature Conservation Committee*. [ONLINE] Available at: http://jncc.defra.gov.uk/page-1523. [Accessed 20 September 2017].

JNCC, 2016b. *Joint Nature Conservation Committee.* [ONLINE] From: Blue mussel beds on sediment; UK Biodiversity Action Plan; Priority Habitat Descriptions. BRIG (ed. Ant Maddock) 2008. Available at: http://jncc.defra.gov.uk/page-5706 [Accessed 20 September 2017].

Johnson, K.M., Wong, J.M., Hoshijima, U., Sugano, C.S. and Hofmann, G.E., 2019. Seasonal transcriptomes of the Antarctic pteropod, *Limacina helicina antarctica*. *Marine Environmental Research*, *143*, 49-59.

Johnston, P.G. and Zucker, I., 1980. Photoperiodic regulation of the testes of adult white-footed mice (*Peromyscus leucopus*). *Biology of Reproduction*, *23*(4), 859-866.

Jones, S.J., Lima, F.P., and Wethey, D.S., 2010. Rising environmental temperatures and biogeography: poleward range contraction of the blue mussel, *Mytilus edulis* L., in the western Atlantic. *Journal of Biogeography*, *37*(12), 2243-2259.

Joosse, J., 1984. Photoperiodicity, rhythmicity and endocrinology of reproduction in the snail *Lymnaea stagnalis*. *Photoperiodic Regulation of Insect and Molluscan Hormones*, Ciba Foundation Symposium 104, 204-220.

Kamae, Y., Uryu, O., Miki, T. and Tomioka, K., 2014. The nuclear receptor genes HR3 and E75 are required for the circadian rhythm in a primitive insect. *PloS One*, *9*(12), e114899.

Kang, C.K., 2000. Seasonal variations in condition, reproductive activity, and biochemical composition of the Pacific oyster, *Crassostrea gigas* (Thunberg), in

suspended culture in two coastal bays of Korea. *Journal of Shellfish Research, 19*, 771-778.

Kang, C.K., Kang, Y.S., Choy, E.J., Kim, D.S., Shim, B.T. and Lee, P.Y., 2007. Condition, reproductive activity, and gross biochemical composition of the Manila clam, Tapes philippinarum in natural and newly created sandy habitats of the southern coast of Korea. *Journal of Shellfish Research, 26*(2), 401-412.

Kapitskaya, M. Z., Li, C., Miura, K., Segraves, W. and Raikhel, A. S., 2000. Expression of the early-late gene encoding the nuclear receptor HR3 suggests its involvement in regulating the vitellogenic response to ecdysone in the adult mosquito. *Molecular and Cellular Endocrinology*, *160*(1), 25-37.

Kawai, Y. and Wada, A., 2007. Diurnal sea surface temperature variation and its impact on the atmosphere and ocean: A review. *Journal of Oceanography, 63*(5), 721-744.

Keeling, P.J. and Doolittle, W.F., 1996. Alpha-tubulin from early-diverging eukaryotic lineages and the evolution of the tubulin family. *Molecular Biology and Evolution, 13*(10), 1297-1305.

Kewley, R. J., Whitelaw, M. L. and Chapman-Smith, A., 2004. The mammalian basic helix–loop–helix/PAS family of transcriptional regulators. *The International Journal of Biochemistry & Cell Biology, 36*(2), 189-204.

Khan, M.A., Parrish, C.C. and Shahidi, F., 2006. Effects of environmental characteristics of aquaculture sites on the quality of cultivated Newfoundland blue mussels (*Mytilus edulis*). *Journal of Agricultural and Food Chemistry*, *54*(6), 2236-2241.

Khavrus, V. and Shelevytsky, I., 2010. Introduction to solar motion geometry on the basis of a simple model. *Physics Education, 45*(6), 641-653.

Kim, W.S., Huh, H.T., Je, J.G. and Han, K.N., 2003. Evidence of two-clock control of endogenous rhythm in the Washington clam, *Saxidomus purpuratus*. *Marine Biology*, *142*(2), 305-309.

Kim, W. S., Huh, H. T., Lee, J. H., Rumohr, H. and Koh, C. H., 1999. Endogenous circatidal rhythm in the Manila clam *Ruditapes philippinarum* (Bivalvia: Veneridae). *Marine Biology*, *134*(1), 107-112.

Klein, D.C., 2007. Arylalkylamine N-acetyltransferase: "the Timezyme". *Journal of Biological Chemistry*, *282*(7), 4233-4237.

Knöbel, L., Breusing, C., Bayer, T., Sharma, V., Hiller, M., Melzner, F. and Stuckas, H., 2019. Comparative de novo assembly and annotation of mantle tissue transcriptomes from the *Mytilus edulis* species complex (*M. edulis*, *M. galloprovincialis*, *M. trossulus*). *Marine Genomics*, 51, 100700.

Koike, N., Hida, A., Numano, R., Hirose, M., Sakaki, Y. and Tei, H., 1998.

Identification of the mammalian homologues of the *Drosophila* timeless gene, Timeless1. *FEBS Letters*, *441*(3), 427-431.

Kojima, S., Shingle, D. L., and Green, C. B. (2011). Post-transcriptional control of circadian rhythms. *Journal of Cell Science*, *124*(3), 311-320.

Korringa, P. 1947. Relations between the moon and periodicity in the breeding of marine animals. *Ecological Society of America*, *17*(3), 347-381.

Koštál, V., 2011. Insect photoperiodic calendar and circadian clock: independence, cooperation, or unity? *Journal of Insect Physiology*, *57*(5), 538-556.

Kostrouchova, M., Krause, M., Kostrouch, Z. and Rall, J.E., 2001. Nuclear hormone receptor CHR3 is a critical regulator of all four larval molts of the nematode *Caenorhabditis elegans*. *Proceedings of the National Academy of Sciences, U.S.A*, *98*(13), 7360-7365.

Kräuchi, K., 2002. How is the circadian rhythm of core body temperature regulated? *Clinical Autonomic Research, 12*, 147- 149.

Kreitzman, L. and Foster, R., 2011. *The rhythms of life: The biological clocks that control the daily lives of every living thing*. Profile books.

Kubo, Y., Takeuchi, T., Okano, K. and Okano, T., 2010. Cryptochrome genes are highly expressed in the ovary of the African clawed frog, *Xenopus tropicalis*. *PloS one*, *5*(2), e9273.

Kumar V. Photoperiodism in higher vertebrates: an adaptive strategy in temporal environment. *Indian Journal of Experimental Biology*, *35*(5):427-37.

Kumar, V. and Mishra, I., 2018. Circannual Rhythms. In: *Encyclopedia of Reproduction*, 1, 442-50.

Kumar, S., Stecher, G. and Tamura, K., 2016. MEGA7: molecular evolutionary genetics analysis version 7.0 for bigger datasets. *Molecular Biology and Evolution*, *33*(7), 1870-1874.

LaCourse, J.R. and Northrop, R.B., 1978. A preliminary study of mechanoreceptors within the anterior byssus retractor muscle of *Mytilus edulis* L. *The Biological Bulletin*, *155*(1), 161-168.

Lafont, R. and Mathieu, M., 2007. Steroids in aquatic invertebrates. *Ecotoxicology*, *16*(1), 109-130.

Lahiri, K., Vallone, D., Gondi, S.B., Santoriello, C., Dickmeis, T. and Foulkes, N.S., 2005. Temperature regulates transcription in the zebrafish circadian clock. *PLoS Biology*, *3*(11), e351.

Lam, V.H. and Chiu, J.C., 2018. Evolution and design of invertebrate circadian clocks. In: *The Oxford Handbook of Invertebrate Neurobiology*.

Larrondo, L.F. and Canessa, P., 2019. The clock keeps on ticking: emerging roles for circadian regulation in the control of fungal physiology and pathogenesis. *Fungal Physiology and Immunopathogenesis*, 121-156.

Laruelle, F., Guillou, J. and Paulet, Y.M., 1994. Reproductive pattern of the clams, Ruditapes decussatus and R. philippinarum on intertidal flats in Brittany. *Journal of the Marine Biological Association of the United Kingdom*, *74*(2), 351-366.

Lawrence, A.J. and Soame, J.M., 2004. The effects of climate change on the reproduction of coastal invertebrates. *Ibis*, *146*, 29-39.

Lee, H., Chen, R., Lee, Y., Yoo, S. and Lee, C., 2009. Essential roles of CKIδ and CKIε in the mammalian circadian clock. *Proceedings of the National Academy of Sciences USA*, *106*(50), 21359-21364.

Lee, J.E. and Edery, I., 2008. Circadian regulation in the ability of *Drosophila* to combat pathogenic infections. *Current Biology*, *18*(3), 195-199.

Li, J., Zhang, Y., Zhang, Y., Mao, F., Xiang, Z., Xiao, S., Ma, H. and Yu, Z., 2017. The first invertebrate NFIL3 transcription factor with role in immune defense identified from the Hong Kong oyster, *Crassostrea hongkongensis*. *Developmental & Comparative Immunology*, *76*, 1-8.

Li, Q., Osada, M. and Mori, K., 2000. Seasonal biochemical variations in Pacific oyster gonadal tissue during sexual maturation. *Fisheries Science*, *66*(3), 502-508.

Li, S., Xie, L., Zhang, C., Zhang, Y., Gu, M. and Zhang, R., 2004. Cloning and expression of a pivotal calcium metabolism regulator: calmodulin involved in shell formation from pearl oyster (*Pinctada fucata*). *Comparative Biochemistry and Physiology Part B: Biochemistry and Molecular Biology*, *138*(3), 235-243.

Lincoln, G.A., Johnston, J.D., Andersson, H., Wagner, G. and Hazlerigg, D.G., 2005. Photorefractoriness in mammals: dissociating a seasonal timer from the circadian-based photoperiod response. *Endocrinology*, *146*(9), 3782-3790.

Linde, A.M., Eklund, D.M., Kubota, A., Pederson, E.R., Holm, K., Gyllenstrand, N., Nishihama, R., Cronberg, N., Muranaka, T., Oyama, T. and Kohchi, T., 2017. Early evolution of the land plant circadian clock. *New Phytologist*, *216*(2), 576-590.

Liu, N., Pan, L., Miao, J., Xu, C. and Zhang, L., 2010. Molecular cloning and sequence analysis and the response of a aryl hydrocarbon receptor homologue gene in the clam *Ruditapes philippinarum* exposed to benzo (a) pyrene. *Comparative Biochemistry and Physiology Part C: Toxicology & Pharmacology*, *152*(3), 279-287.

Liu, P., Miao, J., Song, Y., Pan, L. and Yin, P., 2017. Effects of 2, 2', 4, 4'-tetrabromodipheny ether (BDE-47) on gonadogenesis of the manila clam *Ruditapes philippinarum*. *Aquatic Toxicology*, *193*, 178-186.

Liu, Y.H. and Panda, S., 2017. Circadian Photoentrainment Mechanism in Mammals.

In Biological Timekeeping: Clocks, Rhythms and Behaviour (365-393). Springer, New Delhi.

Livak, K.J. and Schmittgen, T.D., 2001. Analysis of relative gene expression data using real time quantitative data and the $2^{-\Delta\Delta C_T}$ method. *Methods 25*, 402-408.

Lockwood, B.L., Connor, K.M. and Gracey, A.Y., 2015. The environmentally tuned transcriptomes of *Mytilus mussels*. *Journal of Experimental Biology*, *218*(12), 1822-1833.

Lockwood, B.L., Sanders, J.G. and Somero, G.N., 2010. Transcriptomic responses to heat stress in invasive and native blue mussels (genus *Mytilus*): molecular correlates of invasive success. *Journal of Experimental Biology*, *213*(20), 3548-3558.

Lockwood, B.L. and Somero, G.N., 2011. Transcriptomic responses to salinity stress in invasive and native blue mussels (genus *Mytilus*). *Molecular Ecology*, *20*(3), 517-529.

López-Olmeda, J.F., Madrid, J.A. and Sánchez-Vázquez, F.J., 2006. Light and temperature cycles as zeitgebers of zebrafish (*Danio rerio*) circadian activity rhythms. *Chronobiology International*, *23*(3), 537-550.

Lowe, D.M., Moore, M.N. and Bayne, B.L., 1982. Aspects of gametogenesis in the marine mussel *Mytilus edulis* L. *Journal of the Marine Biological Association of the United Kingdom*, *62*(1), 133-145.

Lowe, G.A., 1974. Effect of temperature change on the heart rate of *Crassostrea gigas* and *Mya arenaria* (Bivalvia). *Journal of Molluscan Studies*, *41*(1), 29-36.

Lukat, R., 1978. Circadian growth layers in the cuticle of behaviourally arrhythmic cockroaches (*Blaberus fuscus*, Ins., Blattoidea). *Experientia*, *34*(4), 477-477.

Lumsden, P.J., 2002. Photoperiodism in Plants. In: *Biological Rhythms*. Springer, Berlin, Heidelberg, 181-191.

MacDonald, B.A. and Thompson, R.J., 1988. Intraspecific variation in growth and reproduction in latitudinally differentiated populations of the giant scallop *Placopecten magellanicus* (Gmelin). *The Biological Bulletin*, *175*(3), 361-371.

Majercak, J., Chen, W.F. and Edery, I., 2004. Splicing of the period gene 3′-terminal intron is regulated by light, circadian clock factors, and phospholipase C. *Molecular and Cellular Biology*, *24*(8), 3359-3372.

Mandl, M. and Depping, R., 2014. Hypoxia-inducible aryl hydrocarbon receptor nuclear translocator (ARNT) (HIF-1β): is it a rare exception? *Molecular Medicine*, *20*(1), 215.

Maneiro, V., Silva, A., Pazos, A.J., Sánchez, J.L. and Pérez-Parallé, M.L., 2017. Effects of temperature and photoperiod on the conditioning of the flat oyster (*Ostrea edulis* L.) in autumn. *Aquaculture Research*, *48*(8), 4554-4562.

Maniscalco, M., Nannen, J., Sodi, V., Silver, G., Lowrey, P. and Bidle, K., 2014. Light-dependent expression of four cryptic archaeal circadian gene homologs. *Frontiers in Microbiology*, *5*, 79-88.

Mao, Y., Zhou, Y., Yang, H. and Wang, R., 2006. Seasonal variation in metabolism of cultured Pacific oyster, *Crassostrea gigas*, in Sanggou Bay, China. *Aquaculture*, *253*(1-4), 322-333.

Marchler-Bauer, A., Lu, S., Anderson, J.B., Chitsaz, F., Derbyshire, M.K., DeWeese-Scott, C., Fong, J.H., Geer, L.Y., Geer, R.C., Gonzales, N.R., Gwadz, M., Hurwitz, D.I., Jackson, J.D., Ke, Z., Lanczycki, C.J., Lu, F., Marchler, G.H., Mullokandov, M., Omelchenko, M.V., Millar, A.J., 2004. Input signals to the plant circadian clock. *Journal of Experimental Botany*, *55*(395), 277-283.

Martella, T., 1974. Some factors influencing byssus thread production in *Mytilus edulis* (Mollusca: Bivalvia) Linnaeus, 1758. *Water, Air, & Soil Pollution*, *3*(2), 171-177.

Martin, J.A. and Wang, Z., 2011. Next-generation transcriptome assembly. *Nature Reviews Genetics*, *12*(10), 671-682.

Martínez, G. and Pérez, H., 2003. Effect of different temperature regimes on reproductive conditioning in the scallop *Argopecten purpuratus*. *Aquaculture*, *228*(1-4), 153-167.

Mat, A.M., Massabuau, J., Ciret, P. and Tran, D., 2012. Evidence for a plastic dual circadian rhythm in the oyster *Crassostrea gigas*. *Chronobiology International*, *29*(7), 857-867.

Mat, A.M., Perrigault, M., Massabuau, J.C. and Tran, D., 2016. Role and expression of cry1 in the adductor muscle of the oyster *Crassostrea gigas* during daily and tidal valve activity rhythms. *Chronobiology International*, *33*(8), 949-963.

Mat, A.M. and Handling editor: Howard Browman, 2018. Chronobiology and the design of marine biology experiments. *ICES Journal of Marine Science*, *76*(1), 60-65.

Matsumoto, A., Ukai-Tadenuma, M., Yamada, R.G., Houl, J., Uno, K.D., Kasukawa, T., Dauwalder, B., Itoh, T.Q., Takahashi, K., Ueda, R., Hardin, P.E., Tanimura, T. and Ueda, H.R., 2007. A functional genomics strategy reveals clockwork orange as a transcriptional regulator in the *Drosophila* circadian clock. *Genes and Development*, *21*(13), 1687-700.

Matsumoto, T., Osada, M., Osawa, Y. and Mori, K., 1997. Gonadal estrogen profile and immunohistochemical localization of steroidogenic enzymes in the oyster and scallop during sexual maturation. *Comparative Biochemistry and Physiology Part B*: *Biochemistry and Molecular Biology*, *118*(4), 811-817.

McClintock, J.B. and Watts, S.A., 1990. The effects of photoperiod on gametogenesis in the tropical sea urchin *Eucidaris tribuloides* (Lamarck) (Echinodermata:

Echinoidea). *Journal of Experimental Marine Biology and Ecology*, *139*(3), 175-184.

McClung, C.R., 2006. Plant circadian rhythms. *The Plant Cell*, *18*(4), 792-803.

McClung, C.R., 2019. The plant circadian oscillator. *Biology*, *8(*1), 14.

McDonald, M.J. and Rosbash, M., 2001. Microarray analysis and organization of circadian gene expression in *Drosophila*. *Cell*, *107*(5), 567-578.

McMahon, D.G., Wallace, S.F. and Block, G.D., 1984. Cellular analysis of the *Bulla* ocular circadian pacemaker system. *Journal of Comparative Physiology A*, *155*(3), 379-385.

Mechawar, N. and Anctil, M., 1997. Melatonin in a primitive metazoan: seasonal changes of levels and immunohistochemical visualization in neurons. *Journal of Comparative Neurology*, *387*(2), 243-254.

Meng, L., Zhu, Y., Zhang, N., Liu, W., Liu, Y., Shao, C., Wang, N. and Chen, S., 2014. Cloning and characterization of tesk1, a novel spermatogenesis-related gene, in the tongue sole (*Cynoglossus semilaevis*). *PloS One*, *9*(10), e107922.

Meunier, N., Belgacem, Y. H. and Martin, J. R., 2007. Regulation of feeding behaviour and locomotor activity by takeout in *Drosophila*. *Journal of Experimental Biology*, *210*(8), 1424-1434.

Meuti, M.E., Stone, M., Ikeno, T. and Denlinger, D.L., 2015. Functional circadian clock genes are essential for the overwintering diapause of the Northern house mosquito, *Culex pipiens*. *Journal of Experimental Biology*, *218*(3), 412-422.

Miller, B.H., Olson, S.L., Turek, F.W., Levine, J.E., Horton, T.H. and Takahashi, J.S., 2004. Circadian clock mutation disrupts estrous cyclicity and maintenance of pregnancy. *Current Biology*, *14*(15), 1367-1373.

Millius, A., Ode, K.L. and Ueda, H.R., 2019. A period without PER: understanding 24-hour rhythms without classic transcription and translation feedback loops. *F1000Research*, 8.

Mitchison, T.J. and Cramer, L.P., 1996. Actin-based cell motility and cell locomotion. *Cell*, *84*(3), 371-379.

Miyazaki, Y., Nisimura, T. and Numata, H., 2014. Circannual rhythms in insects. In *Annual, lunar, and tidal clocks*. Springer, Tokyo, 333-350.

Moeser, G.M. and Carrington, E., 2006. Seasonal variation in mussel byssal thread mechanics. *Journal of Experimental Biology*, *209*(10), 1996-2003.

Mohamed, A. A., Wang, Q., Bembenek, J., Ichihara, N., Hiragaki, S., Suzuki, T. and Takeda, M., 2014. N-acetyltransferase (nat) is a Critical Conjunct of Photoperiodism between the circadian system and endocrine axis in *Antheraea pernyi*. *PloS One*, *9*(3), e92680.

Mohammad-Zadeh, L.F., Moses, L. and Gwaltney-Brant, S.M., 2008. Serotonin: a review. *Journal of Veterinary Pharmacology and Therapeutics*, *31*(3), 187-199.

Mohawk, J. A., Green, C. B. and Takahashi, J. S., 2012. Central and peripheral circadian clocks in mammals. *Annual Reviews of Neuroscience*, *35*, 445.

Moreira, R., Pereiro, P., Canchaya, C., Posada, D., Figueras, A. and Novoa, B., 2015. RNA-Seq in *Mytilus galloprovincialis*: comparative transcriptomics and expression profiles among different tissues. *BMC Genomics*, *16*(1), 728.

Morin, L.P., 1999. Serotonin and the regulation of mammalian circadian rhythmicity. *Annals of Medicine*, *31*(1), 12-33.

Morishita, F., Furukawa, Y., Matsushima, O. and Minakata, H., 2010. Regulatory actions of neuropeptides and peptide hormones on the reproduction of molluscs. *Canadian Journal of Zoology*, *88*(9), 825-845.

Morton, B., 2001. The evolution of eyes in the Bivalvia. In: Gibson, R.N., Barnes, M. and Atkinson, R.J.A. eds. 2001. *Oceanography and Marine Biology, An Annual Review*, Volume 39: An Annual Review, *39*, 165-205.

Múgica, M., Sokolova, I.M., Izagirre, U. and Marigómez, I., 2015. Season-dependent effects of elevated temperature on stress biomarkers, energy metabolism and gamete development in mussels. *Marine Environmental Research*, *103*, 1-10.

Muñoz, J.L., Patiño, M.A.L., Hermosilla, C., Conde-Sieira, M., Soengas, J.L., Rocha, F. and Míguez, J.M., 2011. Melatonin in octopus (*Octopus vulgaris*): tissue distribution, daily changes and relation with serotonin and its acid metabolite. *Journal of Comparative Physiology A*, *197*(8), 789-797.

Murakami, A. and Machemer, H., 1982. Mechanoreception and signal transmission in the lateral ciliated cells on the gill of *Mytilus*. *Journal of Comparative Physiology A: Neuroethology, Sensory, Neural, and Behavioral Physiology*, *145*(3), 351-362.

Murgarella, M., Puiu, D., Novoa, B., Figueras, A., Posada, D. and Canchaya, C., 2016. A first insight into the genome of the filter-feeder mussel *Mytilus galloprovincialis*. *PLoS One*, *11*(3), e0151561.

Nawathean, P. and Rosbash, M., 2004. The doubletime and CKII kinases collaborate to potentiate *Drosophila* PER transcriptional repressor activity. *Molecular Cell*, *13*(2), 213-223.

Naylor, E., 2010. *Chronobiology of marine organisms*. Cambridge University Press.

NCBI, National Center for Biotehcnology Information http://www.ncbi.nlm.nih.gov/

Nelson, R.J., Denlinger, D.L., and Somers, D.E. (Eds.). 2009. *Photoperiodism: the biological calendar*. Oxford University Press.

Newcomb, J.M., Kirouac, L.E., Naimie, A.A., Bixby, K.A., Lee, C., Malanga, S., Raubach, M. and Watson III, W.H., 2014. Circadian rhythms of crawling and swimming in the nudibranch mollusc *Melibe leonina*. *The Biological Bulletin*, *227*(3), 263-273.

Newell, R.I., Hilbish, T.J., Koehn, R.K. and Newell, C.J., 1982. Temporal variation in the reproductive cycle of *Mytilus edulis* L.(Bivalvia, Mytilidae) from localities on the east coast of the United States. *The Biological Bulletin*, *162*(3), 299-310.

Nicholls, T.J., Goldsmith, A.R. and Dawson, A., 1988. Photorefractoriness in birds and comparison with mammals. *Physiological reviews*, *68*(1), 133-176.

Nie, H., Jiang, L., Huo, Z., Liu, L., Yang, F. and Yan, X., 2016. Transcriptomic responses to low temperature stress in the Manila clam, *Ruditapes philippinarum*. *Fish & Shellfish Immunology*, *55*, 358-366.

Nishiwaki-Ohkawa, T. and Yoshimura, T., 2016. Molecular basis for regulating seasonal reproduction in vertebrates. *Journal of Endocrinology*, *229*(3), R117-R127.

Norberg, B., Brown, C. L., Halldorsson, O., Stensland, K. and Björnsson, B. T., 2004. Photoperiod regulates the timing of sexual maturation, spawning, sex steroid and thyroid hormone profiles in the Atlantic cod (*Gadus morhua*). *Aquaculture*, *229*(1), 451-467.

Northrop, R.B., 2000. *Introduction to dynamic modelling of neuro-sensory systems*. CRC Press.

Numata, H. and Udaka, H., 2010. Photoperiodism in Mollusks. In: RJ Nelson, DL Denlinger, DE Somers, eds. *Photoperiodism: The Biological Calendar* Oxford University Press: Oxford, UK, 173-192.

Nunes, M.V. and Saunders, D., 1999. Photoperiodic time measurement in insects: a review of clock models. *Journal of Biological Rhythms*, *14*(2), 84-104.

O'Connor, T.P., 2002. National distribution of chemical concentrations in mussels and oysters in the USA. *Marine Environmental Research*, *53*(2), 117-143.

Oishi, T., Nagai, K., Harada, Y., Naruse, M., Ohtani, M., Kawano, E. and Tamotsu, S., 2004. Circadian rhythms in amphibians and reptiles: ecological implications. *Biological Rhythm Research*, *35*(1-2), 105-120.

Okada, Y., Yamaura, K., Suzuki, T., Itoh, N., Osada, M. and Takahashi, K.G., 2013. Molecular characterization and expression analysis of chitinase from the Pacific oyster *Crassostrea gigas*. *Comparative Biochemistry and Physiology Part B: Biochemistry and Molecular Biology*, *165*(2), 83-89.

O'Reilly, L.P., Watkins, S.C. and Smithgall, T.E., 2011. An unexpected role for the clock protein timeless in developmental apoptosis. *PloS One*, *6*(2), e17157.

Osada, M., Nakamura, S. and Kijima, A., 2007. Quantitative analysis of pattern of

gonial proliferation during sexual maturation in Japanese scallop *Patinopecten yessoensis*. *Fisheries Science*, *73*(6), 1318.

Owczarek, S. and Berezin, V., 2012. Neuroplastin: cell adhesion molecule and signalling receptor. *The International Journal of Biochemistry & Cell Biology*, *44*(1), 1-5.

Pairett, A.N. and Serb, J.M., 2013. De novo assembly and characterization of two transcriptomes reveal multiple light-mediated functions in the scallop eye (Bivalvia: Pectinidae). *PloS One*, *8*(7), e69852.

Park, K., Lee, J.S., Kang, J.C., Kim, J.W. and Kwak, I.S., 2015. Cascading effects from survival to physiological activities, and gene expression of heat shock protein 90 on the abalone *Haliotis discus hannai* responding to continuous thermal stress. *Fish & Shellfish Immunology*, *42*(2), 233-240.

Paul, M.J., Zucker, I. and Schwartz, W.J., 2008. Tracking the seasons: the internal calendars of vertebrates. *Philosophical Transactions of the Royal Society B: Biological Sciences*, *363*(1490), 341-361.

Paulet, Y.M. and Boucher, J., 1991. Is reproduction mainly regulated by temperature or photoperiod in *Pecten maximus*? *Invertebrate Reproduction & Development*, *19*(1), 61-70.

Paulus, E.V. and Mintz, E.M., 2012. Developmental disruption of the serotonin system alters circadian rhythms. *Physiology and Behavior*, *105*(2), 257-263.

Pavelka, J., Shimada, K. and Kostal, V., 2003. TIMELESS: a link between fly's circadian and photoperiodic clocks? *European Journal of Entomology*, *100*(2), 255-266.

Pavlicek, J., Sauzet, S., Besseau, L., Coon, S. L., Weller, J. L., Boeuf, G., Gaildrat, P., Omelchenko, M.V., Koonin, E.V., Falcón, J. and Klein, D. C., 2010. Evolution of AANAT: expansion of the gene family in the cephalochordate amphioxus. *BMC Evolutionary Biology*, *10*(1), 154.

Payne, S.H., 2015. The utility of protein and mRNA correlation. *Trends in Biochemical Sciences*, *40*(1), 1-3.

Payton, L., Perrigault, M., Bourdineaud, J.P., Marcel, A., Massabuau, J.C. and Tran, D., 2017a. Trojan horse strategy for non-invasive interference of clock gene in the oyster *Crassostrea gigas*. *Marine Biotechnology*, *19*(4), 361-371.

Payton, L., Perrigault, M., Hoede, C., Massabuau, J.C., Sow, M., Huvet, A., Boullot, F., Fabioux, C., Hegaret, H. and Tran, D., 2017b. Remodeling of the cycling transcriptome of the oyster *Crassostrea gigas* by the harmful algae *Alexandrium minutum*. *Scientific Reports*, *7*(1), 3480.

Payton, L., Sow, M., Massabuau, J.C., Ciret, P. and Tran, D., 2017c. How annual course of photoperiod shapes seasonal behavior of diploid and triploid oysters,

Crassostrea gigas. *PloS one*, *12*(10), e0185918.

Payton, L. and Tran, D., 2019. Moonlight cycles synchronize oyster behaviour. *Biology Letters*, *15*(1), 20180299.

Pazos, A.J., Román, G., Acosta, C.P., Abad, M. and Sánchez, J.L., 1997. Seasonal changes in condition and biochemical composition of the scallop *Pecten maximus* L. from suspended culture in the Ria de Arousa (Galicia, NW Spain) in relation to environmental conditions. *Journal of Experimental Marine Biology and Ecology*, *211*(2), 169-193.

Peek, C.B., Levine, D.C., Cedernaes, J., Taguchi, A., Kobayashi, Y., Tsai, S.J., Bonar, N.A., McNulty, M.R., Ramsey, K.M. and Bass, J., 2017. Circadian clock interaction with HIF1α mediates oxygenic metabolism and anaerobic glycolysis in skeletal muscle. *Cell Metabolism*, *25*(1), 86-92.

Pegoraro, M., Gesto, J.S., Kyriacou, C.P. and Tauber, E., 2014. Role for circadian clock genes in seasonal timing: testing the Bünning hypothesis. *PLoS genetics*, *10*(9), e1004603.

Peres, R., Amaral, F. G., Marques, A. C. and Neto, J. C., 2014. Melatonin Production in the Sea Star *Echinaster brasiliensis* (Echinodermata). *The Biological Bulletin*, *226*(2), 146-151.

Peres, R., Reitzel, A.M., Passamaneck, Y., Afeche, S.C., Cipolla-Neto, J., Marques, A.C. and Martindale, M.Q., 2014. Developmental and light-entrained expression of melatonin and its relationship to the circadian clock in the sea anemone *Nematostella vectensis*. *EvoDevo*, *5*(1), 26.

Peschel, N., Chen, F.K., Szabo, G. and Stanewsky, R., 2009. Light-dependent interactions between the *Drosophila* circadian clock factors *Cryptochrome*, *Jetlag*, and *Timeless*. *Current Biology*, *19*(3), 241-247.

Perrigault, M. and Tran, D., 2017. Identification of the molecular clockwork of the oyster *Crassostrea gigas*. *PloS One*, *12*(1), e0169790.

Petes, L.E., Menge, B.A., Chan, F. and Webb, M.A., 2008a. Gonadal tissue color is not a reliable indicator of sex in rocky intertidal mussels. *Aquatic Biology*, *3*(1), 63-70.

Petes, L.E., Menge, B.A. and Harris, A.L., 2008b. Intertidal mussels exhibit energetic trade-offs between reproduction and stress resistance. *Ecological Monographs*, *78*(3), 387-402.

Petpiroon, S. and Morgan, E., 1983. Observations on the tidal activity rhythm of the periwinkle *Littorina nigrolineata* (Gray). *Marine and Freshwater Behaviour and Physiology*, *9*(3), 171-192.

Petrone, L., 2016. *Circadian clock and light input system in the sea urchin larva* (Doctoral dissertation, UCL (University College London)).

Picard, D., 2002. Heat-shock protein 90, a chaperone for folding and regulation. *Cellular and Molecular Life Sciences CMLS*, *59*(10), 1640-1648.

Piontkivska, H., Chung, J. S., Ivanina, A. V., Sokolov, E. P., Techa, S. and Sokolova, I. M., 2011. Molecular characterization and mRNA expression of two key enzymes of hypoxia-sensing pathways in eastern oysters *Crassostrea virginica* (Gmelin): Hypoxia-Inducible Factor α (HIF-α) and HIF-prolyl hydroxylase (PHD). *Comparative Biochemistry and Physiology Part D: Genomics and Proteomics*, *6*(2), *103*-114.

Pisarev, A.V., Skabkin, M.A., Pisareva, V.P., Skabkina, O.V., Rakotondrafara, A.M., Hentze, M.W., Hellen, C.U. and Pestova, T.V., 2010. The role of ABCE1 in eukaryotic posttermination ribosomal recycling. *Molecular Cell*, *37*(2), 196-210.

Pittendrigh, C.S., 1960, January. Circadian rhythms and the circadian organization of living systems. In *Cold Spring Harbor symposia on quantitative biology* (Vol. 25, 159-184). Cold Spring Harbor Laboratory Press.

Pittendrigh, C.S., 1972. Circadian surfaces and the diversity of possible roles of circadian organization in photoperiodic induction. *Proceedings of the National Academy of Sciences USA*, *69*(9), 2734-2737.

Place, S.P., O'Donnell, M.J. and Hofmann, G.E., 2008. Gene expression in the intertidal mussel *Mytilus californianus*: a physiological response to environmental factors on a biogeographic scale. *Marine Ecology Progress Series*, *356*, 1-14.

Plautz, J.D., Kaneko, M., Hall, J.C. and Kay, S.A., 1997. Independent photoreceptive circadian clocks throughout *Drosophila*. *Science*, *278*, 1632-1635.

Poulain, C., Lorrain, A., Flye-Sainte-Marie, J., Amice, E., Morize, E. and Paulet, Y.M., 2011. An environmentally induced tidal periodicity of microgrowth increment formation in subtidal populations of the clam *Ruditapes philippinarum*. *Journal of Experimental Marine Biology and Ecology*, *397*(1), 58-64.

Prego-Faraldo, M.V., Martínez, L. and Méndez, J., 2018. RNA-Seq analysis for assessing the early response to DSP toxins *in Mytilus galloprovincialis* digestive gland and gill. *Toxins*, *10*(10), 417.

Prisco, M., Agnese, M., De Marino, A., Andreuccetti, P. and Rosati, L., 2017. Spermatogenic cycle and steroidogenic control of spermatogenesis in *Mytilus galloprovincialis* collected in the Bay of Naples. *The Anatomical Record*, *300*(10), 1881-1894.

Pronker, A.E., Nevejan, N.M., Peene, F., Geijsen, P. and Sorgeloos, P., 2008. Hatchery broodstock conditioning of the blue mussel *Mytilus edulis* (Linnaeus 1758). Part I. Impact of different micro-algae mixtures on broodstock performance. *Aquaculture International*, *16*(4), 297-307.

Raingeard, D., Bilbao, E., Cancio, I. and Cajaraville, M.P., 2013. Retinoid X receptor (RXR), estrogen receptor (ER) and other nuclear receptors in tissues of the mussel

Mytilus galloprovincialis: cloning and transcription pattern. *Comparative Biochemistry and Physiology Part A: Molecular & Integrative Physiology*, *165*(2), 178-190.

Ram, J.L., Crawford, G.W., Walker, J.U., Mojares, J.J., Patel, N., Fong, P.P. and Kyozuka, K., 1993. Spawning in the zebra mussel (*Dreissena polymorpha*): activation by internal or external application of serotonin. *Journal of Experimental Zoology*, *265*(5), 587-598.

Rao, K.P., 1954. Tidal rhythmicity of rate of water propulsion in *Mytilus*, and its modifiability by transplantation. *Biological Bulletin*, *106*(3), 353-359.

Rao, M.B., 1980. Studies on the oxygen consumption of a tropical intertidal limpet *Cellana radiata* (Born): effect of body size and tidal rhythm. *Hydrobiologia*, *71*(1-2), 175-179.

Reddy, P., Zehring, W.A., Wheeler, D.A., Pirrotta, V., Hadfield, C., Hall, J.C. and Rosbash, M., 1984. Molecular analysis of the period locus in *Drosophila* melanogaster and identification of a transcript involved in biological rhythms. *Cell*, 38(3), 701-710.

Reischig, T. and Stengl, M., 2003. Ectopic transplantation of the accessory medulla restores circadian locomotor rhythms in arrhythmic cockroaches (Leucophaea maderae). *Journal of Experimental Biology*, *206*(11), 1877-1886.

Reitzel, A. M., Behrendt, L. and Tarrant, A. M., 2010. Light entrained rhythmic gene expression in the sea anemone *Nematostella vectensis*: the evolution of the animal circadian clock. *PLoS One*, *5*(9), e12805.

Rensing, L., Meyer-Grahle, U. and Ruoff, P., 2001. Biological timing and the clock metaphor: oscillatory and hourglass mechanisms. *Chronobiology International*, *18*(3), 329-369.

Rensing, L. and Ruoff, P., 2002. Temperature effect on entrainment, phase shifting, and amplitude of circadian clocks and its molecular bases. *Chronobiology International*, *19*(5), 807-864.

Renthlei, Z., Gurumayum, T., Borah, B.K. and Trivedi, A.K., 2019. Daily expression of clock genes in central and peripheral tissues of tree sparrow (*Passer montanus*). *Chronobiology International*, *36*(1), 110-121.

Rittschof, D. and McClellan-Green, P., 2005. Molluscs as multidisciplinary models in environment toxicology. *Marine Pollution Bulletin*, *50*(4), 369-373.

Rivas, G.B., Teles-de-Freitas, R., Pavan, M.G., Lima, J.B., Peixoto, A.A. and Bruno, R.V., 2018. Effects of light and temperature on daily activity and clock gene expression in two mosquito disease vectors. *Journal of Biological Rhythms*, *33*(3), 272-288.

Roberts, L., Cheesman, S., Breithaupt, T. and Elliott, M., 2015. Sensitivity of the mussel *Mytilus edulis* to substrate-borne vibration in relation to anthropogenically

generated noise. *Marine Ecology Progress Series*, 538, 185-195.

Robertson, C.L., Song, J.S., Thanki, N., Yamashita, R.A., Zhang, D., Zhang, N., Zheng, C. and Bryant, S.H., 2011. CDD: A conserved domain database for the functional annotation of proteins. *Nucleic Acids Research, 39*(D), 225-229.

Robson, A.A., De Leaniz, C.G., Wilson, R.P. and Halsey, L.G., 2010. Effect of anthropogenic feeding regimes on activity rhythms of laboratory mussels exposed to natural light. *Hydrobiologia, 655*(1), 197-204.

Rodhouse, P.G., Roden, C.M., Burnell, G.M., Hensey, M.P., McMahon, T., Ottway, B. and Ryan, T.H., 1984. Food resource, gametogenesis and growth of *Mytilus edulis* on the shore and in suspended culture: Killary Harbour, Ireland. *Journal of the Marine Biological Association of the United Kingdom*, *64*(3), 513-529.

Rodland, D.L., Schöne, B.R., Helama, S., Nielsen, J.K. and Baier, S., 2006. A clockwork mollusc: Ultradian rhythms in bivalve activity revealed by digital photography. *Journal of Experimental Marine Biology and Ecology*, *334*(2), 316-323.

Rodríguez-Rúa, A., Prado, M.A., Romero, Z. and Bruzon, M., 2003. The gametogenic cycle of *Scrobicularia plana* (da Costa, 1778) (Mollusc: Bivalve) in Guadalquivir estuary (Cádiz, SW Spain). *Aquaculture*, *217*(1-4), 157-166.

Roenneberg, T. and Merrow, M., 2005. Circadian clocks – the fall and rise of physiology. *Nature Reviews 6*, 965-971.

Romero, M.P., García-pergañeda, A., Guerrero, J.M. and Osuna, C., 1998. Membrane-bound calmodulin in *Xenopus laevis* oocytes as a novel binding site for melatonin. *The FASEB Journal*, *12*(13), 1401-1408.

Romero, M.R., Pérez-Figueroa, A., Carrera, M., Swanson, W.J., Skibinski, D.O. and Diz, A.P., 2019. RNA-seq coupled to proteomic analysis reveals high sperm proteome variation between two closely related marine mussel species. *Journal of Proteomics*, *192*, 169-187.

Rosati, L., Agnese, M., Abagnale, L., Aniello, F., Andreuccetti, P. and Prisco, M., 2019. The mussel *Mytilus galloprovincialis* in the Bay of Naples: New insights on oogenic cycle and its hormonal control. *The Anatomical Record*, *302*(6), 1039-1049.

Rosen, M.D., 1977. The ultrastructure and evolutionary significance of the cerebral ocelli of *Mytilus edulis*, the bay mussel (Doctoral dissertation, Department of Biology, Sonoma State University).

Rubin, E.B., Shemesh, Y., Cohen, M., Elgavish, S., Robertson, H.M. and Bloch, G., 2006. Molecular and phylogenetic analyses reveal mammalian-like clockwork in the honey bee (*Apis mellifera*) and shed new light on the molecular evolution of the circadian clock. *Genome Research*, *16*(11), 1352-1365.

Ruiz, C., Abad, M., Sedano, F., Garcia-Martin, L.O. and Lopez, J.S., 1992. Influence of seasonal environmental changes on the gamete production and biochemical

composition of Crassostrea gigas (Thunberg) in suspended culture in El Grove, Galicia, Spain. *Journal of Experimental Marine Biology and Ecology*, *155*(2), 249-262.

Ruoff, P., 2004. Temperature-Compensation in Biological Clocks: Models and Experiments. In *Function and Regulation of Cellular Systems*. Birkhäuser, Basel, 19-29.

Rush, B.L., Murad, A., Emery, P. and Giebultowicz, J.M., 2006. Ectopic CRYPTOCHROME renders TIM light sensitive in the *Drosophila* ovary. *Journal of Biological Rhythms*, *21*(4), 272-278.

Sakai, T., Tamura, T., Kitamoto, T. and Kidokoro, Y., 2004. A clock gene, period, plays a key role in long-term memory formation in *Drosophila*. *Proceedings of the National Academy of Sciences USA*, *101*(45), 16058-16063.

Sakaida, F., Kudoh, J.I. and Kawamura, H., 2000. A-HIGHERS—The system to produce the high spatial resolution sea surface temperature maps of the western North Pacific using the AVHRR/NOAA. *Journal of oceanography*, *56*(6), 707-716.

Saout, C., Quéré, C., Donval, A., Paulet, Y.M. and Samain, J.F., 1999. An experimental study of the combined effects of temperature and photoperiod on reproductive physiology of *Pecten maximus* from the Bay of Brest (France). *Aquaculture*, *172*(3), 301-314.

Santina, P.D. and Naylor, E., 1994. Endogenous rhythms in the homing behaviour of the limpet *Patella vulgata* Linnaeus. *Journal of Molluscan Studies*, *60*(1), 87-91.

Sarachana, T., Xu, M., Wu, R.C. and Hu, V.W., 2011. Sex hormones in autism: androgens and estrogens differentially and reciprocally regulate RORA, a novel candidate gene for autism. *PloS One*, *6*(2), e17116.

Sartor, F., Eelderink-Chen, Z., Aronson, B., Bosman, J., Hibbert, L.E., Dodd, A.N., Kovács, Á.T. and Merrow, M., 2019. Are There Circadian Clocks in Non-Photosynthetic Bacteria? *Biology*, *8*(2), 41-59.

Sato, T.K., Yamada, R.G., Ukai, H., Baggs, J.E., Miraglia, L.J., Kobayashi, T.J., Welsh, D.K., Kay, S.A., Ueda, H.R. and Hogenesch, J.B., 2006. Feedback repression is required for mammalian circadian clock function. *Nature Genetics*, *38*(3), 312-319.

Sauman, I., Briscoe, A.D., Zhu, H., Shi, D., Froy, O., Stalleicken, J., Yuan, Q., Casselman, A. and Reppert, S.M., 2005. Connecting the navigational clock to sun compass input in monarch butterfly brain. *Neuron*, *46*(3), 457-467.

Saunders, D.S., 2005. Erwin Bünning and Tony Lees, two giants of chronobiology, and the problem of time measurement in insect photoperiodism. *Journal of Insect Physiology*, *51*(6), 599-608.

Saunders, D.S., 2009. Photoperiodism in insects: migration and diapause responses. In: Nelson, R.J., Denlinger, D.L., and Somers, D.E. 2009. *Photoperiodism: The*

Biological Calendar. Oxford University Press, 218-257.

Saunders, D.S., 2014. Insect photoperiodism: effects of temperature on the induction of insect diapause and diverse roles for the circadian system in the photoperiodic response. *Entomological Science*, *17*(1), 25-40.

Scheiermann, C., Kunisaki, Y. and Frenette, P.S., 2013. Circadian control of the immune system. *Nature Reviews Immunology*, *13*(3), 190-198.

Schibler, U., 2005. The daily rhythms of genes, cells and organs: Biological clocks and circadian timing in cells. *EMBO Reports*, *6*(S1), S9-S13.

Schibler, U., Ripperger, J. and Brown, S.A., 2003. Peripheral circadian oscillators in mammals: time and food. *Journal of Biological Rhythms*, *18*(3), 250-260.

Schierwater, B. and Hauenschild, C., 1990. A photoperiod determined life-cycle in an oligochaete worm. *The Biological Bulletin*, *178*(2), 111-117.

Schmittgen, T.D. and Livak, K.J., 2008. Analyzing real-time PCR data by the comparative CT method. *Nature Protocols*, *3*(6), 1101-1108.

Schneider, R., Linka, R.M. and Reinke, H., 2014. HSP90 affects the stability of BMAL1 and circadian gene expression. *Journal of Biological Rhythms*, *29*(2), .87-96.

Schnytzer, Y., Simon-Blecher, N., Li, J., Ben-Asher, H.W., Salmon-Divon, M., Achituv, Y., Hughes, M.E. and Levy, O., 2018. Tidal and diel orchestration of behaviour and gene expression in an intertidal mollusc. *Scientific Reports*, *8*(1), 4917.

Schulze, T., Prager, K., Dathe, H., Kelm, J., Kießling, P. and Mittag, M., 2010. How the green alga *Chlamydomonas reinhardtii* keeps time. *Protoplasma*, *244*(1-4), 3-14.

Seed, R., 1969. The ecology of *Mytilus edulis* L. (Lamellibranchiata) on exposed rocky shores. *Oecologia*, *3*(3-4), 277-316.

Seed, R., 1976. Ecology, *in*: Bayne, B.L. (Ed.) (1976). *Marine mussels: their ecology and physiology. Cambridge University Press*, Vol 10: 13-65.

Sharma, V.K. and Chandrashekaran, M.K., 2005. Zeitgebers (time cues) for biological clocks. *Current Science*, *89*(7), 1136-1146.

Shearman, L.P., Sriram, S., Weaver, D.R., Maywood, E.S., Chaves, I., Zheng, B., Kume, K., Lee, C.C., Hastings, M.H. and Reppert, S.M., 2000. Interacting molecular loops in the mammalian circadian clock. *Science*, *288*(5468), 1013-1019.

Shirasu, N., Shimohigashi, Y., Tominaga, Y. and Shimohigashi, M., 2003. Molecular cogs of the insect circadian clock. *Zoological Science*, *20*(8), 947-955.

Smaal, A. C., 2002. European mussel cultivation along the Atlantic coast: production status, problems and perspectives. *Hydrobiologia*, *484*(1-3), 89-98.

Smith, J.R. and Strehlow, D.R., 1983. Algal-induced spawning in the marine mussel *Mytilus californianus* 4. *International Journal of Invertebrate Reproduction*, *6*(2), 129-133.

Sonnenfeld, M., Ward, M., Nystrom, G., Mosher, J., Stahl, S. and Crews, S., 1997. The Drosophila tango gene encodes a bHLH-PAS protein that is orthologous to mammalian Arnt and controls CNS midline and tracheal development. *Development*, *124*(22), 4571-4582.

Steeves, T.D., King, D.P., Zhao, Y., Sangoram, A.M., Du, F., Bowcock, A.M., Moore, R.Y. and Takahashi, J.S., 1999. Molecular cloning and characterization of the human CLOCK gene: expression in the suprachiasmatic nuclei. *Genomics*, *57*(2), 189-200.

Stevenson, T.J., 2018. Epigenetic regulation of biological rhythms: an evolutionary ancient molecular timer. *Trends in Genetics*, 34(2), 90-100.

Stone, E.F., Fulton, B.O., Ayres, J.S., Pham, L.N., Ziauddin, J. and Shirasu-Hiza, M.M., 2012. The circadian clock protein Timeless regulates phagocytosis of bacteria in *Drosophila*. *PLoS Pathogens* 8(1), e1002445. doi: 10.1371/journal.ppat.1002445

Suchanek, T.H., 1978. The ecology of Mytilus edulis L. in exposed rocky intertidal communities. *Journal of Experimental Marine Biology and Ecology*, *31*(1), 105-120.

Sugiura, Y., 1962. Electrical induction of spawning in two marine invertebrates (Urechis unicinctus, hermaphroditic *Mytilus edulis*). *The Biological Bulletin*, *123*(1), 203-206.

Sun, X.J., Zhou, L.Q., Tian, J.T., Liu, Z.H., Wu, B., Dong, Y.H., Yang, A.G. and Ma, W.M., 2016. Transcriptome survey of phototransduction and clock genes in marine bivalves. *Genetic Molecular Research*, *15*(4), gmr15048726

Sundram, V., Ng, F.S., Roberts, M.A., Millán, C., Ewer, J. and Jackson, F.R., 2012. Cellular requirements for LARK in the *Drosophila* circadian system. *Journal of Biological Rhythms*, *27*(3), 183-195.

Swan, J.A., Golden, S.S., LiWang, A. and Partch, C.L., 2018. Structure, function, and mechanism of the core circadian clock in cyanobacteria. *Journal of Biological Chemistry*, *293*(14), 5026-5034.

Sweeney, B.M. and Hastings, J.W., 1960, January. Effects of temperature upon diurnal rhythms. In *Cold Spring Harbor symposia on quantitative biology* (Vol. 25, 87-104). Cold Spring Harbor Laboratory Press.

Syrová, Z., Doležel, D., Šaumann, I. and Hodkova, M., 2003. Photoperiodic regulation of diapause in linden bugs: are period and Clock genes involved? *Cellular and Molecular Life Sciences CMLS*, 60(11), 2510-2515.

Taanman, J.W., 1999. The mitochondrial genome: structure, transcription, translation and replication. *Biochimica et Biophysica Acta (BBA)-Bioenergetics*, *1410*(2), 103-123.

Tan, Y., Merrow, M. and Roenneberg, T., 2004. Photoperiodism in *Neurospora crassa*. *Journal of Biological Rhythms, 19*(2), 135-143.

Tahara, Y., Aoyama, S. and Shibata, S., 2017. The mammalian circadian clock and its entrainment by stress and exercise. *The Journal of Physiological Sciences, 67*(1), 1-10.

Tanabe, T., Osada, M., Kyozuka, K., Inaba, K. and Kijima, A., 2006. A novel oocyte maturation arresting factor in the central nervous system of scallops inhibits serotonin-induced oocyte maturation and spawning of bivalve mollusks. *General and Comparative Endocrinology, 147*(3), 352-361.

Tauber, E., Last, K.S., Olive, P.J. and Kyriacou, C.P., 2004. Clock gene evolution and functional divergence. *Journal of Biological Rhythms, 19*(5), 445-458.

Taylor, S., Wakem, M., Dijkman, G., Alsarraj, M. and Nguyen, M., 2010. A practical approach to RT-qPCR—publishing data that conform to the MIQE guidelines. *Methods, 50*(4), S1-S5.

Temmerman, L., Meelkop, E., Janssen, T., Bogaerts, A., Lindemans, M., Husson, S.J., Beets, I. and Schoofs, L., 2011. *C. elegans* homologs of insect clock proteins: a tale of many stories. *Annals of the New York Academy of Sciences, 1220*(1), 137-148.

Tessmar-Raible, K., Raible, F. and Arboleda, E., 2011. Another place, another timer: Marine species and the rhythms of life. *Bioessays, 33*, 165-172.

Tian, Y., Han, X. and Tian, D.L., 2012. The biological regulation of ABCE1. *IUBMB Life, 64*(10), 795-800.

Tobback, J., Boerjan, B., Vandersmissen, H.P. and Huybrechts, R., 2011. The circadian clock genes affect reproductive capacity in the desert locust *Schistocerca gregaria*. *Insert Biochemistry and Molecular Biology, 41*, 313-321.

Tomanek, L. and Zuzow, M.J., 2010. The proteomic response of the mussel congeners Mytilus galloprovincialis and M. trossulus to acute heat stress: implications for thermal tolerance limits and metabolic costs of thermal stress. *Journal of Experimental Biology, 213*(20), 3559-3574.

Tomioka, K., 2014. Chronobiology of crickets: a review. *Zoological Science, 31*(10), 624-632.

Tomioka, K. and Matsumoto, A., 2010. A comparative view of insect circadian clock systems. *Cellular and Molecular Life Sciences, 67*(9), 1397-1406.

Tomioka, K. and Matsumoto, A., 2015. Circadian molecular clockworks in non-model insects. *Current Opinion in Insect Science, 7*, 58-64.

Tomioka, K., Uryu, O., Kamae, Y., Umezaki, Y. and Yoshii, T., 2012. Peripheral circadian rhythms and their regulatory mechanism in insects and some other

arthropods: a review. *Journal of Comparative Physiology B*, *182*, 729-740.

Tosches, M.A., Bucher, D., Vopalensky, P. and Arendt, D., 2014. Melatonin signaling controls circadian swimming behavior in marine zooplankton. *Cell*, *159*(1), 46-57.

Tournier, B.B., Dardente, H., Simonneaux, V., Vivien-Roels, B., Pévet, P., Masson-Pévet, M. and Vuillez, P., 2007. Seasonal variations of clock gene expression in the suprachiasmatic nuclei and pars tuberalis of the European hamster (*Cricetus cricetus*). *European Journal of Neuroscience*, *25*(5), 1529-1536.

Tournier, B.B., Menet, J.S., Dardente, H., Poirel, V.J., Malan, A., Masson-Pévet, M., Pévet, P and Vuillez, P., 2003. Photoperiod differentially regulates clock genes' expression in the suprachiasmatic nucleus of Syrian hamster. *Neuroscience*, *118*(2), 317-322.

Tran, D., Ciutat, A., Mat, A., Massabuau, J. C., Hégaret, H., Lambert, C., Le Goic, N. and Soudant, P., 2015. The toxic dinoflagellate *Alexandrium minutum* disrupts daily rhythmic activities at gene transcription, physiological and behavioral levels in the oyster *Crassostrea gigas*. *Aquatic Toxicology*, *158*, 41-49.

Tran, D., Nadau, A., Durrieu, G., Ciret, P., Parisot, J. and Massabuau, J., 2011. Field chronobiology of a molluscan bivalve: how the moon and sun cycles interact to drive oyster activity rhythms. *Chronobiology International*, *28*(4), 307-317.

Ünsal-Kaçmaz, K., Mullen, T.E., Kaufmann, W.K. and Sancar, A., 2005. Coupling of human circadian and cell cycles by the timeless protein. *Molecular and Cellular Biology*, *25*(8), 3109-3116.

Van Gelder, R.N., 2006. Timeless genes and jetlag. *Proceedings of the National Academy of Sciences, USA 103*(47), 17583-17584.

Vanagt, T., Vincx, M. and Degraer, S., 2008. Can sandy beach molluscs show an endogenously controlled circatidal migrating behaviour? Hints from a swash rig experiment. *Marine Ecology*, *29*, 118-125.

Vandesompele, J., De Preter, K., Pattyn, F., Poppe, B., Van Roy, N., De Paepe, A. and Speleman, F., 2002. Accurate normalization of real-time quantitative RT-PCR data by geometric averaging of multiple internal control genes. *Genome Biology*, *3*(7), 1-12.

VanGuilder, H.D., Vrana, K.E., and Freeman, W.M., 2008. Twenty-five years of quantitative PCR for gene expression analysis. *Biotechniques*, *44*(5), 619.

Vaze, K.M. and Sharma, V.K., 2013. On the adaptive significance of circadian clocks for their owners. *Chronobiology International*, *30*(4), 413-433.

Velez, C., Figueira, E., Soares, A.M. and Freitas, R., 2017. Effects of seawater temperature increase on economically relevant native and introduced clam species. *Marine Environmental Research*, *123*, 62-70.

Villalba, A., 1995. Gametogenic cycle of cultured mussel, *Mytilus galloprovincialis*,

in the bays of Galicia (NW Spain). *Aquaculture*, *130*(2-3), 269-277.

Vitaterna, M.H., Takahashi, J.S. and Turek, F.W., 2001. Overview of circadian rhythms. *Alcohol Research & Health*, *25*(2), 85-93.

Vogel, C. and Marcotte, E.M., 2012. Insights into the regulation of protein abundance from proteomic and transcriptomic analyses. Nature Reviews Genetics, *13*(4), 227-232.

Vriend, J. and Reiter, R. J., 2015. Melatonin feedback on clock genes: a theory involving the proteasome. *Journal of Pineal Research*, *58*(1), 1-11.

Waite, H.R., Sanchez, K.G. and Forward Jr, R.B., 2017. Entrainment of the circadian rhythm in larval release of the crab *Dyspanopeus sayi* by temperature cycles. *Marine and Freshwater Behaviour and Physiology*, *50*(1), 41-54.

Wang, T. and Brown, M.J., 1999. mRNA quantification by real time TaqMan polymerase chain reaction: validation and comparison with RNase protection. *Analytical Biochemistry*, *269*(1), 198-201.

Wang, G., Harpole, C.E., Trivedi, A.K. and Cassone, V.M., 2012. Circadian regulation of bird song, call, and locomotor behavior by pineal melatonin in the zebra finch. *Journal of Biological Rhythms*, *27*(2), 145-155.

Wayne, N.L., 2001. Regulation of seasonal reproduction in mollusks. *Journal of Biological Rhythms*, *16*(4), 391-402.

Wayne, N.L. and Block, G.D., 1992. Effects of photoperiod and temperature on egg-laying behavior in a marine mollusk, *Aplysia californica*. *Biology Bulletin*, *182*, 8-14.

Weil, Z.M. and Crews, D., 2010. Photoperiodism in amphibians and reptiles. In: RJ Nelson, DL Denlinger, DE Somers, eds 2010. *Photoperiodism: The Biological Calendar*; Oxford University Press: Oxford, UK, 399-419.

Weiss, I.M. and Schönitzer, V., 2006. The distribution of chitin in larval shells of the bivalve mollusk *Mytilus galloprovincialis*. *Journal of Structural Biology*, *153*(3), 264-277.

Welsh, D.K., Yoo, S.H., Liu, A.C., Takahashi, J.S. and Kay, S., 2004. Bioluminescence imaging of individual fibroblasts reveals persistent, independently phased circadian rhythms of clock gene expression. *Current Biology*, *14*, 2289-2295.

West, A., Dupré, S.M., Yu, L., Paton, I.R., Miedzinska, K., McNeilly, A.S., Davis, J.R.E., Burt, D.W. and Loudon, A.S.I., 2013. Npas4 is activated by melatonin, and drives the clock gene Cry1 in the ovine pars tuberalis. *Molecular Endocrinology*, *27*(6), 979-989.

Westerbom, M., Mustonen, O., Jaatinen, K., Kilpi, M. and Norkko, A., 2019. Population dynamics at the range margin: Implications of climate change on sublittoral blue mussels (*Mytilus trossulus*). *Frontiers in Marine Science*, *6*, 292.

Whitehead, K., Pan, M., Masumura, K.I., Bonneau, R. and Baliga, N.S., 2009. Diurnally entrained anticipatory behavior in archaea. *PloS one*, *4*(5).

Whitmore, D., Foulkes, N.S. and Sassone-Corsi, P., 2000. Light acts directly on organs and cells in culture to set the vertebrate circadian clock. *Nature*, *404*(6773), 87.

Whitmore, D., Foulkes, N.S., Strähle, U. and Sassone-Corsi, P., 1998. Zebrafish Clock rhythmic expression reveals independent peripheral circadian oscillators. *Nature Neuroscience*, *1*(8), 701.

Wilkinson, C.J., Carl, M. and Harris, W.A., 2009. Cep70 and Cep131 contribute to ciliogenesis in zebrafish embryos. *BMC Cell Biology*, *10*(1), 17.

Williams, B. G. and Pilditch, C. A., 1997. The entrainment of persistent tidal rhythmicity in a filter-feeding bivalve using cycles of food availability. *Journal of Biological Rhythms*, *12*(2), 173-181.

Wilson, R., Reuter, P. and Wahl, M., 2005. Muscling in on mussels: new insights into bivalve behaviour using vertebrate remote-sensing technology. *Marine Biology, 147*(5), 1165-1172.

Wong, M.L., and Medrano, J.F., 2005. Real-time PCR for mRNA quantitation. *Biotechniques*, *39*(1), 75.

Woo, K.C., Kim, T.D., Lee, K.H., Kim, D.Y., Kim, S., Lee, H.R., Kang, H.J., Chung, S.J., Senju, S., Nishimura, Y. and Kim, K.T., 2011. Modulation of exosome-mediated mRNA turnover by interaction of GTP-binding protein 1 (GTPBP1) with its target mRNAs. *The FASEB Journal*, *25*(8), 2757-2769.

Xie, F., Xiao, P., Chen, D., Xu, l., and Zhang, B., 2012. miRDeepFinder: a miRNA analysis tool for deep sequencing of plant small RNAs. *Plant Molecular Biology 80*(1), 75-84.

Xu, J., Tan, A. and Palli, S.R., 2010. The function of nuclear receptors in regulation of female reproduction and embryogenesis in the red flour beetle, *Tribolium castaneum*. *Journal of Insect Physiology*, *56*(10), 1471-1480.

Xu, X., Xu, M., Zhou, X., Jones, O.B., Moharomd, E., Pan, Y., Yan, G., Anthony, D.D. and Isaacs, W.B., 2013. Specific structure and unique function define the hemicentin. *Cell & Bioscience*, *3*(1), 27.

Yamada, H. and Yamamoto, M., 2011. Association between circadian clock genes and diapause incidence in *Drosophila triauraria*. *PLOS One* 6(12), e27493. Doi:10.1371/journal.pone.0027493

Yanez, J. and Meissl, H., 1996. Secretion of the methoxyindoles melatonin, 5-methoxytryptophol, 5-methoxyindoleacetic acid, and 5-methoxytryptamine from trout pineal organs in superfusion culture: effects of light intensity. *General and Comparative Endocrinology*, *101*(2), 165-172.

Yang, B., Zhang, M., Li, L., Pu, F., You, W. and Ke, C., 2015. Molecular analysis of atypical family 18 Chitinase from Fujian Oyster *Crassostrea angulata* and its physiological role in the digestive system. *PloS One*, *10*(6), e0129261.

Yang, J. S., Dai, Z. M., Yang, F. and Yang, W. J., 2006. Molecular cloning of *Clock* cDNA from the prawn, *Macrobrachium rosenbergii*. *Brain Research*, *1067*(1), 13-24.

Yang, Y., Zhao, G. and Winkler, M.E., 1996. Identification of the pdxK gene that encodes pyridoxine (vitamin B6) kinase in Escherichia coli K-12. *FEMS Microbiology Letters*, *141*(1), 89-95.

Yang, Z., Wu, H. and Li, Y., 2012. Toxic effect on tissues and differentially expressed genes in hepatopancreas identified by suppression subtractive hybridization of freshwater pearl mussel (*Hyriopsis cumingii*) following microcystin-LR challenge. *Environmental Toxicology*, *27*(7), 393-403.

Yerushalmi, S. and Green, R.M., 2009. Evidence for the adaptive significance of circadian rhythms. *Ecology Letters*, *12*(9), 970-981.

Young, M.W., 2000. Life's 24-hour clock: molecular control of circadian rhythms in animal cells. *Trends in Biomedical Sciences, 25*, 601-606.

Young, M.W. and Kay, S.A., 2001. Time zones: a comparative genetics of circadian clocks. *Nature Reviews Genetics 2*, 702-715.

Yuan, Q., Lin, F., Zheng, X. and Sehgal, A., 2005. Serotonin modulates circadian entrainment in *Drosophila*. *Neuron*, *47*(1), 115-127.

Zaldibar, B., Cancia, I. and Marigómez, I., 2004. Circatidal variation in epithelial cell proliferation in the mussel digestive gland and stomach. *Cell Tissue Research, 318*, 395-402.

Zann, L.P., 1973. Interactions of the circadian and circatidal rhythms of the littoral gastropod *Melanerita atramentosa* Reeve. *Journal of Experimental Marine Biology and Ecology*, *11*(3), 249-261.

Zarnoch, C.B. and Schreibman, M., 2012. Growth and reproduction of eastern oysters, Crassostrea virginica in a New York City estuary: implications for restoration. *Urban habitats*, *7*(1).

Zeng, Z., Ni, J. and Ke, C., 2013. Expression of glycogen synthase (GYS) and glycogen synthase kinase 3β (GSK3β) of the Fujian oyster, *Crassostrea angulata*, in relation to glycogen content in gonad development. *Comparative Biochemistry and Physiology Part B: Biochemistry and Molecular Biology*, *166*(3-4), 203-214.

Zeng, H., Qian, Z., Myers, M.P. and Rosbash, M., 1996. A light-entrainment mechanism for the *Drosophila* circadian clock. *Nature*, *380*(6570), 129.

Zhadan, P.M., 2005. Directional sensitivity of the Japanese scallop *Mizuhopecten*

yessoensis and Swift scallop *Chlamys swifti* to water-borne vibrations. *Russian Journal of Marine Biology*, *31*(1), 28-35.

Zhang, E.E., Liu, A.C., Hirota, T., Miraglia, L.J., Welch, G., Pongsawakul, P., Liu, X., Atwood, A., Huss III, J.W., Janes, J., Su, A.I., Hogenesch, J.B. and Kay, S.A., 2009. A genome-wide RNAi screen for modifiers of the circadian clock in human cells. *Cell*, *139*(1), 199-210.

Zhang, E.E. and Kay, S.A., 2010. Clocks not winding down: unravelling circadian networks. *Nature Reviews Molecular Cell Biology*, *11*(11), 764-776.

Zhang, G., Fang, X., Guo, X., Li, L., Luo, R., Xu, F., Yang, P., Zhang, L., Wang, X., Qi, H., Xiong, Z., Que, H., Xie, Y., Hollands, P.W.H., Paps, J., Zhu, Y., Wu, F., Chen, Y., Wang, J., Peng, C., Meng, J., Yang, L., Liu, J., Wen, B., Zhang, N., Huang, Z., Zhu, Q., Feng, Y., Mount, A., Hedgecock, D., Xu, Z., Liu, Y., Domazet-Lošo, T., Du, Y., Sun, X., Zhang, S., Liu, B., Cheng, P., Jian, X., Ki, J., Fan, D., Wang, W., Fu, W., Wang, B., Zhang, J., Peng, Z., Li, Y., Li, N., Wang, J., Chen, M., He., Y., Tan, F., Song, X., Zheng, Q., Huang, R., Yang, H., Du, X., Chen, L., Yang, M., Gaffney, P.M., Wang, S., Luo, L., She, Z., Ming, Y., Huang, W., Zhang, S., Huang, B., Zhang, Y., Qu, T., Ni, P., Miao, G., Wang, J., Wang, Q., Steinberg, C.E.W., Wang, H., Li, N., Qian, L., Zhang, G., Li, Y., Yang, H., Liu, X., Wang, J., Yin, Y. and Wang, J., 2012. The oyster genome reveals stress adaptation and complexity of shell formation. *Nature*, *490*(7418), 49-54.

Zhao, W., Chen, L., Qin, J., Wu, P., Zhang, F., Li, E. and Tang, B., 2011. MnHSP90 cDNA characterization and its expression during the ovary development in oriental river prawn, *Macrobrachium nipponense*. *Molecular Biology Reports*, *38*(2), 1399-1406.

Zhao, S., Fung-Leung, W.P., Bittner, A., Ngo, K. and Liu, X., 2014. Comparison of RNA-Seq and microarray in transcriptome profiling of activated T cells. *PloS one*, *9*(1).

Zhdanova, I.V. and Reebs, S.G., 2006. Circadian rhythms in fish. In *Fish physiology*, 24, p.197-238.

Zhou, H., Qu, Y., Wu, H., Liao, C., Zheng, J., Diao, X. and Xue, Q., 2010. Molecular phylogenies and evolutionary behavior of AhR (aryl hydrocarbon receptor) pathway genes in aquatic animals: implications for the toxicology mechanism of some persistent organic pollutants (POPs). *Chemosphere*, *78*(2), 193-205.

Zhu, L., Liu, W., Tan, Q.Q., Lei, C.L. and Wang, X.P., 2017. Differential expression of circadian clock genes in two strains of beetles reveals candidates related to photoperiodic induction of summer diapause. *Gene*, *603*, 9-14.

Zippay, M.L., and Helmuth, B. (2012). Effects of temperature change on mussel, *Mytilus*. *Integrative Zoology*, *7*(3), 312-327.

Zisapel, N., 2018. New perspectives on the role of melatonin in human sleep, circadian rhythms and their regulation. *British Journal of Pharmacology*, *175*(16), 3190-3199.

Zuker, M., 2003. Mfold web server for nucleic acid folding and hybridization prediction. *Nucleic Acids Research. 31*(13), 3406-15.